

JOURNAL OF

CHROMATOGRAPHY

INCLUDING ELECTROPHORESIS AND OTHER SEPARATION METHODS

EDITORS

U. A. Th. Brinkman (Amsterdam)
 R. W. Giese (Boston, MA)
 J. K. Haken (Kensington, N.S.W.)
 K. Macek (Prague)
 L. R. Snyder (Orinda, CA)

EDITORS, SYMPOSIUM VOLUMES,

E. Heftmann (Orinda, CA), Z. Deyl (Prague)

EDITORIAL BOARD

D. W. Armstrong (Rolla, MO)
 W. A. Aue (Halifax)
 P. Boček (Brno)
 A. A. Boulton (Saskatoon)
 P. W. Carr (Minneapolis, MN)
 N. H. C. Cooke (San Ramon, CA)
 V. A. Davankov (Moscow)
 Z. Deyl (Prague)
 S. Dilli (Kensington, N.S.W.)
 F. Erni (Basle)
 M. B. Evans (Hatfield)
 J. L. Glajch (N. Billerica, MA)
 G. A. Guiochon (Knoxville, TN)
 P. R. Haddad (Kensington, N.S.W.)
 I. M. Hais (Hradec Králové)
 W. S. Hancock (San Francisco, CA)
 S. Hjertén (Uppsala)
 Cs. Horváth (New Haven, CT)
 J. F. K. Huber (Vienna)
 K.-P. Hupe (Waldbronn)
 T. W. Hutchens (Houston, TX)
 J. Janák (Brno)
 P. Jandera (Pardubice)
 B. L. Karger (Boston, MA)
 J. J. Kirkland (Wilmington, DE)
 E. sz. Kováts (Lausanne)
 A. J. P. Martin (Cambridge)
 L. W. McLaughlin (Chestnut Hill, MA)
 E. D. Morgan (Keele)
 J. D. Pearson (Kalamazoo, MI)
 H. Poppe (Amsterdam)
 F. E. Regnier (West Lafayette, IN)
 P. G. Righetti (Milan)
 P. Schoenmakers (Eindhoven)
 R. Schwarzenbach (Dübendorf)
 R. E. Shoup (West Lafayette, IN)
 A. M. Siouffi (Marseille)
 D. J. Strydom (Boston, MA)
 N. Tanaka (Kyoto)
 S. Terabe (Hyogo)
 K. K. Unger (Mainz)
 R. Verpoorte (Leiden)
 Gy. Vigh (College Station, TX)
 J. T. Watson (East Lansing, MI)
 B. D. Westerlund (Uppsala)

EDITORS, BIBLIOGRAPHY SECTION

Z. Deyl (Prague), J. Janák (Brno), V. Schwarz (Prague)

JOURNAL OF CHROMATOGRAPHY

INCLUDING ELECTROPHORESIS AND OTHER SEPARATION METHODS

Scope. The *Journal of Chromatography* publishes papers on all aspects of chromatography, electrophoresis and related methods. Contributions consist mainly of research papers dealing with chromatographic theory, instrumental development and their applications. The section *Biomedical Applications*, which is under separate editorship, deals with the following aspects: developments in and applications of chromatographic and electrophoretic techniques related to clinical diagnosis or alterations during medical treatment; screening and profiling of body fluids or tissues with special reference to metabolic disorders; results from basic medical research with direct consequences in clinical practice; drug level monitoring and pharmacokinetic studies; clinical toxicology; analytical studies in occupational medicine.

Submission of Papers. Manuscripts (in English; four copies are required) should be submitted to: Editorial Office of *Journal of Chromatography*, P.O. Box 681, 1000 AR Amsterdam, Netherlands, Telefax (+31-20) 5862 304, or to: The Editor of *Journal of Chromatography*, *Biomedical Applications*, P.O. Box 681, 1000 AR Amsterdam, Netherlands. Review articles are invited or proposed by letter to the Editors. An outline of the proposed review should first be forwarded to the Editors for preliminary discussion prior to preparation. Submission of an article is understood to imply that the article is original and unpublished and is not being considered for publication elsewhere. For copyright regulations, see below.

Publication. The *Journal of Chromatography* (incl. *Biomedical Applications*) has 39 volumes in 1992. The subscription prices for 1992 are:

J. Chromatogr. (incl. *Cum. Indexes*, Vols. 551–600) + *Biomed. Appl.* (Vols. 573–611):

Dfl. 7722.00 plus Dfl. 1209.00 (p.p.h.) (total ca. US\$ 4880.25)

J. Chromatogr. (incl. *Cum. Indexes*, Vols. 551–600) only (Vols. 585–611):

Dfl. 6210.00 plus Dfl. 837.00 (p.p.h.) (total ca. US\$ 3850.75)

Biomed. Appl. only (Vols. 573–584):

Dfl. 2760.00 plus Dfl. 372.00 (p.p.h.) (total ca. US\$ 1711.50).

Subscription Orders. The Dutch guilder price is definitive. The US\$ price is subject to exchange-rate fluctuations and is given as a guide. Subscriptions are accepted on a prepaid basis only, unless different terms have been previously agreed upon. Subscriptions orders can be entered only by calendar year (Jan.–Dec.) and should be sent to Elsevier Science Publishers, Journal Department, P.O. Box 211, 1000 AE Amsterdam, Netherlands, Tel. (+31-20) 5803 642, Telefax (+31-20) 5803 598, or to your usual subscription agent. Postage and handling charges include surface delivery except to the following countries where air delivery via SAL (Surface Air Lift) mail is ensured: Argentina, Australia, Brazil, Canada, China, Hong Kong, India, Israel, Japan*, Malaysia, Mexico, New Zealand, Pakistan, Singapore, South Africa, South Korea, Taiwan, Thailand, USA. *For Japan air delivery (SAL) requires 25% additional charge of the normal postage and handling charge. For all other countries airmail rates are available upon request. Claims for missing issues must be made within three months of our publication (mailing) date, otherwise such claims cannot be honoured free of charge. Back volumes of the *Journal of Chromatography* (Vols. 1–572) are available at Dfl. 217.00 (plus postage). Customers in the USA and Canada wishing information on this and other Elsevier journals, please contact Journal Information Center, Elsevier Science Publishing Co. Inc., 655 Avenue of the Americas, New York, NY 10010, USA, Tel. (+1-212) 633 3750, Telefax (+1-212) 633 3990.

Abstracts/Contents Lists published in Analytical Abstracts, Biochemical Abstracts, Biological Abstracts, Chemical Abstracts, Chemical Titles, Chromatography Abstracts, Clinical Chemistry Lookout, Current Contents/Life Sciences, Current Contents/Physical, Chemical & Earth Sciences, Deep-Sea Research/Part B: Oceanographic Literature Review, Excerpta Medica, Index Medicus, Mass Spectrometry Bulletin, PASCAL-CNRS, Pharmaceutical Abstracts, Referativnyi Zhurnal, Research Alert, Science Citation Index and Trends in Biotechnology.

See inside back cover for Publication Schedule, Information for Authors and information on Advertisements.

© 1992 ELSEVIER SCIENCE PUBLISHERS B.V. All rights reserved.

0021-9673/92/\$05.00

No part of this publication may be reproduced, stored in a retrieval system or transmitted in any form or by any means, electronic, mechanical, photocopying, recording or otherwise, without the prior written permission of the publisher, Elsevier Science Publishers B.V., Copyright and Permissions Department, P.O. Box 521, 1000 AM Amsterdam, Netherlands.

Upon acceptance of an article by the journal, the author(s) will be asked to transfer copyright of the article to the publisher. The transfer will ensure the widest possible dissemination of information.

Submission of an article for publication entails the authors' irrevocable and exclusive authorization of the publisher to collect any sums or considerations for copying or reproduction payable by third parties (as mentioned in article 17 paragraph 2 of the Dutch Copyright Act of 1912 and the Royal Decree of June 20, 1974 (S. 351) pursuant to article 16 b of the Dutch Copyright Act of 1912) and/or to act in or out of Court in connection therewith.

Special regulations for readers in the USA. This journal has been registered with the Copyright Clearance Center, Inc. Consent is given for copying of articles for personal or internal use, or for the personal use of specific clients. This consent is given on the condition that the copier pays through the Center the per-copy fee stated in the code on the first page of each article for copying beyond that permitted by Sections 107 or 108 of the US Copyright Law. The appropriate fee should be forwarded with a copy of the first page of the article to the Copyright Clearance Center, Inc., 27 Congress Street, Salem, MA 01970, USA. If no code appears in an article, the author has not given broad consent to copy and permission to copy must be obtained directly from the author. All articles published prior to 1980 may be copied for a per-copy fee of US\$ 2.25, also payable through the Center. This consent does not extend to other kinds of copying, such as for general distribution, resale, advertising and promotion purposes, or for creating new collective works. Special written permission must be obtained from the publisher for such copying.

No responsibility is assumed by the Publisher for any injury and/or damage to persons or property as a matter of products liability, negligence or otherwise, or from any use or operation of any methods, products, instructions or ideas contained in the materials herein. Because of rapid advances in the medical sciences, the Publisher recommends that independent verification of diagnoses and drug dosages should be made.

Although all advertising material is expected to conform to ethical (medical) standards, inclusion in this publication does not constitute a guarantee or endorsement of the quality or value of such product or of the claims made of it by its manufacturer.

This issue is printed on acid-free paper.

CONTENTS

(Abstracts/Contents Lists published in *Analytical Abstracts, Biochemical Abstracts, Biological Abstracts, Chemical Abstracts, Chemical Titles, Chromatography Abstracts, Current Contents/Life Sciences, Current Contents/Physical, Chemical & Earth Sciences, Deep-Sea Research/Part B: Oceanographic Literature Review, Excerpta Medica, Index Medicus, Mass Spectrometry Bulletin, PASCAL-CRNS, Referativnyi Zhurnal, Research Alert and Science Citation Index*)

REGULAR PAPERS

Column Liquid Chromatography

- Contribution of specifiable hydrophobic interactions to chiral recognition
by W. H. Pirkle, J.-P. Chang and J. A. Burke, III (Urbana, IL, USA) (Received January 8th, 1992) 1
- Effects of stationary phase ligand density on high-performance ion-exchange chromatography of proteins
by D. Wu and R. R. Walters (Ames, IA, USA) (Received January 16th, 1992) 7
- Separon HEMA modified for immobilized metal ion affinity chromatographic separation of proteins
by P. Šmíd, J. Plicka and I. Kleinmann (Prague, Czechoslovakia) (Received December 30th, 1991) 15
- Evaluation of restricted access media for high-performance liquid chromatographic analysis of sulfonamide antibiotic residues in bovine serum
by J. D. Brewster, A. R. Lightfield and R. A. Barford (Philadelphia, PA, USA) (Received January 10th, 1992) 23
- Simultaneous determination of amounts of major phospholipid classes and their fatty acid composition in erythrocyte membranes using high-performance liquid chromatography and gas chromatography
by K. Eder, A. M. Reichlmayr-Lais and M. Kirchgessner (Freising-Weihenstephan, Germany) (Received January 10th, 1992) 33
- Determination of muramic acid by high-performance liquid chromatography-plasma spray mass spectrometry
by I. Elmroth, L. Larsson, G. Wester Dahl and G. Odham (Lund, Sweden) (Received January 8th, 1992) 43
- Screening for amines by dansylation and automated high-performance liquid chromatography
by N. P. J. Price (London, UK), J. L. Firmin (Norwich, UK) and D. O. Gray (London, UK) (Received December 30th, 1991) 51
- High-performance liquid chromatographic analysis of benzodiazepines using diode array, electrochemical and thermospray mass spectrometric detection
by I. S. Lurie, D. A. Cooper and R. F. X. Klein (McLean, VA, USA) (Received January 6th, 1992) 59
- Investigation of enantioselectivity and enantiomeric elution order of propranolol and its ester derivatives on an ovomucoid-bonded column
by J. Haginaka, C. Seyama, H. Yasuda and K. Takahashi (Hyogo, Japan) (Received January 7th, 1992) 67
- Control of the retention selectivity of rare earth octaethylporphyrins in reversed-phase high-performance liquid chromatography using amines as mobile phase additives
by Y. Shibata, K. Saitoh and N. Suzuki (Miyagi, Japan) (Received January 28th, 1992) 73

Gas Chromatography

- Structure elucidation of saccharides in anthocyanins and flavonols by means of methylation analysis and gas chromatography
by W. E. Glässgen, R. Hofmann, M. Emmerling, G. D. Neumann and H. U. Seitz (Tübingen, Germany) (Received January 10th, 1992) 81
- Mass spectrometric identification of products formed during degradation of ethyl dimethylphosphoramidocyanidate (tabun)
by P. A. D'Agostino and L. R. Provost (Medicine Hat, Canada) (Received January 8th, 1992) 89
- Determination of organotin species by capillary gas chromatography with alternating current plasma emission detection
by J. M. Ombaba and E. F. Barry (Lowell, MA, USA) (Received January 21st, 1992) 97
- Determination of selenium by capillary gas chromatography after high-temperature derivatization with 1,2-diamino-3,5-dibromobenzene
by K. Johansson and Å. Olin (Uppsala, Sweden) (Received January 20th, 1992) 105

(Continued overleaf)

Contents (continued)

Electrophoresis

Fluorescence detector cell for use in an integrated electrically driven separation system
 by P. K. de Bokx, E. E. A. Gillissen, P. van de Weijer, M. H. J. Bekkers, C. H. M. van Bommel and H.-G. Janssen
 (Eindhoven, Netherlands) (Received January 27th, 1992) 115

Assay of protein drug substances present in solution mixtures by fluorecamine derivatization and capillary electrophoresis
 by N. A. Guzman, J. Moschera, C. A. Bailey, K. Iqbal and A. W. Malick (Nutley, NJ, USA) (Received January 9th,
 1992) 123

Systematic optimization of capillary electrophoretic separation of sulphonamides
 by C. L. Ng, H. K. Lee and S. F. Y. Li (Singapore, Singapore) (Received January 13th, 1992) 133

SHORT COMMUNICATIONS

Column Liquid Chromatography

High-performance liquid chromatographic separation of *cis-trans* isomers of proline-containing peptides. I. Separation on cyclo-
 dextrin-bonded silica
 by S. Friebe and G. J. Krauss (Halle/S., Germany) and H. Nitsche (Heidelberg, Germany) (Received November 28th,
 1991) 139

Identification and determination of honokiol and magnolol from *Magnolia officinalis* by high-performance liquid chromatogra-
 phy with photodiode-array UV detection
 by T.-H. Tsai (Taipei Hsien, Taiwan) and C.-F. Chen (Taipei, Taiwan) (Received January 17th, 1992) 143

Studies on stress metabolites. XVI. High-performance liquid chromatographic analysis of cruciferous phytoalexins using complex
 ternary mobile phase gradients
 by K. Monde and M. Takasugi (Sapporo, Japan) (Received January 29th, 1992) 147

 *
 * In articles with more than one author, the name of the author to whom correspondence should be addressed is indicated *
 * in the article heading by a 6-pointed asterisk (*). *
 *
 *

Analysis of Substances in the Gaseous Phase

by *E. Smolková-Keulemansová and L. Feltl, Charles University, Department of Analytical Chemistry, Prague, Czechoslovakia*
Series Editor *G. Svehla, Department of Chemistry, University College, Cork, Ireland*

Nowadays, there are increasing demands for the control and specification of all aspects of industrial manufacturing. There is also a growing need to understand various biological processes and conditions for agricultural production, and concern for protection of the environment and human health. These factors have made it imperative to develop adequate methods for the analysis of gaseous substances or substances that can be converted to the gaseous state. It is not only necessary to apply known and developed methods correctly, but novel analytical procedures must also be found. Instrumentation should be improved and the applications of these methods will have to be extended.

The present volume provides a comprehensive description of the state-of-the-art and of future possibilities in the analysis of gaseous substances. In the individual chapters the following themes have been discussed: the theoretical basis for the methods, a description of the instrumentation and the steps necessary in actual analyses and an outline of the principal areas in which each method can be employed. Both classical methods that are still useful for the solution of analytical problems using simple instrumentation,

and the newest methods in the field are described. Special attention is paid to modern electrochemical and spectroscopic methods, and to methods based on a number of physical principles. Gas chromatography is discussed in the greatest detail because of its specially important position in modern analytical chemistry.

The book should be well received by the analytical public and should be extremely useful to students and workers in scientific research laboratories and in fields dealing with environmental protection.

Contents: 1. Introduction. 2. The History of the Chemistry of Gases. 3. Characteristics of Gas Analysis. 4. Determination of the Temperature, Pressure and Volume. 5. Sample Storage and Treatment. 6. Qualitative and Semi-Quantitative Methods of Gas Analysis. 7. Methods of Quantitative Analysis. 8. Chemical and Physico-Chemical Methods of Gas Analysis. 9. Physical Methods of Gas Analysis. 10. Gas Chromatography. Bibliography. Subject Index.

1991 xiv + 480 pages

Price: US \$ 205.00 / Dfl. 400.00

Subscription price:

US \$ 184.50 / Dfl. 360.00

ISBN 0-444-89122-6



Elsevier Science Publishers

P.O. Box 211, 1000 AE Amsterdam, The Netherlands

P.O. Box 882, Madison Square Station, New York, NY 10159, USA

CHROMATOGRAPHY ABSTRACTS

by E.R. Adlard *and* P.A. Sewell .

Volume 35 (1 volume in 10 issues):
ISSN 0268-6287. Subscription price: £529.00

AUDIENCE:

Analytical, research and industrial chemists

AIMS AND SCOPE

Chromatography Abstracts are designed to provide an essential service to chromatographers throughout the world. A team of well-qualified abstractors continuously scans all the major world journals for papers reporting advances in chromatographic techniques and their application to specific problems. A feature of the Abstracts is the detailed annual subject index, helping readers to locate information on a particular topic rapidly and, if desired, transfer this information to a data base. For the convenience of readers the Abstracts are divided into three sections on Gas, Liquid and Miscellaneous methods. The latter section includes thin-layer, supercritical fluid, gel permeation and affinity chromatography as well as associated techniques such as electrophoresis and field flow fractionation.

The Abstracts are sponsored by the Chromatographic Society and reflect the expanding interests of the Society by means of a gradual extension to cover other aspects of separation science, in addition to their comprehensive coverage of the ever-increasing chromatographic literature.



Orders and requests for sample copies should be sent to:

ELSEVIER SCIENCE PUBLISHERS LTD

Crown House, Linton Road, Barking, Essex, IG11 8JU, UK

for customers in North America

Elsevier Science Publishers, Journal Information Center,
655 Avenue of the Americas, New York, NY 10010, USA

JOURNAL OF CHROMATOGRAPHY

VOL. 598 (1992)

JOURNAL of CHROMATOGRAPHY

INCLUDING ELECTROPHORESIS AND OTHER SEPARATION METHODS

EDITORS

U. A. Th. BRINKMAN (Amsterdam), R. W. GIESE (Boston, MA), J. K. HAKEN (Kensington, N.S.W.), K. MACEK (Prague),
L. R. SNYDER (Orinda, CA)

EDITORS, SYMPOSIUM VOLUMES

E. HEFTMANN (Orinda, CA), Z. DEYL (Prague)

EDITORIAL BOARD

D. W. Armstrong (Rolla, MO), W. A. Aue (Halifax), P. Boček (Brno), A. A. Boulton (Saskatoon), P. W. Carr (Minneapolis, MN),
N. H. C. Cooke (San Ramon, CA), V. A. Davankov (Moscow), Z. Deyl (Prague), S. Dilli (Kensington, N.S.W.), F. Erni (Basle), M.
B. Evans (Hatfield), J. L. Glajch (N. Billerica, MA), G. A. Guiochon (Knoxville, TN), P. R. Haddad (Kensington, N.S.W.), I. M.
Hais (Hradec Králové), W. S. Hancock (San Francisco, CA), S. Hjertén (Uppsala), Cs. Horváth (New Haven, CT), J. F. K. Huber
(Vienna), K.-P. Hupe (Waldbronn), T. W. Hutchens (Houston, TX), J. Janák (Brno), P. Jandera (Pardubice), B. L. Karger
(Boston, MA), J. J. Kirkland (Wilmington, DE), E. sz. Kováts (Lausanne), A. J. P. Martin (Cambridge), L. W. McLaughlin
(Chestnut Hill, MA), E. D. Morgan (Keele), J. D. Pearson (Kalamazoo, MI), H. Poppe (Amsterdam), F. E. Regnier (West
Lafayette, IN), P. G. Righetti (Milan), P. Schoenmakers (Eindhoven), R. Schwarzenbach (Dübendorf), R. E. Shoup (West
Lafayette, IN), A. M. Siouffi (Marseille), D. J. Strydom (Boston, MA), N. Tanaka (Kyoto), S. Terabe (Hyogo), K. K. Unger
(Mainz), R. Verpoorte (Leiden), Gy. Vigh (College Station, TX), J. T. Watson (East Lansing, MI), B. D. Westerlund (Uppsala)

EDITORS, BIBLIOGRAPHY SECTION

Z. Deyl (Prague), J. Janák (Brno), V. Schwarz (Prague)



ELSEVIER
AMSTERDAM — LONDON — NEW YORK — TOKYO

J. Chromatogr., Vol. 598 (1992)

ห้องสมุดกรมวิทยาศาสตร์บริการ

© 1992 ELSEVIER SCIENCE PUBLISHERS B.V. All rights reserved.

0021-9673/92/\$05.00

No part of this publication may be reproduced, stored in a retrieval system or transmitted in any form or by any means, electronic, mechanical, photocopying, recording or otherwise, without the prior written permission of the publisher, Elsevier Science Publishers B.V., Copyright and Permissions Department, P.O. Box 521, 1000 AM Amsterdam, Netherlands.

Upon acceptance of an article by the journal, the author(s) will be asked to transfer copyright of the article to the publisher. The transfer will ensure the widest possible dissemination of information.

Submission of an article for publication entails the authors' irrevocable and exclusive authorization of the publisher to collect any sums or considerations for copying or reproduction payable by third parties (as mentioned in article 17 paragraph 2 of the Dutch Copyright Act of 1912 and the Royal Decree of June 20, 1974 (S. 351) pursuant to article 16 b of the Dutch Copyright Act of 1912) and/or to act in or out of Court in connection therewith.

Special regulations for readers in the USA. This journal has been registered with the Copyright Clearance Center, Inc. Consent is given for copying of articles for personal or internal use, or for the personal use of specific clients. This consent is given on the condition that the copier pays through the Center the per-copy fee stated in the code on the first page of each article for copying beyond that permitted by Sections 107 or 108 of the US Copyright Law. The appropriate fee should be forwarded with a copy of the first page of the article to the Copyright Clearance Center, Inc., 27 Congress Street, Salem, MA 01970, USA. If no code appears in an article, the author has not given broad consent to copy and permission to copy must be obtained directly from the author. All articles published prior to 1980 may be copied for a per-copy fee of US\$ 2.25, also payable through the Center. This consent does not extend to other kinds of copying, such as for general distribution, resale, advertising and promotion purposes, or for creating new collective works. Special written permission must be obtained from the publisher for such copying.

No responsibility is assumed by the Publisher for any injury and/or damage to persons or property as a matter of products liability, negligence or otherwise, or from any use or operation of any methods, products, instructions or ideas contained in the materials herein. Because of rapid advances in the medical sciences, the Publisher recommends that independent verification of diagnoses and drug dosages should be made.

Although all advertising material is expected to conform to ethical (medical) standards, inclusion in this publication does not constitute a guarantee or endorsement of the quality or value of such product or of the claims made of it by its manufacturer.

This issue is printed on acid-free paper.

Printed in the Netherlands

CHROM. 23 998

Contribution of specifiable hydrophobic interactions to chiral recognition

William H. Pirkle*, Jen-Ping Chang and J. Andrew Burke, III

School of Chemical Sciences, University of Illinois, Urbana, IL 61801 (USA).

(First received October 28th, 1991; revised manuscript received January 8th, 1992)

ABSTRACT

The reversed-phase chromatographic behavior of several homologous series of racemic analytes was examined using chiral stationary phases (CSPs) derived from (*R*)-*N*-(2-naphthyl)alanine. For those analytes bearing an alkyl substituent on the stereogenic center, the degree of enantioselectivity is observed to increase as the length of this alkyl substituent is increased. This effect is attributed to a reduction in "wetted surface area" when the methylene chain "connecting arm" of the CSP contacts the alkyl substituent of the most retained analyte enantiomer owing to intercalation of this alkyl group between the strands of bonded phase. In these series, the alkyl substituents of the less retained enantiomers are differently oriented during interaction with the CPS and less effectively contact the bonded phase. Although hydrophobic interactions contribute the retention, they need not always contribute to chiral recognition as shown by other series of analytes. Cases may eventually be found where lengthening an alkyl substituent decreases enantioselectivity owing to greater hydrophobic interaction between the CSP and the initially eluted enantiomer.

INTRODUCTION

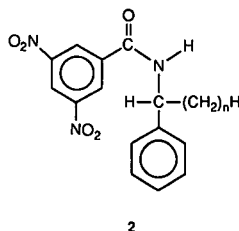
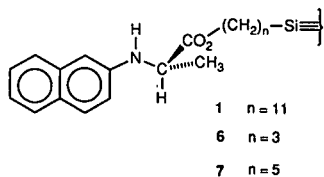
The retention of an analyte on a non-polar stationary phase during reversed-phase chromatography stems principally from the analyte being driven from the mobile phase into (or onto) the non-polar stationary phase so as to reduce the total "wetted surface area" in the system. In the case of enantiomeric analytes, hydrophobic effects provide equal motivation for each enantiomer to partition into (or onto) the stationary phase. However, it is necessary that there be contact between non-polar regions of both the analyte and stationary phase for such partitioning to occur, this contact being responsible for the reduction in "wetted surface area". On chiral stationary phases (CSPs), such contact is, in principle, dependent upon the stereochemistry of the analyte. Hence, enantioselective "hydrophobic interactions" might lead to differential retention of enantiomers. In most instances, such enantioselective hydrophobic interactions will be superimposed upon the more usual "polar effects" invoked to account for chiral recognition. In

other words, hydrophobic interactions may be considered as just another type of intermolecular interaction which contributes to retention under reversed-phase conditions and *may* contribute to chiral recognition. Except for the pioneering efforts of Davankov [1] who has documented the contributions of hydrophobic interactions to chiral recognition during ligand-exchange chromatography, no mechanistic studies have been reported in which the role of these interactions in chiral recognition has been clearly defined. Davankov stands alone in the deliberate incorporation into the CSP of structural features intended to participate in enantioselective hydrophobic interactions. It is true that hydrophobic interactions are invoked as occurring during enantiomer separation on cyclodextrin [2] or protein-derived [3–5] CSPs. However, such effects are usually held to be the source of the major portion of the retention rather than the source of enantioselectivity. It seems fair to say that while hydrophobic effects promote analyte inclusion, differential contributions by hydrophobic interactions to the retention of enantiomers are usually not well understood

and, except for Davankov's work [1], cannot be said to be intentionally included into the design of the CSP.

RESULTS AND DISCUSSION

Because of our interest in chiral recognition mechanisms, we frequently examine homologous series of enantiomeric analytes by reversed-phase chromatography on the CSPs developed in our laboratories. It is found that retention increases as one proceeds through the homologous series but that enantioselectivity generally remains relatively constant. One prior instance of hydrophobic effects contributing to enantioselectivity was noted for an earlier π -basic CSP [6]. However, that system was but briefly studied.



The mechanistic basis by which CSP 1, derived from N-(2-naphthyl)alanine, distinguished between the enantiomers of N-aryl amino acid derivatives in normal-phase eluents is relatively well understood [7,8]. This CSP suffices to separate the enantiomers of many other compounds as well. For example, Fig. 1 shows the relation between n , the number of methylene units in the linear alkyl substituent of N-(3,5-dinitrobenzoyl)- α -amino- α -phenyl alkanes, **2**, and the chromatographic separation factors of the enantiomers, α , when this homologous series of analytes is chromatographed on CSP 1 using either hexane-2-propanol (90:10) or methanol-water (90:10). In the normal mobile phase, α increases until n reaches 5, thereafter decreasing slowly. The retention of both enantiomers decreases as n

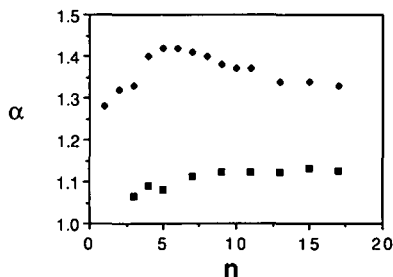


Fig. 1. Dependence of the separation factor, α , for the enantiomers of N-(3,5-dinitrobenzoyl)- α -amino- α -phenyl alkanes on the number of carbons, n , in the linear alkyl substituent. Column, CSP 1 (250 \times 4.6 mm I.D.); mobile phases: \blacksquare = methanol-water (90:10), flow-rate 1.0 ml/min; \blacklozenge = hexane-propanol (90:10), flow-rate, 2.0 ml/min.

increases (Fig. 2). In the reversed mobile phase, retention increases steadily (Fig. 2) as n increases, as does the magnitude of α (Fig. 1). However, α is only 1.06 when $n = 3$ and increases to but 1.13 when $n = 17$, so the hydrophobic contributions to chiral recognition are quite small. Chromatography of similar series of analytes in which the aryl substituents are of greater hydrophobicity (*p*-anisyl, α -naphthyl, β -naphthyl) generates very similar α vs. n curves, retention increasing as expected. This type of observation has been encountered so frequently as to be surprising in the face of Davankov's persuasive reports of the contributions of hydrophobic interactions to chiral recognition [1]. If one truly understood how to utilize hydrophobic interactions to achieve chiral recognition, one might design CSPs capable of separating the enantiomers of relatively

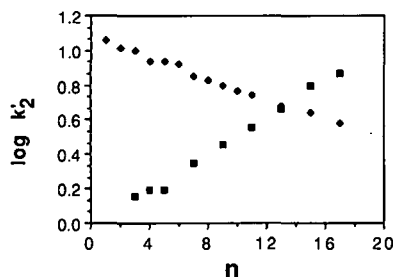
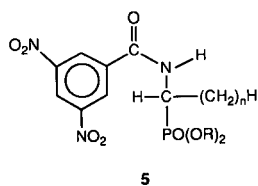
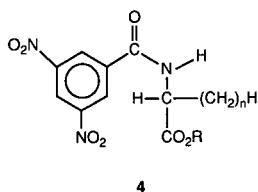
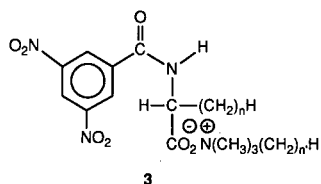


Fig. 2. Dependence of the logarithm of the capacity factor, k'_2 , of the more retained enantiomer of N-(3,5-dinitrobenzoyl)- α -amino- α -phenyl alkanes on the number of carbons, n , in the linear alkyl substituent. Experimental conditions are the same as in Fig. 1. \blacksquare = $\log k'_2$ methanol-water; \blacklozenge = $\log k'_2$ hexane-2-propanol.

unfunctionalized compounds. Being purposely designed to operate under reversed-phase conditions, such CSPs might be useful to those wishing to monitor the enantiomeric composition of drugs or their metabolites in body fluids, possibly complementing present-day cyclodextrin or protein-derived CSPs.

Recently, several homologous series of analytes were encountered which, when chromatographed on CSP 1 using a methanol–water mobile phase, do show significant hydrophobic contributions to chiral recognition. These analytes, depicted in generalized form as 3, 4 and 5, were available from prior



studies. Some aspects of the reversed-phase chromatographic behavior of the type 3 ion pairs have been reported recently [9] as has the direct-phase chromatographic behavior of the ester analytes, 4 [7] and 5 [10]. It is important to note that, on CSP 1 using hexane–2-propanol (80:20), the separation factors for enantiomers of the type 4 and 5 analytes are fairly uniform within each series. Moreover, the enantioselectivity is relatively uninfluenced by the alcohol used to prepare the esters. This indicates that, under normal-phase conditions, intercalative effects, as noted for these analytes on other CSPs [11,12], occur to a minor extent on CSP 1.

Under reversed-phase conditions, the number of methylene units in the alkyl substituent on the ana-

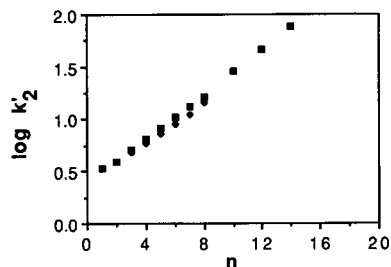


Fig. 3. Variation of the $\log k'_2$ with the number of carbons in the linear alkyl substituent of (■) N-(3,5-dinitrobenzoyl)- α -amino acid ethyl esters and (◆) N-(3,5-dinitrobenzoyl)-2-amino phosphonic acid dimethyl esters. Column, CSP 1; mobile phase, methanol–water (80:20); flow-rate, 1.0 ml/min.

lyte's stereogenic center affects both retention (Fig. 3) and enantioselectivity (Fig. 4) of the ethyl esters of the type 4 α -amino acid derivatives and of the dimethyl esters of the type 5 2-aminophosphonic acid derivatives. Similar observations are made for the enantioselectivity of the type 3 amino acid ion-pair derivatives (Fig. 5 and 6). Significantly, esters derived from these acids and higher alcohols (*n*-butanol, *n*-octanol) show the expected increase in retention under reversed-phase conditions but show no significant change in enantioselectivity relative to the corresponding ethyl esters. A similar observation was made recently when the hydrophobicity of the trimethylalkylammonium ion-pairing reagent was increased [9]. It is evident that, for these analytes, the hydrophobicity of the alkyl substituent on the stereogenic center influences enantioselectivity whereas the hydrophobicity of the alkoxy or ammonium ion portions of these analytes has essen-

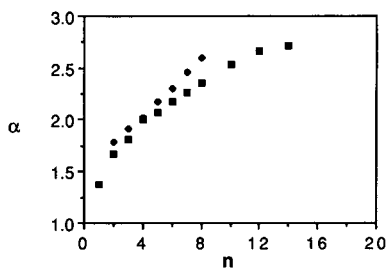


Fig. 4. Effect of the length of the alkyl substituent on the separation factor, α , for the enantiomers of (■) N-(3,5-dinitrobenzoyl)- α -amino acid ethyl esters and (◆) N-(3,5-dinitrobenzoyl)-2-amino phosphonic acid dimethyl esters. Column: CSP 1; mobile phase, methanol–water (80:20); flow-rate 1.0 ml/min.

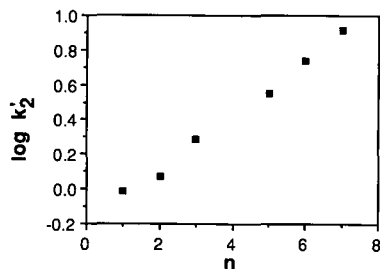


Fig. 5. Dependence of the logarithm of the capacity factor, k'_2 , for the more retained enantiomer on the length of the linear alkyl substituent of the N-(3,5-dinitrobenzoyl)- α -amino acids. Column: CSP 1; mobile phase, methanol-water (70:30) with 5 mM octyltrimethylammonium phosphate with 0.01 M phosphate buffer, pH 6.86; flow-rate, 1.0 ml/min.

tially no such effect, influencing retention only. How may this be rationalized?

It is generally accepted that retention during reversed-phase chromatography stems principally from expulsion of a hydrophobic analyte from the aqueous mobile phase into the non-polar stationary phase. Enantiomers must undergo identical hydrophobic expulsion forces from the achiral mobile phase but, because they may differ in their "fit" to the CSP, may undergo differential hydrophobic interaction. "Fit" is a vague and unsatisfactory term, usually used in the absence of deeper understanding. In the present instance, "fit" is used to mean contact of hydrophobic portions of the analyte with hydrophobic portions of the stationary phase while (presumably) maintaining the stronger interactions normally used to attain chiral recognition. This contact reduces the surface area of these hydrophobic portions which must be wetted by the re-

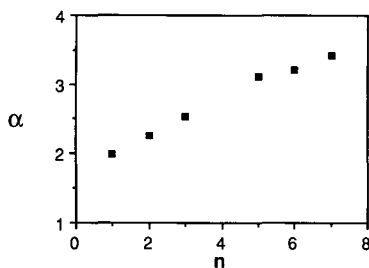


Fig. 6. Relationship between the separation factor, α , for the enantiomers of N-(3,5-dinitrobenzoyl)- α -amino acids on the length of the linear alkyl substituent. Experimental conditions are the same as in Fig. 5.

versed mobile phase. This lowers the energy of the system, contributing to the retention of the analyte. Some contacts occur equally well for either enantiomer, thus contributing equally to the retention of each. Whether or not a group contributes to chiral recognition through hydrophobic interactions bears upon the nature of the chiral recognition process and is of mechanistic relevance.

The elution orders of the enantiomers presently under discussion are the same using either direct or reversed-phase conditions. A chiral recognition mechanism has been advanced which is consistent with the observed elution orders [4], spectroscopic data [8], and the X-ray crystallographic structure [13] of a 1:1 complex of compounds similar in structure to the selector used in CSP 1 and to a type 4 analyte. The origin of the antioselectivity shown by CSP 1 toward the type 4 analytes is relatively well understood in non-polar solvents. It is reasonable to suppose that mechanistically similar processes operate under reversed-phase conditions *although they may be modified to some extent* by hydrophobic interactions, more extensive solvation of polar sites, and a weakening of the electrostatic components of some interactions owing to the higher dielectric constant of the medium. Although not now addressed, changes in the conformational preferences of either the analytes or the CSP or deep-seated changes in the structure of the bonded phase which occur with changes in the mobile phase composition might also influence chromatographic behavior.

The principal interactions occurring in the homochiral [*i.e.*, the (*R,R*) or the (*S,S*)] adsorbate formed from CSP 1 and a type 4 analyte are π - π interaction between the dinitrobenzoyl and naphthyl systems, hydrogen bonding of the dinitrobenzamide NH to the carbonyl oxygen of the CSP's C-terminal carboxyl group, and hydrogen bonding of the CSP's aniline-like NH to the analytes' C-terminal carbonyl oxygen. These interactions occur simultaneously and efficiently while the homochiral components are in low energy conformations. For these interactions to occur similarly in the heterochiral adsorbate, at least one of the components would have to assume a higher energy conformation. In hexane-2-propanol, the heterochiral adsorbates are formed to comparatively small extents. Consequently, their principal structures are uncertain. Similar mechanistic considerations are pre-

sumed to apply to the type 5 analytes where, owing to the Cahn–Ingold–Prelog [14] priority sequence, it is the heterochiral adsorbates which are most stable.

In the structures expected of the more stable diastereomeric adsorbates, study of space-filling models suggests that the alkyl group on the stereogenic center of the analyte parallels the methylene chain “connecting arm” linking the selector to silica. Although the structure of the adsorbate(s) formed from the less retained enantiomer is uncertain, we conclude that the analytes alkyl group is oriented differently. This inference is drawn from the chiral recognition mechanism and from the present observations. These suggest that the hydrophobic contribution to the chiral recognition of the type 3, 4 and 5 analytes stems from contact of the methylene chains of the connecting arm of **1** with the alkyl substituent on the stereogenic center of the most retained analyte enantiomer. The alkyl group of the other enantiomer presumably is oriented differently and, when this group is short, does not efficiently contact non-polar regions of the CSP. As the alkyl groups of the less retained enantiomers become longer, they are better able to establish contact with a non-polar region of the stationary phase (presumably in the neighboring strands) and thus diminish the difference between the hydrophobic interactions undergone by each enantiomer. This leads to the “leveling-off” of enantioselectivity as shown in the α vs. n plots.

Why is the connecting arm of CSP **1** chosen as the site of the hydrophobic interaction which contributes to chiral recognition? This follows from the be-

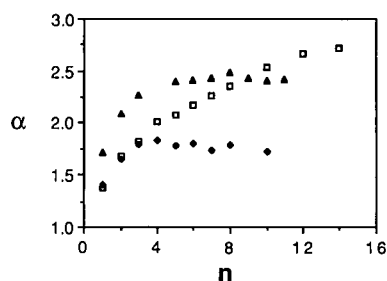


Fig. 7. The dependence of the separation factor, α , for the enantiomers of the ethyl esters of N-(3,5-dinitrobenzoyl)- α -amino acid on the length of the linear alkyl substituent on three CSPs: \square = CSP **1**, \blacklozenge = CSP **6**, \blacktriangle = CSP **7**. Mobile phase, methanol–water (80:20); flow-rate 1.0 ml/min.

havior of the ethyl esters of the type 4 analytes when these are chromatographed on CSPs **1**, **6** and **7**. These CSPs all use the same chiral selector but have, respectively, eleven, three, and five methylene groups in the connecting arms linking the selector to the silica. Fig. 7 presents plots of α , the separation factor for the enantiomers, versus n , the number of carbons in the linear alkyl substituents of the analytes as determined on CSPs **1**, **6** and **7**. The surface coverages of the three CSPs are similar although not identical. Hence, the vertical displacements of the curves may be influenced by the small differences in surface coverages [15]. However, it is the curve shapes which convey the information pertinent to the argument. Note that α initially increases on all three CSPs as the length of the alkyl substituent intercalated between (and presumably more or less parallel to) the strands is of a length comparable to that of the connecting arms. It appears that any further increase in the length of this group requires its reorientation owing to interaction with the underlying silica. The α vs. n curve from CSP **7** shows a pronounced slope change at $n = 5$, whereas the curve from CSP **1** shows no abrupt change in slope. Indeed, α is still increasing at $n = 14$. These curve shapes are clear indication of not only the intercalation of the alkyl substituent of the more retained enantiomer between the strands of bonded phase, but also demonstrate a lesser extent of intercalation by the less retained enantiomer.

The data in this paper make it clear that the effect of hydrophobic interactions upon the enantioselectivity of a CSP is dependent upon the relative orientations and proximities of the nonpolar moieties involved. The hydrophobic interactions reported herein either enhance both retention and enantioselectivity or simply increase retention without altering enantioselectivity. Clearly, it should also be possible for hydrophobic interactions to decrease enantioselectivity. All that is required is that these interactions occur to a greater extent in the least retained enantiomer rather than the most retained enantiomer.

One additional comment on mechanistic differences between non-polar and aqueous mobile phases will be made. Many of the analytes and all of the CSPs we utilize have bulky groups projecting from one “face” so as to control, through steric interactions, the preferred mode of “face-to-face” ap-

proach. These bulky groups are typically hydrophobic. One must wonder whether in reversed-phase solvents, hydrophobic interactions between these groups and non-polar groups in the analytes might lessen the ability of the bulky groups to bias the mode of "face-to-face" approach, thus contributing to the reduction in enantioselectivity which generally accompanies a change from a non-polar to a reversed-phase eluent.

ACKNOWLEDGEMENTS

This work was supported by grants from the National Science Foundation and from Eli Lilly and Company.

REFERENCES

- 1 V. A. Davankov, in V. A. Davankov, J. D. Navratil and H. F. Walton (Editors), *Ligand Exchange Chromatography*, CRC Press, Boca Raton, 1988, Ch. 5; and references cited therein.
- 2 T. J. Ward, D. W. Armstrong, *J. Liq. Chromatogr.*, 9 (1986) 407.
- 3 J. Hermansson and M. Eriksson, *J. Liq. Chromatogr.* 9 (1986) 621.
- 4 G. Schill, I. W. Wainer, S. A. Barkan, *J. Liq. Chromatogr.*, 9 (1986) 641.
- 5 S. Allenmark, *J. Liq. Chromatogr.*, 9 (1986) 425.
- 6 W. H. Pirkle and M. H. Hyun, *J. Chromatogr.*, 322 (1985) 287.
- 7 W. H. Pirkle, T. C. Pochapsky, G. S. Mahler, D. E. Corey, D. S. Reno and D. M. Alessi, *J. Org. Chem.*, 51 (1986) 4991.
- 8 W. H. Pirkle and T. C. Pochapsky, *J. Am. Chem. Soc.*, 109 (1987) 5975.
- 9 W. H. Pirkle, J.-P. Chang and J. A. Burke, III, *J. Chromatogr.*, 479 (1987) 377-86.
- 10 W. H. Pirkle and J. A. Burke, III, *Chirality*, 1 (1989) 57.
- 11 W. H. Pirkle, M. H. Hyun, and B. Bank, *J. Chromatogr.*, 316 (1984) 585.
- 12 W. H. Pirkle, M. H. Hyun, A. Tsipouras, B. C. Hamper and B. Bank, *J. Pharm. Biomed. Anal.*, 2 (1985) 173.
- 13 W. H. Pirkle, J. A. Burke, III and S. R. Wilson, *J. Am. Chem. Soc.*, 111 (1989) 9222-9223.
- 14 R. S. Cahn, C. K. Ingold and V. Prelog, *Experientia*, 12 (1956) 81.
- 15 W. H. Pirkle and R. S. Readnour, *Anal. Chem.*, 63 (1991) 16-20.

Effects of stationary phase ligand density on high-performance ion-exchange chromatography of proteins

Danlin Wu^{*,*} and Rodney R. Walters^{☆☆}

Department of Chemistry, Iowa State University, Ames, IA 50011 (USA)

(First received February 14th, 1991; revised manuscript received January 16th, 1992)

ABSTRACT

Cation-exchange matrices with ligand densities from 10 to 500 $\mu\text{mol/g}$ were prepared by reaction of diglycolic anhydride with diol-bonded silica. Lysozyme and cytochrome *c* were isocratically eluted from these columns under various conditions. The data was used to examine a retention model of proteins in which the slope (*Z* number) of a plot of $\log k'$ vs. $\log (1/\text{sodium ion activity})$ was assumed to represent the number of points of binding between the protein and the matrix. As expected from the model, the *Z* number increased as the ligand density of the matrix increased. However, many qualitative and quantitative deviations from the model were also found, some of which may have been due to heterogeneity of the distribution of the ion-exchange sites on the matrix. An interesting observation was a change in elution order of lysozyme and cytochrome *c* as the ligand density changed; however, this may not have much practical benefit dual to the large band-broadening observed at low ligand densities.

INTRODUCTION

Ion-exchange chromatography is a powerful separation tool for the isolation of proteins. This method has seen rapid growth over the past decade [1,2] and numerous stationary phase materials have been developed to optimize the chromatographic performance [3-8]. The main advantage is the high recovery of proteins in terms of both mass and biological activity. Although the methodology has been frequently applied and the experimental conditions (*i.e.*, mobile phase velocity, pore diameter, column length, salt composition, pH, temperature, loading capacity, etc.) have been extensively investigated [9-13], little is known about the underlying retention mechanism and the factors that contribute to the selectivity.

In a proposed retention model for ion-exchange chromatography of proteins, Kopaciewicz *et al.* [14]

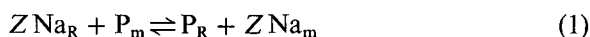
suggested that as a protein comes into contact with the chromatographic stationary phase, only a fraction of the protein surface covers the binding area and that the retention is exponentially related to a parameter called the *Z* number, which is the number of binding sites on a protein surface interacting with the stationary phase. Since the number and distribution of charged groups on the surface of a macromolecule are fixed as well as its chromatographic binding domain, it follows that the *Z* number and retention should be mainly dependent on the stationary phase ligand density. Consequently, the ligand density should have a profound effect on the binding mechanism and chromatographic behavior of macromolecules. For example, in hydrophobic interaction chromatography, the protein retention was found to increase with an increase in ligand density [15]. There have been very few published reports describing the effect of ligand density on the performance of ion-exchange chromatography of proteins. This has primarily been due to the unavailability of supports covering a sufficiently wide range of ligand density.

We have developed a technique [16] for the

* Present address: BASF Corporation, 26 Davis Drive, Research Triangle Park, NC 27709, USA.

** Present address: Drug Metabolism Research, The Upjohn Company, Kalamazoo, MI 49001, USA.

preparation of silica-based supports of variable ligand density by means of controlled reaction of anhydrides with diol-bonded silica. By using this technique, surface ligand densities ranging from a few percent to complete monolayer coverage have been obtained. In this study, cation-exchange supports of different ligand densities were prepared by reaction with diglycolic anhydride. Chromatographic behavior of proteins was subsequently examined as a function of ligand density. The Z number, based on a displacement model proposed by Boardman and Partridge in 1955 [17], was used to characterize retention. The equilibrium of sodium ions, Na^+ , and proteins, P^{n+} , between the resin (R) and mobile phase (m) can be represented by the equation:



where Z is the number of sodium ions displaced when one protein is adsorbed. The mass action expresses the equilibrium as:

$$\frac{[\text{P}_R][\text{Na}_m]^Z}{[\text{P}_m][\text{Na}_R]^Z} = K \quad (2)$$

where K is the equilibrium constant; P_R and P_m are proteins in resin phase and mobile phase; Na_m and Na_R are sodium ions in mobile phase and resin phase, respectively. The equation can be further reduced to the following form:

$$\log k' = Z \log 1/[\text{Na}] + \text{constant } (I) \quad (3)$$

By plotting log capacity factor (k') vs. $\log 1/[\text{Na}]$, Z is thus obtained. The retention model has been widely applied to various high-performance liquid chromatographic (HPLC) systems. For example, Parenter and Wetlaufer [18] were able to demonstrate using cation-exchange chromatography that denatured α -chymotrypsinogen A exhibited a larger Z value than native protein even though it had a shorter retention time. The same authors also measured the log-log slope to fit a gradient elution retention model [19], which made it possible to relate the gradient and isocratic elution retention data. Melander *et al.* [20] used the log-log plot to fit a retention model that takes into account both the ionic and hydrophobic interaction. They also used the same plot to probe the ligand density [20]. The displacement model was evaluated in this study by using protein retention as a function of ligand density in conjunction with Z number.

EXPERIMENTAL

Reagents

Cytochrome *c* (equine) and lysozyme (egg) were from Sigma (St. Louis, MO, USA). Diglycolic anhydride (DGA), benzylamine, and diglycolic acid were from Aldrich (Milwaukee, WI, USA). Nucleosil 300-5 (surface area: $100 \text{ m}^2/\text{g}$) was from Alltech (Deerfield, IL, USA). Tetrahydrofuran (THF), ethanol and diglycolic acid were purified as described previously [16].

Instrumentation

A Model 344 gradient liquid chromatograph (Beckman, Berdeley, CA, USA) was used. Absorbance was monitored at either 280 nm (proteins and acetone) or 262 nm (benzylamine) by a V^4 variable-wavelength absorbance detector (ISCO, Lincoln, NE, USA). Data were collected and processed on an Apple IIe computer via an ADALAB interface board (Interactive Microware, State College, PA, USA).

Methods

All of the carboxylate cation-exchange supports were prepared according to a previously published procedure [16]. The ligand density was quantitated by a ferric hydroxamate ester assay [21]. Briefly, samples containing 0.2–1 μmol of ester in 0.5 ml of distilled ethanol were treated with 0.25 ml of alkaline hydroxylamine reagent and sonicated for 5 min. After 1 h of reaction at room temperature, 4.0 ml of ferric reagent was added followed by 2 min of sonication and an additional 5-min reaction at room temperature. The silica was removed by centrifugation prior to the final absorbance measurement at 530 nm. Dimethyl diglycolate was used as standard.

The carboxylated support was suspended in 0.5 M sodium sulfate and packed into $100 \times 4.1 \text{ mm}$ I.D. columns at 5000 p.s.i. using upward-flow method [22].

Chromatography

The weak mobile phase (A) was 0.01 M sodium phosphate (pH 6.0) and the strong mobile phase (B) was 0.01 M sodium phosphate–0.2 M sodium sulfate (pH 6.0). The sodium concentration was adjusted by premixing A and B in the desired ratio. Chromatography was performed isocratically at room temper-

ature using a flow-rate of 1 ml/min. Aliquots of 10 μl of either a 5 mg/ml protein solution or 10 μM benzylamine solution were injected. In the experiments where k' was measured, the void volume was individually determined for each column by injecting 10 μl of 1% acetone. The experimental error of the Z number measurement was estimated to be $\pm 5\%$ to $\pm 10\%$ depending on the magnitude of the Z number.

The protein adsorption capacities were determined by continuously applying 0.5 mg/ml lysozyme to 6.2 \times 2.1 mm I.D. columns. The breakthrough curves were corrected for the void volume.

The statistical moments were found by using the modified $B/A_{0.5}$ method, where $B/A_{0.5}$ is the peak width ratio at half height [23].

The activity coefficient of sodium ions was not constant over the concentration range studied. This was especially true at high salt concentrations (*e.g.* when % $B > 50\%$), where a two-fold change in % B led to a 15% change in the activity coefficient [24]. To avoid errors due to this, the activity of the ions was used in all calculations.

RESULTS AND DISCUSSION

Ligand quantitation and lysozyme binding capacity

The ligand density was quantitated by means of assay of the ester groups formed when diglycolic anhydride reacted with the diol groups of the matrix [16]. To confirm the assay, k' was measured as a function of ligand density using benzylamine as the probe molecule (eluted isocratically at pH 6.0). Since the k' value of a monovalent molecule like benzylamine should be linearly dependent on the number of ligands in the column, the linearity of a plot of k' vs. ligand density serves to confirm the validity of the ligand density measurements. A linear relationship was observed (Fig. 1) except at the highest ligand density, indicating that the results of ester assay were consistent with retention, at least in the low to intermediate ligand density region of primary interest.

The lysozyme binding capacity vs. ligand density was measured using breakthrough curves. Blank columns containing either no packing material or diol-bonded silica were used to detect the possible presence of nonspecific adsorption. The ion-exchange capacity so obtained was virtually negligible.

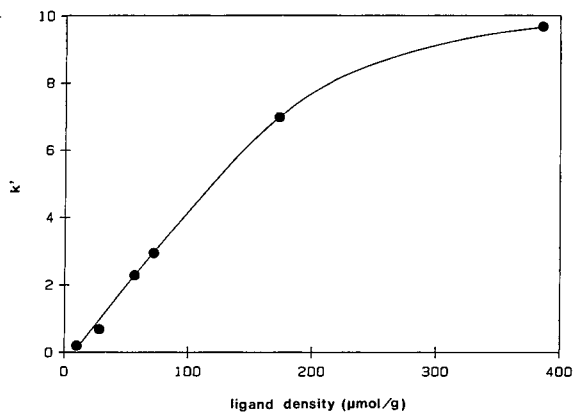


Fig. 1. Ligand density dependence of k' of benzylamine obtained with phosphate buffer, pH 6.0.

This was probably due to the hydrophilic nature of diol phase and the complete coverage of silanol sites. For carboxylated supports, lysozyme capacity was measured after previously saturating the column several times to remove any irreversible adsorption sites. Fig. 2 presents the lysozyme capacity as a function of ligand density. The shape of the curve was substantially different from that seen for a small molecule (Fig. 1). The slope of the curve changed sharply at a ligand density of approximately 70 $\mu\text{mol/g}$. Below that point, the binding capacity increased sharply, while above that point the curve flattened. A calculation of the average distance between the ligands (Table I) reveals that at ligand density of 72 $\mu\text{mol/g}$, the distance between two nearest ligands (15 \AA) was less than the diameter of

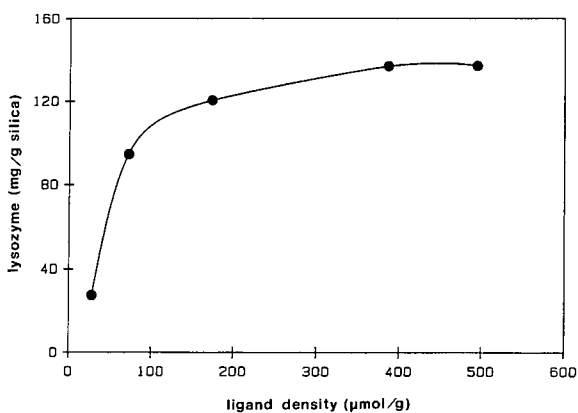


Fig. 2. Ion-exchange capacity for lysozyme as a function of the ligand density.

TABLE I
DISTANCE BETWEEN TWO NEAREST LIGANDS AS A
FUNCTION OF LIGAND DENSITY

Ligand Density ($\mu\text{mol/g}$)	Distance between two nearest ligands (\AA) ^a
10	41
28	24
72	15
173	9.8
386	6.6
494	5.8

^a Calculated based on: $S = (A/CN)^{1/2}$, where S is the average distance between two nearest ligands, C is the ligand density, N is Avogadro's number and A is the surface area given by manufacturer.

lysozyme (*ca.* 20 \AA), enabling the protein to form multiple bonds with the stationary phase. Below 28 $\mu\text{mol/g}$, the two closest ligands averaged 24 \AA or more apart, limiting the protein binding to a single ligand. It appeared from Fig. 2 that once the stationary phase ligand density passed the threshold of multiple binding (*ca.* 70 $\mu\text{mol/g}$) further increases in ligand density did not have much effect on the binding capacity. The maximum binding capacity in Fig. 2 was approximately 28% of a theoretical monolayer of lysozyme. A similar relationship between the protein binding capacity and ligand density was also observed by Alpert and Regnier [25] when hemoglobin was bound to polyethyleneimine-coated (CPE) silica.

Z number and stationary phase heterogeneity

The Z numbers of lysozyme and cytochrome *c*, based on the model proposed by Boardman and Partridge [17], were measured as a function of ligand density and ionic strength, as shown in Fig. 3. The Z number initially increased rapidly with ligand density, but leveled off in the intermediate ligand density region, in a manner similar to that observed in the lysozyme binding capacity measurement of Fig. 2.

The lowest value of the Z number was about 4 at the lowest ligand density (Fig. 3). One would have expected the Z number to decline to 1 at low ligand density, *i.e.*, the protein should have been able to interact with only one ion-exchange site when the spacing of the sites was larger than the diameter of

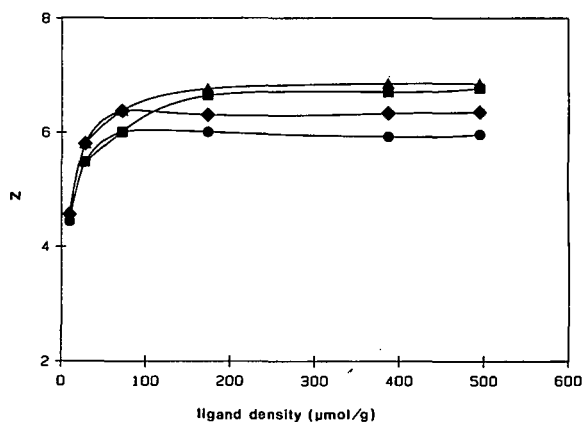


Fig. 3. The Z number of cytochrome *c* (●, ■) and lysozyme (▲, ◆) on various ligand density supports, as measured in the low ionic strength range (▲, ■) and high ionic strength range (◆, ●). For high ionic strength, columns of 100 × 4.1 mm I.D. were used. Other conditions refer to Experimental section.

the protein. Possible reasons for this discrepancy include (a) the irregular and microporous surface of the support, formed from 1–100 nm silica spheres [26], which could interact with several sides of the protein molecule at once and thus increase the apparent protein size, and (b) a heterogeneity in ion-exchange site distribution which could result in clusters of sites, with the Z number primarily determined by the stronger multivalent interactions.

It is noted that the Z numbers obtained in this study were typically non-integer values. This was probably a result of (a) partial ionization of various basic groups in the proteins, which created varying number of charges among individual molecules, giving rise to statistically averaged fractional values; and (b) heterogeneous distribution of ligands on silica surface, leading to an averaging of Z values of protein binding to different locations. Non-integer Z values have been observed with other proteins, *e.g.*, β -lactoglobulin on an anion-exchange column [14].

Z number and ionic strength

Although it is a common observation that an increase in salt concentration would decrease protein retention, it was not clear whether the process involved any change in Z value. In this study, the Z number was measured in different regions of ionic strength, as shown in Fig. 3 and Table II. A

TABLE II
Z NUMBER AS A FUNCTION OF IONIC STRENGTH^a

%B ^a	μ (ionic strength) ^b	Z(lysozyme)	Z(cytochrome c)
60-80	0.37-0.48	6.34	5.93
30-60	0.19-0.37	6.86	6.71
25-35	0.16-0.22	8.59	7.72

^a Range of %B used in the Z measurement.

^b Obtained from a 386 $\mu\text{mol/g}$ column at 1.0 ml/min. $\mu = 1/2 \sum [i]Z_i^2$, where [i] is the molar concentration of an ion, and Z_i is the charge of that ion.

moderate increase in the Z number was observed at various ligand densities when the ionic strength was decreased (Fig. 3), especially on high ligand density columns where a strong mobile phase is usually applied, suggesting that the Z number is ionic strength dependent.

Z number and retention

Although for individual proteins and stationary phases the Z number is determined from the slope of a log-log plot, the model does not predict how the retention (k') should relate to the Z number across a range of matrices of different ligand density. As shown in Fig. 4 for lysozyme and cytochrome c, retention clearly increased with an increase in the Z number, but other parameters must also have affected retention since the curves for the two proteins

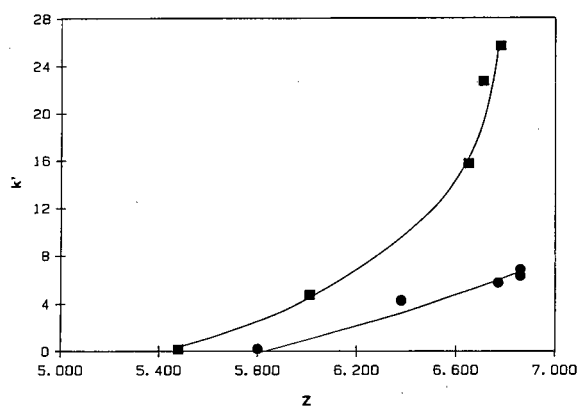


Fig. 4. Capacity factors obtained from isocratic elution of varying ligand density matrices with 50% B vs. the Z number measured in the %B range of 30% to 60% for cytochrome c (■) and lysozyme (●).

were not superimposable. Thus, the number of apparent points of interaction between the protein and the stationary phase must not be the only factor affecting the strength of those interactions.

Additional evidence that the Z number is only one component of retention is indicated by the log-log plot shown in Fig. 5 for lysozyme and cytochrome c on three stationary phases of different ligand densities. Although the slopes, *i.e.*, Z number, of these plots are all similar, note that there is an elution order reversal of the two proteins as the ligand density increased. At a ligand density of about 70 $\mu\text{mol/g}$, both proteins coeluted. Above this density, lysozyme eluted first; below this density, cytochrome c eluted first. The elution order reversal is better represented by the intercept term (I) of eqn. 3, as shown by a plot of I vs. Z (Fig. 6).

The divergence between the Z and retention (k') was also observed by Parenter and Wetlaufer [18] in a denaturation study of α -chymotrypsinogen A, where the denatured protein was found to exhibit a larger Z value but a much shorter retention time.

Band broadening and resolution

In principle, ligand density changes would provide a very useful means of altering selectivity, as shown in Fig. 6. However, it was observed that band-broadening was large at low ligand density, as shown in Fig. 7 for cytochrome c. The medium-to-high density phases exhibited much less broadening.

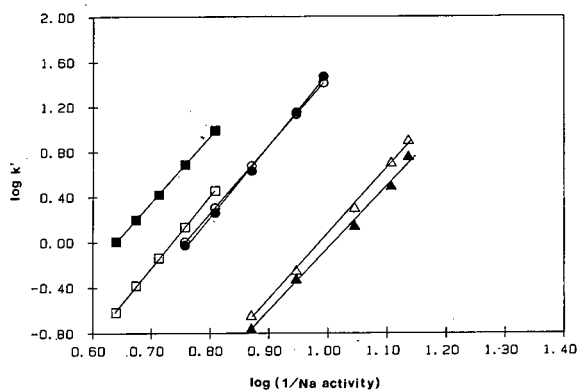


Fig. 5. A plot of the logarithm of capacity factor vs. logarithm of the reciprocal of sodium activity for cytochrome c (▲, ○, ■) and lysozyme (△, ●, □) on supports of ligand density 28 $\mu\text{mol/g}$ (△, ▲), 72 $\mu\text{mol/g}$ (○, ●) and 386 $\mu\text{mol/g}$ (□, ■). Comparison of k' values at different ligand densities shows elution order reversal.

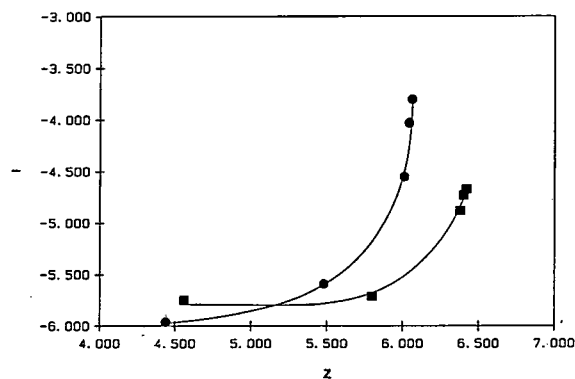


Fig. 6. Intercept I as a function of the Z number for cytochrome c (●) and lysozyme (■).

Lysozyme behaved in a similar manner. The problem was not a result of poor column packing since benzylamine yielded low values for the plate height on both low and high ligand density phases. The possibility of overloading at low ligand density, which could lead to severe tailing, was ruled out by the observation that the elution profile was not affected by a reduction of sample size. Factors which might have affected the band-broadening include heterogeneity of ligand distribution, which presumably is more severe at low ligand density, or changes in the adsorption/desorption rate constants due to changes in the electrical double layer thickness. In any case, the higher ligand density matrices exhibited the best chromatographic resolution.

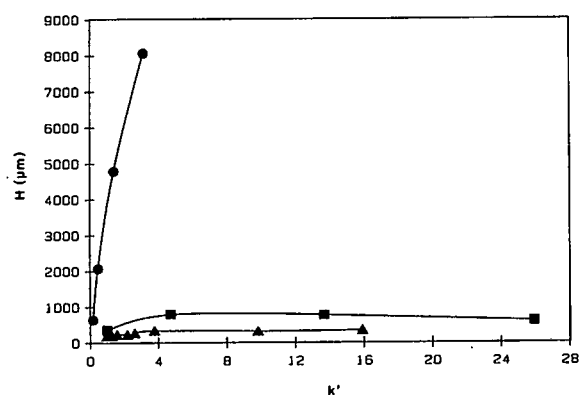


Fig. 7. Plate height vs. capacity factor for cytochrome c on supports of ligand density $28 \mu\text{mol/g}$ (●), $72 \mu\text{mol/g}$ (■) and $386 \mu\text{mol/g}$ (▲). The k' was varied by varying elution salt concentration. The data were derived from those in Fig. 5 by measuring plate height at each k' obtained.

TABLE III

EFFECT OF PHOSPHATE VS. ACETATE BUFFER ON CAPACITY FACTOR OF CYTOCHROME c

%B	k' (phosphate)	k' (acetate)	% change in k'
30	477	612	21.9
40	79.5	115	30.9
50	33.6	37.4	10.1
60	11.2	16.2	30.5

Phosphate bound to cytochrome c

Phosphate is known to bind to cytochrome c and alter its retention on cation exchangers [27]. To characterize the chromatographic behavior of cytochrome c in the presence of phosphate, phosphate and acetate buffers of the same concentration and pH were used to measure the Z number and k' of cytochrome c at a ligand density of $386 \mu\text{mol/g}$. It was found that the Z numbers obtained from these different buffers were essentially the same (phosphate, 6.71; acetate, 6.69) but the k' value was markedly greater in the case of acetate, as shown in Table III. The fact that the Z number did not change with k' further demonstrates that there is no inherent correlation between protein retention (k') and the Z number, even for a given protein.

ACKNOWLEDGEMENT

This work was supported by the National Science Foundation under the Grant CHE-8305057.

REFERENCES

- 1 F. E. Regnier, *Meth. Enzymol.*, 91 (1983) 137.
- 2 F. E. Regnier and K. M. Gooding, *Anal. Biochem.*, 103 (1980) 1.
- 3 A. J. Alpert, *J. Chromatogr.*, 266 (1983) 23.
- 4 A. K. Roy, A. Burgum and S. Roy, *J. Chromatogr. Sci.*, 22 (1984) 84.
- 5 A. J. Alpert and F. E. Regnier, *J. Chromatogr.*, 185 (1979) 375.
- 6 G. Vanecek and F. E. Regnier, *Anal. Biochem.*, 121 (1982) 156.
- 7 J. B. Crowther, P. Griffiths, S. D. Fazio, J. Magram and R. A. Hartwick, *J. Chromatogr. Sci.*, 22 (1984) 221.
- 8 W. Kopaciewicz, M. A. Rounds and F. E. Regnier, *J. Chromatogr.*, 318 (1985) 157.
- 9 K. M. Gooding and M. N. Schmuck, *J. Chromatogr.*, 266 (1983) 633.

- 10 G. Vanecek and F. E. Regnier, *Anal. Biochem.*, 109 (1980) 345.
- 11 T. Tomono, H. Ikeda and E. Tokunaga, *J. Chromatogr.*, 266 (1983) 39.
- 12 R. A. Barford, B. J. Sliwinski and H. L. Rothbart, *J. Chromatogr.*, 185 (1985) 393.
- 13 K. M. Gooding and M. N. Schmuck, *J. Chromatogr.*, 296 (1984) 321.
- 14 W. Kopaciewicz, M. A. Rounds, J. Fausnaugh and F. E. Regnier, *J. Chromatogr.*, 266 (1983) 3.
- 15 J. L. Fausnaugh, L. A. Kennedy and F. E. Regnier, *J. Chromatogr.*, 317 (1984) 141.
- 16 M. E. Landgrebe, D. Wu and R. R. Walters, *Anal. Chem.*, 58 (1986) 1607.
- 17 N. K. Boardman and S. M. Partridge, *Biochem. J.*, 59 (1955) 543.
- 18 E. S. Parenter and D. B. Wetlaufer, *J. Chromatogr.*, 314 (1984) 337.
- 19 E. S. Parenter and D. B. Wetlaufer, *J. Chromatogr.*, 355 (1986) 29.
- 20 W. R. Melander, Z. El Rassi and Cs. Horváth, *J. Chromatogr.*, 469 (1989) 3.
- 21 S. Siggia and J. G. Hanna, *Quantitative Organic Analysis*, Wiley, New York, 4th ed., 1979, pp. 172-183.
- 22 L. R. Snyder and J. J. Kirkland, *Introduction to Modern Liquid Chromatography*, Wiley, New York, 2nd ed., 1979, p. 216.
- 23 D. Anderson and R. R. Walters, *J. Chromatogr. Sci.*, 22 (1984) 353.
- 24 J. S. Fritz and G. H. Schenk, *Quantitative Analytical Chemistry*, Allyn & Bacon, Boston, 4th ed., 1979.
- 25 A. J. Alpert and F. E. Regnier, *J. Chromatogr.*, 185 (1979) 375.
- 26 K. K. Unger, *Porous Silica*, Elsevier, Amsterdam, New York, 1979, p. 4.
- 27 D. L. Brautigan, S. Ferguson-Miller and E. Margoliash, *J. Biol. Chem.*, 253 (1978) 130.

CHROM. 24 022

Separon HEMA modified for immobilized metal ion affinity chromatographic separation of proteins

P. Šmídl, J. Plicka and I. Kleinmann*

Institute for Research, Production and Application of Radioisotopes, Radiova 1, 102 27 Prague 10 (Czechoslovakia)

(First received April 22nd, 1991; revised manuscript received December 30th, 1991)

ABSTRACT

Two sorbents for high-performance immobilized metal ion affinity chromatography were synthesized on the basis of Separon HEMA methacrylate matrices. Iminodiacetic acid was covalently bound on the surface of the sorbents by the means of two spacers of different length. In addition to the fact that both sorbents could be loaded with similar amounts of Cu^{2+} ions, their chromatographic properties were different, which was demonstrated by the separation of four globular proteins.

INTRODUCTION

Numerous proteins are able to form coordinate-covalent bonds with unoccupied coordination sites of metals via electron donor groups resident on their molecular surface. This ability was reported by Porath *et al.* [1] in the development of immobilized metal ion affinity chromatography (IMAC). In this method, the metal ion is immobilized on the surface of the sorbent via a chelating ligand. The ligand was iminodiacetic acid (IDA) covalently bonded to the epoxy-derived Sepharose [1]. This chelating ligand and reaction scheme have been used by most previous workers [2–9]. There are other methods for the synthesis of IDA carriers [10–13], but they are more complicated and usually do not provide more effective sorbents.

IDA has been the most frequent chelating ligand in IMAC; others have been used only rarely [2,11,14]. On the other hand, the choice of immobilized metal ions is much wider. Cu^{2+} , Ni^{2+} , Fe^{3+} and especially Zn^{2+} have been used for the purification of proteins and peptides [2–4,6–8,13–26], but a number of other metals have also been examined [6,8]. Sorbents for IMAC have been synthesized on the basis of hydrophilic organic matrices [1,2,4–10] or silica gel [3,11–13]. In high-performance (HP)

IMAC, silica gel or sufficiently rigid organic sorbents (Superose, TSK gel PW and some others) are used. Whereas the former offer better efficiency, the latter are much more hydrolytically stable and permit work even with alkaline buffered eluents.

Elution of adsorbed proteins is carried out using a pH gradient (sometimes increasing [21] but mainly decreasing [15–20,22,24–26]) or by increasing the concentration of amino acids, imidazole and ammonia in the eluent [2,4,22,23,27–29].

In addition to the separation and purification of proteins and peptides, IMAC can serve as a valuable tool in the study of their structure and topography [5,13,17,30]. In addition, IMAC sorbents can be used as regenerable carriers for immobilization of enzymes in biotechnology [31].

In this paper, we report the synthesis of two sorbents for HP-IMAC, based on Separon HEMA microparticulate hydrophilic methacrylate sorbents. The sorbents differed in the spacer arm length and in the hydrophilicity of the matrix.

The aim of this work was to confirm if the modification of Separon HEMA-BIO 1000 can provide a better matrix for IDA attachment than Separon HEMA 1000 E. In addition, we wished to verify whether the separation of proteins on the IMAC sorbents prepared could be influenced by

ionic or hydrophobic interactions when the concentration of sodium chloride recommended in the literature was used.

EXPERIMENTAL

Sorbents

Separon HEMA 1000 E and HEMA-BIO 1000 (this sorbent was indicated as Separon HEMA 1000 H in a previous paper [32]) were purchased from Tessek (Prague, Czechoslovakia). Both sorbents were declared by the producer to have a molecular weight exclusion limit 10^6 and a wide pore-size distribution. The particle size is 10 μm .

Chemicals

Iminodiacetic acid (IDA) was obtained from Janssen Chimica (Beerse, Belgium), 1,4-butanediol diglycidyl ether (BUDGE) from Aldrich-Chemie (Steinheim, Germany), imidazole from Serva (Heidelberg, Germany) and ethylenediaminetetraacetic acid disodium salt (EDTA), NaCl, $\text{Na}_2\text{HPO}_4 \cdot \text{H}_2\text{O}$, and $\text{CuSO}_4 \cdot 5\text{H}_2\text{O}$ from Lachema (Brno, Czechoslovakia). Chicken egg white lysozyme (Lys), bovine pancreatic ribonuclease-A (RNase) and horse skeletal muscle myoglobin (Myo) were purchased from Sigma (St. Louis, MO, USA) and human transferrin (Tra) from Serva.

Chromatography

All experiments were performed with a Model 2150 high-performance liquid chromatographic pump, a low-pressure gradient mixer, a Model 2152 LC controller, a C6W-HC injector, a Model 2140 rapid spectral detector and a Data Print computer from Pharmacia-LKB (Bromma, Sweden). Sorbents were packed into stainless-steel columns (100 \times 4 mm I.D.). A pressure of 2.5 MPa was maintained during the whole operation.

The loading of sorbents with copper was done by washing the column successively with 5 ml of 0.05 *M* EDTA, 10 ml of water, 7.5 ml of 0.1 *M* CuSO_4 solution and 10 ml of water. The flow-rate was 0.5 ml/min.

Synthesis of sorbents

Separon HEMA-BIO 1000-BUDGE. This epoxy-activated product was prepared by a slightly modified version of the method published by Porath *et al.*

[1]. A 5-g amount of Separon HEMA-BIO 1000 was suspended in a mixture of 18 ml of 0.4 *M* NaOH, 18 ml of BUDGE and 25 mg of NaBH_4 . The suspension was stirred for 8 h at 25°C, then washed with 300 ml of water and 50 ml of acetone and dried overnight at 35°C.

Separon HEMA 1000 E-IDA. Two reaction conditions were applied to bond IDA to the epoxy-activated sorbent Separon HEMA 1000 E.

Reaction scheme I is Porath's method [1]. A 4.5-g amount of IDA disodium salt and 80 mg of NaBH_4 were diluted in 83 ml of 2 *M* Na_2CO_3 , then 5 g of Separon HEMA 1000 E were suspended in this solution and stirred for 8 h at 65°C. The suspension was subsequently kept at 65°C overnight, then the sorbent was filtered, washed with 0.1 *M* NaOH, water and acetone and dried for 6 h at 65°C.

In reaction scheme II, 8.7 g of IDA and 4.1 g of NaOH were diluted in 23 ml of water and the pH was adjusted to 10.0 with concentrated H_3PO_4 . A 5-g amount of the matrix mentioned above was suspended in this solution and the suspension was kept at 65°C for 24 h. The suspension was shaken vigorously at 15-min periods for the first 8 h. Washing and drying were carried out as in reaction scheme I, then the sorbents were suspended in 100 ml of a 1 *M* solution of ethanolamine and kept for 8 h at 65°C with occasional shaking.

Separon HEMA-BIO 1000-Budge-IDA. This epoxy-activated matrix was treated by both reaction schemes described for Separon HEMA 1000 E.

Determination of content of epoxy groups in matrices

The method published by Pribyl [33] was used. A 0.2-g amount of sorbent was suspended in 20 ml of a 0.5 *M* solution of tetrabutylammonium bromide in glacial acetic acid and titrated with a 0.1 *M* solution of perchloric acid in glacial acetic acid. The equivalence point was determined potentiometrically.

Analysis of synthesized sorbents

The content of IDA in the prepared sorbents was determined by elemental analysis for nitrogen. Its loading capacity for copper was determined in the following way: 0.2–0.3 g of dry IDA sorbent was suspended in 25 ml of 0.05 *M* $\text{CuSO}_4 \cdot 5\text{H}_2\text{O}$ solution and mixed for 30 min. The sorbent was then filtered and washed with 100 ml of 0.1 *M* acetate buffer (pH 4.5) containing 0.5 *M* NaCl and with 50

ml of water. Cu^{2+} ions were then eluted with 100 ml of 0.05 M EDTA and measured spectrophotometrically at 735 nm.

RESULTS

Two synthesis routes, outlined in Fig. 1, were used for the preparation of IDA sorbents. The reaction of IDA with epoxy-activated matrices was carried out under strongly alkaline conditions with 2 M Na_2CO_3 (reaction scheme I) or at pH 10.0 (reaction scheme II). The results are summarized in Table I. The concentration of epoxy groups in Separon HEMA 1000 E (henceforth referred to as HEMA E) was 850 $\mu\text{mol/g}$ of dry material (this value is declared by the producer) and Separon HEMA-BIO 1000-BUDGE (henceforth referred to as HEMA-BUDGE) contained 520 $\mu\text{mol/g}$ of glycidyl groups (this value was determined by the method described under Experimental).

The ability of both sorbents for aminolysis was tested by reaction with a large excess of a 1 M solution of ethanolamine (EA) at 65°C for 8 h. The molar content of nitrogen, equal to the proportion of converted epoxy groups, was determined by elemental analysis. A small increase in mass due to EA attachment was considered in the calculations.

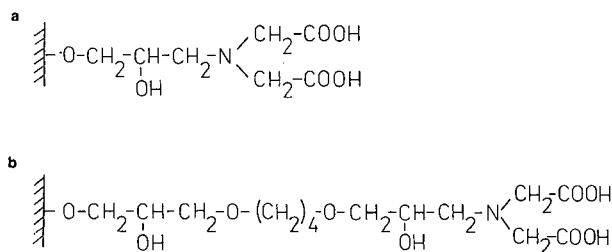


Fig. 1. Structures of (a) Separon HEMA 1000 E-IDA and (b) Separon HEMA-BIO 1000-BUDGE-IDA.

The average values for nitrogen in three parallel experiments were 660 $\mu\text{mol/g}$ for HEMA E and 425 $\mu\text{mol/g}$ for HEMA-BUDGE. It is probable that hydrolysis of epoxy groups proceeded simultaneously because no epoxy groups were determined after EA treatment. The hydrolysis of epoxy groups with 2 M Na_2CO_3 was also followed. No epoxy groups were determined after treatment for 24 at 65°C. The content of IDA was determined by elemental analysis for nitrogen in the same way as for EA.

Apart from the content of glycidyl groups, the main difference between the matrices discussed here is that these groups are attached directly to the

TABLE I

INFLUENCE OF MATRIX AND REACTION SCHEME ON SOME SORBENT PARAMETERS

No.	Sorbent ^a	Reaction scheme	Content of epoxy groups in matrix ($\mu\text{mol/g}$)	Content of N after reaction with IDA ($\mu\text{mol/g}$)	Content of N after reaction with EA ^b ($\mu\text{mol/g}$)	Content of Cu ($\mu\text{mol/g}$)
1	Separon HEMA 1000 E-IDA I	I	850	Below detection limit	Below detection limit	11
2a	Separon HEMA 1000 E-IDA II	II	850	332	610	135
2b	Separon HEMA 1000 E-IDA II	II	850	332	334	137
3	Separon HEMA-BIO 1000-BUDGE-IDA I	I	520	180	184	121
4	Separon HEMA-BIO 1000-BUDGE-IDA II	II	520	220	390	147

^a All data are averages of two parallel experiments for HEMA-BUDGE and three parallel experiments for HEMA E.

^b The treatment with ethanolamine was performed after the reaction with IDA.

surface in HEMA E whereas they are situated at the end of a relatively long spacer in HEMA-BUDGE.

It is interesting that IDA was bonded on HEMA-BUDGE under the conditions of reaction scheme I, whereas HEMA E did not bind any IDA if 2 M Na₂CO₃ was applied (see sorbents 1 and 3, Table I). The epoxy groups present in the matrices were hydrolysed during the reaction in 2 M Na₂CO₃. No reaction with EA was observed (see Table I).

When reaction scheme II was applied, almost the same proportion of epoxy groups was converted into IDA moieties (about 56%) in both matrices. The subsequent reaction with EA decomposed non-converted glycidyl groups. The final content of nitrogen (see sorbents 2 and 4, Table I) was lower than that obtained by the direct reaction with EA, probably owing to the hydrolysis proceeding during reaction with IDA. It seems that steric effects do not play a significant role in the conversion of epoxides into IDA groups under the given conditions. Even an extended reaction time (48 h) did not increase the degree of conversion with either sorbent.

On the other hand, steric effects can play a role in the loading of sorbents with Cu²⁺. HEMA-BUDGE carrying IDA at the end of the spacer arm is capable of retaining a relatively larger amount of metal (67% of IDA groups) than HEMA E (42% of IDA groups), where the original glycidyl groups were attached directly to the surface of the matrix (see sorbents 2a, 3 and 4, Table I). Fleminger *et al.* [34] discussed a similar property of bonded epoxy groups.

The situation was different when reaction scheme I was applied. Whereas the content of IDA was only 18% lower in comparison with reaction scheme II when using HEMA-BUDGE, virtually no IDA was found after the reaction with HEMA E (see sorbent 1, Table I). The fact that no IDA was bound and no residual epoxy groups were present after the reaction can be explained only by the preferred hydrolysis of epoxy groups during the reaction with 2 M Na₂CO₃. The glycidyl groups attached directly to the surface of the matrix are probably less accessible for IDA than the same groups situated at the end of the spacer in HEMA-BUDGE and, in addition, the hydrolysis is much faster in 2 M Na₂CO₃ than at pH 10.0. Hence it is possible that virtually all epoxy groups of HEMA E were hydrolysed before they could be converted into IDA groups.

The question of whether EA bonded during the decomposition of residual epoxy groups could influence the loading of the sorbent with copper was also solved. The sorbent prepared according to reaction scheme II was treated partly with EA and partly with Na₂CO₃ after the reaction with IDA to decompose residual glycidyl groups. No difference was found in the loading capacity with copper (see sorbents 2a and 2b, Table I).

An additional difference between the two types of IDA sorbents is in the "effective" loading capacity. If the number of micromoles of IDA present on the sorbent is the limiting value for Cu²⁺ content, then HEMA E retained about 49% of this capacity (see sorbents 2a and 2b, Table I) whereas for HEMA-BUDGE this value was about 67% (see sorbents 3 and 4, Table I). This means that not all IDA ligands chelated Cu²⁺ ions with the same strength and some metal ions were washed out with acidic buffer or not all IDA ligands are accessible to Cu²⁺ ions [34].

To compare the abilities of the two sorbents in the chromatography of proteins, they were used for the separation of a model mixture of four globular proteins under the conditions optimized for each of the sorbents individually. Although the amount of Cu²⁺ chelated was nearly identical for both columns, substantial differences were observed. The resolution of proteins was much better on HEMA-BUDGE and they eluted as sharper peaks (see Figs. 2 and 3).

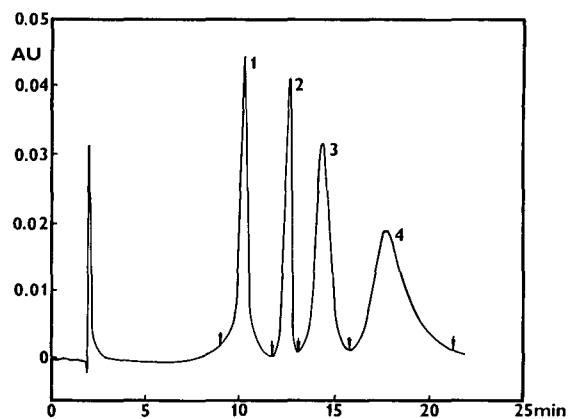


Fig. 2. Separation of model mixture on Separon HEMA 1000 E-IDA-Cu (see sorbent 2a in Table I). Column, 100 × 4 mm I.D.; flow-rate, 0.5 ml/min; gradient from 2 to 25 mM imidazole in 0.02 M Na₂HPO₄-0.5 M NaCl (pH 7.0) in 20 min. Proteins: 1 = Lys; 2 = RNase; 3 = Myo; 4 = Tra. A 50-μg amount of each protein was loaded. Absorbance was measured at 280 nm.

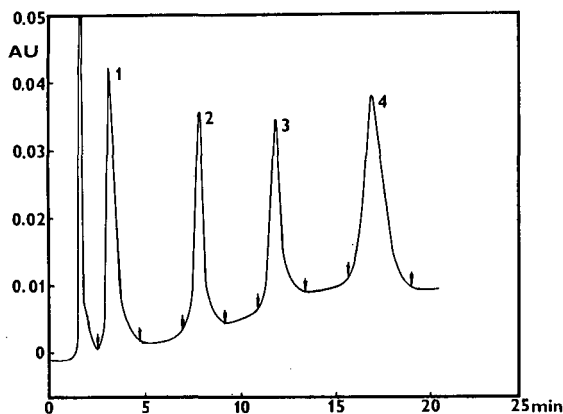


Fig. 3. Separation of model proteins on separon HEMA-BIO 1000-BUDGE-IDA-Cu (see sorbent 4 in Table I). For proteins and conditions, see Fig. 2.

In addition to the chromatographic resolution, the reproducibility of Cu^{2+} loading and its leakage during gradient elution are important factors concerning the routine application of this type of sorbent. The following experiments were made: columns were loaded with copper (see Experimental) and the gradient elution of the four above-mentioned proteins was performed. The volumes of effluent marked by arrows (see Figs. 2 and 3) were collected and the amounts of copper were determined. The columns were then washed with EDTA and water and repeatedly loaded with copper. The amount of copper loaded was also determined. The results of five repeated experiments are summarized

in Table II. The loading reproducibility was better than 3% and copper leakage occurring with the concentration gradient of imidazole was negligible. Repeated gradient elution of the model mixture without washing out and new loading of copper shows that this very small loss of metal cannot influence the capacity factors of proteins. In these experiments we also measured spectrophotometrically the recovery of proteins and in all instances obtained values from 90% to 95%.

The following study was performed with HEMA-BUDGE only. It was mentioned above that part of the IDA moieties are free from Cu^{2+} and so their carboxyl groups can act as ion-exchanging groups. In the following experiments, the influence of the concentration of NaCl in the eluent was tested. The aim was to establish the contribution of ion-exchange effects to the retention of proteins. The results are given in Table III. The large shifts in the retention times of Lys and Tra obtained with 0.1 M NaCl can be explained in the following way. The electrostatic interaction of free carboxyl groups of IDA are not suppressed sufficiently with 0.1 M NaCl, so Lys (a protein positively charged and retained on cation exchangers at pH 7.0) was retained more with lower concentrations of NaCl. The opposite situation was observed with Tra (a protein negatively charged at pH 7.0), which is excluded by negatively charged carboxyl groups at pH 7.0 and in 0.1 M NaCl. The retention time of Lys decreased and that of Tra increased when the concentration of NaCl increased. The charges of two other proteins, Myo and RNase, are nearly

TABLE II

TEST OF Cu LEAKAGE DURING THE ELUTION OF PROTEINS WITH IMIDAZOLE GRADIENT

Exp. No.	Separon HEMA 1000 E-IDA-Cu				Content of Cu in column (μg)	Separon HEMA-BIO 1000-BUDGE-IDA-Cu				Content of Cu in column (μg)
	Content of Cu in peak of protein (μg)					Content of Cu in peak of protein (μg)				
	Lys	RNase	Myo	Tra		Lys	RNase	Myo	Tra	
1	0.2	0.1	0.2	0.5	3415	0.2	0.1	0.2	0.6	3581
2	0.2	0.1	0.2	0.5	3200	0.1	0.1	0.2	0.6	3645
3	0.2	0.1	0.2	0.5	3245	0.1	0.1	0.2	0.5	3511
4	0.5	0.2	0.8	1.8	3245	0.1	0.1	0.3	0.7	3397
5	0.3	0.2	0.5	1.5	3245	0.1	0.1	0.2	0.6	3664

TABLE III
INFLUENCE OF NaCl CONCENTRATION IN THE ELUENT ON PROTEIN RETENTION

Sorbent: Separon HEMA-BIO 1000-BUDGE-IDA-Cu. Gradient conditions: (A) 0.02 M phosphate buffer-NaCl as indicated-0.002 M imidazole (pH 7.0); (B) 0.02 M phosphate buffer-NaCl as indicated-0.025 M imidazole (pH 7.0); gradient from 0 to 100% B in 20 min.

NaCl concentration (mol/l)	t_R (min)			
	Lys	RNase	Myo	Tra
0.1	6.34	6.87	11.14	12.11
0.5	3.25	7.94	11.97	17.30

balanced at pH 7.0, so the change in the t_R values of these proteins was small when the concentration of NaCl was changed.

We also followed the contribution of hydrophobic interactions of proteins with the sorbent when a combination of an increasing gradient of imidazole and a decreasing gradient of $(\text{NH}_4)_2\text{SO}_4$ was applied. The results are summarized in Table IV. It is seen that the retention of all the proteins increased with increasing concentration of $(\text{NH}_4)_2\text{SO}_4$ in eluent A. This means that hydrophobic interactions play some role in the separation

TABLE IV
INFLUENCE OF SIMULTANEOUSLY INCREASING IMIDAZOLE GRADIENT AND DECREASING $(\text{NH}_4)_2\text{SO}_4$ GRADIENT ON PROTEIN SEPARATION

Sorbent: HEMA-BIO 1000-BUDGE-IDA-Cu. Gradient conditions: (A) 0.02 M phosphate buffer-0.5 M NaCl-0.002 M imidazole- $(\text{NH}_4)_2\text{SO}_4$ as indicated (pH 7.0); (B) 0.02 M phosphate buffer-0.5 M NaCl-0.025 M imidazole (pH 7.0); gradient from 0 to 100% B in 20 min. For the last line: (A) 0.02 M phosphate buffer-0.5 M NaCl-3.0 M $(\text{NH}_4)_2\text{SO}_4$ (pH 7.0); (B) 0.02 M phosphate buffer-0.5 M NaCl (pH 7.0); gradient from 0 to 100% B in 20 min.

$(\text{NH}_4)_2\text{SO}_4$ concentration (mol/l)	t_R (min)			
	Lys	RNase	Myo	Tra
0	3.25	7.94	11.97	17.35
1.5	8.45	11.27	15.54	19.04
2.0	12.40	13.70	17.34	20.60
3.0	13.40	10.20	7.70	11.82

process, in addition to the interactions with immobilized metal, only at a high concentration of $(\text{NH}_4)_2\text{SO}_4$. This is also demonstrated by the last line in Table IV. In this instance the sorbent without immobilized Cu^{2+} was used. Because the hydrophobicity of the sorbent was low, a higher initial concentration was used to obtain comparable retention of solutes. Because the IMAC mechanism did not take part in the separation process in this instance, a change in retention order occurred and the most hydrophobic protein, Lys, was eluted as the last peak.

DISCUSSION

Two types of IDA-Separons were prepared. Whereas the reaction of IDA with epoxy-derived sorbents at pH 10.0 gave similar results, Porath *et al.*'s method [1] of synthesis (in 2 M Na_2CO_3) was successful only with the BUDGE-derived Separon where the epoxy groups are situated at the end of a long spacer arm. The steric hindrance of glycidyl groups attached directly to the surface of HEMA E probably plays a role in combination with the more rapid hydrolysis in 2 M Na_2CO_3 , because no epoxy groups were left after the treatment in Na_2CO_3 . Steric effects are not so important with HEMA-BUDGE and this sorbent gave similar results with both types of reaction. Steric effects can also affect the loading of the sorbent with Cu^{2+} . The "effective" loading capacity of HEMA-BUDGE was higher than that of HEMA E even if the content of IDA was higher in HEMA E.

The two types of sorbents show different chromatographic properties. Even if the chromatographic conditions were optimized for each type of sorbent, better resolution of the mixture of model proteins was observed on BUDGE-derived IDA-Separon. This improvement in resolution was not caused simply by narrowing of peaks, which was significant only with transferrin. The better resolution is a consequence of the favourable changes in the retention times of the model proteins. It seems that the spacer ligand affects not only the width of the peaks but also the mutual relationships between the retention times of proteins. The influence of ionic and hydrophobic interactions is negligible under the conditions of separation. A similar effect of the spacer was also observed with modified

Separon HEMA sorbents for hydrophobic interaction chromatography [32]. The introduction of a spacer between a matrix and a ligand probably reduces some undesirable interactions of proteins with the sorbent surface and positively influences the steric effects and mass transport during separation.

Synthesized Separon HEMA-BIO1000-BUDGE-IDA is a stable and rigid material. The elution of copper during separations is very low and the retention times of standards are reproducible even after 50 gradient cycles without new loading of the metal.

A paper dealing with practical applications of this sorbent is in preparation.

REFERENCES

- 1 J. Porath, J. Carlsson, I. Olsson and G. Belfrage, *Nature (London)*, 238 (1975) 598.
- 2 J. Porath and B. Olin, *Biochemistry*, 22 (1983) 1621.
- 3 Z. El Rassi and Cs. Horváth, *J. Chromatogr.*, 359 (1983) 241.
- 4 Y. Kato, K. Nakamura and T. Hashimoto, *J. Chromatogr.*, 354 (1986) 511.
- 5 M. C. Smith, T. C. Furman and Ch. Pidgeon, *Inorg. Chem.*, 26 (1987) 1965.
- 6 L. Andersson and J. Porath, *Anal. Biochem.*, 154 (1986) 250.
- 7 C. A. Borrebaeck, B. Lonnerdal and M. E. Etzer, *FEBS Lett.*, 130 (1981) 194.
- 8 J. Porath, B. Olin and B. Grandstrand, *Arch. Biochem. Biophys.*, 225 (1983) 543.
- 9 E. S. Sayeda and J. Porath, *J. Chromatogr.*, 323 (1985) 247.
- 10 A. Godzicka-Józesiak and J. Augustyniak, *J. Chromatogr.*, 131 (1977) 91.
- 11 M. Gimpel and K. Unger, *Chromatographia*, 16 (1982) 117.
- 12 M. Gimpel and K. Unger, *Chromatographia*, 17 (1983) 200.
- 13 N. T. Miller, B. Feibush and B. L. Karger, *J. Chromatogr.*, 316 (1984) 519.
- 14 B. Monjon and J. Solms, *Anal. Biochem.*, 160 (1987) 88.
- 15 K. C. Chadha, P. M. Grob, A. J. Mikulski, L. R. Davis, Jr., and E. Sulkowski, *J. Gen. Virol.*, 43 (1979) 701.
- 16 E. Bollin, Jr. and E. Sulkowski, *Arch. Virol.*, 88 (1978) 149.
- 17 M. P. Scully and V. V. Kakkar, *Biochim. Biophys. Acta*, 700 (1982) 130.
- 18 J. P. Salier, J. P. Martin, P. Lambin, H. McPhee and K. Hochstrasser, *Anal. Biochem.*, 109 (1980) 273.
- 19 M. Yoshimoto and M. Laskowski, Sr., *Prep. Biochem.*, 12 (1982) 235.
- 20 T. Kurecki, L. F. Kress and M. Laskowski, Sr., *Anal. Chem.*, 99 (1979) 415.
- 21 G. Muszyńska, L. Andersson and J. Porath, *Biochemistry*, 25 (1986) 6850.
- 22 S. A. Al-Mashikhi and S. Nakai, *Agric. Biol. Chem.*, 51 (1987) 2881.
- 23 H. Kikuchi and M. Watanabe, *Anal. Biochem.*, 145 (1981) 109.
- 24 J. P. Lebreton, *FEBS Lett.*, 80 (1977) 351.
- 25 T. T. Yip, Y. Y. Tam, Y. C. Kong, M. C. Belew and J. Porath, *FEBS Lett.*, 187 (1985) 345.
- 26 M. G. Reclinbaugh and W. H. Campbell, *Plant. Physiol.*, 71 (1983) 205.
- 27 M. Conlon and R. F. Murphy, *Biochem. Soc. Trans.*, 4 (1976) 860.
- 28 M. Below, T. T. Yip, L. Andersson and R. Ehrnström, *Anal. Biochem.*, 164 (1987) 457.
- 29 I. Ohkobo, T. Kondo and N. Tanigushi, *Biochim. Biophys. Acta*, 616 (1980) 89.
- 30 E. Sulkowski, K. Vastola, D. Oleszek and W. von Muenchhausen, in T. C. J. Gribnau, J. Visser and R. J. F. Nivard (Editors), *Affinity Chromatography and Related Techniques*, Elsevier, Amsterdam, 1982, p. 313.
- 31 P. R. Coulet, J. Carlsson and J. Porath, *Biotechnol. Bioeng.*, 23 (1981) 663.
- 32 P. Šmidl, I. Kleinmann, J. Plicka and V. Svoboda, *J. Chromatogr.*, 523 (1990) 311.
- 33 M. Pribyl, *Fresenius' Z. Anal. Chem.*, 303 (1980) 113.
- 34 G. Fleminger, T. Wolf, E. Hadas and B. Solomon, *J. Chromatogr.*, 510 (1990) 311.

Evaluation of restricted access media for high-performance liquid chromatographic analysis of sulfonamide antibiotic residues in bovine serum

Jeffrey D. Brewster*, Alan R. Lightfield and Robert A. Barford

US Department of Agriculture, ARS, Eastern Regional Research Center, 600 East Mermaid Lane, Philadelphia, PA 19118 (USA)

(First received October 29th, 1991; revised manuscript received January 10th, 1992)

ABSTRACT

Three commercially-available high-performance liquid chromatographic columns packed with restricted access media were evaluated for suitability in multi-residue direct injection analysis at the ng/ml level. The internal surface reversed-phase and shielded hydrophobic phase columns were not sufficiently retentive to separate all analytes from the tail of the matrix peak. Coelution of some of the analytes was also observed with these columns. The semi-permeable surface column was significantly more retentive and selective, providing good separation of analyte and matrix peaks. With this column, an analytical protocol requiring no organic solvents was developed for the assay of six sulfonamides at a detection limit of 25 ng/ml.

INTRODUCTION

The injection of biological fluids into conventional high-performance liquid chromatographic (HPLC) systems results in rapid degradation of performance, typically evidenced by increased back-pressure and reduced efficiency. These effects are usually attributed to precipitation and irreversible or slowly-reversible adsorption of proteins on the stationary phase. Sample clean-up procedures which remove protein prior to injection are therefore needed for conventional HPLC analysis of small molecules in biological samples. These clean-up steps are generally slow, difficult to automate, and employ large quantities of toxic organic solvents. As a result, much of the time and cost of current methods for drug residue analysis are associated with sample preparation, and the full capabilities of modern, automated HPLC systems are seldom realized.

One approach to removing the sample preparation bottleneck is to automate the clean-up operation [1], preferably utilizing methods which reduce [2] or eliminate [3,4] organic solvent consumption.

Another approach is the use of stationary phases which permit the direct injection of proteinaceous samples. Several dozen phases have been developed specifically for HPLC of protein-containing samples [5,6]. These phases are generally referred to as restricted access media (RAM), and a number of such columns are now commercially available. Direct injection HPLC on RAM columns has been applied to the analysis of a large number of pharmaceuticals [5] at therapeutic levels (10–100 µg/ml) in human body fluids, but to our knowledge it has not been used for quantitative determinations at concentrations (1–100 ng/ml) relevant to residue analysis (a detection limit of 5 ng/ml has been claimed in one report [7], but quantitative results were demonstrated only at µg/ml levels). The ability to determine traces of drug and pesticide residues in foods without sample preparation would greatly enhance the speed and cost-effectiveness of food safety monitoring programs. Elimination of sample treatment steps would also reduce the time required for development and optimization of new analytical methods. We therefore initiated a study of several commercially available columns in order to assess

the use of RAM for detection of ng/ml levels of drug residues, using the sulfonamide antibiotics in bovine serum as a test system. We briefly discuss here the columns used in this study, and refer the reader to recent review articles [5,6] for detailed information on history, nomenclature, synthesis, mode of operation, and applications of restricted access media. Three different types or classes of packings were studied: the internal surface reversed-phase (ISRP) type [8], the shielded hydrophobic phase (SHP) type [9], and the semi-permeable surface (SPS) type [10]. ISRP packings consist of small-pore silica particles having a bonded phase with hydrophilic properties at the outer surface and hydrophobic properties within the pores. The packings are generated in three steps: bonding of a hydrophilic group to the silica; capping the hydrophilic group with a hydrophobic species (polypeptide in the original work); and enzymatic cleavage of the hydrophobic end group at the particle surface to expose the hydrophilic sub-phase. The commercial ISRP column used here (GFF-II) employs a glycidoxypropyl hydrophilic sub-phase and a glycine-phenylalanine-phenylalanine hydrophobic cap. The SHP uses hydrophobic moieties (disubstituted aromatic rings) embedded by a proprietary process in a hydrophilic polyethylene oxide polymer network bonded to a silica support. The SPS phase utilizes hydrophilic polyoxyethylene "tails" bound to alkylated silica particles. The column used in this work had a C₁₈ alkyl group, but packings with other hydrophobic moieties are available. Size exclusion plays the dominant role in restricting retention of protein in the ISRP, while chemical effects (*e.g.* hydrophobic interactions) are claimed to predominate with the SHP and SPS phases. However, it has been pointed out that size exclusion may also be the dominant mechanism for limiting protein retention in the SPS and SHP packings due to the small pore size of the silica used for these phases [6]. Despite differences in structure and chemistry, all three columns exhibit similar behavior: large molecules (proteins) are prevented from interacting with the stationary phase and are eluted in or near the void volume, while low-molecular-weight analytes are retained and separated by mechanisms similar to those operating in conventional reversed-phase HPLC. Comparison of the columns was facilitated by the fact that all had identical dimensions (150 ×

4.6 mm) and support particle size (5 μm), and exhibited similar efficiency for test compounds (plate count > 50 000 m⁻¹).

EXPERIMENTAL

Reagents and solutions

Sulfamethazine (SMZ), sulfamerazine (SM), sulfapyridine (Sp) and sulfathiazole (STZ) were obtained from Sigma (St. Louis, MO, USA) and sulfanilamide (SA) was from J. T. Baker (Phillipsburg, NJ, USA). N⁴-acetylsulfamethazine (N4-ASMZ) was prepared from sulfamethazine and acetic anhydride (gift of Dr. Owen W. Parks, USDA, Philadelphia, PA, USA). Reagent grade dibasic potassium phosphate, phosphoric acid, sodium acetate, ammonium acetate and acetic acid were obtained from Thomas Scientific (Swedesboro, NJ, USA). Dimethylsulfoxide and Tween 40 (Aldrich, Milwaukee, WI, USA) were used as received. Spectrapor dialysis tubing, 10 000 molecular weight cutoff (Arthur H. Thomas Co., Philadelphia, PA, USA) was rinsed in distilled water before use. House-purified HPLC grade water was used in all mobile phases and solutions. Mobile phases were filtered through 0.45-μm membranes and degassed with helium before use. Bovine serum albumin (Sigma) was received in freeze-dried form and reconstituted as needed using HPLC-grade water. Stock solutions of the sulfonamide drugs were prepared in methanol and added to serum to generate the spiked serum samples. Serum samples were stored at 4°C and filtered through 0.45-μm syringe-top filters prior to injection. Beef and pork samples were prepared by blending 2.5 g muscle tissue with 15 ml water for 1 min in a Polytron mixer (Brinkmann Instr., Westbury, NY, USA), centrifuging the homogenate 5 min at 3000 g, and adding stock solutions of the sulfonamide drugs to the supernatant.

Apparatus

The HPLC system consisted of an HP 1050 quaternary pump (Hewlett-Packard, Avondale, PA, USA), a Model 7125 loop injector (Rheodyne, Cotati, CA, USA), a Spectroflow 773 variable-wavelength detector (Kratos Analytical, Ramsey, NJ, USA), and an HP 3396A integrator (Hewlett-Packard). A Fiatron CH-30 column heater (Alltech, State College, PA, USA) was used for some analy-

ses. The shielded hydrophobic phase (SHP) column used was the Hisep (Supelco, Bellefonte, PA, USA), the internal surface reversed-phase (ISRP) column was the GFF-II (Regis, Morton Grove, IL, USA), and the semi-permeable surface (SPS) column was the SPS-C18 (Regis). All columns were packed with 5- μ m particles and had dimensions of 150 \times 4.6 mm I.D.

Procedures

Each analytical column was protected by a commercially-packed guard column containing the same packing and by a 2- μ m in-line filter. Unless otherwise noted, mobile phase flow-rate was 1.0 ml/min, temperature was ambient (20–30°C), injection size was 20 μ l, and detection was performed at 265 nm with a 1-s detector risetime. Phosphate buffers were used in the pH range 5.7–7.5, and sodium acetate buffers were used for lower pH. For analyses at levels below 100 ng/ml, the column was temperature-controlled at 30°C and a detector rise time of 5 s was used. For studies of injection size response, the injection valve was fitted with a 100- μ l loop which was partially filled with a syringe to obtain the desired injection volume. Chromatographic performance was evaluated periodically using benzene and toluene as analytes with a 70% methanol mobile phase. Guard columns were backflushed or replaced when elevated backpressure or reduced efficiency were observed.

RESULTS AND DISCUSSION

The nominal goal of this work was development of an HPLC method for direct injection analysis of a mixture of sulfonamides in bovine serum with a detection limit below 100 ng/ml. The success of RAM technology in determinations of individual drugs at therapeutic levels (*ca.* 10 μ g/ml) suggested that this goal could be readily met. However, initial experiments showed that simple extrapolation from results obtained at therapeutic levels was not possible. A typical chromatogram of phenobarbital in serum at the 10 μ g/ml level (Fig. 1a) showed an isolated analyte peak on a flat baseline. At the 100 ng/ml level (Fig. 1b), the long tail of the matrix peak became apparent, and the steeply sloping background under the analyte peak (SMZ) made detection and quantitation very difficult. The need for

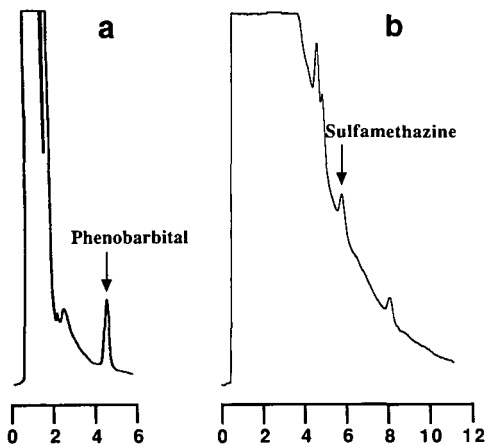


Fig. 1. RAM analyses at therapeutic and trace levels. (a) Phenobarbital (12.5 μ g/ml) in human serum, 625 ng injected. SHP column, 150 \times 4.6 mm I.D.; mobile phase, 180 mM ammonium acetate-acetonitrile (95:5); flow-rate 2.0 ml/min; wavelength, 240 nm; injection volume, 50 μ l. (Reproduced with permission from Supelco Chromatography Products Catalog 28, p. 178). (b) Sulfamethazine (100 ng/ml) in bovine serum, 2 ng injected. SHP column, 150 mm \times 4.6 mm I.D.; mobile phase, 100 mM pH 7 phosphate-acetonitrile (90:10); flow-rate, 1.0 ml/min; wavelength, 265 nm; injection volume, 20 μ l. Time in min.

significant reduction in the tailing of the matrix peak and/or much greater retention of the analyte was clear.

At the time this work was initiated, two types of RAM phases, the ISRP and the SHP, were commercially available. The performance of these columns was similar, and we discuss them together below. Several months later, a series of SPS columns having C₈, C₁₈, CN, and phenyl functionality was introduced. We chose to evaluate the C₁₈ column from this series as it was expected to provide the greatest degree of analyte retention and similarity to the conventional C₁₈ columns used for sulfonamide analysis [11,12].

The sulfonamide antibiotics were chosen as model compounds for several reasons: they are widely used in animal husbandry and of considerable regulatory interest: they are often administered in mixtures of several sulfonamide types; they exhibit a fairly wide range of capacity factors in reversed-phase HPLC; and their chromatographic behavior on reversed-phase columns is well known. The principal metabolite of SMZ, N4-ASMZ, was included as a representative metabolite which may be used as a marker SMZ exposure.

ISRP and SHP columns

In order to identify optimum separation conditions, the chromatographic behavior of the matrix and analytes was studied as a function of pH, organic modifier concentration, and organic modifier type. In an effort to reduce tailing of the matrix peaks a number of mobile phase additives were also examined. Dialysis of the sample to remove lower-molecular-weight matrix components suspected of causing tailing was also investigated.

Organic modifier type. A number of organic modifiers, including methanol, acetonitrile, isopropanol, THF, and dioxane were evaluated. In the narrow range of modifier concentrations (0–10%) which gave acceptable capacity factor (k') values, none of the modifiers offered any significant improvement in selectivity or efficiency over acetonitrile. Little or no effect on elution or tailing of the matrix peaks was observed with variation in modifier type.

Organic modifier concentration and pH. The retention times of the sulfonamide antibiotics on the SPS column as a function of pH and acetonitrile concentration are shown in Fig. 2. Retention times varied little with pH, even at pH values above the pK_a of the analytes. Capacity values for the analytes were much lower than those observed with conventional C_{18} phases under similar conditions, and coelution of analytes prevented full resolution of the mixture. The retention time of the matrix peaks was also a slowly varying function of mobile phase composition,

although the presence of several large matrix peaks presented problems with analyte interference.

Retention times of the sulfonamides on the ISRP column as a function of pH and acetonitrile concentration are shown in Fig. 3. In contrast to the SPS phase, analyte retention behavior varied considerably with changes in pH and modifier concentration. However, the matrix peaks also exhibited complex changes in retention time and peak height when mobile phase composition was varied, making selection of conditions which minimized matrix interference difficult. Similar complex behavior has been observed in separations of peptides on ISRP columns [13]. The pH dependence of analyte retention was qualitatively similar to that observed with conventional C_{18} phases and reflected the ionization of the drugs at high pH. Elution order was similar to that observed with C_{18} phases, but k' values were much smaller. The effect of low pH was studied for the ISRP column with 0.1% trifluoroacetic acid (pH 2) as the mobile phase. Under these conditions, the free aromatic amine of the antibiotics was protonated, and all the analytes except N4-ASMZ eluted within 2 to 3 min. Even without organic modifier, the early-eluting compounds could not be resolved from the major matrix peak, and the steeply sloping tail of the matrix peak prevented reliable detection and integration of the analytes at low concentration. No conditions were found which gave complete resolution of all six analytes.

Mobile phase additives. The addition of protein

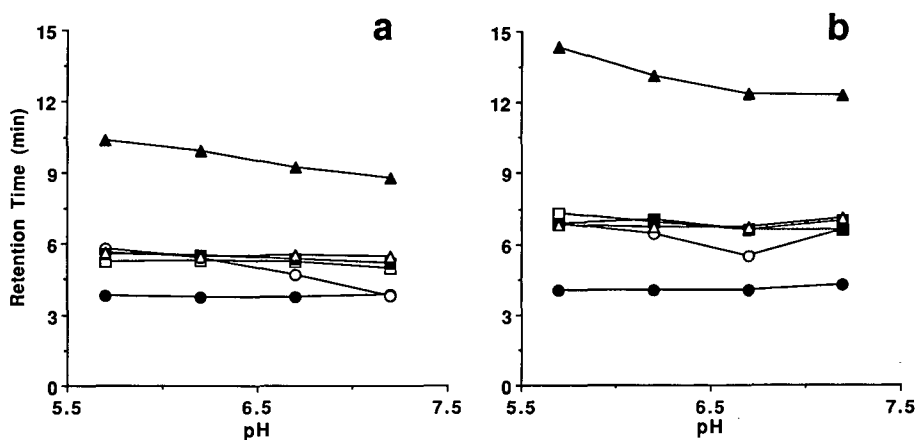


Fig. 2. Retention of sulfonamide antibiotics on SHP column as a function of mobile phase pH. Buffer, 100 mM phosphate; flow-rate, 1.5 ml/min; wavelength, 265 nm. (a) mobile phase, buffer-acetonitrile (90:10); (b) mobile phase, buffer-acetonitrile (95:5). ● = SA, ○ = SM, ■ = SMZ, □ = N4-ASMZ, ▲ = STZ, △ = SP.

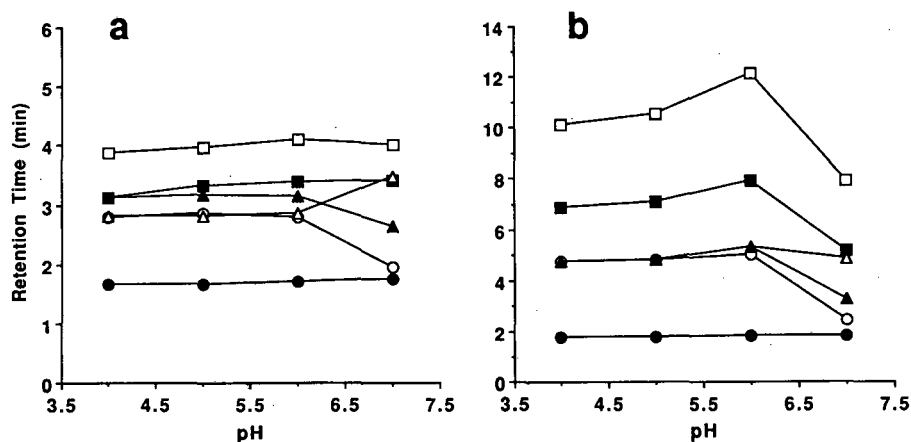


Fig. 3. Retention of sulfonamide antibiotics on ISRP column as a function of mobile phase pH. Buffers, 100 mM phosphate (pH 6, 7), 100 mM sodium acetate (pH 4, 5); flow-rate, 1.5 ml/min; wavelength, 265 nm. (a) mobile phase, buffer-acetonitrile (95:5), (b) mobile phase, buffer. ● = SA, ○ = SM, ■ = SMZ, □ = N4-ASMZ, ▲ = STZ, △ = SP.

solubilizing agents such as dimethylsulfoxide (2%) and Tween (0.1%) to the mobile phase as a means of reducing the tailing of the matrix peaks was explored without success. Addition of 50 ng/ml of serum to the mobile phase did result in noticeable suppression of matrix peak tailing, but was not sufficient to permit reliable detection/quantitation of

the early eluting components. Suppression of matrix peak tailing diminished slowly over several hundred column volumes after switching to mobile phase without added serum.

Dialysis. It was hypothesized that the tailing of the matrix peak was due to slow elution of small proteins and peptides which had penetrated into the pores or hydrophobic region of the stationary phase. To test this theory, a sample of serum was dialysed overnight against pH 6.0 buffer with a 10 000 molecular weight cutoff cellulose membrane to remove low- and intermediate-molecular-weight components. Chromatograms of dialysed and undialysed serum on the SHP column are shown in Fig. 4. Two sharp peaks at 2.1 and 2.5 min (off scale at this attenuation) were eliminated by dialysis, but no significant reduction in matrix peak tailing was apparent.

Buffer concentration. Buffer concentration was varied from 10–500 mM at pH 6 with minimal effect on either the serum peak shape or analyte retention times for buffer concentration greater than 50 mM. Small shifts in retention time observed at lower buffer concentrations could be counteracted by slightly acidifying the serum before injection. The retention time changes were attributed to lack of buffer capacity resulting in transient alteration of mobile phase pH by the sample.

Optimum results. Based on the retention behavior of the analytes and matrix constituents, optimum

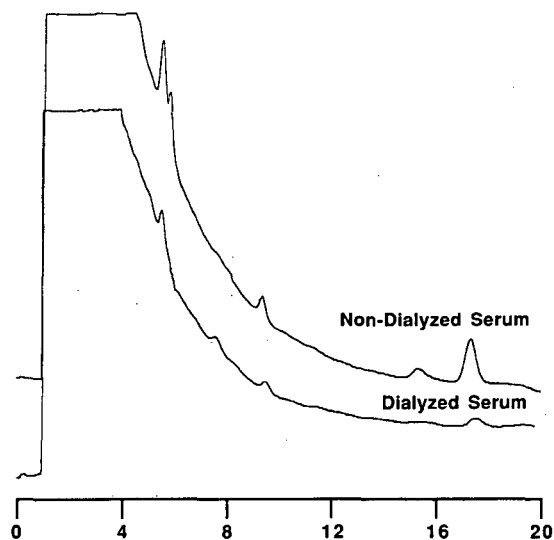


Fig. 4. Effect of dialysis on serum. Column, SHP, 150 × 4.6 mm I.D.; mobile phase, 100 mM pH 7 phosphate-acetonitrile (90:10); flow-rate, 1.0 ml/min; wavelength, 265 nm; injection volume, 20 μ l. Time in min.

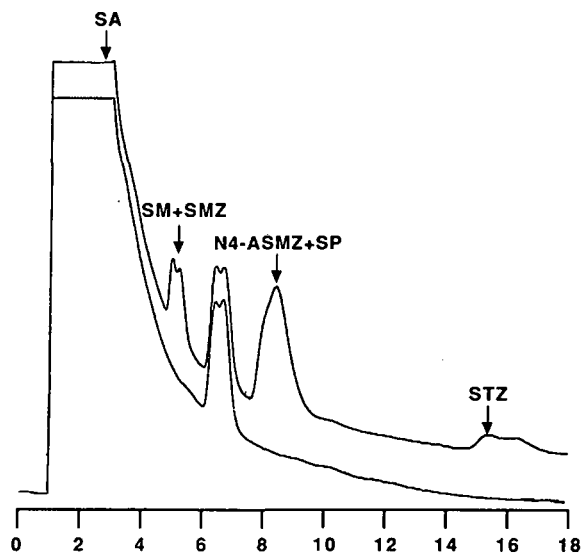


Fig. 5. Optimum separation of sulfonamides on SHP column. Sample, sulfonamide mixture (300 ng/ml) in serum; column, SHP, 150 × 4.6 mm I.D.; mobile phase, 100 mM pH 6 phosphate-acetonitrile (95:5); flow-rate, 1.0 ml/min; wavelength, 265 nm; injection volume, 20 μ l; temperature 30°C. Upper chromatogram, sample; lower chromatogram, serum blank. Time in min:

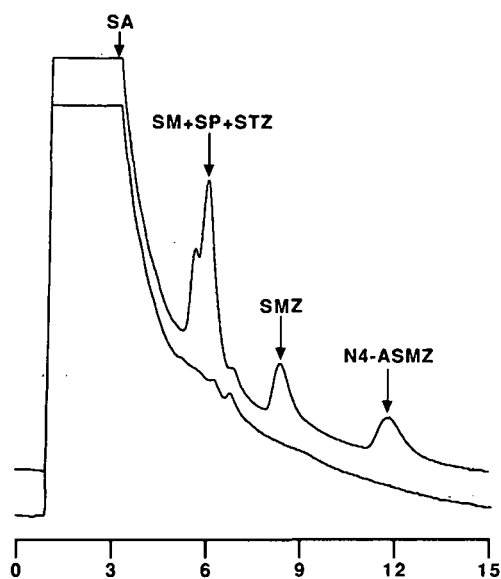


Fig. 6. Optimum separation of sulfonamides on ISRP column. Sample, sulfonamides (300 ng/ml) in serum; column, ISRP, 150 × 4.6 mm I.D.; mobile phase, 100 mM pH 6 phosphate-acetonitrile (99:1); flow-rate, 1.0 ml/min; wavelength, 265 nm; injection volume, 20 μ l; temperature, 30°C. Upper chromatogram, sample; lower chromatogram, serum blank. Time in min.

conditions for analyte detection were determined. Choice of optimum conditions required some compromise between maximum resolution of analytes from each other, and minimum interference from matrix peaks. A chromatogram illustrating the optimum separation obtained with the SHP column is shown in Fig. 5. The large matrix peaks at 6.5 min were not identified. Only three analytes could be resolved, and the SA peak was not separated from the matrix. However, five of the analytes could be detected individually or in appropriate mixtures, without matrix interference.

A chromatogram of the sulfa mixture on the ISRP column at pH 6 is shown in Fig. 6. SA coeluted with the matrix peaks on the ISRP column, and three of the analytes (SM, SP and STZ) coeluted. While other pH values afforded better resolution of the analytes from each other, severe matrix interferences at those pH values prevented detection of several analytes. The conditions shown permitted five of the analytes to be detected (though not simultaneously) without matrix interference. Both columns were exposed to over 100 injections of serum (20 μ l) without appreciable degradation of performance.

SPS-C18 column

The chromatographic behavior of the matrix and analytes was also studied as a function of pH, organic modifier concentration and organic modifier type for the SPS column. Because the analytes were adequately separated from the matrix peaks with this column, the use of mobile phase additives was not explored. Several other matrices were examined with promising results.

Organic modifier type. Methanol, acetonitrile, propanol, tetrahydrofuran and dioxane were evaluated as organic modifiers. Over the limited range of modifier concentrations (0–10%) which gave acceptable k' values, none of the modifiers offered any significant improvement in selectivity or efficiency over acetonitrile. Little or no effect on elution or tailing of the matrix peaks was observed.

Organic modifier concentration and pH. The retention times of the analytes as a function of pH and acetonitrile concentration are shown in Fig. 7. Retention of the analytes on the SPS column was significantly greater than with the ISRP and SHS columns, though still considerably less than observed with conventional C₁₈ phases. The pH depend-

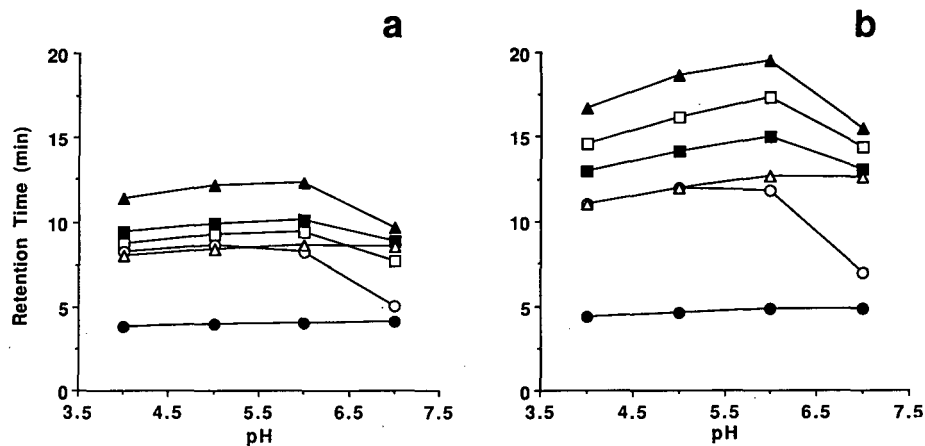


Fig. 7. Retention of sulfonamide antibiotics on SPS column as a function of mobile phase pH. Buffers, 100 mM phosphate (pH 6.7), 100 mM sodium acetate (pH 4.5); flow-rate, 1.0 ml/min; wavelength, 265 nm. (a) mobile phase, buffer-acetonitrile (95:5); (b) mobile phase, buffer. ● = SA, ○ = SM, ■ = SMZ, □ = N4-ASMZ, ▲ = STZ, △ = SP.

ence was qualitatively similar to that observed with C_{18} phases and indicated decreased retention due to ionization of the drugs at high pH. Over the first several weeks of column use, retention times for the sulfonamides decreased approximately 30%, and

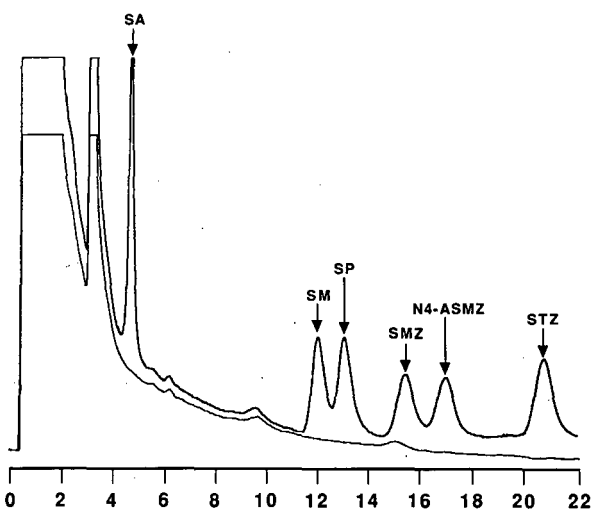


Fig. 8. Sulfonamides on SPS column. Sample, sulfonamides (300 ng/ml) in serum; column, SPS, 150 × 4.6 mm I.D.; mobile phase, 100 mM pH 6 phosphate; flow-rate, 1.0 ml/min; wavelength, 265 nm; injection volume, 20 μ l; temperature, 30°C. Upper chromatogram, sample; lower chromatogram, serum blank. Time in min.

then reached a steady value which remained unchanged for months. Virtually no change in retention time for benzene and toluene was observed over this time frame, however. SMZ and STZ, which initially coeluted, were well resolved following this "conditioning" period. We are working with the column manufacturer to determine protocols for conditioning columns in order to obtain stable retention rapidly, and results of these studies will be reported elsewhere. Resolution of all six sulfonamides could be achieved at pH 6 with both 0.5% acetonitrile and unmodified mobile phases. The separation is relatively robust, and pH and modifier concentration may be altered to avoid interferences without compromising resolution of the analytes. A chromatogram of the test mixture using unmodified buffer as the mobile phase is shown in Fig. 8.

Temperature and ionic strength. Temperature and ionic strength variations were studied for the SPS-C18 column and found to provide minimal improvement in the separation. Temperature changes in the range 25–45°C resulted in predictable reduction of k' with increasing temperature, but did not improve resolution or peak shape significantly. Ionic strength was studied by holding buffer concentration at 50 mM, pH at 6.0, and acetonitrile concentration at 2%, and varying KCl concentration from 0 to 1 M. Retention time increases ranging from 0.2 min for sulfanilamide to 2.7 min for sulfathiazole

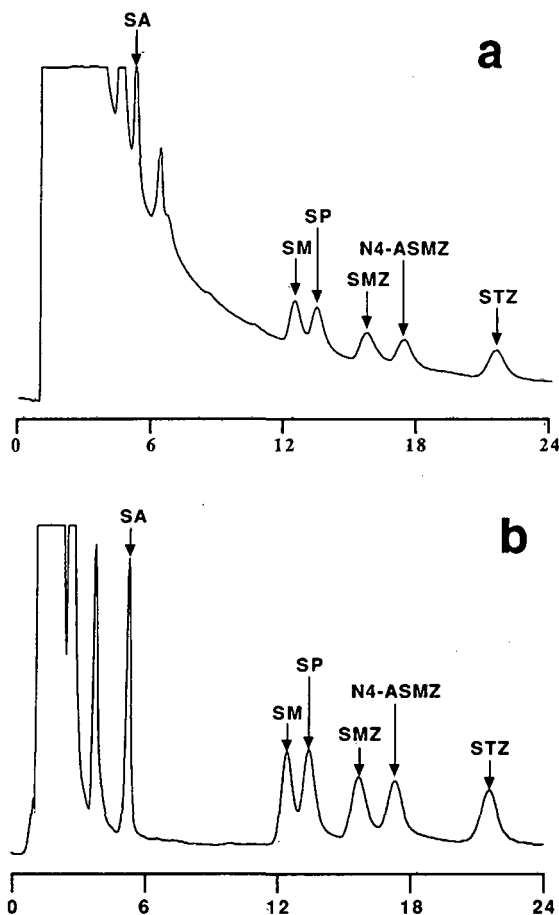


Fig. 9. Analysis of milk and beef homogenate on SPS column. (a) 300 ng/ml sulfonamide mixture in beef tissue homogenate; (b) 300 ng/ml sulfonamide mixture in milk. Mobile phase, 100 mM pH 6 phosphate; flow-rate, 1.0 ml/min; wavelength, 265 nm; injection volume, 20 μ l; temperature, 30°C. Time in min.

were observed for all components as KCl concentration was varied from 0 to 1 M. While retention time could be manipulated by adjusting ionic strength, little gain in selectivity between analytes and virtually no effect on matrix tailing was observed.

Injection size. The effect of sample size on peak area was investigated using 300 ng/ml sulfamethazine in serum. Peak area increased linearly with injection volume over the range tested (10–100 μ l). Injection volumes greater than 50 μ l resulted in an initial 200–400 p.s.i. pressure increase which decayed over several minutes. Additional peaks also

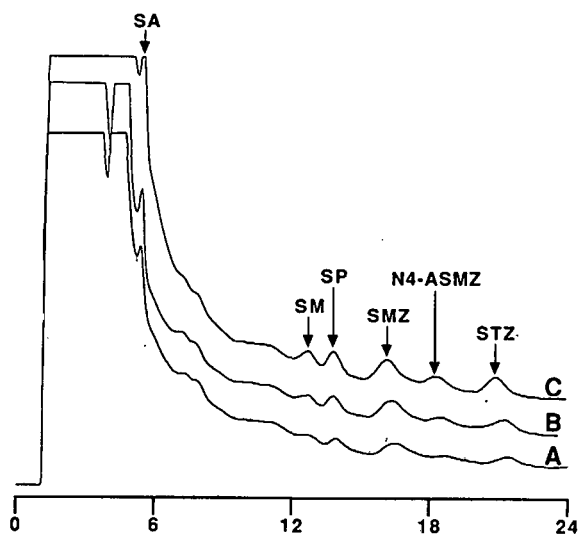


Fig. 10. Limit of detection for sulfonamides on SPS column. Bovine serum spiked with sulfonamides at concentrations of (A) 25 ng/ml, (B) 50 ng/ml, (C) 75 ng/ml. Mobile phase, 100 mM pH 6 phosphate; flow-rate, 1.0 ml/min; wavelength, 265 nm; injection volume, 50 μ l; temperature, 30°C. Time in min.

appeared at unpredictable times in the chromatograms, apparently due to late eluting species from earlier injections. With 100- μ l injections, the pre-column became partially plugged and separation efficiency was noticeably reduced within 3–5 injections. This behavior was in contrast to that of ISRP columns, which are known to accommodate injection sizes up to 660 μ l [14]. Injection size was subsequently limited to 50 μ l to maximize column performance and lifetime.

Other matrices. Beef tissue homogenate, pork tissue homogenate and milk were spiked with the sulfonamide mixture and chromatographed under the same conditions used for bovine serum. Results for the beef and milk samples are shown in Fig. 9. Chromatograms of pork homogenate were very similar to those of beef. It should be noted that the beef homogenate contained only 2.5 g tissue per 15 ml, and that the sulfonamides were added at a level of 300 ng/ml to the homogenate. The matrix peaks were therefore much smaller relative to the analyte peaks than in the case of the serum or milk samples. Nonetheless, direct injection analysis of milk and homogenized tissue using RAM columns appears to be very promising as a method for residue analysis in these matrices.

Limit of detection. A series of serum samples spiked with 10–100 ng/ml of the sulfonamides was analysed to estimate the limit of detection and limit of quantitation for 50- μ l injections. Chromatograms of spiked serum at 25, 50, and 75 ng/ml levels are shown in Fig. 10. From this data, a limit of detection of 25 ng/ml and a limit of quantitation of 50 ng/ml was conservatively estimated for all of the components. Other techniques such as electrochemical detection might be used to achieve lower detection limits.

CONCLUSIONS

The utility of RAM for analysis of multiple analytes in biological matrices at ng/ml levels has been demonstrated for sulfonamide antibiotics in serum. At the sensitivity required to detect these low concentrations, a steeply sloping background due to tailing of the serum matrix was observed which prevented reliable detection of analytes with $k' < 5$ at low (50 ng/ml) concentrations. Due to limited retention and selectivity, the ISRP and SHP columns were unsuitable for analysis of all the sulfonamides, but could be used to determine some individual drugs or mixtures with detection limits below 100 ng/ml. The SPS column exhibited the greatest analyte retention and selectivity of the columns tested, and could be used for direct injection, multi-residue

analysis of all six sulfonamides in serum with an estimated detection limit of 25 ng/ml, using minimal sample preparation and no organic solvents.

REFERENCES

- 1 R. W. Frei and K. Zech (Editors), *Selective Sample Handling and Detection in High-Performance Liquid Chromatography (Journal of Chromatography Library, Vol. 39A and B)*, Elsevier, Amsterdam, 1988 (Vol. 39A), 1989 (Vol. 39B).
- 2 W. Th. Kok, K.-P. Hupe and R. W. Frei, *J. Chromatogr.*, 436 (1988) 421.
- 3 A. J. J. Debets, W. Th. Kok, K.-P. Hupe and U. A. Th. Brinkman, *Chromatographia*, 30 (1990) 361.
- 4 J. D. Brewster and E. G. Piotrowski, *J. Chromatogr.*, 585 (1991) 213.
- 5 K. K. Unger, *Chromatographia*, 31 (1991) 507.
- 6 T. C. Pinkerton, *J. Chromatogr.*, 544 (1991) 13.
- 7 C. M. Dawson, T. W. M. Wang, S. J. Rainbow and T. R. Tickner, *Ann. Clin. Biochem.*, 25 (1988) 661.
- 8 J. A. Perry, *J. Liq. Chromatogr.*, 13 (1990) 1047.
- 9 C. P. Desilets, M. A. Rounds, F. E. Regnier, *J. Chromatogr.*, 544 (1991) 25.
- 10 B. Feibush and C. T. Santasania, *J. Chromatogr.*, 544 (1991) 41.
- 11 J. D. Weber and M. D. Smedley, *J. Assoc. Off. Anal. Chem.*, 72 (1989) 445.
- 12 M. M. L. Aerts, W. M. J. Beek and U. A. Th. Brinkman, *J. Chromatogr.*, 435 (1988) 97.
- 13 T. C. Pinkerton and K. A. Koeplinger, *J. Chromatogr.*, 458 (1988) 129.
- 14 T. C. Pinkerton, T. D. Miller and L. J. Janis, *Anal. Chem.*, 61 (1989) 1173.

Simultaneous determination of amounts of major phospholipid classes and their fatty acid composition in erythrocyte membranes using high-performance liquid chromatography and gas chromatography

K. Eder, A. M. Reichlmayr-Lais and M. Kirchgessner*

Institut für Ernährungsphysiologie, Technische Universität München, W-8050 Freising-Weihenstephan (Germany)

(First received October 23rd, 1991; revised manuscript received January 10th, 1992)

ABSTRACT

A method for the simultaneous determination of amounts of major phospholipid classes and their fatty acid composition in erythrocyte membranes is described. The method consists in extraction of phospholipids from erythrocyte membranes, separation of phospholipid classes by high-performance liquid chromatography, methylation of phospholipids and determination of phospholipid-bound fatty acids by capillary gas chromatography. The amounts of phospholipid classes are calculated from the total weight of phospholipid-bound fatty acids and their average molecular weights. The method was applied to erythrocytes from rats. The results show that the method is reproducible and is useful for the determination of amounts of phospholipid classes and their fatty acid composition in small blood samples.

INTRODUCTION

Phospholipids are important constituents of all biological membranes. Both the nature of the polar head groups and the acyl chains influence the physical and chemical properties of membranes [1,2]. Especially in erythrocytes, membrane parameters such as shape, deformability, permeability and osmotic fragility are determined by membrane phospholipids [3–6]. The most important phospholipid classes in erythrocyte membranes are phosphatidylcholine (PC), phosphatidylethanolamine (PE), phosphatidylserine (PS) and sphingomyelin (SM), which contain a variety of aliphatic chains that vary in length and number of double bonds [7–10]. For their determination erythrocyte membrane phospholipids are extracted with various solvents or binary solvent mixtures. The main phospholipid classes are usually separated by one- and two-dimensional thin-layer chromatography (TLC), quantified by measurement of inorganic phosphate and their fatty

acid composition is determined by capillary gas chromatography (GC) after methylation [11–14]. Although TLC is used routinely for the separation of phospholipid classes, it has some disadvantages. The amount of lipid that can be applied to the plate is small and oxidation of polyunsaturated fatty acids during plate development and drying and losses of phospholipids during scraping off can occur [15,16]. Moreover, quantification of phospholipid classes by phosphorimetry is not very exact as only the number of moles of phospholipid and not the molecular weight of the individual phospholipid classes depending on their fatty acid composition is considered.

The aim of this work was to develop a method for the determination of amounts of individual phospholipid classes and their fatty acid composition in erythrocyte membranes which should overcome the disadvantages of the TLC method. For this purpose phospholipid classes extracted from erythrocyte membranes were separated by high-performance

liquid chromatography (HPLC) and the amounts of total bound fatty acids of individual phospholipid classes were determined by capillary GC. Amounts of individual phospholipid classes were then calculated from the sum of their bound fatty acids.

EXPERIMENTAL

Chemicals, standards and blood samples

Phospholipid standards [PC, lyso-PC and lyso-PE from egg yolk; PE (diacyl), PE (plasmalogen), PS and SM from bovine brain; PI from bovine liver; cardiolipin from bovine heart) were purchased from Sigma (Taufkirchen, Germany). The purity of all phospholipid standards was at least 98%.

Fatty acid standards (with a chain length between 8 and 24 carbon atoms) were obtained from Sigma, Roth (Karlsruhe, Germany) and Fluka (Buchs, Switzerland) in the highest purity available. Methylation of standard fatty acids for GC was carried out using boron trifluoride-methanol reagent (Fluka, purissimum) in accordance with Morrison and Smith [17]. All other chemicals were purchased from Merck (Darmstadt, Germany). Blood samples were taken from adult female Sprague-Dawley rats.

Apparatus

Separation of phospholipid classes was carried out on a Merck-Hitachi (Darmstadt, Germany) HPLC system consisting of a gradient pump (L-6200), a diode array (L-3000), a 25 cm × 0.4 cm I. D. Si 60 (5- μ m) cartridge (LiChroCART, Merck), an integrator (D-2000) and a fraction collector (Model 201; Gilson, Villiers-le-Bel, France).

Analysis of fatty acid methyl esters (FAMES) was performed on a Sichromat 2 gas chromatograph (Siemens, Karlsruhe, Germany) equipped with a programmed-temperature vaporizer (PTV), a CP-Sil 88 wall-coated open-tubular (WCOT) fused-silica column (50 m × 0.25 mm I.D., film thickness 0.2 μ m) (Chrompack, Middelburg, Netherlands), a flame ionization detector and an integrator (D-2500, Merck).

Preparation of erythrocyte membranes and extraction of phospholipids

Blood from rats was collected in glass tubes containing heparin to prevent clotting. The fresh blood

was centrifuged (1100 g, 10 min) and plasma and buffy coat were removed by suction. The red cells were washed three times with isotonic saline by centrifugation (1100 g, 10 min) and resuspension. The washed cells were haemolysed by adding 5 ml of distilled water per millilitre of cells and freezing. The red cell membranes were then washed three times according to Hanahan and Ekholm [18] using Tris buffer (pH 7.6). After washing, liquid was drained from the packed membranes by placing the centrifuge tubes upside down. A 1-ml volume of distilled water per gram of packed membranes was added and the membranes were suspended ("membrane solution"). Extraction of phospholipids was carried out with isopropanol by a modification of the method of Peuchant *et al.* [10]. To 1 g of membrane solution 20 ml of isopropanol [containing butylated hydroxytoluene (BHT) as an antioxidant] were added. This mixture was sonicated with a Branson Sonifier for 1 min and was then left to stand for 4 h at room temperature. After extraction the mixture was filtered and the residue was washed twice with 10 ml of isopropanol. The filtrate was evaporated to dryness and the residue consisting of lipids was dissolved in chloroform and diluted to 5 ml with chloroform. This lipid extract was filtered using an HPLC (45- μ m) filter and was then ready for injection into the HPLC system.

Separation of phospholipid classes by HPLC

For separation of phospholipid classes a modification of the method of Seewald and Eichinger [19] based on the simultaneous use of a pH gradient and a polarity gradient was used. The mobile phase

TABLE I
SOLVENT GRADIENTS AND FLOW-RATES USED FOR SEPARATION OF PHOSPHOLIPID CLASSES

Time (min)	A (%)	B (%)	C (%)	Flow-rate (ml/min)
0.0	100	0	0	1.5
5.0	100	0	0	1.5
5.1	0	100	0	1.5
15.0	0	100	0	1.5
15.1	0	100	0	1.0
35.0	0	0	100	1.5
50.0	0	0	100	1.5

was composed of solvent A (acetonitrile), solvent B [acetonitrile–85% phosphoric acid (99.8:0.2)] and solvent C [(methanol–85% phosphoric acid 99.8:0.2)]. The solvent gradients and the flow-rates used are shown in Table I.

A 50- μ l portion of the lipid extract was injected manually into the HPLC system. Separation was carried out at room temperature. The eluted phospholipid classes were detected at 205 nm and collected with a fraction collector for further analysis. To each tube containing the collected eluent with an individual phospholipid class a solution containing a known amount of methyl heptadecanoate (as internal standard for GC determination of FAMES) and BHT (as antioxidant) was added.

Methylation of phospholipid classes

The individual phospholipid classes were evaporated from the mobile phase under vacuum at room temperature. The residues of the phosphoglyceride classes (PC, PE, PS, PE–plasmalogen)

were resuspended in 0.5 ml of chloroform and then 4 ml of 0.5 M methanolic sodium methoxide solution were added. This mixture was stirred at room temperature for 1.5 h. For extraction of FAMES 2 ml of water and 2 ml of hexane were added. The mixture was stirred for a further 10 min, then the hexane phase containing the FAMES was transferred into a vial for analysis. The extraction was repeated by adding a further 2 ml of hexane. The hexane phases were collected and the solvent was evaporated under vacuum at room temperature. The FAMES were dissolved in a small volume (50 μ l) of hexane and were then ready for injection into the GC system. This methylation procedure gave conversions of fatty acids from standard phosphoglyceride classes into FAMES between 97.1 and 103.4% [20].

The residue of sphingomyelin was dissolved in 1 ml of chloroform, transferred into a tube provided with a PTFE-lined screw cap, the solvent was evaporated again and 2 ml of methanolic boron trifluo-

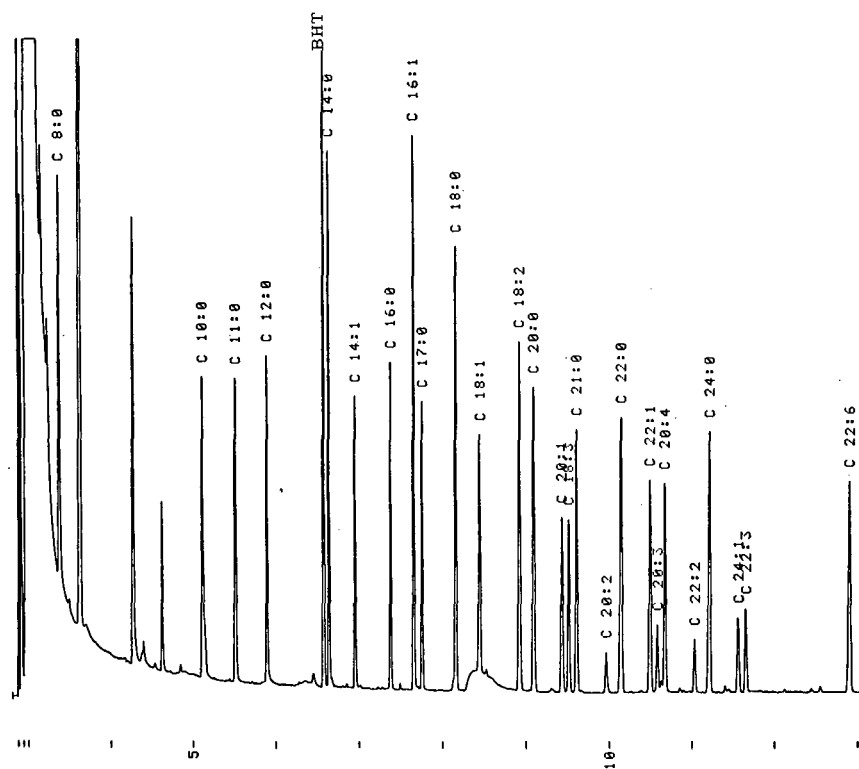


Fig. 1. Separation of standard FAMES using PTV split injection. Splitting ratio, 1:2; amounts of FAMES injected into the injector chamber, 0.8–7 ng. Time scale in minutes.

ride solution (140 g/l) and a small volume (10 μ l) of a solution containing BHT (6 mg/ml) were added. The tube was closed and heated for 15 h at 90°C. This very long period of heating was necessary as it has been shown [20,21] that for complete methylation of sphingomyelin with boron trifluoride-methanol reagent very long periods are required. Thus in our studies [20] the recoveries of FAMES from a sphingomyelin standard were 35.5, 60.4, 82.7 and 99.1% for periods of 1, 2, 6 and 15 h, respectively. FAMES were extracted by adding twice each time 0.75 ml of hexane and water. The hexane phases were collected, the solvent was evaporated and the FAMES were dissolved in a small volume of hexane.

Gas chromatographic analysis of FAMES

A 2- μ l portion of each FAME extract was injected manually into the GC system using a PTV. The PTV programme was 25°C held for 1 min after injection, increased at 800°C/min to 300°C, 300°C held for 10 min, then the PTV was cooled. The oven temperature was 50°C held for 1 min, increased at 30°C/min to 160°C and at 15°C/min to 200°C, 200°C held for 1.5 min, increased at 10°C/min to 225°C, 225°C held for 15 min. Hydrogen was used as the carrier gas at a flow-rate of 2.0 ml/min; the splitting ratio was 1:2. FAMES were calculated using methyl heptadecanoate ester as internal standard. For more details, see ref. 22. A typical separation of standard FAMES with chain lengths between 8 and 24 carbon atoms is shown in Fig. 1.

Calculation of amounts of individual phospholipid classes

Amounts of individual phospholipid classes were calculated as proposed by Seewald and Eichinger [19]. The amount of each individual fatty acid of each phospholipid class was determined by GC. The total fatty acid weight of each phospholipid class was calculated as the sum of the amounts of the individual fatty acids. Using the relative amount of each fatty acid and its molecular weight, an average molecular weight of the fatty acids of each phospholipid class can be calculated. The molecular weight of the phospholipid can be calculated as the sum of the molecular weight of the phospholipid core and the average molecular weight of bound fatty acids. The number of moles of fatty acids can

be calculated as the ratio between total amount of fatty acids and the average molecular weight of the fatty acids bound to each phospholipid class. For PC, PE and PS, the number of moles of phospholipid in the injected extract is half that of the number of their bound fatty acids, and for lyso-phospholipids and sphingomyelin the number of moles of phospholipids and their bound fatty acids is identical. From the number of moles of each phospholipid class and its average molecular weight, the amount in micrograms of each phospholipid class contained in the extract injected into the HPLC system can be calculated.

Quality control

The reproducibility of the method was studied by applying the whole method (Washing of cells, extraction and separation of phospholipids and GC analysis of FAMES) to five aliquots of pooled blood (5 ml each). The recovery of phospholipids was checked by using a phospholipid standard solution containing PC, PE and SM. A 25-ml volume of this

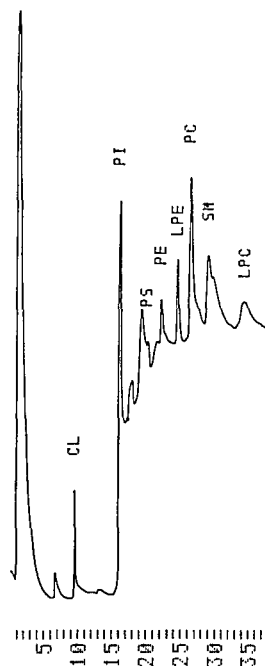


Fig. 2. Separation of standard phospholipid classes by HPLC as described under Experimental. The amounts of phospholipids applied to the column were 20 μ g for PE, 25 μ g for cardiolipin (CL), PI, PS, lyso-PE and lyso-PC and 50 μ g for PC and SM. Time scale in minutes.

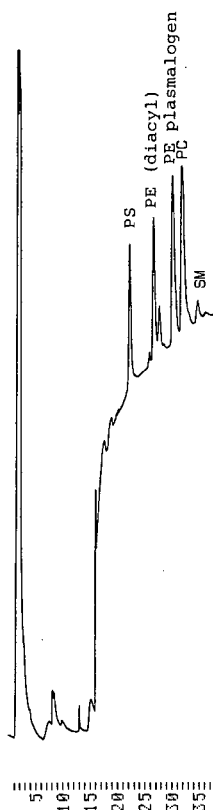


Fig. 3. Separation of rat erythrocyte membrane phospholipids by HPLC as described under Experimental. Peaks represent phospholipids contained in 40 μ l of packed erythrocytes. Time scale in minutes.

solution (containing 3.12 mg of PC, 5.43 mg of PE and 3.21 mg of SM) was treated in the same way as the lipid extract was treated in the method described above. The standard solution was evaporated to dryness and phospholipids were dissolved in chloroform. The solution was diluted up to 5 ml with chloroform and 50 μ l of it were injected into the HPLC system. The subsequent analytical steps were identical with those described above. Phospholipid recoveries were calculated as the ratio between the calculated amount of each phospholipid class and the known amount of each phospholipid class injected into the HPLC system.

RESULTS

The chromatographic separation of standard phospholipid classes [PC, PE, PS, phosphatidylino-

sitol (PI), lyso-PC, lyso-PE, cardiolipin and SM] and phospholipid classes from rat erythrocyte membranes are shown in Figs. 2 and 3. The chromatogram of rat erythrocyte membranes contains peaks of PS, PE, lyso-PE, PC and SM. However, the lyso-PE peak represents the plasmalogen fraction of PE as the use of acidic mobile phases leads to hydrolysis of the labile enol ether binding [23–25].

Fig. 4 shows typical separations of FAMES from rat erythrocyte PC, PE, PE-plasmalogen, PS and SM. The fatty acid composition of these phospholipid classes is given in Table II. Amounts of phospholipid classes per millilitre of cells as calculated by their total bound fatty acids are given in Table III. The relative standard deviations ($n = 5$) were 2.7% for PC, 3.1% for PE (diacyl), 6.3% for PE (plasmalogen), 5.4% for PS, 1.0% for SM and 0.1% for the sum of these phospholipid classes.

The recoveries of phospholipid standards were $98.9 \pm 0.8\%$ for PE (diacyl), $101.8 \pm 4.2\%$ for PC and $96.3 \pm 0.1\%$ for SM, indicating that there were no losses of phospholipid between extraction and fatty acid analysis.

DISCUSSION

In the analysis of phospholipids, TLC is the most widely used separation technique. Although the separation of major phospholipid classes can be easily achieved, this method has disadvantages such as possible losses of phospholipids during scraping off and oxidation of polyunsaturated fatty acids during plate development and drying. Another problem is the quantification of the separated phospholipids. Phosphorimetry, which is the most commonly used technique for the quantification of phospholipids, does not give exact results because different molecular weights of phospholipids depending on their fatty acid composition are not considered. Using HPLC for separation of phospholipid classes, the disadvantages of the TLC method can be avoided. However, phospholipids cannot be quantified directly by UV absorption measurement as the molar absorption coefficients of phospholipids are dependent on their fatty acid composition [26,27]. Therefore, phospholipid classes separated by HPLC must be collected and quantified in a further analytical step.

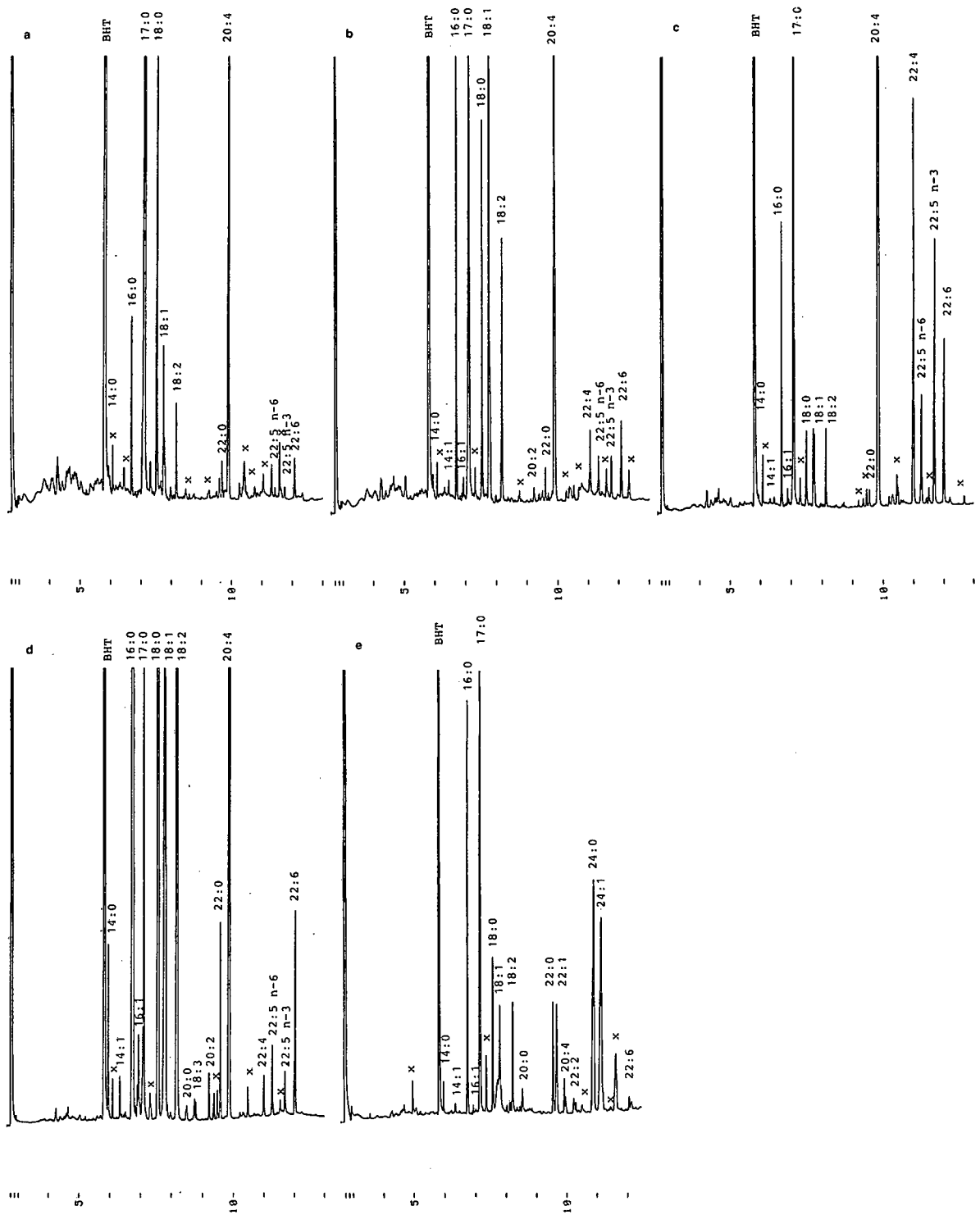


Fig. 4. GC separation of FAMES from rat erythrocyte membrane phospholipid classes. (a) Phosphatidylserine; (b) phosphatidylethanolamine (diacyl); (c) phosphatidylethanolamine (plasmalogen); (d) phosphatidylcholine; (e) sphingomyelin. 17:0 = Internal standard representing *ca.* 4 ng of substance; x = unidentified peaks. Time scale in minutes.

TABLE II

FATTY ACID COMPOSITION (mol%) OF PHOSPHOLIPID CLASSES FROM RAT ERYTHROCYTE MEMBRANES

Values represent means \pm S.D. for five analyses of a pooled blood sample.

Fatty acid	Phospholipid class					
	PS	PE (diacyl)	PE (plasmalogen)	PC	SM	Total
14:0	— ^a	—	—	1.01 \pm 0.02	1.34 \pm 0.05	0.70 \pm 0.02
16:0	7.21 \pm 0.53	13.67 \pm 0.42	5.24 \pm 0.13	39.13 \pm 0.66	23.43 \pm 0.94	27.25 \pm 0.60
16:1	—	0.42 \pm 0.03	—	0.64 \pm 0.01	—	0.40 \pm 0.01
18:0	25.15 \pm 0.68	9.53 \pm 0.16	1.83 \pm 0.08	17.96 \pm 0.50	8.40 \pm 0.53	14.55 \pm 0.39
18:1	8.97 \pm 0.32	22.48 \pm 0.62	3.23 \pm 0.26	10.03 \pm 0.89	7.39 \pm 0.58	9.72 \pm 0.48
18:2	4.56 \pm 0.08	8.82 \pm 0.07	1.73 \pm 0.06	12.16 \pm 0.30	6.94 \pm 0.20	9.07 \pm 0.20
20:0	—	—	—	0.17 \pm 0.00	1.29 \pm 0.04	0.21 \pm 0.00
20:2	—	0.65 \pm 0.03	—	0.34 \pm 0.00	—	0.25 \pm 0.00
20:4	47.48 \pm 1.76	35.21 \pm 0.67	54.43 \pm 0.61	14.19 \pm 0.63	1.79 \pm 0.07	24.16 \pm 0.61
22:0	—	0.81 \pm 0.06	—	1.04 \pm 0.02	4.90 \pm 0.21	1.12 \pm 0.01
22:1	—	—	—	—	5.93 \pm 0.35	0.54 \pm 0.03
22:4	1.36 \pm 0.09	2.29 \pm 0.05	14.32 \pm 0.16	0.35 \pm 0.01	—	2.72 \pm 0.14
22:5 <i>n</i> -6	1.97 \pm 0.16	1.37 \pm 0.03	3.85 \pm 0.17	0.64 \pm 0.01	—	1.26 \pm 0.04
22:5 <i>n</i> -3	0.70 \pm 0.02	1.60 \pm 0.10	9.43 \pm 0.48	0.37 \pm 0.02	—	1.87 \pm 0.14
22:6	2.60 \pm 0.12	3.15 \pm 0.09	5.94 \pm 0.07	1.97 \pm 0.10	0.88 \pm 0.03	2.64 \pm 0.07
24:0	—	—	—	—	18.25 \pm 0.98	1.68 \pm 0.08
24:1	—	—	—	—	19.46 \pm 0.81	1.79 \pm 0.05

^a Dashes indicate that the fatty acid exists only in trace amounts.

Seewald and Eichinger [19] proposed a method for quantification of phospholipids by determination of the total amounts of phospholipid bound fatty acids. This method offers the advantage that in

TABLE III

AMOUNTS OF PHOSPHOLIPID CLASSES IN RAT ERYTHROCYTE MEMBRANES

Values represent means \pm S.D. for five analyses of a pooled blood sample.

Phospholipid	Amount	
	μ g/ml of cells	%
PS	294 \pm 16	8.2
PE (diacyl)	253 \pm 8	7.1
PE (plasmalogen) ^a	878 \pm 55	24.5
PC	1717 \pm 47	47.9
SM	443 \pm 4	12.3
Sum	3584 \pm 4	100.0

^a For calculation of the amount of PE-plasmalogen it was assumed that the aldehyde in the α -position has an average chain length of 17.5 carbon atoms.

a single analysis both the amount of individual phospholipid classes and their fatty acid composition can be determined. In contrast, most other methods require two analyses for the same purpose. A disadvantage of this method for calculation is that the exact determination of phospholipid amounts depends on the determination of all bound fatty acids. In practice, however, when small sample amounts are used it is hardly possible to identify and quantify fatty acids which are present in very small amounts ("minor fatty acids").

In this work, the method of Seewald and Eichinger [19] originally used for the determination of phospholipids from muscle was adapted to erythrocyte membranes from small blood samples. There are many differences between pig muscle and rat erythrocyte membranes. First, in contrast to pig muscle, in most instances rat erythrocytes are available only in small amounts. Second, erythrocyte membranes contain smaller amounts of phospholipids than muscle. Third, phospholipid from erythrocyte membranes contain a greater variety of fatty acids (some of which exist in very small amounts, "minor fatty acids") than phospholipids of pig

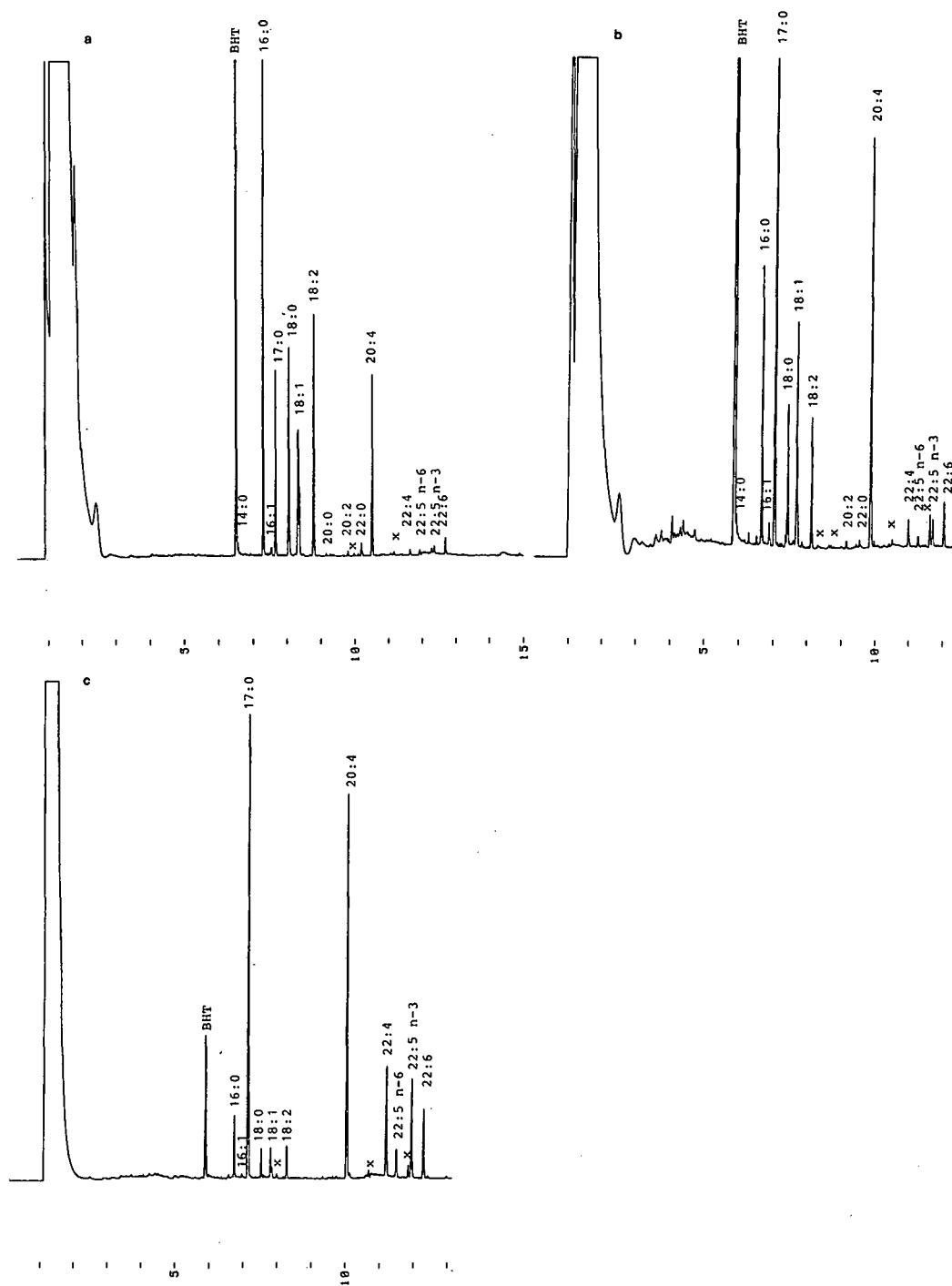


Fig. 5. Chromatograms of FAMEs from the rat erythrocyte membrane phospholipid classes. (a) PC; (b) PE (diacyl); (c) PE (plasmalogen). The results indicate that peak areas of FAMEs which were not identified (x) represent only 1–3% of the peak areas of total FAMEs. 17:0 = Internal standard. Time scale in minutes.

muscle. Owing to these differences, the determination of erythrocyte membrane phospholipids requires a higher sensitivity than the determination of phospholipids from pig muscle.

In the proposed method a high sensitivity was achieved by the following means. The phospholipid and FAME extracts were evaporated and dissolved in a small volume of solvent. Hence sufficient amounts of phospholipids and FAMES could be injected into HPLC and GC systems. Moreover, for GC injection a very small splitting ratio was used. A further possibility for increasing the sensitivity is to repeat the HPLC separation of phospholipid classes and collect phospholipid classes from more than one HPLC separation. This is useful for very small blood samples (less than 1 ml). Preliminary studies have shown that there is a linear correlation ($r = 0.99$) between the amount of fatty acids measured and the number of successive collections of separated phospholipid classes.

The fourth difference between erythrocyte membranes and muscle is the different behaviour of the sample during extraction. Whereas lipids from muscle can be extracted with the widely used Folch extraction [chloroform-methanol (2:1)], this method cannot be applied for extraction of lipids from erythrocyte membranes without problems, as erythrocyte membranes aggregate after addition of the chloroform-methanol mixture, making it difficult to resuspend them [28–30]. However, in another study we found that isopropanol is a good solvent for the extraction of phospholipids from erythrocyte membranes [30]. Another difference is that erythrocyte membranes are to be isolated by some preparative steps such as washing and haemolysis of cells and washing of membranes whereas muscle can be extracted in its original form.

In this work, methylation of phosphoglycerides was carried out at room temperature using methanolic sodium methoxide. Hence a one-vial procedure could be used. Phospholipids contained in the lipid extract were separated by HPLC. The eluent containing separated phospholipids was collected in 10-ml centrifuge tubes and the solvent was evaporated under vacuum at room temperature. Then methanolic sodium methoxide was added and, after methylation, hexane and water were added for extraction of FAMES. Thus losses of phospholipids during transfer from one vial to another could be

completely avoided. This could be seen in the recovery data for phosphoglycerid standards, which were close to 100% (98.9% for PE, 101.8% for PC).

Using the described method, the amounts of the major phospholipid classes PC, PE, PS and SM (which represent approximately 95% of total phospholipids in erythrocyte membranes [31]) and their fatty acid compositions can be determined.

In contrast to diacyl phospholipids, plasmalogens contain one "fatty aldehyde". Using the method described, which is based on fatty acid analysis, it is not possible to determine the exact molecular weight of plasmalogens. Therefore, for calculation of the amounts of PE-plasmalogen it was assumed that the aldehyde contained in the molecule has an average chain length of 17.5 carbon atoms, as data from Farquhar [32] showed that 15.9% of aldehyde molecules in PE-plasmalogen from human erythrocytes contained sixteen carbon atoms, 11.3% contained seventeen carbon atoms and 56.2% contained eighteen carbon atoms. Using this assumption also the amounts of PE-plasmalogen contained in erythrocyte membranes can be calculated. This might be interesting, as PE-plasmalogen, which represents 78% of the total PE in rat erythrocyte membranes (Table III), contains a large portion of long-chain polyunsaturated fatty acids ($C_{20:4}$, $C_{22:4}$, $C_{22:5}$ and $C_{22:6}$) and therefore might be of physiological significance.

The method described shows good reproducibility. The fatty acids determined in the present analyses represent 97–99% of the total phospholipid-bound fatty acids as compared with fatty acid composition data from other investigators [7,8,33]. Therefore, the error in the calculation of amounts of phospholipids caused by bound fatty acids which could not be detected or identified is small. This can also be seen from Fig. 5, illustrating areas of peaks identified and not identified. Moreover, the results for the amounts of phospholipids in rat erythrocyte membranes and also those of the fatty acid composition of individual phospholipid classes are in good agreement with those of other investigators [13,14,33–38]. The method can be applied to small blood samples (less than 1 ml) without loss of precision if the sensitivity of the method is optimized by the means discussed above. Hence the method is useful for blood samples obtained from small laboratory animals such as mice and rats. The method

gives simultaneous results for amounts of the major phospholipid classes and their fatty acid composition in erythrocyte membranes.

REFERENCES

- 1 D. Zakim and D. A. Vessey, in R. H. Herman, R. M. Cohn and P. D. McNamara (Editors), *Principles of Metabolic Control in Mamalian Systems*, Plenum Press, New York, 1980, pp. 337–371.
- 2 C. D. Stubbs and A. D. Smith, *Biochim. Biophys. Acta*, 779 (1984) 89–137.
- 3 F. A. Kuypers, B. Roelofsen, J. A. F. Op den Kamp and L. L. M. van Deenen, *Biochim. Biophys. Acta*, 769 (1984) 337–347.
- 4 F. A. Kuypers, B. Roelofsen, W. Berendsen, J. A. F. Op den Kamp and L. L. M. van Deenen, *J. Cell Biol.*, 99 (1985) 2260–2267.
- 5 H. G. Parsons, R. Hill, P. Pencharz and A. Kuksis, *Biochim. Biophys. Acta*, 860 (1986) 420–427.
- 6 B. Roelofsen, F. A. Kuypers, J. A. F. Op den Kamp and L. L. M. van Deenen, *Biochem. Soc. Trans.*, 17 (1989) 284–286.
- 7 B. D. Beaumelle and H. J. Vial, *J. Chromatogr.*, 356 (1986) 187–194.
- 8 D. R. Wing, D. J. Harvey, P. La Droitte, K. Robinson and S. Belcher, *J. Chromatogr.*, 368 (1986) 103–111.
- 9 M. D. Laryea, P. Cieslicki, E. Dieckmann and U. Wendel, *Clin. Chim. Acta*, 171 (1988) 11–18.
- 10 E. Peuchant, R. Wolff, C. Salles and R. Jensen, *Anal. Biochem.*, 181 (1989) 341–344.
- 11 J. H. Williams, M. Kuchmak and R. F. Witter, *Lipids*, 1 (1966) 391–398.
- 12 R. Stocker, W. B. Cowden, R. L. Tellam, M. J. Weidemann and N. H. Hunt, *Lipids*, 22 (1987) 51–57.
- 13 S. M. Innis, *J. Parent. Nutr.*, 13 (1989) 47–50.
- 14 G. L. Johanning and B. L. O'Dell, *J. Nutr.*, 119 (1989) 1654–1660.
- 15 M. Z. Nichaman, C. C. Sweeley, N. M. Oldham and R. E. Olson, *J. Lipid Res.*, 4 (1963) 484–485.
- 16 E. N. Ashworth, J. B. St. John, M. N. Christiansen and G. W. Patterson, *J. Agric. Food Chem.*, 29 (1981) 881–884.
- 17 W. R. Morrison and L. M. Smith, *J. Lipid Res.*, 5 (1964) 600–608.
- 18 D. J. Hanahan and J. E. Ekholm, *Methods Enzymol.*, 31 (1974) 168–172.
- 19 M. Seewald and H. M. Eichinger, *J. Chromatogr.*, 469 (1989) 271–280.
- 20 K. Eder, A. M. Reichlmayr-Lais and M. Kirchgessner, submitted for publication.
- 21 J. MacGee and M. G. Williams, *J. Chromatogr.*, 205 (1981) 281–288.
- 22 K. Eder, A. M. Reichlmayr-Lais and M. Kirchgessner, *J. Chromatogr.*, 588 (1991) 265–272.
- 23 J. R. Yandrasitz, G. Berry and S. Segal, *J. Chromatogr.*, 225 (1981) 319–328.
- 24 T. L. Kaduce, K. C. Norton and A. A. Spector, *J. Lipid Res.*, 24 (1983) 1398–1403.
- 25 E. B. Hoving, J. Prins, H. M. Rutgers and F. A. J. Muskiet, *J. Chromatogr.*, 434 (1988) 411–416.
- 26 F. B. Jungalwala, J. E. Evans and R. H. McCluer, *Biochem. J.*, 155 (1976) 5–60.
- 27 K. Shimbo, *Agric. Biol. Chem.*, 50 (1986) 2643–2645.
- 28 R. M. C. Dawson, N. Hemington and D. B. Lindsay, *Biochem. J.*, 77 (1960) 226–230.
- 29 G. J. Nelson, in E. G. Perkins (Editor), *Analysis of Lipids and Lipoproteins*, American Oil Chemists Society, Champaign, IL, 1975, pp. 1–22.
- 30 K. Eder, A. M. Reichlmayr-Lais and M. Kirchgessner, submitted for publication.
- 31 G. J. Nelson, in G. J. Nelson (Editor), *Blood Lipids and Lipoproteins: Quantification, Composition and Metabolism*, Wiley-Interscience, New York, 1972, pp. 318–386.
- 32 J. W. Farquhar, *Biochim. Biophys. Acta*, 60 (1962) 80–89.
- 33 S. E. Carlson, P. G. J. D. Carvier and S. G. House, *J. Nutr.*, 116 (1986) 718–725.
- 34 G. J. Nelson, *Biochim. Biophys. Acta*, 144 (1967) 221–232.
- 35 W. Haude, H. Oginscius and E. Goetze, *Acta Biol. Med. Ger.*, 18 (1967) 589–595.
- 36 F. A. Kuypers, S. Abraham, B. Lubin and D. Chiu, *J. Lab. Clin. Med.*, 111 (1988) 529–536.
- 37 J. A. Schouten, A. C. Beynen, C. Popp-Snijders and C. Mulder, *Nutr. Rep. Int.*, 31 (1985) 229–235.
- 38 D. F. Horrobin, Y. S. Huang, S. C. Cunnane and M. S. Manku, *Lipids*, 19 (1984) 806–811.

CHROM. 24 001

Determination of muramic acid by high-performance liquid chromatography–plasma spray mass spectrometry

Ingrid Elmroth*

Department of Technical Analytical Chemistry, University of Lund, Chemical Center, Box 124, 221 00 Lund (Sweden)

Lennart Larsson

Department of Medical Microbiology, University of Lund, Sölveg. 23, 223 62 Lund (Sweden)

Gunilla Westerdahl and Göran Odham

Department of Ecology, Division of Chemical Ecology, University of Lund, Helgonav. 5, 223 62 Lund (Sweden)

(First received October 11th, 1991; revised manuscript received January 8th, 1992)

ABSTRACT

A high-performance liquid chromatographic–plasma spray mass spectrometric method was developed for the determination of muramic acid, a unique compound present in bacterial peptidoglycan. The method included hydrolysis of bacterial samples by hydrochloric acid, purification using a disposable extraction column, and separation using cation-exchange chromatography with a mobile phase composed of ammonium acetate–trifluoroacetic acid–water. Muramic acid was detected in cells of *Bacillus subtilis*; the presence of yeast cells (*Saccharomyces cerevisiae*) in excess amounts did not interfere with the analyses. In contrast to currently applied liquid and gas chromatographic methods, the described method permits highly selective determination of underivatized muramic acid, and may therefore be useful for detecting bacteria and bacterial cell debris in complex biological matrices.

INTRODUCTION

The bacterial cell wall contains several compounds unique to prokaryotic organisms. A basic structure is the peptidoglycan backbone, which consists of alternating molecules of N-acetylglucosamine and N-acetylmuramic acid linked by β -1,4 glycosidic bonds. As N-acetylmuramic acid is absent in non-bacterial biological matter, including other microorganisms (*e.g.*, viruses and fungi) [1,2], it can be used as a chemical marker for determining bacterial cells or cell debris in various environments. With this in mind, muramic acid has been used as the analyte in the chemical detection of peptidoglycan, *e.g.*, in mammalian tissues [3], soil [4], marine sediments [5] and human septic synovial fluids [6]. As opposed to culturing techniques,

which only provide information on the viable portion of bacteria present in a sample, chemical analysis of muramic acid does not discriminate between live and dead cells.

During the past decade, several methods for determining muramic acid by chromatographic and mass spectrometric (MS) techniques have been described. Gas chromatographic (GC) and GC–electron impact (EI) MS analysis of alditol acetate [3,7] and aldonitrile acetate [8,9] derivatives, and of N-heptafluorobutyl ester derivatives [10,11] have been performed. In addition, some investigators have applied high-performance liquid chromatographic (HPLC) methods using either precolumn fluorescence derivatization with *o*-phthaldialdehyde [4,5,12] or postcolumn redox reaction with bis(1,10-phenanthroline)copper(II) as a mediator

for amperometric detection [13]. For all of the described methods, derivatization of the analyte is required in order to achieve high sensitivity and selectivity in the detection.

In this study, an HPLC–MS method was developed for the determination of muramic acid after a minimum of sample pretreatment and without derivatization. To obtain high sensitivity, selected ion monitoring (SIM) was applied. The selectivity of this method is illustrated by the determination of muramic acid in pure cultures of *Bacillus subtilis* and in *B. subtilis* cultures in the presence of excess amounts of yeast (*Saccharomyces cerevisiae*).

EXPERIMENTAL

Materials

The following chemicals were used: muramic acid (purity 99%; Sigma, St. Louis, MO, USA), N-methyl-D-glucamine (purity 99%; Aldrich Chemie, Steinheim, Germany), ammonium acetate and acetonitrile (analytical-reagent grade; Merck, Darmstadt, Germany) and trifluoroacetic acid (purity protein-sequencing grade; Fluka, Buchs, Switzerland). Bond Elut C₁₈ octadecyl solid-phase 1-ml extraction columns were purchased from Analytichem International (Harbor City, CA, USA). Before use, all glassware was washed in 5% Deconex (Borer Chemie, Zuchwil, Switzerland), rinsed several times with hot tap water and distilled water and then heated for 10 h at 400°C.

Microorganisms

Bacillus subtilis (ATCC 6051) was cultivated overnight on blood-agar plates at 37°C. *Saccharomyces cerevisiae* was isolated from baker's yeast by cultivation on Rogosa agar plates (Oxoid, Basingstoke, UK) overnight at 32°C. The bacterial and yeast cells were transferred into 10-ml test-tubes and washed three times by repeated centrifugations and dispersions in distilled water; after the final centrifugation, the sediments were lyophilized.

Chromatography

Different conditions for the chromatographic separations were evaluated using an LDC Model III Constametric pump and either an LDC Spectro-Monitor III variable-wavelength UV detector (operating at 220 nm) or an LDC RefractoMonitor re-

fractive index detector (LDC, Riviera Beach, FL, USA). A Rheodyne (Cotati, CA, USA) Model 7010 injector equipped with a 10- or 20- μ l loop was used to inject samples onto a cation-exchange column (100 \times 4.0 mm I.D.) packed with Nucleosil 5-SA (5- μ m particles) (Macherey–Nagel, Düren, Germany). The mobile phase was a 0.02 M aqueous solution of ammonium acetate with the pH adjusted to 2.5 by addition of trifluoroacetic acid. A flow-rate of 0.7 ml/min was used, and most compounds eluted within 30 min. After analysing biological samples for 1 week, the column was reconditioned with ten column volumes of 1% trifluoroacetic acid to avoid any interference from previously injected, late-eluting compounds.

Separations were also performed using a 100 \times 4.6 mm I.D. column packed with Spherisorb aminopropylsilica gel (5- μ m particles) (Phase Separations, Queensferry, UK) and with acetonitrile–water (82:18, v/v) as the mobile phase (1 ml/min). Biological samples were not analysed with this column.

Chromatography–mass spectrometry

The HPLC–MS experiments were performed on a Waters Model 600 MS delivery system (Millipore, Milford, MA, USA) equipped with a 60- μ l variable-volume loop injector (Rheodyne, Model 7000). The effluent from the column was introduced into a quadrupole mass spectrometer (Model Trio 3; VG, Altrincham, UK) via the standard VG thermospray–plasma spray probe.

Full mass spectra were obtained by scanning from m/z 110 to avoid the solvent ions. The temperature of the capillary vaporizer was 220°C and that of the ion source 235°C. In the plasma spray studies the discharge current was 230 μ A, whereas in the thermospray studies no discharge current was used. When using thermospray the ammonium acetate concentration of the mobile phase (pH 6.8) was increased to 0.1 M. In the selected ion monitoring (SIM) analyses, the ion of m/z 234 was used for determining muramic acid and that of m/z 196 for determining N-methyl-D-glucamine. All the SIM analyses were performed using the plasma spray interface.

When the aminopropylsilica gel column was used, the vaporizer capillary temperature was 250°C, the ion source temperature 230°C and the discharge current 250 μ A.

Sample treatment

Biological samples containing bacteria and/or yeast (0.25–3 mg dry weight) were hydrolysed at 90°C under nitrogen for 2.5 h in 0.5 ml of 6 M HCl. After cooling, water (0.5 ml) and the internal standard N-methyl-D-glucamine (25 µg) were added. The hydrolysates were purified by loading them on the solid-phase extraction columns (conditioned with one volume of methanol and three volumes of water prior to use) and eluting them with 4 × 0.5 ml of water; following this procedure, the samples were lyophilized. The residues were dissolved in 0.5–1 ml of the mobile phase before HPLC–plasma spray MS analysis (see above).

Muramic acid reference compound: calibration, recovery, stability

A calibration graph for pure muramic acid was constructed using the HPLC–MS step with plasma spray SIM analysis (*m/z* 234) in the range 6.5–250 ng. A constant amount (50 ng) of N-methyl-D-glucamine added to each sample served as the internal standard.

To evaluate the recovery of muramic acid and the internal standard in the purification, ten standard samples of a mixture of muramic acid and internal standard (5 µg of each) in 1 ml of 3 M HCl were prepared. Five of the samples were purified, lyophilized as described under *Sample treatment* and analysed by HPLC–plasma spray MS (SIM mode). The remaining five samples were treated in the same manner, but the purification step was omitted. The recoveries were evaluated by comparing the absolute responses of the purified standard samples with those obtained from the unpurified samples.

On chromatography of muramic acid on the cation-exchange column (UV detection) a fraction containing a rapidly eluting compound (retention time 1.6 min), in addition to the muramic acid fraction (retention time 4 min), were collected. The stability of these compounds after storage at 4°C (for 1 and 3 days and 1 and 8 weeks) was studied using HPLC–MS (scanning mode).

Biological samples

All biological samples were analysed using the plasma spray interface. To study the accuracy of the method, 0–22 µg of muramic acid were added to hydrolysates of 250 µg of *B. subtilis*, after which the

samples were subjected to the whole determination procedure (*i.e.*, sample treatment, and HPLC–MS). To determine the recovery of muramic acid, the peak areas were compared with those obtained from reference experiments in which 25 µg of muramic acid (dissolved in the mobile phase) were analysed by HPLC–MS directly (without further sample pre-treatment).

The recovery was calculated as the slope of the graph of the amount of muramic acid found *versus* the known amount added. The amount found was calculated by comparison with the peak area of the reference experiment. A reference sample was analysed immediately before each sample.

To study the precision of using internal standardization, the same experiments were performed after addition of 25 µg of internal standard to the sample and reference solutions.

To determine the amount of muramic acid in *B. subtilis*, 1.4, 0.6 and 0.7 mg dry weight of bacteria were analysed.

In a separate experiment, aliquots of a mixture of bacteria (1.4 mg/ml) and yeast (1.6 mg/ml), prepared as described under *Sample treatment*, were diluted with different volumes of a likewise prepared yeast sample (2.7 mg/ml) to investigate whether the presence of a 5–50-fold excess concentration of yeast in the bacterial samples interfered with the detection of muramic acid.

RESULTS

Chromatography

When using the cation-exchange column, the retention time of muramic acid was 4 min. The compound appeared as a double peak, with the α - and β -anomers partly separated. Either a UV (220 nm) or a refractive index (RI) detector could be used for muramic acid detection, whereas only an RI detector could be used for detection of the internal standard (retention time 8 min). A higher concentration of ammonium acetate or a lower concentration of trifluoroacetic acid in the mobile phase (higher pH) shortened the retention time of muramic acid. The flow-rate (0.7 ml/min) was chosen to fit the vacuum pump capacity of the mass spectrometer.

Using the aminopropylsilica gel column the α - and β -anomers of muramic acid co-eluted at a retention time of 9 min. However, when the mobile

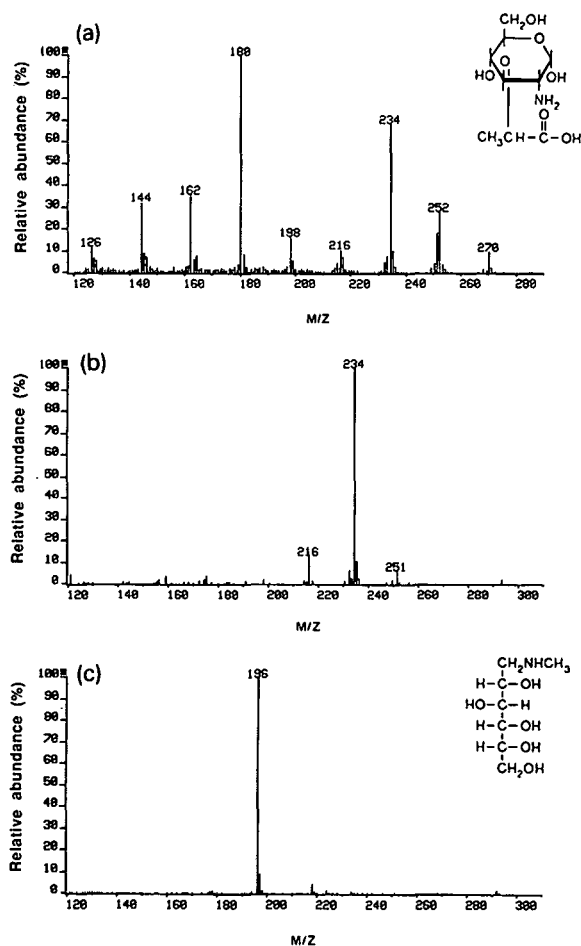


Fig. 1. Mass spectra of (a) muramic acid, (b) a degradation or conversion product of muramic acid and (c) N-methyl-D-glucamine. All three spectra were recorded using HPLC-plasma spray MS.

phase was led from this column into the mass spectrometer, the vaporizer capillary became clogged after a few hours. This phenomenon was not observed when the mobile phase was led directly into the mass spectrometer (*i.e.*, without first passing through the column). Degradation products from the aminopropylsilica gel were considered to be the cause of the problem, and this stationary phase was not used in subsequent analyses.

Chromatography-mass spectrometry

A plasma spray mass spectrum of pure muramic acid after cation-exchange chromatography is

shown in Fig. 1a. The MS ionization conditions were chosen to give a maximum of high-mass fragments. The molecular adduct ion of m/z 252 ($M + 1$) was detected, as were other prominent ions presumably resulting from addition or successive losses of water molecules resulting in fragments of m/z 270 ($+ 1 H_2O$), 234 ($- 1 H_2O$), 216 ($- 2 H_2O$), 198 ($- 3 H_2O$), 180 ($- 4 H_2O$) and 162 ($- 5 H_2O$). The fragment of m/z 162 may also originate from the loss of the carboxylic acid-containing group $COOH-CHOH-CH_3$ (m/z 90) and the fragment of m/z 144 from an additional loss of one molecule of water. The fragmentation patterns of the two anomers of muramic acid were virtually identical.

A rapidly eluting compound (retention time 1.6 min) was detected on injection of the muramic acid reference compound onto the cation-exchange column. Total ion current (TIC) analyses of the collected muramic acid fraction revealed that after 3 days of storage more than 99% of muramic acid remained, after 1 week 97% and after 8 weeks 42%; the amounts of the rapidly eluting compound increased correspondingly. As ions of m/z 216, 234 and 251 were present in its plasma spray mass spectrum (Fig. 1b), the compound was assumed to be a degradation or conversion product of muramic acid. When analysing the fraction containing this compound after storage for up to 8 weeks, muramic acid did not appear, indicating that the degradation or conversion reaction was irreversible.

The molecular adduct ion of m/z 196 ($M + 1$) was seen in the plasma spray mass spectrum of N-methyl-D-glucamine (Fig. 1c).

The fragment of m/z 234 was abundant in the mass spectrum of muramic acid and was therefore used for the muramic acid measurements in the SIM analyses. Analogously, the fragment of m/z 196 was selected for N-methyl-D-glucamine. Fig. 2 shows selected ion current profiles of muramic acid reference compound (13 ng) and N-methyl-D-glucamine (50 ng).

The detection limit for muramic acid was 3 ng at a signal-to-noise ratio of 3:1, and a linear calibration graph was found in the measured interval (Fig. 3). In the purification, the recovery of muramic acid was 96% ($s_{n-1} = 3\%$, $n = 5$) and that of N-methyl-D-glucamine was 108% ($s_{n-1} = 8\%$, $n = 5$).

A thermospray MS fragmentation pattern of muramic acid is shown in Fig. 4. As in the plasma

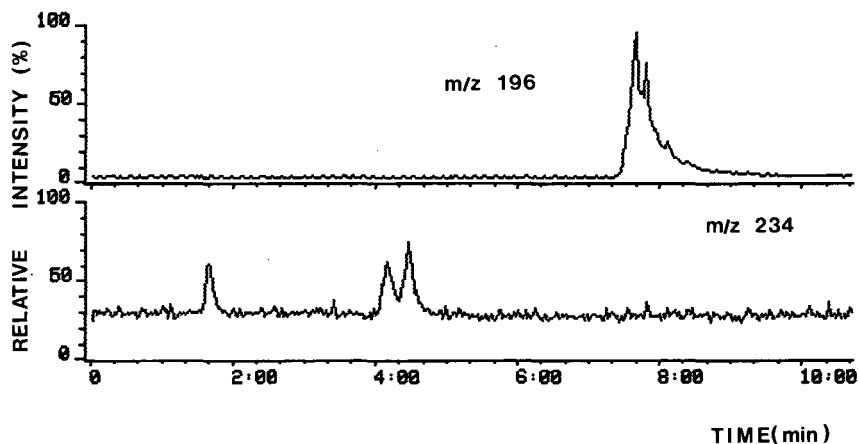


Fig. 2. HPLC-plasma spray MS (SIM) analysis of 13 ng of muramic acid (bottom trace, retention time 4.2–4.4 min, focused at m/z 234) and 50 ng of the internal standard N-methyl-D-glucamine (top trace, retention time 7.6 min, focused at m/z 196).

spray mass spectrum, the molecular adduct ion of m/z 252 ($M+1$) and also ions presumably representing addition or losses of water molecules were found. The ion of m/z 234 was less abundant than when using plasma spray ionization.

Biological samples

The identity of muramic acid in the SIM analyses of the bacteria was ascertained by monitoring three ions: m/z 270, 252 and 234 (Fig. 5). Fig. 6 shows the results of adding increasing amounts of muramic acid to *B. subtilis* samples. The data in Fig. 6a are equivalent to quantification by external standardization. A straight line ($y = 0.84x + 7.9$) was fitted to the data; the slope, corresponding to the absolute

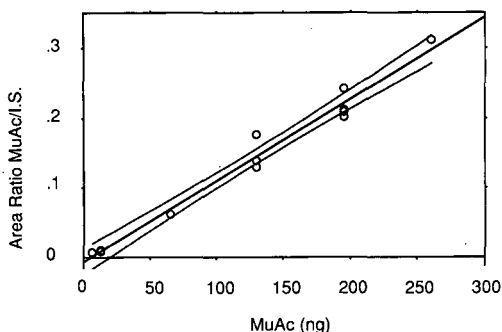


Fig. 3. Calibration graph based on muramic acid and the internal standard (MuAc/I.S.) from HPLC-plasma spray MS (SIM) determinations. The method of least squares was used to fit straight lines to the individual data. A 95% confidence interval of the true area ratio is included.

recovery of muramic acid, was $84 \pm 28\%$ (95% confidence interval); the intercept corresponded to the amount of muramic acid in the bacteria. In the plot in Fig. 6b, internal standardization was used in the quantification; a straight line ($y = 1.5x + 8.9$) was fitted to the data.

The mean amount of muramic acid in dried cells of *B. subtilis* was found to be 2.2% (w/w) (2.1, 2.2, 2.4%).

Fig. 7 illustrates the correlation between the bacterial concentration and the concentration of muramic acid. Notably, the presence of yeast cells in the samples, even in amounts 5–50 times larger compared with bacteria (2.3–2.6 and 0–0.49 mg/ml, respectively), did not interfere with the detection of muramic acid. Muramic acid was not found in pure yeast samples. The superior selectivity of MS over

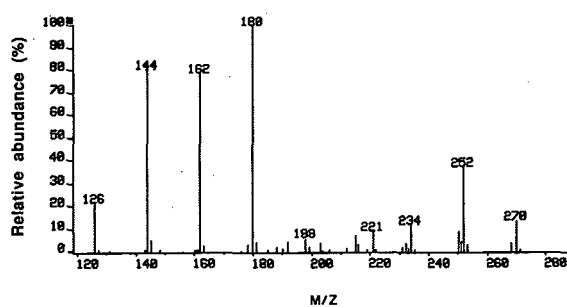


Fig. 4. Mass spectrum of muramic acid obtained using HPLC-thermospray MS.

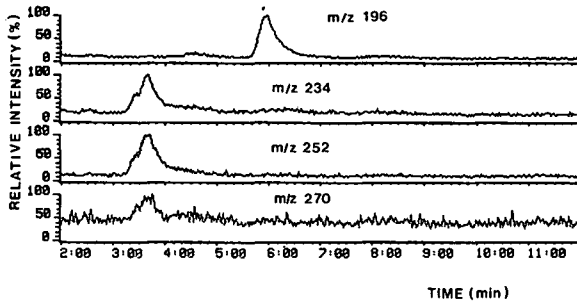


Fig. 5. HPLC-plasma spray MS (SIM) analysis of *Bacillus subtilis* cells monitoring the ions of *m/z* 196 (N-methyl-D-glucamine) and 234, 252 and 270 (muramic acid). The injected amount corresponded to 50 μg (dry weight) of bacteria.

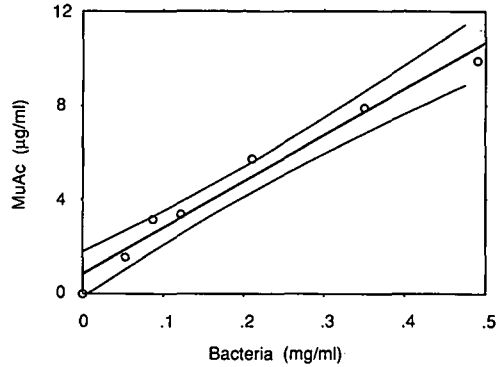


Fig. 7. Muramic acid (MuAc) concentrations in *Bacillus subtilis* preparations in the presence of excess amounts (2.3–2.6 mg/ml, dry weight) of yeast cells (*Saccharomyces cerevisiae*). The method of least squares was used to fit a straight line to the data. A 95% confidence interval of the true amounts of muramic acid is included.

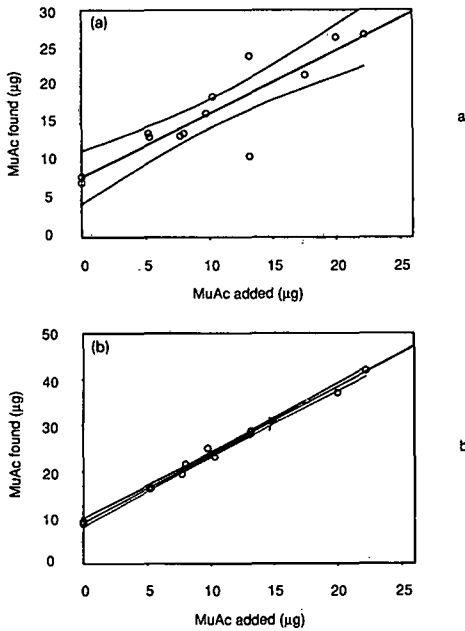


Fig. 6. (a) Test of accuracy of HPLC-plasma spray MS (SIM) analysis of muramic acid added in increasing amounts to *Bacillus subtilis* samples. (b) Comparison of found and added amounts of muramic acid using determination by HPLC-plasma spray MS (SIM) with internal standardization. The method of least squares was used to fit straight lines to the data. 95% confidence intervals of the true amounts of muramic acid amounts are included.

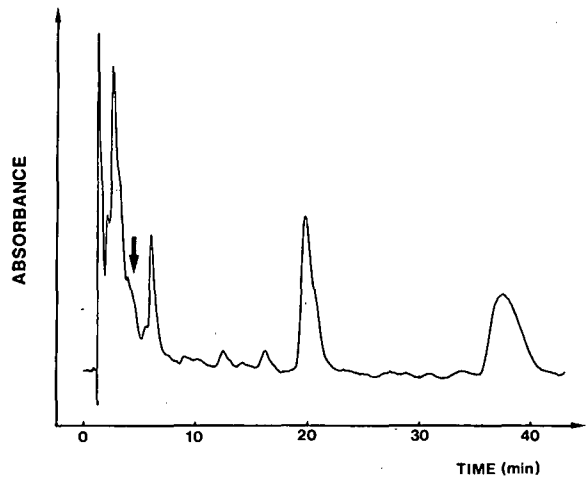


Fig. 8. HPLC-UV detection (220 nm) of a 1:1 (w/w) mixture of cells of *Bacillus subtilis* and yeast (*Saccharomyces cerevisiae*). The arrow indicates the retention time for muramic acid.

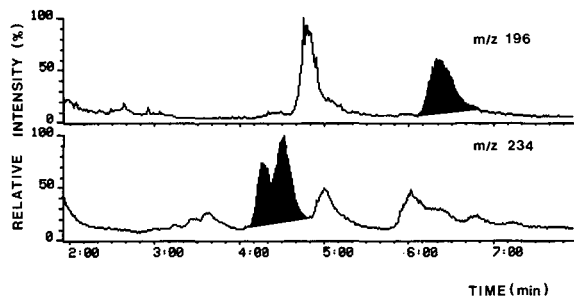


Fig. 9. HPLC-plasma spray MS (SIM) analysis of muramic acid (m/z 234, bottom trace, black peak) and N-methyl-D-glucamine (m/z 196, top trace, black peak) in a 1:5 (w/w) mixture of cells of *Bacillus subtilis* and *Saccharomyces cerevisiae*.

UV detection is illustrated in Figs. 8 and 9, which show analyses of bacteria-yeast hydrolysates. Muramic acid co-eluted with other compounds and could only be detected when the HPLC-MS technique was used. Notably, the sample analysed by HPLC-MS contained a fivefold lower bacteria-to-yeast ratio than the sample analysed with UV detection; the total amount of yeast cells was identical.

DISCUSSION

Muramic acid is a unique compound, as it is present in bacterial peptidoglycan but absent elsewhere in nature. The amount of muramic acid in bacteria varies between different strains and genera, and there is usually more in Gram-positive than in Gram-negative species [9]. Muramic acid has been used as a chemical marker for the determination of bacteria, *e.g.*, in soil [4], and surface microlayers and sediments in marine environments [5]. This acid has also been used for the detection of bacterial cell debris in mammalian tissues in animal models of arthritis [14] and for the detection of bacteria in joint fluids from patients with septic arthritis [6]. Another possible use for muramic acid determination is in the detection of bacterial infections in eukaryotic cell cultures used in biotechnical processes. We have previously reported the application of GC-MS analysis of 3-hydroxymyristic acid in industrial fermentations as a means of detecting trace levels of Gram-negative bacteria [15]. In contrast to GC-MS methods, HPLC-MS allows several microbial constituents, such as amino acids and carbohydrates, to be analysed underivatized. This means

that sample treatment will be simplified considerably and that there will be a decrease in the overall analysis time.

Throughout this study, the samples were dissolved in the mobile phase to ensure constant chromatographic conditions. To avoid long retention times and to obtain good peak shapes, a comparatively short column (100 mm \times 4.0 mm I.D.) was used. After prolonged use, the ability of the column to separate the α - and β -anomers of muramic acid decreased and the retention times were reduced (Fig. 5).

When determining the recovery of muramic acid from bacterial samples (Fig. 6a), the data points were greatly scattered, resulting in a wide confidence interval; this shows the disadvantage of using external standardization where variations in injection volumes and, perhaps of more importance, ionization conditions are not compensated for. The precision was significantly improved by internal standardization (Fig. 6b), although the amounts found were significantly higher than the amounts added, which may indicate some imperfections in the behaviour of the internal standard.

An advantage of using MS as the HPLC detector when analysing complex samples is the high selectivity offered. Because of this selectivity, the muramic acid determinations in this study were possible, even though appreciable amounts of water-soluble cellular hydrolysis products (*e.g.*, carbohydrates, amino acids and peptides) were co-injected owing to the minimum of sample purification. The measurement of three ions typical of muramic acid (m/z 234, 252 and 270), at identical retention times and with similar peak shapes, ascertained the identity of muramic acid in the sample (Fig. 5). There was no indication that co-eluting substances interfered with the determination of muramic acid in *B. subtilis* cells in the presence of high concentrations of *S. cerevisiae* (Figs. 7 and 9). In contrast, UV detection in HPLC analysis of a corresponding sample was insufficient, despite a more favourable bacteria-to-yeast ratio (Fig. 8).

Degradation of muramic acid in water solution has been reported previously [11]. As fragments of m/z 216, 234 and 251 were found in the mass spectrum of the degradation product, it might represent a lactam compound formed by conversion of muramic acid [8,16]. Clearly, the rapid elution of the

product from the cation-exchange column indicates that no interaction occurs. This degradation of muramic acid should be taken into account in quantitative studies of biological samples.

A major advantage of plasma spray over thermospray MS is the wide choice of mobile phases that can be used. This means that whereas thermospray MS requires a volatile ionic buffer with high ionic strength for the ionization, effluents from both normal- and reversed-phase columns can be introduced directly into the MS system under plasma spray conditions. In the thermospray analyses of muramic acid, the ammonium acetate concentration had to be increased from 0.02 to 0.1 M to achieve sufficient ionic strength; this also resulted in a higher pH. Under these conditions, muramic acid was not retarded on the stationary phase. Therefore, to be able to use thermospray analysis of muramic acid in complex matrices, the ammonium acetate has to be added postcolumn.

The development of HPLC-MS techniques has been intensified during recent years, resulting in improvements in reproducibility and sensitivity. The detection limit (3 ng) of the described assay for muramic acid corresponds to about $3 \cdot 10^5$ bacterial cells, provided that muramic acid accounts for 1% of the total cell mass and that the dry weight per cell is $1 \cdot 10^{-12}$ g. HPLC methods utilizing fluorescence detection may offer lower detection limits [4,5], but these methods also entail much lower selectivity than mass spectrometric detection. GC-MS is a sensitive and very useful method for the determination of muramic acid, but the need for derivatization leads to extensive sample handling. At present, GC-MS cannot be used in applications where a short analysis time is required [3,7-9].

The HPLC-MS technique described here may represent an interesting alternative to traditional microbiological methods, *e.g.*, to detect bacterial contamination of eukaryotic cultures in industrial fermentations. For this specific application, rapid

and specific detection of small amounts of the contaminating bacteria is desirable. Owing to the extreme complexity of sample matrices containing eukaryotic cells, cultivation medium and various metabolites, the selectivity of the proposed method should be very valuable.

ACKNOWLEDGEMENTS

We thank Agneta Walhagen and Per Erlandsson for valuable advice concerning the HPLC work and Professor K. G. Wahlund for critically reading the manuscript. This work was supported by the Biotechnology Research Foundation (Sweden).

REFERENCES

- 1 K. H. Schleifer, *Methods Microbiol.*, 18 (1985) 123.
- 2 A. Fox, J. C. Rogers, J. Gilbert, S. L. Morgan, C. H. Davis, S. Knight and P. B. Wyrick, *Infect. Immun.*, 58 (1990) 835.
- 3 J. Gilbert, A. Fox, R. S. Whiton and S. L. Morgan, *J. Microbiol. Methods*, 5 (1986) 271.
- 4 L. Zelles, *Biol. Fertil. Soils*, 6 (1988) 125.
- 5 T. Mimura and J. C. Romano, *Appl. Environ. Microbiol.*, 50 (1985) 229.
- 6 B. Christensson, J. Gilbert, A. Fox and S. L. Morgan, *Arthritis Rheum.*, 32 (1989) 1268.
- 7 A. Fox and S. L. Morgan, in W. H. Nelson (Editor), *Instrumental Methods for Rapid Microbiological Analysis*, Verlag Chemie, Deerfield Beach, FL, 1985, pp. 135-164.
- 8 R. H. Findlay, D. J. W. Moriarty and D. C. White, *Geomicrobiol. J.*, 3 (1983) 135.
- 9 L. W. Eudy, M. D. Walla, S. L. Morgan and A. Fox, *Analyst (London)*, 110 (1985) 381.
- 10 A. Tunlid and G. Odham, *J. Microbiol. Methods*, 1 (1983) 63.
- 11 C. Er, B. Nagy, E. C. Riser, K. H. Schram and P. F. Baker, *Geomicrobiol. J.*, 5 (1987) 57.
- 12 T. Mimura and D. Delmas, *J. Chromatogr.*, 280 (1983) 91.
- 13 N. Watanabe, *J. Chromatogr.*, 316 (1984) 495.
- 14 A. F. Wells, J. A. Hightower, C. Parks, E. Kufoy and A. Fox, *Infect. Immun.*, 57 (1989) 351.
- 15 I. Elmroth, A. Valeur, G. Odham and L. Larsson, *Biotechnol. Bioeng.*, 35 (1990) 787.
- 16 R. S. Whiton, P. Lau, S. L. Morgan, J. Gilbert and A. Fox, *J. Chromatogr.*, 347 (1985) 109.

CHROM. 24 010

Screening for amines by dansylation and automated high-performance liquid chromatography

Neil P. J. Price*,☆

School of Biological Sciences, Queen Mary and Westfield College, University of London, Mile End Road, London E1 4NS (UK)

John L. Firmin

John Innes Institute, John Innes Centre for Plant Science Research, Colney Lane, Norwich NR4 7UH (UK)

David O. Gray

School of Biological Sciences, Queen Mary and Westfield College, University of London, Mile End Road, London E1 4NS (UK)

(First received July 25th, 1991; revised manuscript received December 30th, 1991)

ABSTRACT

A reversed-phase high-performance liquid chromatographic procedure for the determination of a broad range of amines after derivatization with dansyl chloride is presented. Forty-five amines were tested over the concentration range 2–16 μM . Linear calibration graphs passing through the origin were obtained with 25 amines. The method was applied to the identification of biogenic amines from *Agrobacterium*-transformed plant tissue. Reliability and ease of operation make the procedure particularly well suited to automation, permitting the rapid analysis of a large number of samples.

INTRODUCTION

Transformation of plants by *Agrobacterium* sp. has a profound effect on their development and nitrogen metabolism [1,2]. An investigation of the role of amines in the transformation required an automated procedure to analyse a large number of plant tissue extracts for the broadest possible range of primary and secondary amines, with the option of recovering fractions for spectroscopic characterization.

The simultaneous determination of all biogenic amines is difficult because of their structural diversity [3], and in the absence of any other common

moiety their determination has tended to rely on derivatization of the amino group [4,5]. Fluorescamine [6], *o*-phthalaldehyde (OPA) [7] and naphthalene-2,3-dicarboxaldehyde (NDA) [8] have been used for this purpose, but only react with primary amino groups. 4-Chloronitrobenzoxadiazole (NBD) [9] also reacts with secondary amines but, like OPA, the derivatives are often unstable, and not suitable for spectroscopic analysis. Dansyl [10] and benzoyl [11,12] derivatives cannot be detected at as low a concentration or as selectively as the corresponding fluorescent derivatives [13,14].

Dansyl chloride is a particularly well established reagent [15] and gives highly fluorescent sulphonamide derivatives with both primary and secondary amines that are relatively stable, have improved chromatographic properties and are readily isolated from the hydrolysis product, dansyl sulphonate (dansyl-OH), by solvent extraction. Sensitive and

* Present address: Laboratoire de Biologie Moléculaire des Plantes Supérieures, Université de Genève, 1 Ch. de l'Imperatrice, CH-1292 Chambesy/Geneva, Switzerland.

selective detection is possible with a fluorescence detector, and dansylated derivatives have also proved useful for spectroscopic identification [16,17].

However, although well established, the separation of dansylated amines by high-performance liquid chromatography (HPLC) is not particularly suited to automation. Aqueous buffers are often used to improve separation, but continuous use can corrode pumps or, worse, give gradual precipitation [18]. The low solubility of some dansylated amines in aqueous solvent mixtures can also lead to gradual over-pressure problems. We have therefore developed a new method for the determination of a

broad range of amines which is compatible with the use of automated HPLC. Over 40 amines were tested, of which 25 gave linear calibration graphs over the concentration range 2–16 μM . Most earlier methods have tended to focus selectively on a small group of amines, particularly catecholamines [19] or the polyamines [20], and few have been applicable to automation [18].

We also observed that the reaction of agmatine (4-guanidinobutyl-1-amine) with dansyl chloride led to a cleavage of the guanido group and, therefore, the major dansylation product of agmatine was always didansylputrescine.

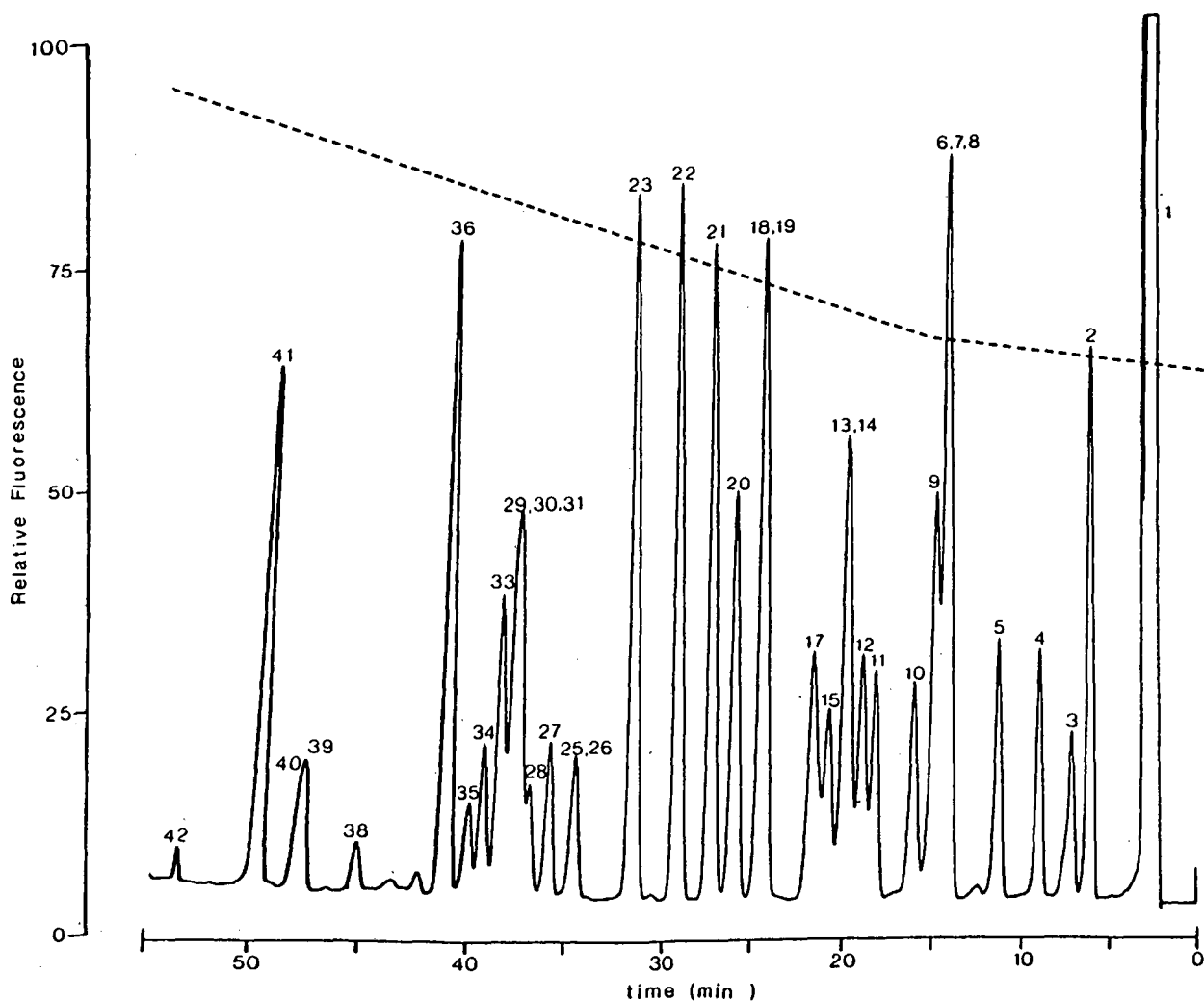


Fig. 1. HPLC of dansylated amine standards separated on a Spheri-5 RP-18 reversed-phase column. The methanol-water gradient shown as a broken line is as described under Experimental. Each peak represents 0.9 nmol of amine. Peak numbers refer to Table I.

EXPERIMENTAL

Agmatine was obtained from Sigma (Poole, UK) (95% pure grade) and from Aldrich (Poole, UK) (99% pure grade). All other chemicals were obtained from Sigma.

The HPLC system consisted of a Model 401 diluter and Model 231 autoinjector (Gilson, Villiers-le-Bel, France), a Rheodyne (Cotati, CA, USA) Model 7010 injector valve fitted with a 50- μ l loop, and two LDC III G Constametric pumps (LDC-Milton Roy, Riviera Beach, FL, USA). A 25 cm \times 4.6 mm I.D. Brownlee Spheri-5 RP-18 reversed-phase C₁₈ (5 μ m particle size) column was used, protected by a similarly packed 3 cm \times 4.6 mm I.D. guard column (Brownlee, Santa Clara, CA, USA). Detection was accomplished with a Perkin-Elmer (Beaconsfield, UK) LS4 spectrofluorimeter (3- μ l cell) set at 340 nm excitation and 540 nm emission (10-nm bandwidth).

A methanol-water gradient (flow-rate 1 ml/min) was used, consisting of three linear sections: 0 min, 60% methanol; 15 min, 67% methanol; 54 min, 95% methanol; 60 min, 60% methanol. A period of 10 min was allowed to re-equilibrate the system after each run.

Derivatization procedure

Amines in aqueous solution (100 μ l; 15 nmol) were derivatized by adding dansyl chloride in acetone (400 μ l; 5 mg/ml). After saturation with solid sodium hydrogencarbonate, the mixture was reacted in the dark for 15 h at room temperature. Excess of acetone was then removed by warming at 60°C for 10 min and the mixture was diluted to 1 ml with water. Dansylated amines were extracted by vortex mixing for 20 s with 3 \times 2 ml of toluene. The phases were separated by centrifugation (2700 g; 10 min) and the upper layer was removed and evaporated to dryness under a stream of air. Plant tissue extracts were derivatized by the same procedure. At all stages exposure to light was kept to a minimum.

The dansylated samples were redissolved in 500 μ l of methanol and centrifuged (9000 g; 4 min). The autoinjector made 30- μ l (0.9-nmol) injections.

RESULTS AND DISCUSSION

A typical chromatogram of dansylated amines is shown in Fig. 1. Forty-five amines were tested, of

which 30 were sufficiently separated to allow recognition from retention data (Table I). Gramine, indole and creatinine did not dansylate under the reaction conditions. Every other amine, with the exception of agmatine, gave a single peak after correcting for the blank, indicating that amines able to undergo dansylation at more than one position were in fact completely derivatized.

In addition to the hydrolysis product, the dansylation reaction always gives rise to dansyldimethylamine and dansylmethylamine from partial cleavage of the dimethylamino moiety [15]. All chromatograms therefore had peaks at 2.2 min (dansyl-OH), 8.6 min (dansylmethylamine) and 13.7 min (dansyldimethylamine). Excess of dansyl chloride co-eluted with the dansyldimethylamine by-product. Ammonia is a common contaminant of samples and reagents, so a peak was usually observed at 5.9 min for dansylated ammonia. Phenolics and thiols are also derivatized, but are easily distinguished from dansylated amines because they fluoresce at higher wavelenths [15].

An application of the method is shown in Fig. 2. Biogenic amines from a crown gall culture of *Cinchona ledgeriana* transformed with *A. tumefaciens* strain A6 were readily separated. Fifteen peaks were identified by reference to the standard retention times in Table I.

Agmatine samples always gave a major didansylputrescine peak (identified by spiking), and sometimes a minor peak presumed to be monodansylagmatine (Fig. 3). The agmatine samples were checked by OPA derivatization [7] and did not contain significant amounts of putrescine, suggesting that the didansylputrescine arose during the dansylation reaction, probably from partial cleavage of the agmatine guanido group. Similar decomposition to a putrescine derivative occurs when agmatine is benzoylated [11,12].

It is common HPLC practice to dissolve samples prior to injection in the solvent mixture to be used at the start of the HPLC gradient. Consequently, aqueous methanol (60%, v/v) was initially used for this purpose. However, it was noted that the detector response was non-linear under these conditions, and that the preinjection solutions were often cloudy. This suggested that some or all of the dansylated amines were at best only partially soluble in 60% (v/v) aqueous methanol. The solubilities of selected

TABLE I
HPLC RETENTION TIMES (t_R) OF DANSYLATED AMINES

All retention times quoted (except for dansylated agmatine) are the means of eight separate readings. Standard deviations (S.D.) were calculated for the same data. The derivative numbers refer to the numbered HPLC peaks shown in Fig. 1.

No.	Derivative	Mean t_R (min)	S.D. (min)	No.	Derivative	Mean t_R (min)	S.D. (min)
1	Dansyl-OH	2.2	0.10	23	1,6-Diaminohexane	31.1	0.19
2	Ammonia	5.9	0.04	24	N-Methylputrescine	34.0	0.12
3	Ethanolamine	6.9	0.08	25	D,L-Octopamine	34.0	0.16
4	Methylamine	8.6	0.05	26	Histamine	34.4	0.12
5	Ethylamine	11.0	0.04	27	3-Methoxy-4-hydroxy- benzylamine	35.3	0.17
6	Dimethylamine	13.7	0.08	28	Serotonin	36.3	0.13
7	Iso-propylamine	13.7	0.08	29	Metanephrine	36.9	0.11
8	Dansyl-Cl	13.7	0.08	30	3-Hydroxy-4-methoxy- phenylethylamine	36.9	0.11
9	n-Propylamine	14.5	0.11	31	3-Methoxy-p-tyramine	37.3	0.13
10	Phenylethanolamine	15.6	0.09	32	1,7-Diaminoheptane	37.4	0.12
11	Norephedrine	17.8	0.11	33	D,L-Synephrine	37.7	0.11
12	Isobutylamine	18.9	0.18	34	p-Tyramine	38.5	0.09
13	n-Butylamine	19.4	0.11	35	o-Tyramine	39.2	0.11
14	Benzylamine	19.4	0.11	36	Spermidine	40.4	0.13
15	Tryptamine	20.4	0.08	37	Homospermidine	41.5	—
16	Agmatine	20.8	—	38	Norepinephrine	44.4	0.13
17	L-Ephedrine	21.3	0.08	39	D,L-Epinephrine	46.6	0.15
18	Isoamylamine	23.8	0.10	40	Dopamine	47.0	0.12
19	2-Phenylethylamine	23.8	0.10	41	Spermine	48.6	0.13
20	1,3-Diaminopropane	25.5	0.11	42	5-Hydroxydopamine	53.6	0.04
21	Putrescine	26.7	0.11				
22	Cadaverine	28.6	0.17				

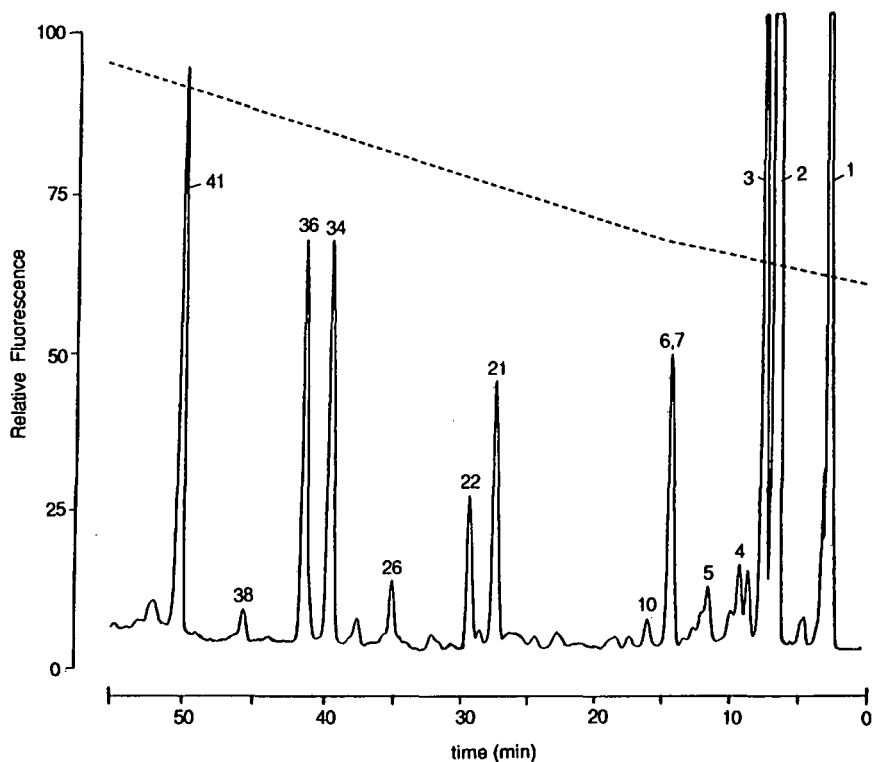


Fig. 2. HPLC separation of dansylated amines from *Cinchona ledgeriana*-*A. tumefaciens* strain A6 crown gall culture (40 mg fresh weight). Conditions as described in the text. Peak numbers refer to Table I.

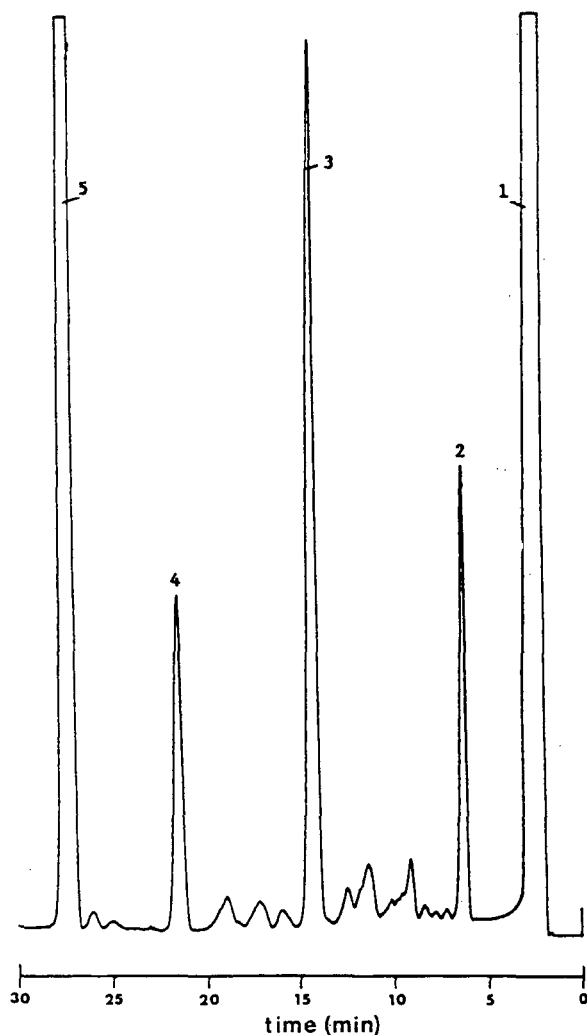


Fig. 3. HPLC of dansylated agmatine. Partial decomposition of the guanido group gives rise to didansylputrescine. Details are described in the text. Peaks: 1 = dansyl-OH; 2 = dansylated ammonia; 3 = excess of dansyl chloride/dansyldimethylamine; 4 = monodansylagmatine; 5 = didansylputrescine.

TABLE II

SOLUBILITIES OF DANSYLATED AMINES AT 25°C

Excess of solid dansylated amine was shaken overnight at 25°C with 0.2 ml of the stated solvent. Duplicate aliquots were taken and diluted to 1.5 ml. The weight of dansylated amine present was determined by measuring the absorbance at the λ_{\max} and applying the previously determined molar absorptivity.

Dansylated amine	Maximum solubility (mmol/ml)			
	Ethyl acetate	Methanol	60% aq. methanol	30% aq. acetonitrile
Spermidine	>8.63	3.2	0.155	0.12
Histamine	24.2	5.9	1.05	0.34
Diaminopropane	>24.9	>52.0	3.25	4.05
Cadaverine	>9.14	>9.7	1.84	0.22
Putrescine	0.92	0.38	0.10-0.13	0.12
Ammonia	4.51	10.0	2.26	1.78

TABLE III
RELATIVE FLUORESCENCE INTENSITIES OF DANSYLATED AMINES

Dansylated amine	No. of dansyl groups ^a	Relative fluorescence intensity		
		%F ^b per 0.1 nmol	Normalized ^c	<i>r</i> ^d
Spermine	4	47.77	100.0	1.000
Spermidine	3	29.17	61.1	0.999
Cadaverine	2	21.23	44.5	0.998
Putrescine	2	20.83	43.6	0.997
1,6-Diaminohexane	2	20.40	42.7	0.999
Ethanolamine	1	18.33	38.4	1.000
<i>n</i> -Propylamine	1	18.13	38.0	0.999
Ethylamine	1	17.90	37.5	1.000
Iso butylamine	1	15.63	32.7	0.999
Synephrine	2	14.57	30.5	1.000
1,3-Diaminopropane	2	12.90	27.0	1.000
Ephedrine	1	12.70	26.6	0.999
3-Methoxy- <i>p</i> -tyramine	2	12.30	25.8	1.000
Phenylethanolamine	1	12.06	25.3	0.999
<i>p</i> -Tyramine	2	11.23	23.5	0.998
Norephedrine	1	10.40	21.8	1.000
Tryptamine	1	9.80	20.5	0.998
3-Methoxy-4-hydroxybenzylamine	2	8.97	18.8	0.997
Epinephrine	3	8.13	17.0	0.999
Dopamine	3	5.83	12.2	0.999
Norepinephrine	3	4.57	9.6	0.999
<i>o</i> -Tyramine	1	4.17	8.7	0.999
5-Hydroxydopamine	4	2.07	4.3	0.997
Histamine	2	1.67	3.5	1.000
Serotonin	2	1.47	3.1	1.000

^a Number of dansyl moieties on each derivative.

^b Percentage fluorescence, an arbitrary scale based on peak height.

^c Relative fluorescence intensities normalized on the tetradansylspermine response (nominally assigned as 100).

^d Correlation coefficients, calculated from four replicates per point.

dansylated amines were measured in 100% methanol, 60% (v/v) aqueous methanol, 100% ethyl acetate and 30% (v/v) aqueous acetonitrile. The results, shown in Table II, suggested that low solubility in 60% (v/v) aqueous methanol might indeed be a factor. After making the preinjection dilutions in 100% methanol, 25 out of 28 amines tested (Table III) gave reproducible ($r > 0.997$) linear calibration graphs over the concentration range 2–16 μM , all with zero intercept. Ammonia, methylamine and dimethylamine derivatives were the exceptions, probably because of the high background levels arising from the dansylation reaction.

The relative fluorescence intensities of the dansylated amines obtained from the gradients of the

calibration graphs are given in Table III. With 340-nm excitation and 540-nm emission, settings chosen to optimize the detection of derivatives with a range of different emission wavelengths, tetradansylspermine had the highest relative fluorescence intensity measured, and was 33 times more fluorescent than didansylserotonin. The detection limits varied with the relative intensities, but were generally of the order of 5–10 pmol (signal-to-noise ratio = 3).

Simplicity, ease of operation and reliability are prerequisites of automated HPLC. It is particularly important that there is no gradual accumulation of precipitates. We therefore avoided the use of buffers, and also determined the solubility of some dansylamines in aqueous solvents. We found that

comparable methods used to determine a broad range of amines [13,14] were unsuitable for automation, and eventually led to problems of over-pressure. Other workers [18] have reported that precipitates gradually form in the phosphate buffer used by Hayman *et al.* [14]. In contrast, Seiler [15] used a simple methanol-water gradient, but did not consider the low and variable solubilities of dansylated amines. The method described here overcomes both of these disadvantages. In one instance the HPLC system was run continuously for 72 h, the autoinjector making 66 injections without encountering any problems, and in our experience the method is particularly suited to screening for novel amines from plant tissue.

ACKNOWLEDGEMENTS

We thank the Science and Engineering Research Council for financial support (N.P.J.P.) and Dr. R. J. Robins of the AFRC Food Research Institute, Norwich, UK, for the gift of transformed plant tissue.

REFERENCES

- 1 J. Martin-Tanguy, D. Tepfer, M. Paynot, D. Burtin, L. Heisler and C. Martin, *Plant Physiol.*, 92 (1990) 912.
- 2 S. D. Mitchell, J. L. Firmin and D. O. Gray, *Biochem. J.*, 221 (1984) 891.
- 3 T. A. Smith, *Annu. Rev. Plant Physiol.*, 36 (1985) 117.
- 4 N. Seiler, *J. Chromatogr.*, 379 (1986) 157.
- 5 K. Imai, T. Toyooka and H. Miyano, *Analyst (London)*, 109 (1984) 1365.
- 6 K. Imai, P. Bohlen, S. Stein and S. Udenfriend, *Arch. Biochem. Biophys.*, 161 (1974) 161.
- 7 D. F. Bushey, D. M. Law and P. J. Davies, *Anal. Biochem.*, 167 (1987) 36.
- 8 T. Kawasaki, T. Higushi, K. Imai and O. S. Wong, *Anal. Biochem.*, 180 (1989) 279.
- 9 R. S. Fager, C. B. Cutina and E. W. Abrahamson, *Anal. Biochem.*, 53 (1973) 590.
- 10 J. K. Lin and J. K. Chang, *Anal. Chem.*, 47 (1985) 1634.
- 11 H. E. Flores and A. W. Galston, *Plant Physiol.*, 69 (1982) 701.
- 12 R. D. Slocum, H. E. Flores, A. W. Galston and L. H. Weinstein, *Plant Physiol.*, 89 (1989) 512.
- 13 N. Seiler, B. Knodgen and F. Eisenbeiss, *J. Chromatogr.*, 145 (1978) 29.
- 14 A. R. Hayman, D. O. Gray and S. V. Evans, *J. Chromatogr.*, 325 (1985) 462.
- 15 N. Seiler, *Methods Biochem. Anal.*, 18 (1970) 259.
- 16 A. R. Hayman and D. O. Gray, *Phytochemistry*, 28 (1989) 673.
- 17 D. A. Durden, B. A. Davis and A. A. Boulton, *Biomed. Mass Spectrom.*, 1 (1974) 83.
- 18 J. R. L. Smith, A. U. Smart, F. E. Hancock and M. V. Twigg, *J. Chromatogr.*, 547 (1991) 447.
- 19 R. W. Roos and C. A. Lau-Cam, *J. Chromatogr.*, 555 (1991) 278.
- 20 Y. Saeki, N. Uehara and S. Shirakawa, *J. Chromatogr.*, 145 (1978) 221.

High-performance liquid chromatographic analysis of benzodiazepines using diode array, electrochemical and thermospray mass spectrometric detection

Ira S. Lurie*, Donald A. Cooper and Robert F. X. Klein

Special Testing and Research Laboratory, Drug Enforcement Administration, 7704 Old Springhouse Road, McLean, VA 22102-3494 (USA)

(First received October 15th, 1991; revised manuscript received January 6th, 1992)

ABSTRACT

Twenty benzodiazepines were examined via a combination of high-performance liquid chromatography (HPLC)–diode array–dual electrochemical detection and HPLC–thermospray mass spectrometric detection. Although UV detection at 230 nm resulted in extensive overlap of the benzodiazepines, each compound gave unique UV spectra. Twenty percent of the benzodiazepines tested gave response ratios via oxidation detection, and the values obtained were unique. All compounds except chlorazepate gave MH^+ ions as the base peak via thermospray-mass spectrometric detection with filament off; additional ions were detected for many compounds. Using single ion chromatograms all benzodiazepines can be chromatographically resolved.

INTRODUCTION

Benzodiazepines are a commonly prescribed group of drugs well known for their sedative, hypnotic and anticonvulsant effects. Because of their potential for abuse, their analysis is of forensic interest. Typical submissions to forensic laboratories consist of solid-dosage forms and biological specimens.

Gas chromatography (GC) with flame ionization [1–4], electron-capture [4] and mass spectrometric (MS) detection [2–5] have been employed for the analysis of benzodiazepines. Some of these compounds are difficult to analyze via GC because of thermal decomposition [2–4]; in addition, derivatization may be required because of adsorption of benzodiazepines containing hydroxy groups on active sites of the GC column [5].

High-performance liquid chromatography (HPLC) [6–9] has been used for the direct analysis of these compounds. Analysis via retention time alone using single-wavelength detection which lacks specificity is commonly employed. The use of dual-

wavelength detection [9,10], diode array detection [9], electrochemical detection in the reduction mode [11,12] and MS detection [13] have all been used to increase specificity of analysis. Huang *et al.* [13] used a heated pneumatic nebulizer interface with atmospheric pressure ionization mass spectrometry for the analysis of 5 benzodiazepines.

In this paper a multi-detection approach for the HPLC analysis of benzodiazepines is reported. These compounds were examined via a combination of HPLC–diode array–dual electrochemical detection in the oxidation mode and HPLC–thermospray MS detection. The structures for the 20 benzodiazepines examined in this study are shown in Fig. 1.

EXPERIMENTAL

Equipment

Two HPLC systems were employed in this study. For diode array and electrochemical detection, a Series 4 liquid chromatograph (Perkin-Elmer, Norwalk, CT, USA) fitted with an ISS 100 autosampler

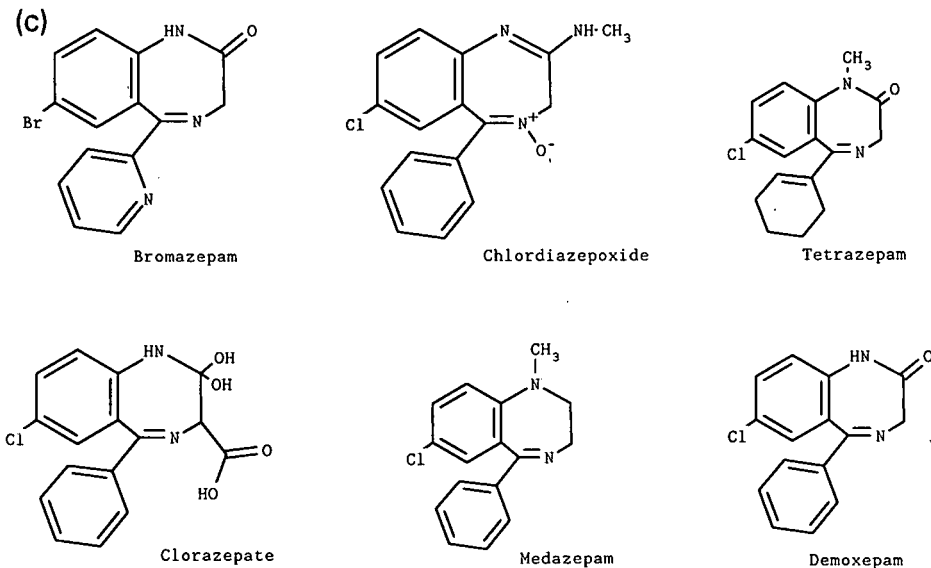
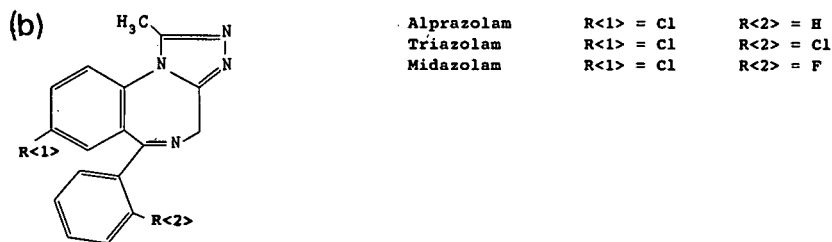
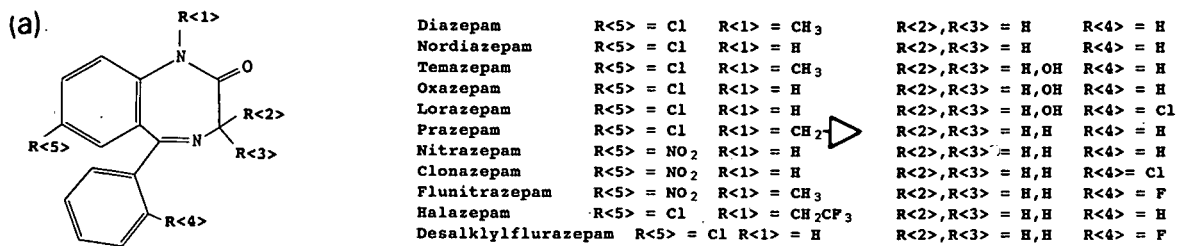


Fig. 1. Structures of benzodiazepines. For explanation of a-c see text.

(Perkin-Elmer); a Partisil ODS-3, 5- μ m column (11.0 cm \times 4.7 mm I.D.) (Whatman, Clifton, NJ, USA); a 1040 M diode array detection system (Hewlett-Packard, Waldbronn, Germany); and an

LC-4B dual amperometric detector fitted with a dual TL-5 glassy carbon electrode cell in the parallel mode, and a Ag/AgCl reference detector with the top half of the cell serving as the auxiliary electrode

(Bionalytical Systems, West Lafayette, IN, USA) were used. For UV and thermospray MS detection, a Series 4 liquid chromatograph fitted with a valve injector (Rheodyne, Cotati, CA, USA), a Partisil ODS-3, 5- μ m column, an LC85 UV detector (Perkin-Elmer), a switching valve (Rheodyne), an electronically activated switching valve (Valco), a thermospray interface (Vestec Corporation, Houston, TX, USA) and a 4630 quadrupole mass spectrometer (Finnigan MAT, San Jose, CA, USA) were employed. The manual switching valve was used for either flow or column injection while the electronically activated switching valve was used to divert sample either to the thermospray source or to waste.

Materials

Acetonitrile and ammonium acetate were HPLC grade. Water suitable for HPLC analysis and thermospray-mass spectrometric analysis was obtained from a Milli-Q system (Millipore Corporation). All other chemicals were reagent grade. Benzodiazepine drug standards of United States Pharmacopeia/National Formulary quality were employed.

The HPLC mobile phase was internally mixed from solvent reservoirs containing acetonitrile or 0.1 M ammonium acetate buffer.

Chromatographic procedure

For HPLC analysis using the diode array and electrochemical detectors 1 mg of benzodiazepine standard was dissolved in 20.0 ml mobile phase prior to a 10- μ L injection onto the liquid chromatograph. When analyzing benzodiazepines using UV and thermospray MS detection, 1 mg of standard or 1 mg each of several standards were dissolved in 20.0 ml mobile phase prior to 50–200- μ L injections onto the liquid chromatograph.

HPLC mobile phase consisted of 0.1 M ammonium acetate–acetonitrile (60:40, v/v) at a flow-rate of 1.3 ml/min.

Mass spectrometric procedure

The column effluent was introduced into the mass spectrometer via a thermospray LC–MS interface. The vaporizer was operated at 220°C while a source block temperature of 250°C was used. The repeller was set at 45 V. The mass spectrometer was operated under full scan acquisition (m/z 104–500) with a 3-s scan.

RESULTS AND DISCUSSION

As shown in Table I there is extensive overlap in retention times between the various benzodiazepines examined via HPLC and UV detection at 230 nm. However, all compounds gave unique UV spectra via diode array detection, *i.e.*, no two spectra directly overlapped. Overall a large number of the spectra can be divided into 3 broad categories. Category 1, as shown in Fig. 2a, contains the generalized 1,4-benzodiazepine structure shown in Fig. 1a. For this category, R<5> = Cl, R<4> = H, Cl or F, R<1> = H, CH₃ or cyclopropylmethyl and R<2>, R<3> = H, H or H, OH. All compounds except lorazepam have UV maxima at 228.5 nm (lorazepam 232.5 nm). In addition, all compounds have UV maxima at 318 nm. Category 2 spectra, as shown in Fig. 2b, also contain the generalized 1,4-benzodiazepine structure shown in Fig. 1a. For this category R<5> = NO₂, R<4> = H, Cl or F and R<1> = H or CH₃. Flunitrazepam and clonazepam have UV maxima at 252.5 nm while nitrazepam has a UV maximum at 258.5 nm. In addition, all 3 compounds have UV maxima at 310.5 nm.

TABLE I

RETENTION DATA AND DUAL ELECTROCHEMICAL RESPONSE RATIOS FOR BENZODIAZEPINES

Compound	Retention time (min)	Area 1.1 V / Area 1.0 V
Clorazepate	1.2, 1.3	
Bromazepam	2.6	
Demoxepam	2.7	
Oxazepam	3.4	10.5
Lorazepam	3.8	13.2
Chlordiazepoxide	4.0	63.8
Nitrazepam	4.1	
Clonazepam	4.5	
Alprazolam	4.6	
Triazolam	4.8	
Desalkylflurazepam	4.9	
Nordiazepam	5.4	
Temazepam	5.5	
Flunitrazepam	5.8	
Diazepam	8.2	
Midazolam	11.5	
Tetraazepam	13.5	
Prazepam	17.2	
Halazepam	17.5	
Medazepam	23.1	1.38

Category 3, as shown in Fig. 2c, contain the generalized benzodiazepine structure shown in Fig. 1b. For this category $R<1> = \text{Cl}$ and $R<2> = \text{H, Cl}$ or F. The spectra of the remaining benzodiazepines are shown in Fig. 2d. Clorazepate injected via the autosampler gives 2 peaks with identical UV spectra near the solvent front, which suggests that peak splitting may be occurring. The cause of this phenomena is not clear.

Using dual electrochemical detection in the parallel mode at oxidation potentials of 1.0 and 1.1 V, certain benzodiazepines were found to be electrochemically active. As shown in Table I, the values obtained were unique. The electrooxidation mechanism of chlordiazepoxide, lorazepam, medazepam and oxazepam have been previously examined

[14,15] by means other than HPLC. The use of dual electrochemical detection in series with diode array detection results in a significantly higher degree of specificity of detection.

Caution must be exercised in using electrochemical ratios because of potentially poor day-to-day reproducibility [16]. Changes in ratios can result from drifts in the reference-electrode redox potential, from over-potential effects or from variations in temperature. The injection-to-injection reproducibility is much better. The dual electrochemical ratio for medazepam on a given day did not change by more than 5% over a 7-h period. Therefore, suspected compounds should be confirmed by standard injection on the same day of analysis.

In addition, all the benzodiazepines analyzed in

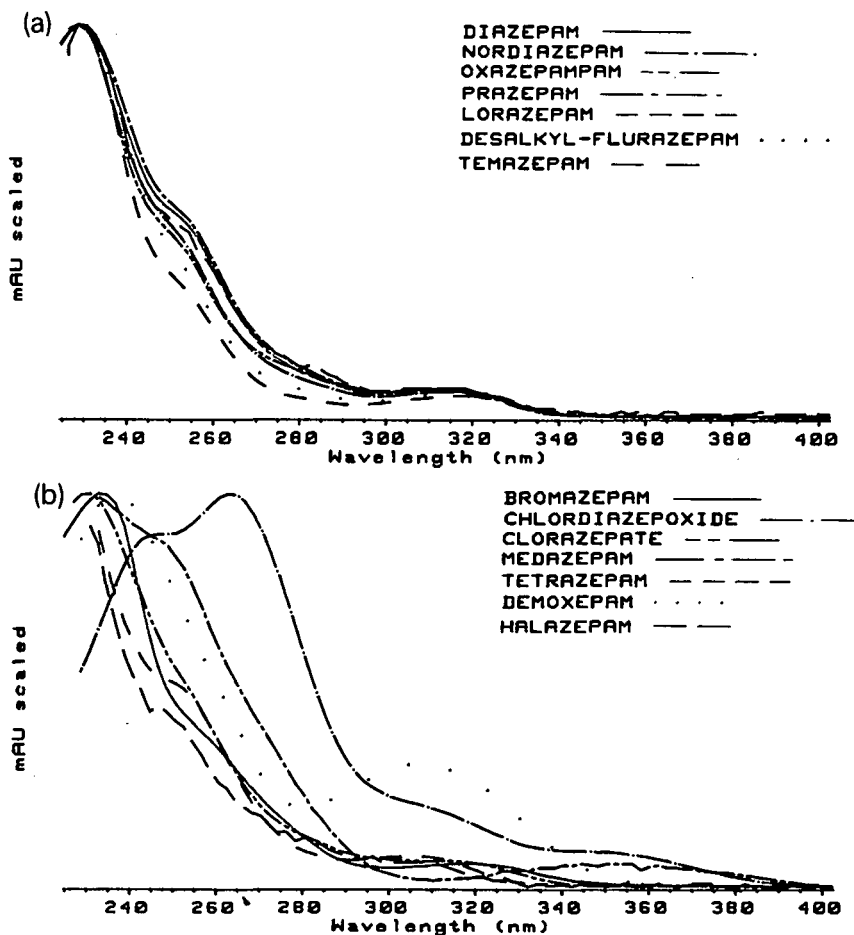


Fig. 2.

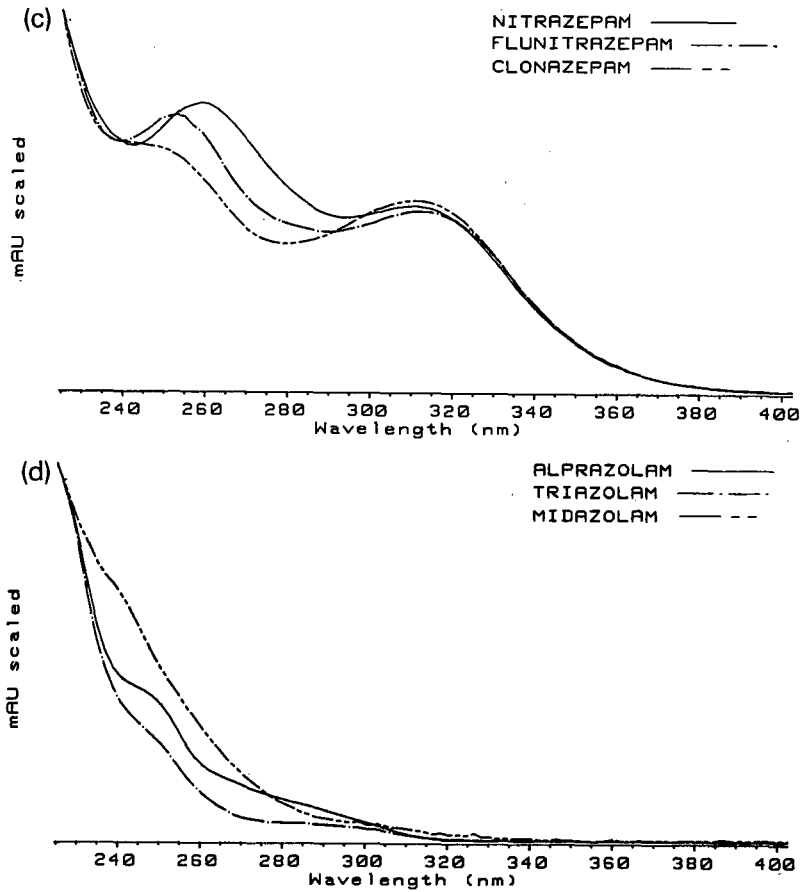


Fig. 2. UV spectra of benzodiazepines. For explanation of a-d see text.

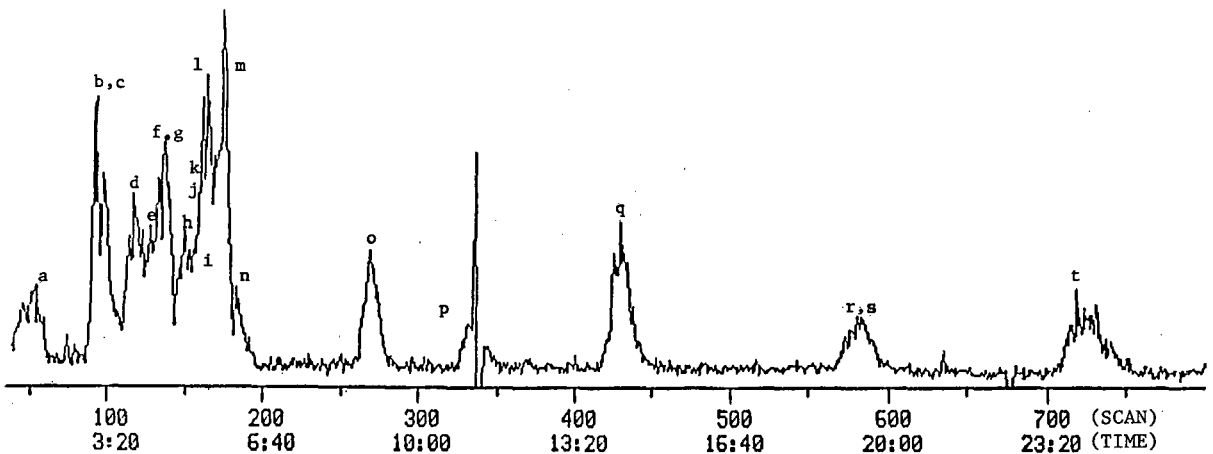


Fig. 3. Reconstructed ion chromatogram for LC-MS of a mixture of standard benzodiazepines. Peaks: a = clorazepate; b = bromazepam; c = demoxepam; d = oxazepam; e = lorazepam; f = chlordiazepoxide; g = nitrazepam; h = clonazepam; i = alprazolam; j = triazolam; k = desalkylflurazepam; l = nordiazepam; m = temazepam; n = flunitrazepam; o = diazepam; p = midazolam; q = tetrazepam; r = prazepam; s = halazepam; t = medazepam. Times scale in min:s.

this study would be expected to give electrochemical response ratios in the reduction mode [12] due to the presence of a diphenylimine moiety. This is in contrast to the higher specificity of detection in the oxidation mode, where only 20% of the compounds were electrochemically active. However, analysis in the reduction mode requires a slow reflux of the eluent to deoxygenate the mobile phase and the presence of coulometric detector prior to a mercury electrode for high-sensitivity work [12].

HPLC-MS, as shown in Fig. 3, was also investigated for the analysis of benzodiazepines. A summary of the spectral data for the thermospray-mass spectrometric detection of the benzodiazepines obtained with filament off is shown in Table II. In all instances except clorazepate, the $[M + H]^+$ ion is the base peak. For clorazepate, the base peak is the $[M + H - CO_2 - H_2O]^+$ ion. This ion is formally identical to the MH^+ ion derived from nordiazepam. It should be noted that although nordiazepam and clorazepate give very similar mass spectra, their retention times as shown in Table I are vastly differ-

ent and thus these compounds are chromatographically distinct. It has been shown that at a slightly basic pH (mobile phase pH for this study 6.8), the decarboxylation of clorazepate to nordiazepam is delayed [6]. For most of the benzodiazepines the only ion of any consequence is $[M + H]^+$. Demoxepam and chlordiazepoxide, both containing N-oxides, exhibit a small relative abundance of $[M + H - O]^+$ ions. In addition, oxazepam and lorazepam, both containing H and OH groups at the <2> and <3> positions, exhibit a relatively high abundance of $[M + H - H_2O]^+$ ions. It is unclear at this point why temazepam, which also contains H and OH groups at the <2> and <3> positions, does not also show this loss. It is of interest to note that most of the benzodiazepines contain either a single Cl, Br or two Cl atoms. Because of natural isotopic abundances of these halogens, additional characteristic mass fragment ions are observed which increase the specificity of the mass spectral data.

Besides providing characteristic mass fragment

TABLE II
MASS SPECTRA (THERMOSPRAY IONIZATION) OF BENZODIAZEPINES

Relative abundance in parentheses.

Benzodiazepine	<i>m/z</i>		
	$[M + H]^+$	$[M + H - O]^+$	$[M + H - H_2O]^+$
Clorazepate	271(100) ^a		
Bromazepam	316(100)		
Demoxepam	287(100)	271(1)	
Oxazepam	287(100)		269(56)
Lorazepam	321(100)		303(55)
Chlordiazepoxide	300(100)	284(1)	
Nitrazepam	282(100)		
Clonazepam	316(100)		
Alprazolam	309(100)		
Triazolam	343(100)		
Desalkylflurazepam	289(100)		
Nordiazepam	271(100)		
Temazepam	301(100)		
Flunitrazepam	314(100)		
Diazepam	285(100)		
Midazolam	326(100)		
Tetrazepam	289(100)		
Prazepam	325(100)		
Halazepam	353(100)		
Medazepam	271(100)		

^a $[M + H - CO_2 - H_2O]^+$

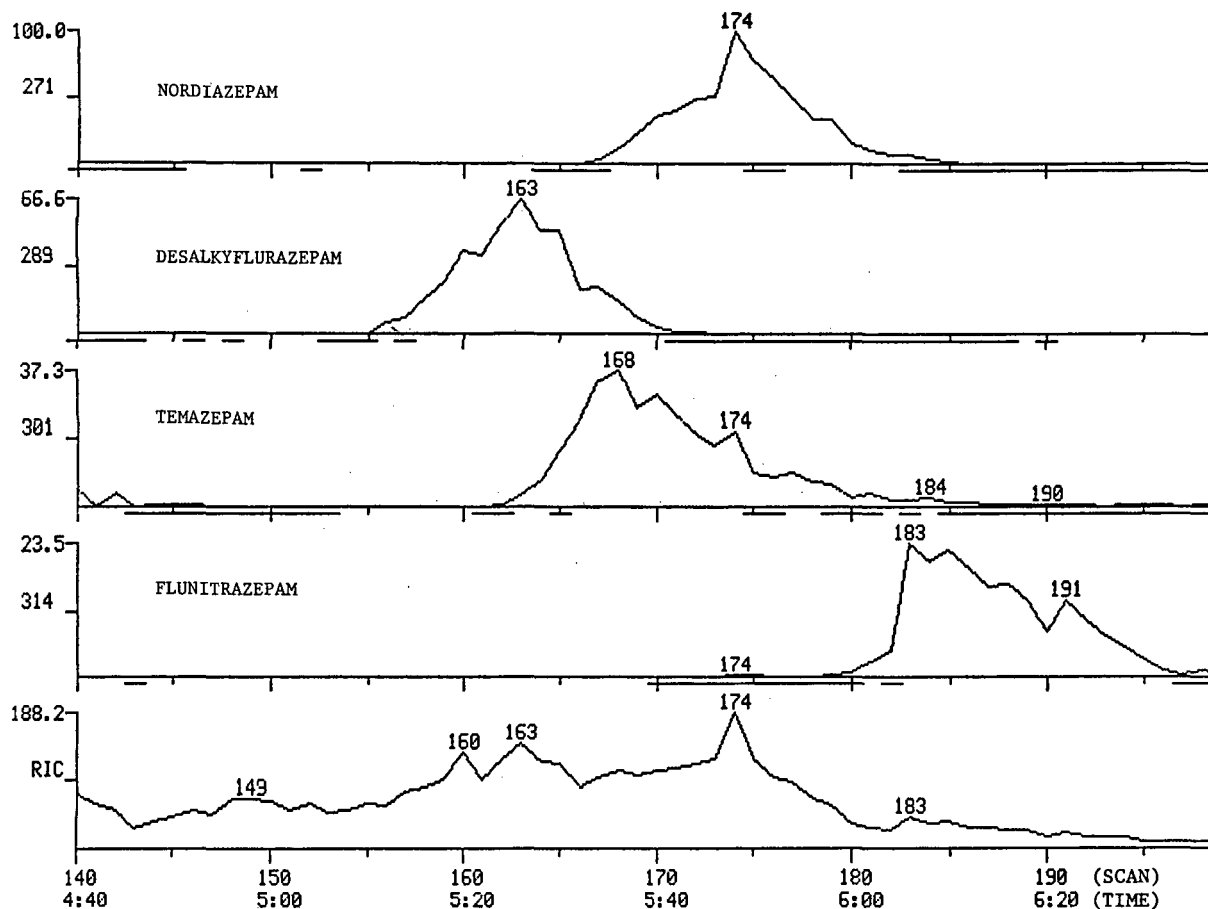


Fig. 4. Ion chromatograms and reconstructed ion chromatogram for LC-MS of a mixture of standard benzodiazepines. Time scale in min:s.

ions, one of the great utilities of HPLC-thermospray MS detection is the ability to perform single-ion monitoring (SIM) to deconvolute complex chromatograms. This capability is illustrated in Fig. 4, where 4 benzodiazepines that overlap in a reconstructed ion chromatogram can be resolved using SIM. In fact, all 20 benzodiazepines can be chromatographically resolved using SIM.

CONCLUSION

The combination of complimentary diode array, dual electrochemical and thermospray MS detection greatly increases the specificity of HPLC analysis of benzodiazepines. This technique is potentially applicable to both solid-dosage forms and biological specimens.

ACKNOWLEDGEMENT

The authors thank Charles Harper for the preparation of the figures containing chemical structures.

REFERENCES

- 1 M. Chiarotti, N. De Giovanni and A. Fiori, *J. Chromatogr.*, 358 (1986) 169.
- 2 M. Japp, K. Garthwaite, A. V. Geeson and M. D. Osselton, *J. Chromatogr.*, 439 (1988) 317.
- 3 S. I. Weston, M. Japp, J. Partridge and M. D. Osselton, *J. Chromatogr.*, 538 (1991) 277.
- 4 W. Sadee and E. van der Kleijn, *J. Pharm. Sci.*, 60 (1971) 135.
- 5 C. D. Coassolo, C. Aubert, P. Coassolo and J. P. Cano, *J. Chromatogr.*, 487 (1989) 295.
- 6 F. T. Noggle and C. R. Clark, *J. Assoc. Off. Anal. Chem.*, 62 (1979) 799.

- 7 R. Gill, B. Law and J. P. Gibbs, *J. Chromatogr.*, 356 (1986) 37.
- 8 P. Mura, A. Piriou, P. Fraillon, Y. Papet and D. Reiss, *J. Chromatogr.*, 416 (1987) 303.
- 9 F. T. Noggle, C. R. Clark, and J. De Ruitter, *J. Liq. Chromatogr.*, 13 (1990) 4005.
- 10 J. D. Wittwer, *J. Liq. Chromatogr.*, 3 (1980) 1713.
- 11 W. Lund, M. Hannisdal and T. Greibokk, *J. Chromatogr.*, 173 (1979) 249.
- 12 J. B. F. Lloyd and D. A. Parry, *J. Chromatogr.*, 449 (1988) 281.
- 13 E. C. Huang, T. Wachs, J. J. Conboy and J. D. Henion, *Anal. Chem.*, 13 (1990) 713A.
- 14 W. F. Smyth and A. Ivastia, *Analyst (London)*, 110 (1985) 1377.
- 15 W. F. Smyth, J. S. Burmicz and A. Ivastia, *Analyst (London)*, 107 (1982) 1019.
- 16 X. D. Ding and I. S. Krull, *J. Liq. Chromatogr.*, 6 (1983) 2173.

Investigation of enantioselectivity and enantiomeric elution order of propranolol and its ester derivatives on an ovomucoid-bonded column

Jun Haginaka*, Chikako Seyama, Hiroyuki Yasuda and Koichi Takahashi

Faculty of Pharmaceutical Sciences, Mukogawa Women's University, 11–68, Koshien Kyuban-cho, Nishinomiya, Hyogo 663 (Japan)

(First received September 10th, 1991; revised manuscript received January 7th, 1992)

ABSTRACT

The enantioselectivity and enantiomeric elution order of racemic propranolol (PP) and its ester derivatives (O-acetyl, -propionyl, -butyryl and -valeryl) on an ovomucoid (OVM)-bonded silica column were investigated with respect to eluent pH (from 3 to 7) and organic modifier (2-propanol, ethanol, methanol and acetonitrile). The enantioselectivity was dependent on the eluent pH and organic modifier used. Reversal of the enantiomeric elution order of racemic PP and its ester derivatives occurred around eluent pH 5–7 and/or by variation of the organic modifier used. The results reveal that chiral recognition or binding properties may be altered by a change in eluent pH and/or addition of organic solvents. Reversal of the enantiomeric elution order suggests that there may be more than one binding site on the OVM-bonded column, and/or that at least two chiral recognition mechanisms may operate on the OVM-bonded column with regard to PP and its ester derivatives. Also, a conformational change of the OVM bonded structure might be caused by a change in eluent pH and/or addition of organic modifier.

INTRODUCTION

Recently, several chiral stationary phases have been developed for the direct resolution of enantiomers by high-performance liquid chromatography (HPLC) [1]. Protein-bonded stationary phases have been widely used for the chiral resolution of racemic compounds, especially racemic drugs, by HPLC. These proteins include albumins such as bovine serum albumin [2] and human serum albumin [3], glycoproteins such as α_1 -acid glycoprotein (AGP) [4] and ovomucoid (OVM) [5] and enzymes such as α -chymotrypsin [6] and trypsin [7]. Above all, glycoprotein-bonded phases are promising candidates for the chiral resolution of various racemic solutes owing to their wide chiral recognition properties, their stability against changes in eluent pH and type and content of organic modifier and their relatively high efficiency compared with other protein-bonded phases. An OVM-bonded column, developed by Miwa *et al.* [5], has been uti-

lized for the chiral separation of acidic and basic solutes [8–13].

Reversal of the enantiomeric elution order was reported on Pirkle-type columns, based on (*R*)-*N*-(3,5-dinitrobenzoyl)phenylglycine [14] and (*S*)- or (*R*)-1-(α -naphthyl)ethylamine with (*S*)- or (*R*)-valine [15]. Also, it was observed on cellulose columns, based on cellulose tribenzoate [16] and cellulose tris(3,5-dimethylphenylcarbamate) [17]. It was reported [18] that the inversion of the enantiomeric elution order for pseudoephedrine occurred on an AGP-based column with the addition of octanoic acid to the eluent. In a previous paper [11], we reported the inversion of the enantiomeric elution order of propranolol (PP) and its ester derivatives on an OVM-bonded column. This paper deals with the investigation of the enantioselectivity and enantiomeric elution order of PP and its ester derivatives on an OVM-bonded column with respect to eluent pH (from 3 to 7) and organic modifier (2-propanol, ethanol, methanol and acetonitrile).

EXPERIMENTAL

Reagents and materials

Racemic PP hydrochloride was purchased from Wako (Osaka, Japan) and (*R*)- and (*S*)-PP hydrochlorides from Aldrich (Milwaukee, WI, USA). The racemic *O*-acetyl (Ac), -propionyl (Pro), -butyryl (Bu) and -valeryl (Val) esters of PP were synthesized according to the procedures reported previously [19]. The (*R*)- and (*S*)-PP derivatives were prepared by the same procedure. The structures of PP and its ester derivatives are shown in Fig. 1. Methanol, ethanol, 2-propanol and acetonitrile of HPLC grade were obtained from Wako. Other reagents were of analytical-reagent grade and were used as received.

Water purified with a Nanopure II unit (Barnstead, Boston, MA, USA) was used for the preparation of the eluent and sample solutions.

Chromatography

The HPLC system consisted of a Model 880-PU pump, a VL-614 injector (both from Japan Spectroscopic, Tokyo, Japan) equipped with a 100- μ l loop and an RF-540 spectrofluorimeter (Shimadzu, Kyoto, Japan) with excitation at 285 nm and emission at 340 nm. An OVM-bonded silica column (Ultron ES-OVM, particle diameter 5 μ m, 150 \times 4.6 mm I.D.) (Shinwa Chemical Industries, Kyoto, Japan) was used with a guard column (10 \times 4.0 mm I.D.) (Shinwa Chemical Industries) packed with the same material. The flow-rate was maintained at 1.0 ml/min. Chromatograms were recorded and integrated with a Chromatopac C-R6A integrator (Shi-

madzu). Capacity factors (k') were calculated using the equation $k' = (t_R - t_0)/t_0$, where t_R and t_0 are elution times of retained and unretained solutes, respectively. The retention time of an unretained solute, t_0 , was measured by injecting a solution with an organic modifier content slightly different from that of the eluent used. Enantioseparation factors (α) were calculated using the equation $\alpha = k'_2/k'_1$, where k'_1 and k'_2 are the capacity factors of the first- and second-eluted peaks, respectively. All separations were performed at 25°C using a Lauda RMS 6 low-temperature thermostat (Hansen, Kobe, Japan).

The eluents used are specified in the legends of the figures and tables.

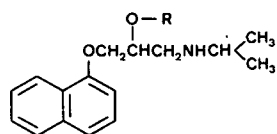
Sample preparations

A known amount of PP or its ester derivatives was dissolved in water and the solution was diluted with the eluent to the desired concentration. A 20- μ l aliquot of the sample solution was loaded on to the column. The on-column amount was less than 0.2 nmol.

RESULTS AND DISCUSSION

In a previous paper [11], we reported that an increase in the organic modifier content and/or a decrease in the eluent pH resulted in a decreased retention of PP and its ester derivatives. Also, the enantioselectivity and enantiomeric elution order of PP and its ester derivatives on an OVM-based column are dependent on the organic modifier used. In this study, the effects of eluent pH and organic modifier on the enantioselectivity and enantiomeric elution order of PP and its ester derivatives were investigated. The eluent pH was varied over the range 3–7 and the organic modifiers used were 2-propanol, acetonitrile, ethanol and methanol at various concentrations.

Fig. 2 shows the effect of eluent pH on the retention, enantioselectivity and enantiomeric elution order of PP and its ester derivatives, with 17.5% of 2-propanol as organic modifier. Almost the same retentions of PP and its ester derivatives were obtained with 20%, 30% and 50% acetonitrile, ethanol and methanol organic modifier contents, respectively. However, the enantioselectivity and enantiomeric elution order of PP and its ester deriv-



R	Abbreviation
H	PP
COCH ₃	Ac-PP
COCH ₂ CH ₃	Pro-PP
COCH ₂ CH ₂ CH ₃	Bu-PP
COCH ₂ CH ₂ CH ₂ CH ₃	Val-PP

Fig. 1. Structures of propranolol and its ester derivatives used in this study.

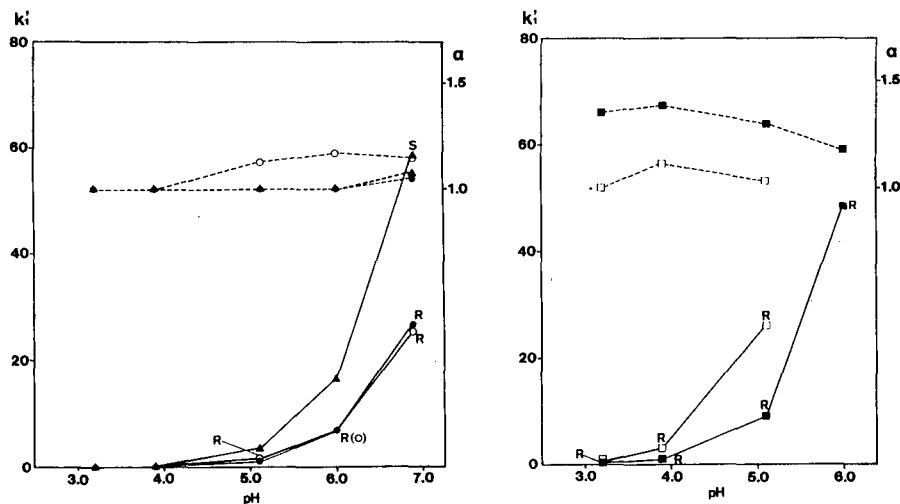


Fig. 2. Effect of eluent pH on retention and enantioselectivity of PP and its ester derivatives. Solid lines, k' ; dashed lines, α . Eluent: 20 mM phosphate buffer (pH 3.2, 3.9, 5.1, 6.0, 6.9) containing 17.5% of 2-propanol. *R* and *S* indicate the first-eluted enantiomer. ● = PP; ○ = Ac-PP; ▲ = Pro-PP; ■ = Bu-PP; □ = Val-PP.

atives are dependent on the organic modifier in addition to the eluent pH.

As PP, Ac-PP and Pro-PP were not retained with acidic eluents and Bu-PP and Val-PP were not eluted with neutral eluents, by changing the organic modifier content the enantiomeric elution order was investigated as described below. Tables I–IV show the effects of eluent pH and type and content of organic modifier on the enantioselectivity and enantiomeric elution order of PP and its ester derivatives when the organic modifier content was altered. Although a decrease or almost no change in enantioselectivity for PP and its ester derivatives was observed with increase in organic modifier content, the enantiomeric elution order was not affected by a change in the organic modifier content studied, except that both enantiomers were co-eluted. When an eluent of pH < 5.1 was used, PP was eluted with the enantiomeric elution order of *S* followed by *R* (*S/R*) with all organic modifiers. Reversal of the elution order occurred with an eluent of pH 6.9 or pH > 6.0. The enantiomeric elution order of Ac-PP was *R/S* except when the eluent of pH > 6.0 was used with addition of methanol. When acetonitrile was used as an organic modifier, Pro-PP was eluted with the enantiomeric elution order *S/R* for all eluent pH values. When an alkanol was

used as the organic modifier, the elution order of Pro-PP was *R/S* with an eluent of acidic pH and *S/R* with the eluent of neutral pH. When ethanol, methanol or acetonitrile was used as the organic modifier, the enantiomeric elution order of Bu-PP was *R/S* with an eluent of acidic pH and *S/R* with an eluent of neutral pH. When 2-propanol was used, the enantiomeric elution order of Bu-PP was *R/S* for all eluent pH values. The enantiomeric elution order of Val-PP, depending on the eluent pH and organic modifier used, was complicated. When acetonitrile was used as the organic modifier, the enantiomeric elution order was *R/S* over the range of eluent pH studied, whereas with methanol the elution order was *S/R*. When 2-propanol was used, the elution order was *R/S* for eluent pH < 5.1 and *S/R* for pH > 6.0. With ethanol as the organic modifier the elution order was *S/R* except for the eluent of pH 3.9.

The above results indicate that chiral recognition or binding properties may be altered by a change in eluent pH and/or addition of organic solvents. Reversal of the enantiomeric elution order suggests that there may be more than one binding site on the OVM-bonded column, and/or that at least two chiral recognition mechanisms may operate on the OVM-bonded column with regard to PP and its es-

TABLE I

ENANTIOMERIC ELUTION ORDER OF PP AND ITS ESTER DERIVATIVES ON AN OVM COLUMN WITH 2-PROPANOL AS ORGANIC MODIFIER^a

pH ^b	Parameter	PP	AC-PP	Pro-PP	Bu-PP	Val-PP
3.2	k'_1 (modifier, %) ^c	1.35 (0.5)	1.20 (2.5)	3.75 (2.5)	2.27 (8)	7.76 (8)
	α^d	1.00	1.33	1.33	1.53	1.09
	Elution order	—	<i>R/S</i>	<i>R/S</i>	<i>R/S</i>	<i>R/S</i>
3.9	k'_1 (modifier, %)	3.10 (2.5)	3.19 (5)	10.8 (5)	6.92 (10)	33.5 (10)
	α	1.14	1.26	1.25	1.55	1.16
	Elution order	<i>S/R</i>	<i>R/S</i>	<i>R/S</i>	<i>R/S</i>	<i>R/S</i>
5.1	k'_1 (modifier, %)	17.4 (5)	12.0 (7.5)	10.5 (15)	9.02 (20)	24.4 (20)
	α	1.08	1.34	1.10	1.38	1.20
	Elution order	<i>S/R</i>	<i>R/S</i>	<i>R/S</i>	<i>R/S</i>	<i>R/S</i>
6.0	k'_1 (modifier, %)	49.7 (7.5)	5.95 (20)	41.1 (15)	35.0 (20)	33.9 (25)
	α	1.04	1.15	1.00	1.28	1.13
	Elution order	<i>S/R</i>	<i>R/S</i>	—	<i>R/S</i>	<i>S/R</i>
6.9	k'_1 (modifier, %)	11.5 (25)	8.64 (25)	15.9 (25)	38.5 (25)	22.4 (30)
	α	1.06	1.11	1.06	1.05	1.31
	Elution order	<i>R/S</i>	<i>R/S</i>	<i>S/R</i>	<i>R/S</i>	<i>S/R</i>

^a The eluent used was a mixture of 20 mM phosphate buffer and various concentrations of 2-propanol.^b Eluent pH before addition of organic modifier.^c The k'_1 value indicates the capacity factor of the first-eluted peak and the percentage of organic modifier used is given in parentheses.^d Separation factor of the enantiomers.

TABLE II

ENANTIOMERIC ELUTION ORDER OF PP AND ITS ESTER DERIVATIVES ON AN OVM COLUMN WITH ACETONITRILE AS ORGANIC MODIFIER^a

pH ^b	Parameter	PP	AC-PP	Pro-PP	Bu-PP	Val-PP
3.2	k'_1 (modifier, %) ^c	2.53 (0.5)	4.65 (2.5)	14.5 (2.5)	23.6 (5)	10.2 (10)
	α^d	1.00	1.00	1.12	1.11	1.58
	Elution order	—	—	<i>S/R</i>	<i>R/S</i>	<i>R/S</i>
3.9	k'_1 (modifier, %)	14.5 (2.5)	8.96 (7)	6.00 (10)	24.9 (10)	9.76 (15)
	α	1.06	1.04	1.16	1.17	1.93
	Elution order	<i>S/R</i>	<i>R/S</i>	<i>S/R</i>	<i>R/S</i>	<i>R/S</i>
5.1	k'_1 (modifier, %)	13.5 (10)	5.97 (15)	3.65 (20)	8.87 (20)	16.6 (20)
	α	1.00	1.21	1.11	1.20	2.17
	Elution order	—	<i>R/S</i>	<i>S/R</i>	<i>R/S</i>	<i>R/S</i>
6.0	k'_1 (modifier, %)	6.31 (20)	30.7 (15)	16.6 (20)	14.1 (25)	8.97 (30)
	α	1.10	1.21	1.20	1.17	2.13
	Elution order	<i>R/S</i>	<i>R/S</i>	<i>S/R</i>	<i>R/S</i>	<i>R/S</i>
6.9	k'_1 (modifier, %)	21.3 (20)	4.74 (30)	7.14 (30)	14.1 (30)	23.9 (30)
	α	1.21	1.05	1.23	1.11	1.46
	Elution order	<i>R/S</i>	<i>R/S</i>	<i>S/R</i>	<i>S/R</i>	<i>R/S</i>

^a The eluent used was a mixture of 20 mM phosphate buffer and various concentrations of acetonitrile.^{b-d} See footnotes to Table I.

TABLE III

ENANTIOMERIC ELUTION ORDER OF PP AND ITS ESTER DERIVATIVES ON AN OVM COLUMN WITH ETHANOL AS ORGANIC MODIFIER^a

pH ^b	Parameter	PP	AC-PP	Pro-PP	Bu-PP	Val-PP
3.2	k'_1 (modifier, %) ^c	1.12 (1)	2.50 (1)	7.69 (1)	4.80 (10)	55.3 (5)
	α^d	1.20	1.45	1.61	1.28	1.07
	Elution order	S/R	R/S	R/S	R/S	S/R
3.9	k'_1 (modifier, %)	2.07 (10)	4.21 (10)	14.8 (10)	8.94 (15)	91.3 (10)
	α	1.19	1.22	1.13	1.26	1.08
	Elution order	S/R	R/S	R/S	R/S	R/S
5.1	k'_1 (modifier, %)	7.35 (15)	11.7 (15)	37.5 (15)	34.0 (20)	15.1 (30)
	α	1.12	1.19	1.00	1.17	1.18
	Elution order	S/R	R/S	—	R/S	S/R
6.0	k'_1 (modifier, %)	16.7 (20)	21.9 (20)	9.55 (30)	22.5 (30)	43.7 (30)
	α	1.03	1.12	1.13	1.14	1.37
	Elution order	S/R	R/S	S/R	S/R	S/R
6.9	k'_1 (modifier, %)	16.4 (30)	11.2 (35)	15.3 (35)	12.3 (40)	17.9 (40)
	α	1.06	1.07	1.15	1.19	1.46
	Elution order	R/S	R/S	S/R	S/R	S/R

^a The eluent used was a mixture of 20 mM phosphate buffer and various concentrations of ethanol.^{b-d} See footnotes to Table I.

TABLE IV

ENANTIOMERIC ELUTION ORDER OF PP AND ITS ESTER DERIVATIVES ON AN OVM COLUMN WITH METHANOL AS ORGANIC MODIFIER^a

pH ^b	Parameter	PP	AC-PP	Pro-PP	Bu-PP	Val-PP
3.2	k'_1 (modifier, %) ^c	1.43 (5)	3.57 (5)	3.29 (15)	11.9 (15)	7.14 (25)
	α^d	1.14	1.38	1.30	1.38	1.16
	Elution order	S/R	R/S	R/S	R/S	S/R
3.9	k'_1 (modifier, %)	8.47 (10)	23.6 (10)	3.41 (25)	7.84 (30)	20.3 (30)
	α	1.15	1.26	1.14	1.22	1.23
	Elution order	S/R	R/S	R/S	R/S	S/R
5.1	k'_1 (modifier, %)	15.6 (20)	17.7 (25)	7.79 (40)	18.5 (40)	34.5 (40)
	α	1.08	1.07	1.18	1.20	1.65
	Elution order	S/R	R/S	S/R	S/R	S/R
6.0	k'_1 (modifier, %)	13.2 (40)	17.5 (40)	31.0 (40)	20.1 (50)	
	α	1.08	1.10	1.36	1.65	
	Elution order	R/S	S/R	S/R	S/R	
6.9	k'_1 (modifier, %)	13.5 (50)	12.1 (50)	18.8 (50)		
	α	1.16	1.17	1.50		
	Elution order	R/S	S/R	S/R		

^a The eluent used was a mixture of 20 mM phosphate buffer and various concentrations of methanol.^{b-d} See footnotes to Table I.

ter derivatives. Also, a conformational change of the OVM bonded structure might be caused by a change in eluent pH and/or addition of organic modifier [20,12]. Taking into account the pK_a value of PP (9.45) [21], PP and its ester derivatives are protonated over the range of eluent pH studied. At eluent pH 5–7, where reversal of the enantiomeric elution order occurs, OVM is negatively charged because of the isoelectric point of OVM (3.8–4.3). Also, the organic modifier might compete with solutes at chiral recognition or binding site(s). Hence electrostatic interactions and the type of organic modifier might play an important role in the chiral recognition of PP and its ester derivatives on an OVM-bonded column.

ACKNOWLEDGEMENTS

The authors thank Shinwa Chemical Industries (Kyoto, Japan) for the loan of the Ultron ES-OVM column. This work was supported in part by a Grant-in-Aid for Scientific Research (No. 01771951) from the Ministry of Education, Science and Culture, Japan.

REFERENCES

- 1 G. Gubitz, *Chromatographia*, 30 (1990) 555; and references cited therein.
- 2 S. Allenmark, B. Bomgren and H. Boren, *J. Chromatogr.*, 237 (1982) 473.
- 3 E. Domenici, C. Bertucci, P. Salvadori, G. Felix, I. Cahagne, S. Motellier and I. W. Wainer, *Chromatographia*, 29 (1990) 170.
- 4 J. Hermansson, *J. Chromatogr.*, 269 (1983) 71.
- 5 T. Miwa, M. Ichikawa, M. Tsuno, T. Hattori, T. Miyakawa, M. Kayano and Y. Miyake, *Chem. Pharm. Bull.*, 35 (1987) 682.
- 6 I. W. Wainer, P. Jadaud, G. R. Schonbaum, S. V. Kadodkar and M. P. Henry, *Chromatographia*, 25 (1988) 903.
- 7 S. Thelohan, Ph. Jadaud and I. W. Wainer, *Chromatographia*, 28 (1989) 551.
- 8 T. Miwa, T. Miyakawa, M. Kayano and Y. Miyake, *J. Chromatogr.*, 408 (1987) 316.
- 9 M. Okamoto and N. Nakazawa, *J. Chromatogr.*, 504 (1990) 445.
- 10 G. Tamai, M. Edani and H. Imai, *Biomed. Chromatogr.*, 4 (1990) 157.
- 11 J. Haginaka, J. Wakai, K. Takahashi, H. Yasuda and T. Katagi, *Chromatographia*, 29 (1990) 587.
- 12 J. Iredale, A.-F. Aubry and I. Wainer, *Chromatographia*, 31 (1991) 329.
- 13 K. M. Kirkland, K. L. Nielson and D. A. McCombs, *J. Chromatogr.*, 545 (1991) 43.
- 14 T. D. Doyle and I. W. Wainer, *J. High Resolut. Chromatogr. Chromatogr. Commun.*, 7 (1984) 38.
- 15 N. Oi, H. Kitahara and R. Kira, *J. Chromatogr.*, 535 (1990) 213.
- 16 M. H. Gaffney, R. M. Stiffin and I. W. Wainer, *Chromatographia*, 27 (1989) 15.
- 17 Y. Fukui, A. Ichida, T. Shibata and K. Mori, *J. Chromatogr.*, 515 (1990) 85.
- 18 J. Hermansson and G. Schill, in M. Zief and L. J. Crane (Editors), *Chromatographic Chiral Separation*, Marcel Dekker, New York, 1988, p. 245.
- 19 W. L. Nelson and R. B. Walker, *Res. Commun. Chem. Pathol. Pharmacol.*, 22 (1978) 435.
- 20 I. Kato, J. Schrode, W. J. Kohr and M. Laskowski, Jr., *Biochemistry*, 26 (1987) 193.
- 21 *Drug Data Handbook 1990*, ADIS Press, New York, 1990.

Control of the retention selectivity of rare earth octaethylporphyrins in reversed-phase high-performance liquid chromatography using amines as mobile phase additives

Yoshihiko Shibata, Koichi Saitoh and Nobuo Suzuki*

Department of Chemistry, Faculty of Science, Tohoku University, Sendai, Miyagi 980 (Japan)

(First received September 24th, 1991; revised manuscript received January 28th, 1992)

ABSTRACT

The reversed-phase liquid chromatographic retention behaviour of the complexes of octaethylporphyrin (OEP) with eleven trivalent rare earth (REs), viz., Y, Sm, Eu, Gd, Tb, Dy, Ho, Er, Tm, Yb and Lu, on an octadecyl-bonded silica gel column is described. All these complexes can be eluted without demetallation with a methanol–water mixture that contains a small amount (about 1%) of acetylacetonate and an amine. The retention order of the RE–OEP complexes depends on the amine used. With a mono-*n*-alkylamine and a di-*n*-alkylamine, the retention of the RE–OEP complex decreases with increasing atomic number of the REs within the lanthanide series, whereas the reverse tendency occurs with a trialkylamine and a dialkylamine possessing branched alkyl side-chains or alcoholic side-chains. In all instances, the retention of the Y complex is close to that of the Dy complex. Successful separation of the OEP complexes of Lu, Yb, Tm, Er and Sm in 20 min is demonstrated with dihexylamine.

INTRODUCTION

There has been increased interest in the separation of metalloporphyrins from the biomedical [1], geological [2] and analytical [3] viewpoints. High-performance liquid chromatography (HPLC) is the most powerful tool for the separation of these compounds today [4]. HPLC separations of a limited number of metal complexes of synthetic porphyrins, have been investigated, e.g. porphine [5], haematoporphyrin [6], *meso*-tetraphenylporphine (TPP) [7], *meso*-tetrakis (*p*-tolyl)porphine [8] and pheophorbide-a (not a porphyrin, but a compound with a chlorin structure) [9].

In general, the separation of metalloporphyrins with different central metal ions is more difficult than the separation of different porphyrin complexes of a certain metal, because the metal ion is surrounded by a bulky macrocyclic porphyrin structure to which various organic substituents are at-

tached. The separation of metalloporphyrins becomes increasingly difficult as the metals become more similar chemically. The feasibility of the reversed-phase HPLC separation of the TPP complexes of trivalent rare earths (REs) was previously confirmed [10]. It was found that the separation selectivity for the RE–TPP complexes varied with the type of amine added to the mobile phase.

This work was undertaken to examine the effects of amines on the chromatographic retention characteristics of the RE complexes of octaethylporphyrin (OEP), which had been frequently used as a model porphyrin, similarly to TPP, in studies relating to porphyrin. OEP differs from TPP in its molecular structure. In the TPP molecule, four relatively bulky phenyl groups are bonded with four *meso*-carbons to the porphyrin nucleus, whereas in OEP eight ethyl groups are bonded to eight β -pyrrolic positions.

EXPERIMENTAL

Materials

The free acid form of OEP (H_2oep) was obtained from Strem Chemicals (Newburyport, MA, USA). The complexes of OEP with RE (III) (RE = Y, Sm, Eu, Gd, Tb, Dy, Ho, Er, Tm, Yb, Lu) were synthesized by reacting H_2oep (60 mg, 0.11 mmol) with the corresponding RE acetylacetonate [RE(acac)₃] (110–130 mg, 0.25 mmol) while refluxing in 1,2,4-trichlorobenzene (12 ml) in a stream of nitrogen, a modification of the method used for the preparation of a mixed ligand complex of an RE with TPP and acetylacetonate, RE(tpp) (acac) [11]. The reaction mixture diluted with 200 ml of toluene and then poured onto a neutral alumina column (70 mm × 12.5 mm I.D.). After complete elution of the unreacted H_2oep with toluene–acetone (30:1, v/v), the RE complex was eluted with dimethyl sulphoxide–water (80:20, v/v). The eluate was mixed with water (1:1) and the RE–OEP complex was extracted with dichloromethane. After removal of the solvent, the complex was obtained as a crystalline material of reddish violet needles or as an amorphous solid. When examined by UV–VIS spectrophotometry, each material gave two sharp absorption peaks corresponding to the so-called α -band and β -band peaks in the 500–600-nm region, implying that the material was a metal complex of porphyrin [12]. A significant peak appeared in the mass spectrum (recorded with desorption electron impact ionization) at an m/z value consistent with the molecular ion [RE(oep) (acac)]⁺; for example, the Lu(III) complex gave a peak at m/z 806. The complexes thus prepared were identified as mixed-ligand complexes with tetradentate oep and bidentate acetylacetonate (acac) anions, RE(oep) (acac). The structural formula of this complex is illustrated in Fig. 1, assuming that it is analogous to that of RE(tpp) (acac) [13]. The term RE–OEP complex is hereafter taken to mean RE(oep) (acac), unless indicated otherwise.

Acetylacetonate (Hacac), octylamine (OA), diethylamine (DEA), dipropylamine (DPA), diisopropylamine (DIPA), dihexylamine (DHA), diethanolamine (DEOLA), triethylamine (TEA), tripropylamine (TPA), dichloromethane and sodium hydroxide (NaOH) were of analytical-reagent grade (Wako, Osaka, Japan). Methanol and water were distilled in glass.

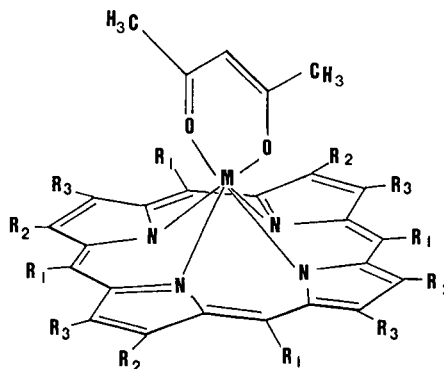


Fig. 1. Structural formula of the RE–OEP ($R_1 = H$; $R_2 = R_3 = \text{ethyl}$) and the RE–TPP ($R_1 = \text{phenyl}$; $R_2 = R_3 = H$) complexes. M indicates the RE(III) ion.

HPLC

A Twinkle solvent delivery pump, a VL-611 sample injection valve (Jasco, Tokyo, Japan) and a Model SPD-M6A photodiode-array UV–VIS spectrophotometric detector (Shimadzu, Kyoto, Japan) were used with a Model TSK ODS-80TM column (150 mm × 4.6 mm I.D.) packed with octadecyl-bonded silica gel (5 μm) (Tosoh, Tokyo, Japan).

The mobile phase was prepared, unless indicated otherwise, by adding an amine to the mixture of methanol–water–Hacac (95:5:1, v/v/v) so that the amine was of equimolar concentration with respect to Hacac in the final solution (about 0.1 M). In order to avoid damaging the column, when NaOH was used in place of an amine, it was added to the methanol–water–Hacac mixture so as to be approximately half the equimolar concentration with respect to Hacac in the final composition of the mixture. The flow-rate of the mobile phase was 1 ml/min.

The sample solution of an RE–OEP complex was prepared at a concentration of about 0.1 mM in dichloromethane containing DEA (2%, v/v) and a 10- μl aliquot of each solution was injected into the column. All experiments were carried out at $25 \pm 1^\circ\text{C}$.

RESULTS AND DISCUSSION

Capacity factors

The OEP complexes of light lanthanides, particularly of Sm(III) and Eu(III), showed low stability

in common solvents such as methanol, acetonitrile, acetone, dichloromethane and benzene: demetallation of the complexes occurred within 1 h after the preparation of the solutions at about the 0.1-mM level. These complexes could be stabilized by addition of a small amount of an amine, such as DEA, to the solution, as for RE complexes of TPP [4]. The solution of an RE–OEP complex to be applied in HPLC was prepared in dichloromethane–DEA (50:1, v/v).

The capacity factor (k') of an RE–OEP complex was calculated from its retention volume and the column void volume, which was assumed to be equal to the retention volume of sodium nitrate (a nearly saturated solution was injected). The k' value was determined from triplicate measurements, with a relative standard deviation of less than 1%.

Effects of amines on the retention of the RE–OEP complexes

No RE–OEP complex could be eluted from the HPLC column with a mixture of methanol and water (e.g., 95:5, v/v) or methanol alone; in every instance, H₂oep was not detected in the eluate. [The k' value of H₂oep was the smallest ($k' = 4.24$) when using methanol as the mobile phase, and increased with increasing water concentration in the methanol–water mixture.] This implied that the dissociation of the OEP ligand from the RE complex did not occur to any detectable extent, and that the complex adsorbed strongly on the column packing material.

The OEP complexes of Lu(III), Yb(III), Tm(III) and Er(III) could be eluted with a mobile phase containing Hacac, e.g., with methanol–water–Hacac (95:5:1, v/v/v). All other RE–OEP complexes were eluted successfully by addition of both Hacac and an amine, such as DEA, to the mobile phase.

It was considered that the dissociation of the anionic bidentate ligand, acac[−], from the RE–OEP complex occurred in the Hacac-free mobile phase, and resulted in a cationic species, [RE(oep)]⁺, that was adsorbed by a cation-exchange site (presumably dissociated silanol group) on the surface of the alkyl-bonded silica gel. Similar phenomena have been reported for the TPP complexes of trivalent metals, such as Mn(tpp)Cl and Co(tpp)Cl, in reversed-phase HPLC, where strong adsorption of the complexes was suppressed by addition of am-

monium chloride to the mobile used [15]. Higher acac[−] concentrations in the mobile phase were considered to eliminate the anomalous retention behaviour of the RE–OEP complex by suppression of the following dissociation:



One of the functions of the amine added to the mobile phase is to act as a base and promote the dissociation of the weak acid Hacac, thereby increasing the concentration of the acac[−] anion. In this respect, all amines (and also simple inorganic bases, such as NaOH) are expected to be useful mobile phase additives for the successful elution of RE–OEP complexes.

It was confirmed, by means of real-time monitoring of the UV–VIS spectra of the eluate with a photodiode-array spectrophotometric detector, that undesirable chemical reactions did not occur to any detectable extent between the injected complex and the metal components of the HPLC system.

Effects of the molecular structure of the amine additive

When a methanol–water–Hacac–amine mixture was used as the mobile phase, the k' of the RE–OEP complexes and also their retention sequence varied with the type of amine used, as shown in Fig. 2. With mobile phases containing monoalkylamines, such as OA, and dialkylamines, such as DEA, DPA and DHA, the k' of RE–OEP increased with decreasing atomic number (Z) of the RE within the lanthanide series. On the other hand, with trialkylamines, such as TEA and TPA, the opposite trend was observed for these metal complexes. It is shown in Fig. 3 that the retention trends observed with DIPA and DEOLA are different from those obtained with other dialkylamines, but similar to the trends observed with trialkylamines (see Fig. 2). If amines functioned only as bases promoting the dissociation of the weak acid, Hacac, the retention order should depend little on the molecular structure of the amine, and should be similar to the trends observed with NaOH. In fact, when NaOH was used in the place of an amine, the k' values decreased with decreasing Z of the lanthanides, as shown in Fig. 3. This retention trend is similar to those observed with DIPA and trialkylamines, such as TEA and TPA, and DIPA.

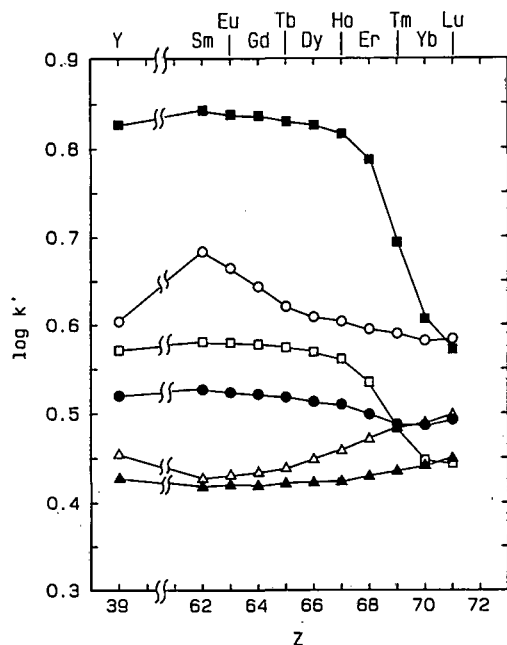
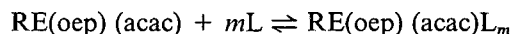


Fig. 2. Relationship between the retention of RE-OEP complexes and the atomic number (Z) of the RE. Mobile phase: methanol-water-Hacac-amine (95:5:1: x , v/v). Amines: \circ = OA ($x = 1.6$); \bullet = DEA ($x = 1.0$); \square = DPA ($x = 1.3$); \blacksquare = DHA ($x = 2.3$); \triangle = TEA ($x = 1.3$); \blacktriangle = TPA ($x = 1.8$).

Function of the amine additive

Trivalent REs can have coordination numbers (CN) larger than 6 [16]. Accordingly, the coordination sphere of the RE ion in an RE-OEP is not necessarily saturated by the tetradentate ligand OEP and bidentate acac, rather coordination with an additional ligand (L) in the mobile phase, such as water, methanol or an amine, may be possible:



In the case of RE-TPP complexes in dimethyl sulphoxide, a CN of 8 was determined for the light lanthanides from Ce to Tb and a CN of 7 for the heavy lanthanides from Dy to Lu [17].

It is reasonable to predict that the stronger the coordinative interaction that occurs between the RE ion and the hydrophilic ligand(s) such as water and/or methanol, the more the capacity factor of the RE-oep is reduced in the reversed-phase system. The retention trend for the RE-OEP complexes observed without an amine (see Fig. 3 with NaOH instead of an amine) implies that the coord-

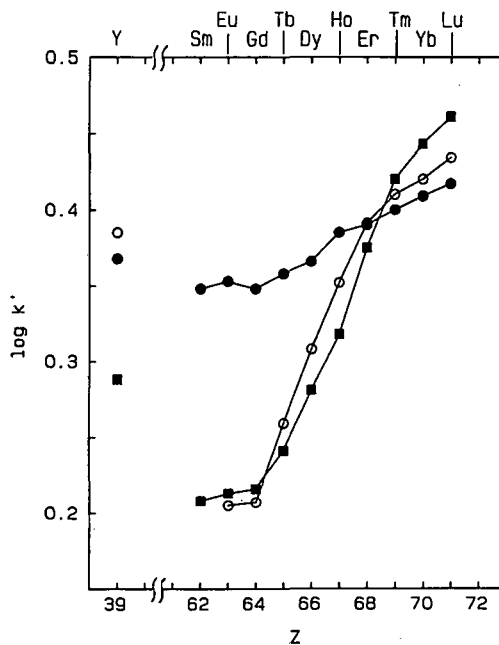


Fig. 3. Relationship between the retention of RE-OEP complexes and the atomic number (Z) of the RE. Mobile phase: \bullet = methanol-water-Hacac-DIPA (95:5:1:1.4, v/v); \circ = methanol-water-Hacac-DEOLA (95:5:1:0.93, v/v); \blacksquare = 0.045 M NaOH in methanol-water-Hacac (95:5:1, v/v).

dination strength of such hydrophilic ligand(s) increases with decreasing atomic number of the lanthanide.

Amines are stronger electron donors than water and methanol. Most amines possess hydrophobic alkyl moieties in their molecules. When an amine coordinates to the RE ion in a OEP complex more strongly than water and methanol, the k' of the RE-OEP complex may be larger than those observed without the amine in the reversed-phase system. The results shown in Figs. 2 and 3 imply that the stability of the additional coordination of the mono- and dialkylamines to the RE ion in the OEP complexes tends to increase with decreasing atomic number of the lanthanide. Also, trialkylamines (TEA and TPA) and the dialkylamines with branched alkyl side-chains (DIPA) cannot coordinate to the RE ion as strongly as the mono- and di- n -alkylamines. This suggests that the structure of the alkyl moiety of the amine affects the strength of the additional coordination of the amine to the RE ions in the RE-OEP complexes.

The RE(III) ionic radii are larger than the best fit (64 pm) for the cavity in the N_4 -moiety of porphyrin [18]. In a mixed complex of RE with porphyrin and acetylacetonate, the RE ion is displaced from the porphyrin plane towards the additional ligand, acac (see Fig. 1), and the estimated out-of-plane distance increases with increasing ionic radius of the RE [13,19]. It is assumed that the longer the out-of-plane distance, the stronger is the interaction between the RE ion and the additional ligand. Also, the bulkier the alkyl moiety in the vicinity of the nitrogen atom in an amine molecule, the greater is the extent of its steric hindrance to the coordination of the amine with the RE ion.

It was previously found that the retention sequence of RE-TPP complexes depended on the type of amine used as the mobile phase additive [10]. Such peculiar retention characteristics were explained in terms of the steric effects of the alkyl moiety of the amine on the coordination to the RE ion complexed with both porphyrin and acetylacetonate.

The retention trends of RE-OEP complexes observed with and without amines are represented as a

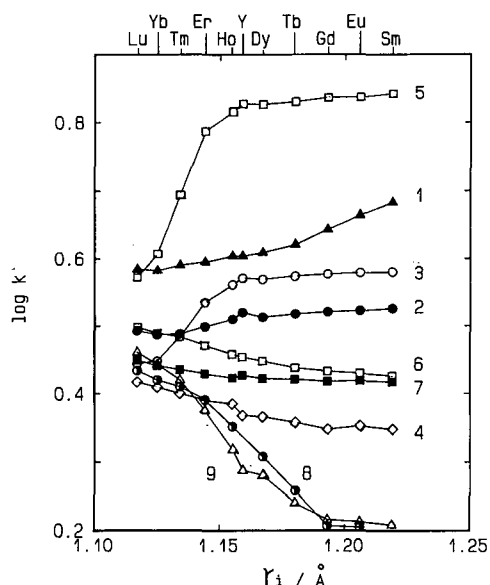


Fig. 4. Retention of RE-OEP complexes as a function of the ionic radius (r_i) of the RE(III) (r_i values for $CN = 8$). Basic mobile phase additives: 1 = OA; 2 = DEA; 3 = DPA; 4 = DIPA; 5 = DHA; 6 = TEA; 7 = TPA; 8 = DEOLA; 9 = NaOH. For the mobile phase compositions, see Figs. 2 and 3.

function of the ionic radius (r_i) of the RE in Fig. 4, where the r_i values for a CN of 8 [20] are applied. It is noted that the k' value of the complex of Y(III) lies, in every instance, near to that of the complex of Dy(III), whose ionic radius is close to that of Y(III). With mono- and di- n -alkylamines, the k' of RE-OEP tends to increase monotonously with increasing r_i of the RE. The opposite retention trends observed with trialkylamines is regarded as being due to the bulky alkyl moieties of these amines. The steric effect of branched alkyl groups appears clearly in the comparison of DIPA and DPA, which possess the same numbers of carbon atoms in their alkyl moieties. The retention trend observed with DEOLA, which is similar to that with NaOH, is attributed to the polar alcoholic structure of the side-chains in the molecule; the formation of the hydrophilic DEOLA adduct of an RE-OEP complex resulted in a reduction of the k' of the RE complex.

Control of the elution sequence

Methanol and water were used as the main components of the mobile phase to which Hacac and

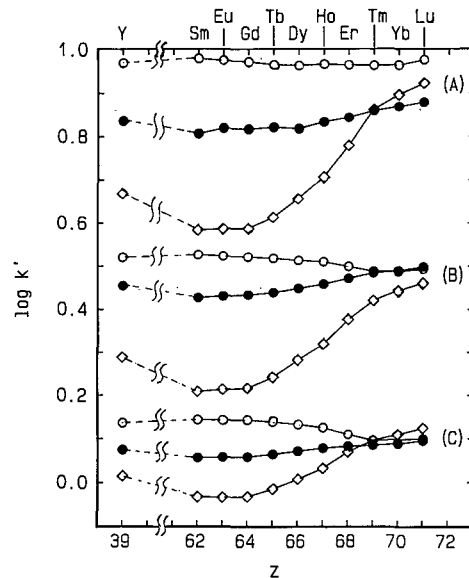


Fig. 5. Effect of the mobile phase composition on the retention of RE-OEP complexes. Mobile phase: (A) methanol-water-Hacac-base (90:10:1: x , v/v/v); (B) methanol-water-Hacac-base (95:5:1: x , v/v/v); (C) methanol-Hacac-base (100:1: x , v/v). Bases: \circ = DEOA ($x = 1$); \bullet = TEA ($x = 1.3$); \diamond = NaOH (0.045 M).

amine were added. When the methanol-to-water ratio in the mobile phase was increased, the k' value decreased considerably for each RE-OEP complex, whereas their retention order changed little, as illustrated in Fig. 5 as an example. This means that the elution sequence for these complexes varies little with either the methanol or the water content of the mobile phase. According to the results shown in Figs. 2-4, the selectivities for the RE-OEP complexes can be varied with basic mobile phase additives such as amines and NaOH. It can be predicted that the elution order of the OEP complexes follows the increasing atomic number of the lanthanides when using trialkylamines, DIPA, DEOLA and NaOH as the mobile phase additives, whereas the reverse elution order is possible with a di-*n*-alkylamine or OA.

Separations of the RE-OEP complexes with different elution orders are demonstrated in Fig. 6.

Comparison with RE complexes of TPP

The effects of amines on the retention behaviour of RE-OEP complexes are compared here with those of RE-TPP complexes [10]. When the mobile

phase contains a trialkylamine, the retention trends for RE-OEP complexes are similar to those for RE-TPP; the capacity factor increases with increasing atomic numbers of lanthanides, as shown in Fig. 7. However, with respect to the effects of dialkylamines, such as DPA, the retention trends for the complexes of OEP are different from those for the complexes of TPP. With the TPP complexes, the capacity factor tends to decrease with increasing atomic number of the RE for relatively light lanthanides from Sm to Tb, whereas the reverse trend, which is similar to the results obtained with trialkylamines, is obtained for the complexes of heavy lanthanides from Dy to Lu. The capacity factors of the OEP complexes decrease monotonically with increasing atomic number of the lanthanide. This implies that the additional coordination of the dialkylamine with heavy lanthanides in the OEP complexes is stronger than in the TPP complexes.

According to the results shown in Fig. 7, the retention sequences for the complexes of heavy lanthanides in particular differ between the TPP complexes and OEP complexes, even though a dialkylamine is used. In an actual HPLC separation as

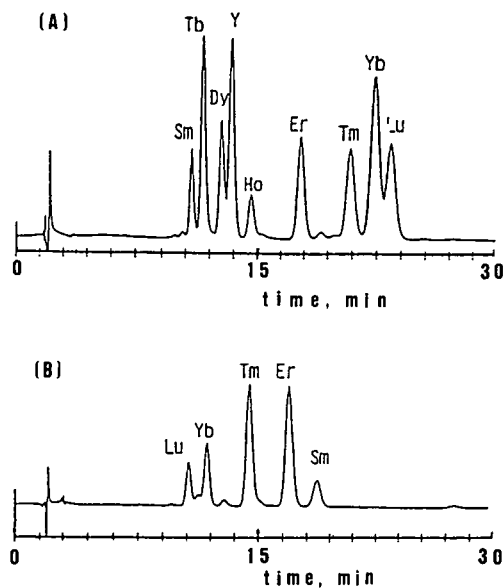


Fig. 6. HPLC separation of the RE-OEP complexes. Column: 50- μ m TSK Gel ODS-80TM (150 mm \times 4.6 mm I.D.). Mobile phase: (A) 0.045 M NaOH in methanol-water-Hacac (87:13:1, v/v/v); (B) methanol-water-Hacac-DHA (93:7:1:2.3, v/v/v); flow-rate, 1.0 ml/min. Detection at 565 nm.

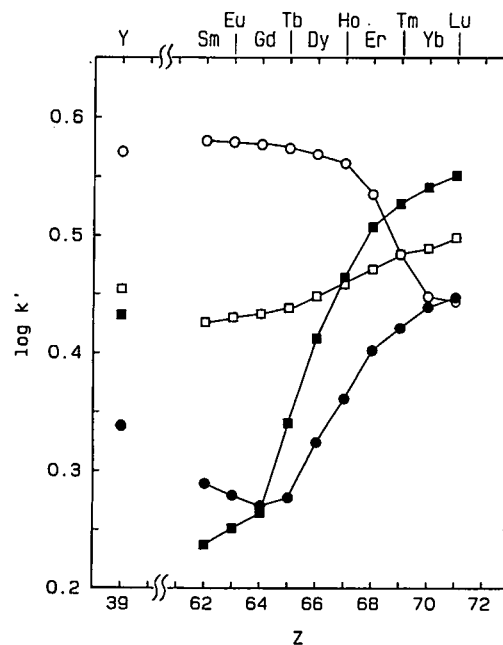


Fig. 7. Comparison of the retention trends for RE-OEP complexes (O, \square) and RE-TPP complexes (\bullet , \blacksquare). Mobile phase: O, \bullet = methanol-water-Hacac-DPA (95:5:1:1.3, v/v/v); \square , \blacksquare = methanol-water-Hacac-TEA (95:5:1:1.3, v/v/v).

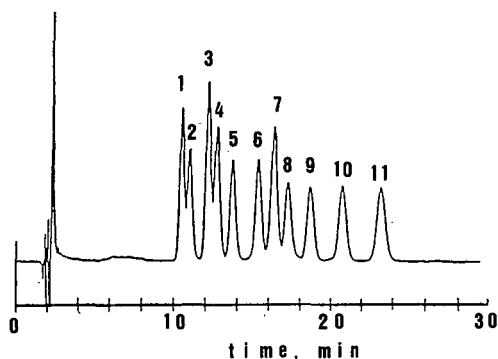


Fig. 8. HPLC separation of RE porphyrins. Mobile phase: methanol-water-Hacac-DPA (89:11:1:1.3, v/v); flow-rate, 1 ml/min. Detection at 555 nm. Column: as in Fig. 6. Peaks: 1 = Gd-TPP; 2 = Tb-TPP; 3 = Dy-TPP; 4 = Y-TPP; 5 = Ho-TPP; 6 = Er-TPP; 7 = Tm-TPP; 8 = Yb-OEP; 9 = Tm-OEP; 10 = Er-OEP; 11 = Sm-OEP.

demonstrated in Fig. 8, seven TPP complexes (peak 1-7) are eluted in order to the atomic numbers of the lanthanides, and then four OEP complexes (peaks 8-11) are separated in the reverse order of the atomic numbers of the RE.

CONCLUSIONS

An amine added to the mobile phase with a small amount of Hacac functions as a base which enhances the stability of the RE-OEP complexes to be separated and, accordingly, suppresses their undesirable adsorption on the stationary phase material. The second useful function of the amine is with regard to the selectivity and the elution sequence for the RE-OEP complexes. The retention selectivity depends on the amine used. The separation of RE-OEP complexes in increasing order of the atomic number of the REs is achieved with a trialkylamine as well as NaOH. The separation sequence can be reversed by changing the amine to either a mono-*n*-alkylamine, such as OA, or a di-*n*-alkylamine, such as DHA. The effect of dialkylamines in particular on the retention sequence of RE-OEP complexes is different from that for RE-TPP complexes.

ACKNOWLEDGEMENT

This work was supported by a Grant-in-Aid for Scientific Research from the Ministry of Education, Science and Culture.

REFERENCES

- 1 A. Kappas and G. D. Drummond, *J. Clin. Invest.*, 77 (1986) 335.
- 2 R. H. Filby and J. F. Branthaver (Editors), *Metal Complexes in Fossil Fuels*, American Chemical Society, Washington, DC, 1986.
- 3 K. L. Cheng, K. Ueno and T. Imamura, *Handbook of Organic Analytical Reagents*, CRC Press, Boca Raton, FL, 1982, p. 355.
- 4 V. Varadi, F. R. Longo and A. D. Adler, in D. Dolphin (Editor), *The Porphyrins*, Vol. I, Academic Press, New York, 1978, p. 581.
- 5 Y. Wakui, K. Saitoh and N. Suzuki, *Chromatographia*, 22 (1986) 160.
- 6 N. Suzuki, K. Saitoh and Y. Sugiyama, *Chromatographia*, 21 (1986) 509.
- 7 K. Saitoh, M. Kobayashi and N. Suzuki, *J. Chromatogr.*, 243 (1982) 291.
- 8 M. Kobayashi, K. Saitoh and N. Suzuki, *Chromatographia*, 20 (1985) 72.
- 9 K. Adachi, K. Saitoh and N. Suzuki, *J. Chromatogr.*, 347 (1988) 99.
- 10 K. Saitoh, Y. Shibata and N. Suzuki, *J. Chromatogr.*, 542 (1991) 351.
- 11 C. P. Wong, *Inorg. Synth.*, 22 (1983) 152.
- 12 K. M. Smith, *Porphyrins and Metalloporphyrins*, Elsevier, Amsterdam, 1975, pp. 884-885.
- 13 C.-P. Wong, R. F. Venteicher and W. D. Horrocks, Jr., *J. Am. Chem. Soc.*, 96 (1974) 7149.
- 14 N. Suzuki, K. Saitoh and Y. Shibata, *J. Chromatogr.*, 504 (1990) 179.
- 15 N. Suzuki, T. Takeda and K. Saitoh, *Chromatographia*, 22 (1986) 43.
- 16 A. Zalkin, D. H. Templeton and D. G. Karraker, *Inorg. Chem.*, 8 (1969) 2680.
- 17 A. Iwase and S. Tada, *Nippon Kagaku Kaishi*, 1 (1973) 60.
- 18 W. Buchler, in K. M. Smith (Editor), *Porphyrins and Metalloporphyrins*, Elsevier, Amsterdam, 1975, p. 191.
- 19 W. D. Horrocks, Jr. and C. P. Wong, *J. Am. Chem. Soc.*, 98 (1976) 7157.
- 20 R. D. Shannon, *Acta Crystallogr.*, Sect. A, 32 (1975) 751.

CHROM. 24 005

Structure elucidation of saccharides in anthocyanins and flavonols by means of methylation analysis and gas chromatography

Werner Edgar Glässgen, Roswitha Hofmann, Michael Emmerling^{*}, Günter Dieter Neumann and Hanns Ulrich Seitz^{*}

Botanisches Institut, Allgemeine Botanik und Pflanzenphysiologie, Universität Tübingen, Auf der Morgenstelle 1, W-7400 Tübingen (Germany)

(First received October 28th, 1991; revised manuscript received January 10th, 1992)

ABSTRACT

The monosaccharide composition of anthocyanins and flavonols was elucidated by capillary gas chromatography after derivatization to the corresponding alditol acetates. Methylation analysis using gas chromatography revealed the types of linkages in these saccharides. Three anthocyanins isolated from carrot cell suspension cultures were shown to contain galactose, xylose and glucose in equimolar amounts, forming a branched triglycoside. Therefore, the structures of these carrot anthocyanins could be identified as cyanidin 3-(6^C-glucosyllathyroside) and the same triglycoside acylated with sinapic or ferulic acid.

INTRODUCTION

The carbohydrate part of flavonoids is usually investigated by using paper (PC) or thin-layer chromatography (TLC) after acid or enzymic hydrolysis or after peroxide degradation of the aglycone [1,2]. Sugar analyses using gas chromatography (GC) require the conversion of the sugars into volatile derivatives. Two techniques for derivatization have been reported: trimethylsilylation of the sugars [3] and reduction of the sugars to their alditols followed by peracetylation to form the alditol acetates [4,5]. In order to reveal the monosaccharide composition of anthocyanidin and flavonol glycosides, we applied a slightly different procedure for alditol acetate formation [6] and separated the resulting derivatives using capillary GC.

Additional information about the linkages between the sugars was obtained by methylation analysis, a technique commonly used in the structure elucidation of proteoglycans, polysaccharides and oligosaccharides [6–9]. The carbon atoms involved in glycosidic bonds could be identified by methylation of the sugars prior to hydrolysis and subsequent reduction, acetylation and GC.

These GC techniques were used to examine the glycoside component of three anthocyanins isolated from carrot cell suspension cultures. The structure of the major pigment of these cells has been reported to be cyanidin 3-(sinapoylxylosylglucosylgalactoside) [10,11] with a linear triglycoside chain [12]. Recently, the question arose whether the trisaccharide of the pigment could be branched through the galactose moiety with the acyl group located on the glucose residue [13,14]. Methylation analysis provided a suitable means of deciding between these two structure proposals by determining the positions of the linkages.

^{*} Present address: Plant Cell Biology Research Centre, School of Botany, University of Melbourne, Parkville, Victoria 3052, Australia.

EXPERIMENTAL

Chemicals

Cyanidin 3-glucoside was a gift from Professor J. B. Harborne, University of Reading, UK; cyanin, hyperoside, quercitrin and rutin were purchased from Roth (Karlsruhe, Germany). Hyperoside and quercitrin were purified before use by TLC on cellulose (20 × 20 cm plates, 0.1-mm layer; Merck, Darmstadt, Germany) with chloroform–acetic acid–water (50:45:5) as solvent. The compounds were detected under UV light (354 nm, R_F = 0.35 for hyperoside and 0.32 for quercitrin) and eluted with methanol. Amberlite IR-120 was obtained from Fluka (Buchs, Switzerland).

Dimethylsulphanyl carbanion (potassium salt) was synthesized from potassium hydride and dimethyl sulphoxide (DMSO) using the method of Harris *et al.* [6] with minor modifications [15]. Partially methylated alditol acetate (PMAA) standards were prepared according to York *et al.* [8] and identified by gas chromatography–mass spectrometry (GC–MS) [15].

Isolation of anthocyanins

Anthocyanins were isolated from suspension-cultured cells of an Afghan cultivar of *Daucus carota* L. [16] maintained as described previously [17]. Cells were extracted with methanol–acetic acid–water (50:8:42) using a mortar and pestle. After washing with ethyl acetate, anthocyanins were purified by repeated PC in the descending mode on Whatman 3MM paper with *n*-butanol–acetic acid–water (4:1:5, upper phase, overrun) and with 15% acetic acid as solvents, followed by column chromatography on

Sephadex LH-20 (17 × 2 cm I.D., gravity flow) using 8% acetic acid as the eluent. The purity of the samples was monitored at 530 nm by reversed-phase high-performance liquid chromatography (HPLC) on a Hypersil ODS (5 μm) column (250 × 5 mm I.D.) (Grom, Herrenberg, Germany) using a gradient with 10% formic acid in water (solvent A) and in methanol (solvent B), with solvent B increasing from 10% to 13% within 10 min, to 20% during 10–20 min, to 40% during 20–25 min and to 98% during 25–30 min at a flow-rate of 1.0 ml/min. The major compound (1) proved to be identical with the substance characterized by Harborne and co-workers [10,13] by co-chromatography with HPLC and TLC on cellulose with three solvents (Table I).

Deacylation of anthocyanins and identification of acyl residues

Alkaline hydrolysis was carried out according to Albach *et al.* [18] with 10% potassium hydroxide solution for 4 h in the dark at room temperature. The hydrolysate was acidified with prewashed Amberlite IR-120 (H⁺ form). The liberated hydroxycinnamic acids were extracted with diethyl ether and identified (Table I) by HPLC on a Hypersil ODS (5 μm) column (250 × 5 mm I.D.) (Grom) using a linear gradient with 5% acetic acid and methanol as solvents (from 10 to 40% methanol in 20 min at a flow-rate of 1.5 ml/min, detected at 280 nm). Caffeic acid (elution time 7.77 min), *p*-coumaric acid (11.79 min), ferulic acid (13.66 min), sinapic acid (14.36 min) and *p*-hydroxybenzoic acid (6.03 min) were used as standards. The aqueous phase containing the deacylated pigments was also subjected to sugar analysis.

TABLE I

CHROMATOGRAPHIC DATA FOR THREE CARROT ANTHOCYANINS FROM HPLC AND TLC

For HPLC, see Experimental. TLC on cellulose (0.1 mm, 20 × 20 cm) (Merck). Solvent 1 = *n*-butanol–acetic acid–water (4:1:5, upper phase); solvent 2 = 1% hydrochloric acid; solvent 3 = acetic acid–hydrochloric acid–water (15:3:82).

Anthocyanin	Elution time in HPLC (min)	R_F in TLC			Acyl group
		Solvent 1	Solvent 2	Solvent 3	
1	22.38	17.5	15	28.5	Sinapic acid
2	24.36	21	15	31	Ferulic acid
3	17.15	14	32	58	—

Peroxide degradation

Degradation of the aglycone of the purified anthocyanins was performed by treatment with 2 M ammonia solution and 30% hydrogen peroxide as described by Markham [3]. The remaining carbohydrate parts of the anthocyanins were derivatized for GC analysis.

Monosaccharide analysis

Samples containing 50–500 μg of flavonoid standard or purified anthocyanin were dried in a stream of nitrogen and dissolved in 490 μl of water. After the addition of 50 μg of *myo*-inositol as internal standard, the samples were brought to 2 M trifluoroacetic acid (TFA) and hydrolysed at 120°C for 60 min. The liberated aglycones could be extracted from the hydrolysate with ethyl acetate and identified by TLC or HPLC. The TFA was then removed by evaporation with nitrogen and the monosaccharides were reduced and acetylated according to Harris *et al.* [6] to obtain volatile alditol acetates. Aromatic acyl groups are probably detached from the saccharides during this procedure. The alditol acetates were extracted with 1.5 ml of dichloromethane and the organic phase was washed four times with water. Then the dichloromethane was removed in a stream of filtered air and the dry samples were stored at -18°C . For GC analysis, the samples were dissolved in 50 μl of dichloromethane.

GC was performed on a Shimadzu GC-9A instrument equipped with a flame ionization detector (275°C). Separation of the alditol acetates was carried out on an SP-2340 capillary column (30 m \times 0.25 mm I.D.) isothermally at 235°C. The carrier gas was nitrogen at an inlet pressure of 4.5 bar. Volumes of 1.0–1.5 μl of the samples were injected into a glass inlet at 275°C with a splitting ratio of 10:1. The alditol acetates were identified by comparing their relative retention times with respect to *myo*-inositol hexaacetate with those of known standards. Quantification was based on relative response factors obtained by the analysis of standard mixtures of monosaccharides.

Methylation analysis

A modification of the procedure described by Harris *et al.* [6] was used [15]. Rutin in different amounts ranging from 0.2 to 0.8 mg or 0.2–2 mg of purified anthocyanins were dried carefully in a

Speed Vac and taken up in 0.2 ml of dry DMSO. A 0.2-ml volume of dimethylsulphanyl carbanion (potassium salt) was added under argon and the samples were stirred at ambient temperature for at least 60 min. During this deprotonation [7], aromatic acyl groups are likely to be removed from the anthocyanins by alkaline hydrolysis. The samples were cooled on ice and 150 μl of methyl iodide were added to the frozen samples. After thawing and mixing, the methylation reaction was allowed to proceed for at least 1 h or overnight. Subsequently, 3 ml of chloroform–methanol (2:1, v/v) were added and the organic phase was washed four times with 2 ml of water. The methylated samples were then dried under a stream of filtered air at 40°C. A 50- μg amount of *myo*-inositol was added as an internal standard and the permethylated saccharides were hydrolysed in 2 M TFA. This procedure also removes the aglycones from the saccharide part. The partially methylated monosaccharides were then reduced and acetylated as described above for the monosaccharide analysis.

GC was performed on a Shimadzu GC-9A instrument equipped with a DB-1701 capillary column (30 m \times 0.25 mm I.D., 0.25- μm film thickness) with temperature programming from 180 to 240°C at 2.5°C/min. The carrier gas, injector and detector were as described above. The peaks were identified by comparing their relative retention times with those of PMAA standards analysed by GC-MS. Cellobiose was used as the external standard. Quantitative results were obtained by using the relative response factors provided by Sweet *et al.* [19].

RESULTS AND DISCUSSION

Monosaccharide composition

The derivatization of the sugar residues to their alditol acetates produces volatile derivatives suitable for GC analysis [4]. A mixture of the alditol acetates derived from eight standard sugars and the internal standard *myo*-inositol was well separated by capillary GC (Fig. 1a). The alditol acetates could also be chromatographed with the column and GC programme used for methylation analysis.

The investigation of the flavonoid standards quercitrin (= quercetin 3-rhamnoside), hyperoside (= quercetin 3-galactoside), rutin (= quercetin 3-rhamnosylglucoside), cyanin (= cyanidin 3,5-di-

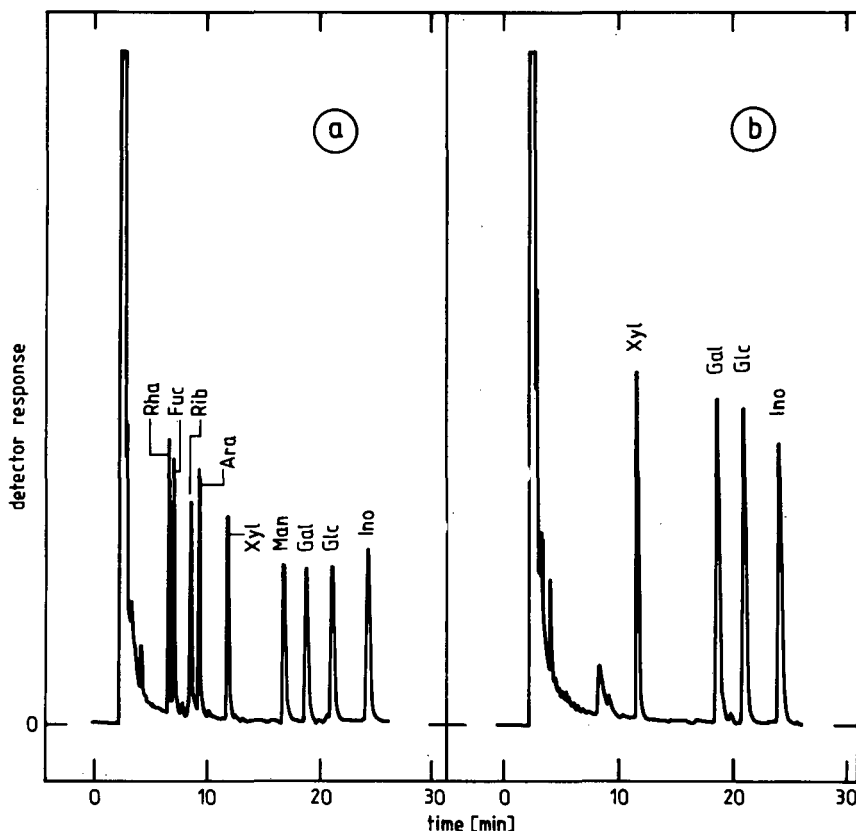


Fig. 1. GC separation of alditol acetates on a Shimadzu GC-9A instrument equipped with an SP-2340 capillary column (30 m \times 0.25 mm I.D.) run isothermally at 235°C with flame ionization detection. Derivatization of the samples was carried out as described under Experimental. (a) Standard mixture containing alditol acetates derived from Rha = rhamnose, Fuc = fucose, Rib = ribose, Ara = arabinose, Xyl = xylose, Man = mannose, Gal = galactose, Glc = glucose and Ino = *myo*-inositol. (b) Alditol acetates derived from the purified major anthocyanin from carrot cell suspension cultures with *myo*-inositol as internal standard.

glucoside) and cyanidin 3-glucoside yielded the expected monosaccharide derivatives (data not shown). In the chromatograms for quercitrin and hyperoside, some impurities were present: traces of glucose could be identified, probably originating from the cellulose TLC plates. The flavonoid aglycones were split off during acid hydrolysis and could be extracted with ethyl acetate and identified by TLC or HPLC.

Capillary GC of the alditol acetates derived from the major anthocyanin of carrot cell cultures after TFA hydrolysis and derivatization yielded three peaks (Fig. 1b) which could be clearly identified as xylitol pentaacetate, galactitol hexaacetate and glucitol hexaacetate by comparison with the standard mixture (Fig. 1a). Hence the carbohydrate compo-

nent of the pigment is composed of xylose, glucose and galactose in equimolar amounts. These results confirm earlier findings by Harborne *et al.* [10] and Hopp and Seitz [11] obtained with PC and TLC. Two further carrot anthocyanins proved to have the same monosaccharide composition. Hemingson and Collins [20] tried to determine the monosaccharides in carrot anthocyanins using a similar method, but had problems with extraneous sugars probably originating from the chromatography paper. Their identification of two mono- and two diglycosides is obviously connected with degradation products [10].

The monosaccharide composition of samples containing as little as 50 μ g of purified pigment could be unambiguously determined with the outlined proce-

ture. In contrast, GC analysis of sugars after trimethylsilylation requires about 250–500 μg [3]. Despite some limitations (difficulties with ketoses and some sugar pairs have been discussed [5]), this derivatization technique has proved to be a useful method for identifying most of the monosaccharides naturally occurring in anthocyanins and other flavonoids.

Methylation analysis

The PMAA obtained by methylation of the free hydroxyl groups, hydrolysis of the glycosidic bonds and subsequent acetylation were separated by capillary GC and identified by comparison with PMAA standards and the external standard cellobiose [15]. Cellobiose yielded two peaks originating from a terminal glucose residue bound through C-1 and a glucose bound through C-4. Rutin exhibited one peak clearly representing a 1,5,6-tri-O-acetyl-2,3,4-tri-O-methylglucitol and a peak that could not be distinguished from a terminal rhamnose (2,3,4-tri-O-methylrhamnositol). These two peaks corresponded to the expected derivatives which were present in equimolar amounts (data not shown). A series with different quantities of rutin from 200 to 800 μg was analysed, revealing that 200 μg were sufficient for detection. Thus, methylation analysis requires much smaller amounts of analyte than ^{13}C NMR studies necessary for structure elucidation with spectroscopic methods.

Methylation analysis of the glycoside part of the major carrot anthocyanin yielded three PMAA peaks separated with capillary GC (Fig. 2). Their relative retention times (RRT) compared with the internal standard were 0.330 (peak 1), 0.455 (peak 2) and 0.835 (peak 3). Peak 3 corresponded well to 1,2,5,6-tetra-O-acetyl-3,4-di-O-methylgalactitol (RRT 0.838) and definitely not to a tri-O-acetyltri-O-methylgalactitol (RRT 0.586–0.687) [15]. This unequivocally proved that the galactose residue is branched at the 2- and 6-positions, as had been postulated from fast atom bombardment (FAB) MS data [21]. Peak 1 represented 1,5-di-O-acetyl-2,3,4-tri-O-methylxylitol and peak 2 1,5-di-O-acetyl-2,3,4,6-tetra-O-methylglucitol originating from terminal xylopyranose and glucopyranose, respectively. Chromatograms of the external standard cellobiose confirmed the peak identification. The three peaks represented equimolar amounts as calculated

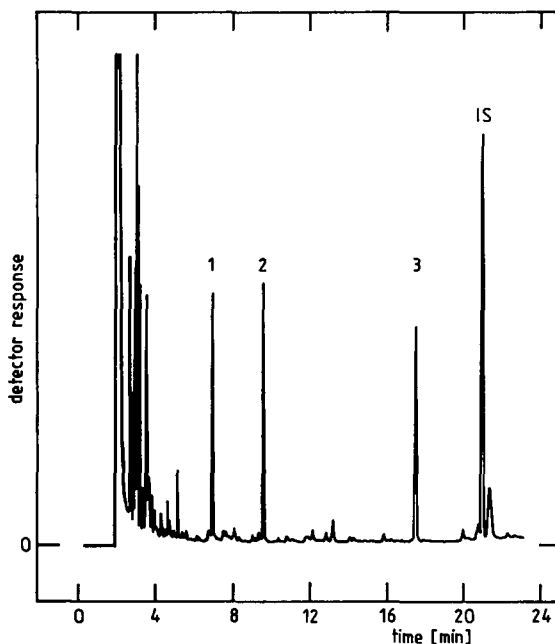


Fig. 2. GC analysis of partially methylated alditol acetates prepared from the purified major anthocyanin component of carrot cell cultures. GC was performed on a Shimadzu GC-9A instrument equipped with a DB-1701 capillary column (30 m \times 0.25 mm I.D., 0.25- μm film thickness) with a temperature gradient from 180 to 240°C at 2.5°C/min and flame ionization detection. IS = Internal standard (*myo*-inositol).

from the relative response factors [19]. Hence the results on the monosaccharide composition are corroborated by methylation analysis.

The occurrence of nine methylated hydroxyl groups on derivatization of the trisaccharide indicated that the acyl group must have been removed prior to methylation by the alkali treatment with dimethylsulphinyl carbanion. The attachment site of the acyl group therefore cannot be determined with this technique. Attempts to evaluate the position of this linkage by GC analysis of methylated samples of anthocyanins [18,22,23] were hampered in each instance by the removal of the acyl group during methylation. Considering the detection of sinapoylglucose fragments with FAB-MS [21], the acyl group must be attached to the glucose moiety. On the basis of indirect evidence, the glucose–galactose link has been concluded to be β (1–6) [12]. As the acyl group was clearly identified to be sinapic acid by HPLC

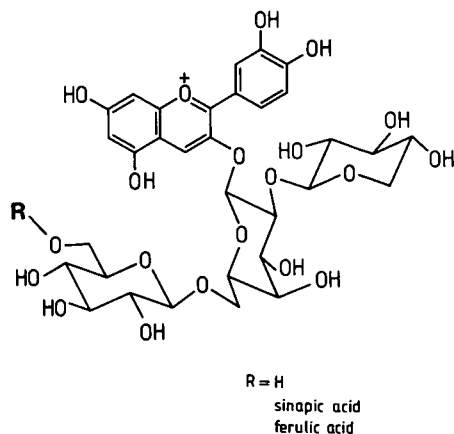


Fig. 3. Structures of three anthocyanins from carrot cell suspension cultures.

(data not shown), the structure of the major anthocyanin from carrot cell suspension cultures is cyanidin 3-(6^G-glucosyllathyroside), *i.e.*, cyanidin 3-O-(2''-xylopyranosyl-6''-glucopyranosylgalactopyranoside), acylated with sinapic acid. This conclusion is consistent with NMR data obtained recently [24]. Another two anthocyanins derived from the same cell culture were analysed. They exhibited the same carbohydrate component but contained ferulic acid or had no acyl residue (Fig. 3).

A comparable methylation procedure with methyl iodide in dimethylformamide in the presence of silver oxide has been described for the examination of acylated betacyanins [23]. The identification of partially methylated sugars by PC and TLC made possible the discovery of a branched trisaccharide in the betacyanins of *Bougainvillea glabra* [25].

Deacylation of the anthocyanins with potassium hydroxide prior to derivatization had no substantial effect on either the methylation data or on the monosaccharide analysis. Since peroxide degradation of the cyanidin aglycone did not improve the GC profiles either, we suggest that both derivatization procedures are carried out without additional pretreatment. The advantage of the outlined GC analyses is their sensitivity and the option of combining them with detection by mass spectrometry. The monosaccharide composition can be elucidated with only 25 μg of carbohydrate. Complete methylation allows reliable determinations of the interglycosidic linkages (except the α or β configuration at the

anomeric carbon atoms) and terminal sugars with samples containing as little as 200 μg of purified pigment. Methylation analysis is especially suitable for investigations of complex glycosides, *e.g.*, for branched saccharides in anthocyanins and other flavonoids.

ACKNOWLEDGEMENTS

The authors thank Professor J. B. Harborne and J. Greenham (University of Reading, UK) for their help with anthocyanin purification, for valuable discussions and for a sample of cyanidin 3-glucoside. They are also grateful to Professor K. Poralla (Department of Biology, Tübingen) for enabling them to carry out some GC analyses on his Shimadzu GC-9A instrument. W.E.G. and M.E. were supported by fellowships (Graduierten-Förderung) of the Land Baden-Württemberg. This work was supported by the Deutsche Forschungsgemeinschaft (DFG).

REFERENCES

- 1 B. V. Chandler and K. A. Harper, *Aust. J. Chem.*, 14 (1961) 586.
- 2 D. Strack and V. Wray, in J. B. Harborne (Editor), *Methods in Plant Biochemistry, Vol. 1, Plant Phenolics*, Chapman & Hall, London, 1989, Ch. 9, p. 325.
- 3 K. R. Markham, *Techniques of Flavonoid Identification (Biological Techniques Series)*, Academic Press, London, 1982.
- 4 D. A. Kolterman, *Phytochem. Bull.*, 16 (1984) 22.
- 5 K. R. Markham, in J. B. Harborne (Editor), *Methods in Plant Biochemistry, Vol. 1, Plant Phenolics*, Chapman & Hall, London, 1989, Ch. 6, p. 197.
- 6 P. J. Harris, R. J. Henry, A. B. Blakeney and B. A. Stone, *Carbohydr. Res.*, 127 (1984) 59.
- 7 S. Hakomori, *J. Biochem. (Tokyo)*, 55 (1964) 205.
- 8 W. S. York, A. G. Darvill, M. McNeil, T. T. Stevenson and P. Albersheim, *Methods Enzymol.*, 118 (1986) 3.
- 9 M. Emmerling and H. U. Seitz, *Planta*, 182 (1990) 174.
- 10 J. B. Harborne, A. M. Mayer and N. Bar-Nun, *Z. Naturforsch., Teil C*, 38 (1983) 1055.
- 11 W. Hopp and H. U. Seitz, *Planta*, 170 (1987) 74.
- 12 J. B. Harborne, *Biochem. System. Ecol.*, 4 (1976) 31.
- 13 J. B. Harborne and R. J. Grayer, in J. B. Harborne (Editor), *The Flavonoids—Advances in Research since 1980*, Chapman & Hall, London, 1988, Ch. 1, p. 1.
- 14 R. Brouillard, in J. B. Harborne (Editor), *The Flavonoids—Advances in Research since 1980*, Chapman & Hall, London, 1988, Ch. 16, p. 525.
- 15 M. Emmerling, *Ph.D. Thesis*, Tübingen, 1990.
- 16 W. Alfermann and E. Reinhard, *Experientia*, 27 (1971) 353.

- 17 W. Noé, C. Langebartels and H. U. Seitz, *Planta*, 149 (1980) 283.
- 18 R. F. Albach, R. E. Kepner and A. D. Webb, *J. Food Sci.*, 30 (1965) 69.
- 19 D. P. Sweet, R. H. Shapiro and P. Albersheim, *Carbohydr. Res.*, 40 (1975) 217.
- 20 J. C. Hemingson and R. P. Collins, *J. Nat. Prod. (Lloydia)*, 45 (1982) 385.
- 21 J. B. Harborne and R. Self, unpublished results.
- 22 D. E. Gueffroy, R. E. Kepner and A. D. Webb, *Phytochemistry*, 10 (1971) 813.
- 23 L. Minale, M. Piatelli, S. De Stefano and R. A. Nicolaus, *Phytochemistry*, 5 (1966) 1037.
- 24 W. E. Glässgen, V. Wray, D. Strack, J. W. Metzger and H. U. Seitz, *Phytochemistry*, in press (1992).
- 25 F. Imperato, *Phytochemistry*, 14 (1975) 2526.

Mass spectrometric identification of products formed during degradation of ethyl dimethylphosphoramidocyanidate (tabun)

P. A. D'Agostino* and L. R. Provost

Defence Research Establishment Suffield, P.O. Box 4000, Medicine Hat, Alberta T1A 8K6 (Canada)

(First received September 17th, 1991; revised manuscript received January 8th, 1992)

ABSTRACT

The major sample components in dichloromethane extracts of munitions-grade tabun decontaminated with methanol–potassium hydroxide, including nine compounds not previously associated with tabun, were identified following capillary column gas chromatographic–mass spectrometric analysis. Electron impact fragmentation ions provided valuable structural information for the unknown sample components, but the presence of little or no molecular ion information for many of the components made identification difficult. Ammonia chemical ionization analysis was required to provide the complementary molecular ion information necessary for identification or tentative identification of these compounds. All the major sample components exhibited significant $(M+H)^+$ and $(M+NH_4)^+$ pseudo-molecular ions and in some cases structurally significant chemical ionization fragmentation ions during capillary column ammonia chemical ionization gas chromatographic–mass spectrometric analysis.

INTRODUCTION

The possible ratification of a United Nations Chemical Weapons Convention has prompted many nations to consider the ramifications of chemical warfare agent destruction. Destruction of organophosphorus chemical warfare agents may be done by chemical and/or thermal means, with chemical degradation often being preferred for small-scale operations. Regardless of the destruction method, it will be critical to both the Chemical Weapons Convention inspectorate and environmental concerns, that adequate analytical methods be available to monitor both the destruction of chemical warfare agents and the resultant reaction products.

Capillary column gas chromatography with flame ionization detection (GC–FID) may be used for the detection of chemical warfare agents [1,2]. However, it is generally agreed that the Chemical Weapons Convention will require confirmation of chemical warfare agents and their degradation

products by mass spectrometry (MS). Electron impact (EI) ionization has been used for the verification of organophosphorus chemical warfare agents, as the EI mass spectra of numerous chemical warfare agents, their decomposition products and related compounds have been published [3–8]. EI mass spectra generally provide excellent structural information [9], but the presence of little or no molecular ion information often hinders the identification of unknown organophosphorus compounds. Chemical ionization mass spectrometry (CI-MS) [10] has been used with increasing frequency to provide molecular ion information for organophosphorus compounds [11] with isobutane and other CI gases [4,12] having been used in the analysis of organophosphorus chemical warfare agents. More recently, the efficacy of ammonia CI-MS [13] has been demonstrated for phosphorous oxyacids [14], for several organophosphorus pesticides [15–17], during tandem MS study [18,19] and for the identification of unknown components of interest to the Chemical Weapons Convention in tabun [5,8] and

VX [7] formulations. Ammonia CI-MS was particularly valuable in the formulation analyses and was therefore used in this project for the identification of unknown organophosphorus degradation products in decontaminated munitions grade tabun.

A small-scale chemical destruction of the organophosphorus chemical warfare agent, ethyl dimethylphosphoramidocyanidate (tabun), was carried out using methanol-potassium hydroxide and the resultant solutions stored awaiting high-temperature incineration at the Defence Research Establishment Suffield. Samples of the decontaminated munitions-grade tabun were extracted with dichloromethane and subjected to capillary column GC-MS analysis to verify complete destruction of the tabun. EI-MS and ammonia CI-MS analysis of the dichloromethane extracts indicated the presence of a number of compounds due to methanolysis that were not previously associated with the munitions grade tabun [8]. The primary objective of this study was the MS identification of these unknown components, as this information would be of value to others involved in the verification of chemical warfare agent destruction.

EXPERIMENTAL

Munitions-grade tabun and dichloromethane extracts of the munitions-grade tabun decontaminated with methanol-potassium hydroxide were provided by personnel involved in a project that will rid the Defence Research Establishment Suffield Experimental Proving Grounds of chemical waste. All samples were stored in PTFE-lined screw-capped vials at 4°C prior to GC analysis. Anhydrous-grade ammonia (99.99%) was used during CI-MS analyses (Liquid Carbonic Ltd.).

Munitions-grade tabun and dichloromethane extracts of decontaminated munitions-grade tabun samples were analysed by capillary column GC-MS under both EI and ammonia CI conditions. Analyses were carried out with a VG 70/70E mass spectrometer equipped with a Varian 3700 gas chromatograph. All GC injections were cool on-column onto 15 m × 0.32 mm I.D. J&W capillary columns coated with either DBWAX or DB-1701 films (0.25 μm) with the following temperature programme: 50°C (2 min), then 10°C/min to 230°C. Helium was used as the carrier gas with a linear velocity of ap-

proximately 100 cm/s. EI conditions were as follows: electron energy, 70 eV; source temperature, 200°C; emission, 100 μA and source pressure, $5 \cdot 10^{-7}$ Torr. Ammonia CI conditions were as follows: electron energy, 50 eV; source temperature, 130°C; emission, 500 μA and source pressure, $9 \cdot 10^{-5}$ Torr. All EI and CI full scanning data were obtained over 400 to 35 u at 1 s/decade with an accelerating voltage of 6 kV.

RESULTS AND DISCUSSION

Twenty-four organophosphorus compounds were detected during capillary column GC-MS analysis of the munitions-grade tabun and dichloromethane extracts of the decontaminated munitions-grade tabun (Table I). Fig. 1 illustrates a typical chromatogram obtained for munitions-grade tabun using the DBWAX column. Following methanol-potassium hydroxide decontamination of the munitions-grade tabun, a number of new sample components were resolved through the use of both DBWAX (Fig. 2) and DB-1701 (Fig. 3) columns. Tabun and two other cyano substituted organophosphorus compounds, observed in munitions-grade tabun [8], were not detected in samples decontaminated with methanol-potassium hydroxide. Electron impact mass spectra provided valuable structural information for the unknown compounds, but the presence of little or no molecular ion information hindered identification.

Ammonia CI-MS, a technique being used with increasing frequency to provide the complementary molecular ion information for organophosphorus chemical warfare agents, greatly aided the identification of the decontamination products of munitions-grade tabun. All the compounds identified during chromatographic analysis of munitions-grade tabun and the decontamination products of the munitions-grade tabun exhibited pseudo-molecular ions during ammonia CI-MS and in many cases structurally significant CI fragmentation ions due to the neutral loss of C_xH_{x+2} (where $x = 2$ or 3) from the largest alkoxy (OC_xH_{x+2}) substituent.

Figs. 4 and 5 illustrate the EI and ammonia CI mass spectra of organophosphorus compounds not previously reported in munitions-grade tabun [8]. Five of the compounds, isopropyl methyl ethylphosphonate (Fig. 4a), diisopropyl ethylphospho-

TABLE I

COMPOUNDS IDENTIFIED IN MUNITIONS-GRADE TABUN AND DECONTAMINATED MUNITIONS-GRADE TABUN

Peak Nos. refer to chromatograms in Figs. 1, 2 and 3. Asterisks indicate presence in munitions (M)-grade tabun or in decontaminated (D) munitions-grade tabun.

Peak No.	Mol. wt.	M	D	Compound
1	166	*	*	Isopropyl methyl ethylphosphonate
2	194	*	*	Diisopropyl ethylphosphonate
3	209	*	*	Diisopropyl dimethylphosphoramidate ^a
4	140	—	*	Trimethyl phosphate
5	153	—	*	Dimethyl dimethylphosphoramidate
6	181	—	*	Isopropyl methyl dimethylphosphoramidate
7	195	*	*	Ethyl isopropyl dimethylphosphoramidate ^a
8	167	—	*	Ethyl methyl dimethylphosphoramidate
9	224	*	*	Triisopropyl phosphate ^a
10	—	—	*	Unknown ^b
11	181	*	*	Diethyl dimethylphosphoramidate ^a
12	182	—	*	Ethyl isopropyl methyl phosphate
13	210	*	*	Diisopropyl ethyl phosphate ^a
14	168	—	*	Diethyl methyl phosphate
15	196	*	*	Diethyl isopropyl phosphate ^a
16	182	*	*	Triethyl phosphate ^a
17	194	*	*	Methyl pinacolyl methylphosphonate
18	194	*	*	Isopropyl tetramethylphosphorodiamidate ^a
19	166	—	*	Methyl tetramethylphosphorodiamidate
20	180	*	*	Ethyl tetramethylphosphorodiamidate ^a
21	176	*	—	Isopropyl dimethylphosphoramidocyanidate ^a
22	162	*	—	Ethyl dimethylphosphoramidocyanidate (Tabun) ^a
23	161	*	—	Tetramethylphosphorodiamidic cyanide ^a
24	154	—	*	Dimethyl ethyl phosphate

^a Compound previously identified in munitions-grade tabun (ref. 8)

^b EI data were not interpretable and no ammonia CI data were obtained.

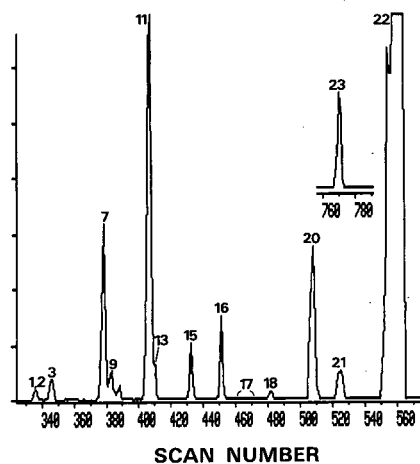


Fig. 1. Capillary column GC-MS total ion current chromatogram of munitions-grade tabun obtained under electron impact ionization conditions. Sample components are identified in Table I. Conditions: 15 m × 0.32 mm I.D. J&W DBWAX; 50°C (2 min), 10°C/min to 230°C (5 min); 1 MS Scan = 1.3 s).

nate (Fig. 4b), dimethyl dimethylphosphoramidate (Fig. 4c), ethyl methyl dimethylphosphoramidate (Fig. 4e) and methyl pinacolyl methylphosphonate (Fig. 5c), exhibited EI mass spectra similar to those published by the Finnish Research Project for Chemical Warfare Verification [3,20], and tentative identification was possible on this basis. Further evidence, particularly for the three compounds which do provide molecular ion information under EI conditions (isopropyl methyl ethylphosphonate, diisopropyl ethylphosphonate and methyl pinacolyl methylphosphonate) was obtained during ammonia CI analysis. $(M+H)^+$ and $(M+NH_4)^+$ pseudomolecular ions were observed for these three compounds as well as for the other two compounds that exhibit molecular ions under EI conditions. Background subtraction, performed on all the ammonia CI mass spectra presented, was not always effective

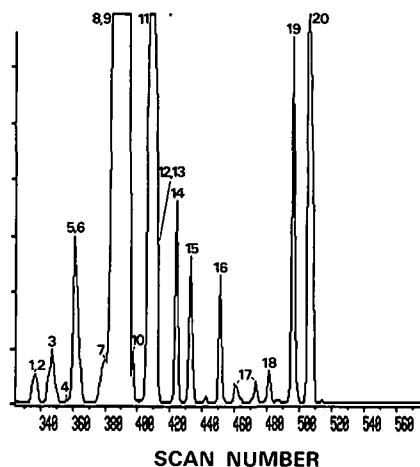


Fig. 2. Capillary column GC-MS total ion current chromatogram of dichloromethane extract of methanol-potassium hydroxide decontaminated munitions-grade tabun obtained under electron impact ionization conditions. Sample components are identified in Table I. Component 9 was minor compared to component 8. Conditions: 15 m \times 0.32 mm I.D. J&W DBWAX; 50°C (2 min), 10°C/min to 230°C (5 min); 1 MS Scan = 1.3 s.

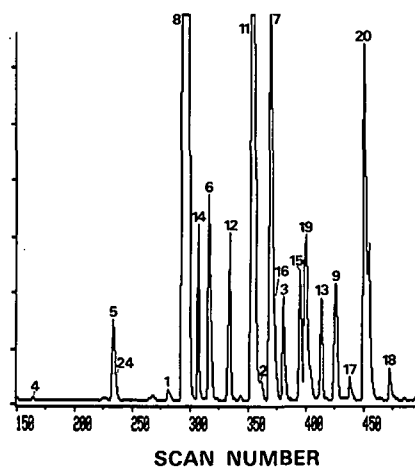


Fig. 3. Capillary column GC-MS total ion current chromatogram of dichloromethane extract of methanol-potassium hydroxide decontaminated munitions-grade tabun obtained under electron impact ionization conditions. Sample components are identified in Table I. Conditions: 15 m \times 0.32 mm I.D. J&W DB-1701; 50°C (2 min), 10°C/min to 250°C (5 min); 1 MS Scan = 1.3 s.

in completely reducing the low mass CI background ions ($< m/z$ 100) for several minor components (*i.e.*, Figs. 4a and b).

The remaining five compounds were identified on the basis of interpretation of both the EI and ammonia CI data acquired. Isopropyl methyl dimethylphosphoramidate (Fig. 4d) exhibited EI ions at m/z 181, 166, 139, 122 and 108, likely due to M^+ , $(M-CH_3)^+$, $(M-C_3H_6)^+$, $(M-OC_3H_7)^+$ and $[N(CH_3)_2P(O)OH]^+$, respectively. The base ion at m/z 44, due to $[N(CH_3)_2]^+$, was typically observed as the base ion during prior analysis of other dimethylphosphoramidates [5,8]. The m/z 181 ion was confirmed as the molecular ion during ammonia CI by the presence of $(M+H)^+$ and $(M+NH_4)^+$ pseudo-molecular ions at m/z 182 and 199 respectively.

Ethyl isopropyl methyl phosphate was characterized by EI fragmentation ions at m/z 167, 141, 139, 113 and 95, likely due to $(M-CH_3)^+$, $(M-C_3H_5)^+$, $(M-C_3H_7)^+$, $[(OH)_3P(OCH_3)]^+$ and $[(OH)P(O)(OCH_3)]^+$, respectively. Molecular ion information, absent in the EI data, was provided during ammonia CI analysis. Pseudo-molecular ions at m/z 183 and 200, due to $(M+H)^+$ and $(M+NH_4)^+$, respectively, and CI fragmentation

ions due to the loss of C_3H_6 from both pseudo-molecular ions (m/z 141 and 158) were observed (Fig. 5a).

Diethyl methyl phosphate exhibited a weak EI molecular ion at m/z 168 and several diagnostic EI fragmentation ions at m/z 153, 141, 113, 95 and 81, likely due to $(M-CH_3)^+$, $(M-C_2H_3)^+$, $[(OH)_3P(OCH_3)]^+$, $[(OH)P(O)(OCH_3)]^+$ and $[(OH)_2P(O)]^+$, respectively (Fig. 5b). The molecular weight of the compound was confirmed by the presence of pseudo-molecular ions at m/z 169 and 186, due to $(M+H)^+$ and $(M+NH_4)^+$, respectively, and CI fragmentation ions due to the loss of C_2H_4 from both pseudo-molecular ions (m/z 141 and 158) were observed.

Methyl tetramethylphosphorodiamidate was characterized by an intense molecular ion at m/z 166, an EI fragmentation ion due to loss of $N(CH_3)_2$ from the molecular ion (m/z 122) and the ion diagnostic of dimethylphosphoramidates at m/z 44 due to $[N(CH_3)_2]^+$ (Fig. 5d). The ammonia CI mass spectrum contained pseudo-molecular ions at m/z 167 and 184 due to $(M+H)^+$ and $(M+NH_4)^+$, respectively.

Dimethyl ethyl phosphate exhibited EI fragmen-

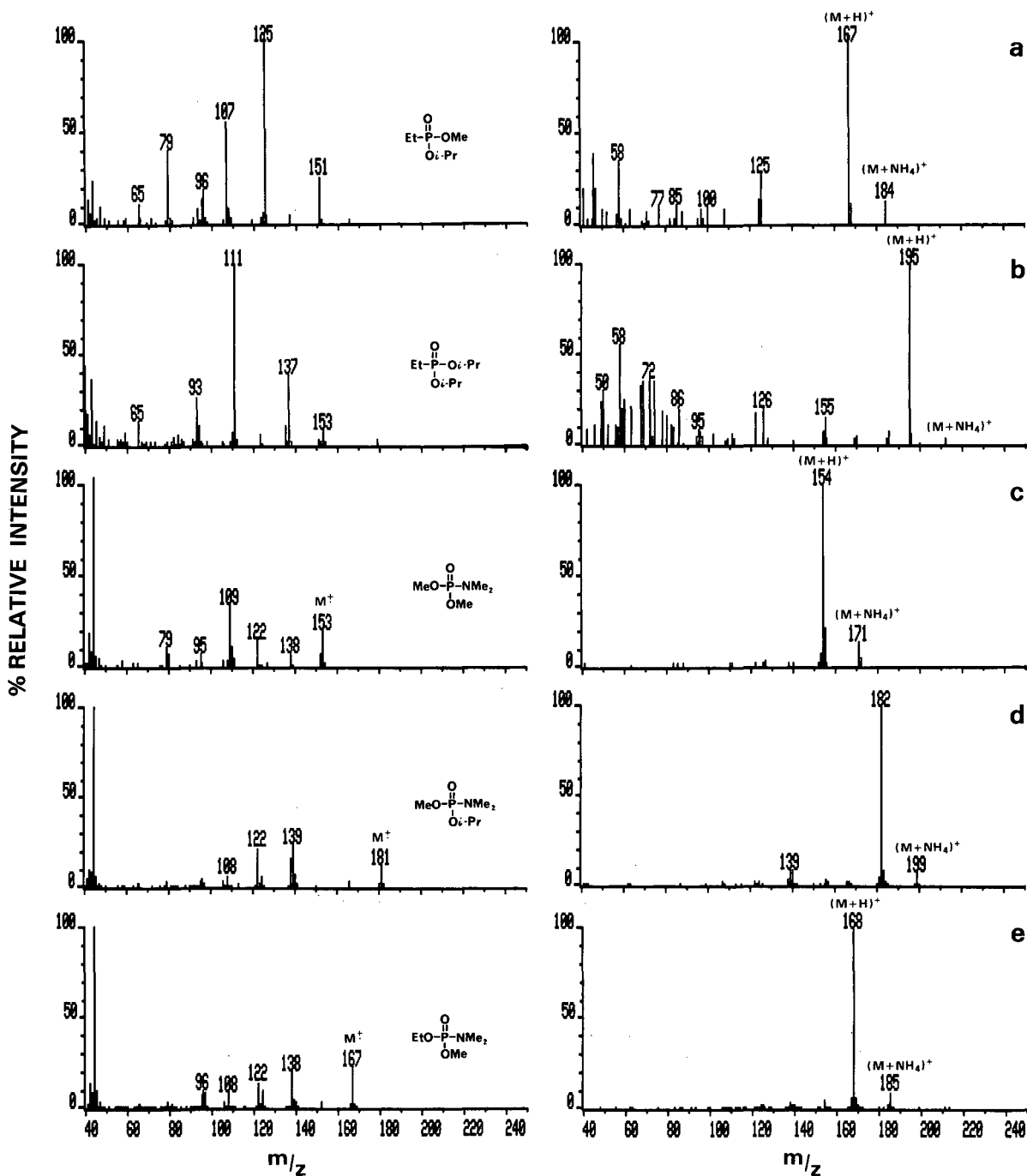


Fig. 4. Electron impact (left) and ammonia chemical ionization (right) mass spectra obtained for (a) isopropyl methyl ethylphosphonate, (b) diisopropyl ethylphosphonate, (c) dimethyl dimethylphosphoramidate, (d) isopropyl methyl dimethylphosphoramidate and (e) ethyl methyl dimethylphosphoramidate. Et = Ethyl; *i*-Pr = isopropyl; Me = methyl.

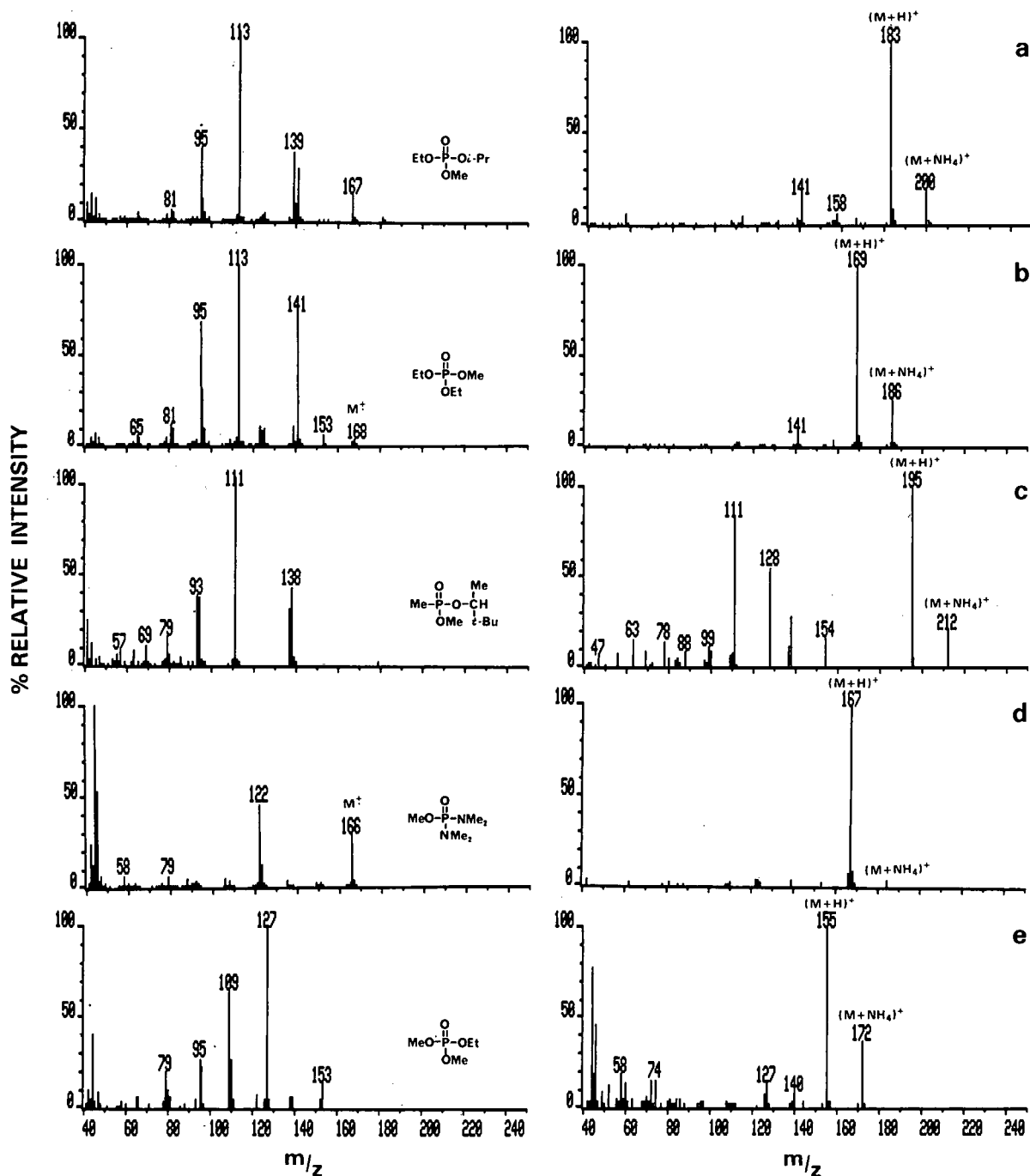


Fig. 5. Electron impact (left) and ammonia chemical ionization (right) mass spectra obtained for (a) ethyl isopropyl methyl phosphate, (b) diethyl methyl phosphate, (c) methyl pinacol methylphosphonate, (d) methyl tetramethylphosphorodiamidate and (e) dimethyl ethyl phosphate. *t*-Bu = *tert*-Butyl; other abbreviations as in Fig. 4.

tation ions at m/z 153, 127, 109 and 95 likely due to $(M-H)^+$, $(M-C_2H_3)^+$, $(M-OC_2H_5)^+$ and $[(OH)P(O)(OCH_3)]^+$, respectively (Fig. 5e). Support for a molecular weight of 154 was provided by the presence of pseudo-molecular ions at m/z 155 and 172, due to $(M+H)^+$ and $(M+NH_4)^+$, respectively.

The methanolysis product of tabun, ethyl methyl dimethylphosphoramidate $[(EtO)(CN)P(O)(NMe_2)]$, was the major component identified during GC-MS analysis of the decontaminated munitions-grade tabun (Figs. 2 and 3). Compounds, such as methyl tetramethylphosphorodiamidate and dimethyl dimethylphosphoramidate, could be expected after methanolysis of, for example, the munitions-grade tabun component, tetramethylphosphorodiamidic cyanide. Most of the other methanolysis products could be rationalized in a similar manner. The ammonia CI mass spectrum of trimethyl phosphate acquired was similar to published data [14] and the presence of this minor component was confirmed with a standard. An unusual compound methyl pinacolyl methylphosphonate (two chromatographic peaks due to diastereoisomeric pair) was found in both the munitions-grade tabun and the decontaminated munitions-grade tabun extract. This compound, present at a very low level relative to the other sample components in munitions-grade tabun (Fig. 1), was likely due to contamination of the tabun with a small amount of the organophosphorus chemical warfare agent, soman or a related pinacolyl containing compound. The P-Et compounds, diisopropyl ethylphosphonate and isopropyl methyl ethylphosphonate (peaks 1 and 2), may also be tabun contaminants. Pyrophosphates identified in munitions-grade tabun [8] were not observed in the dichloromethane extracts of the decontaminated tabun.

CONCLUSIONS

The major sample components in dichloromethane extracts of munitions-grade tabun decontaminated with methanol-potassium hydroxide, including nine compounds not previously associated with tabun, were identified following capillary column GC-MS analysis. Electron impact fragmentation ions provided valuable structural information for the unknown sample components, but the presence of little or no molecular ion information for many of the components made identification difficult. All

the major sample components exhibited significant $(M+H)^+$ and $(M+NH_4)^+$ pseudo-molecular ions and in some cases structurally significant CI fragmentation ions during capillary column ammonia chemical ionization GC-MS analysis. Use of the provided EI-MS and ammonia CI-MS data is anticipated during capillary column GC-MS analysis of chemical destruction samples by other laboratories involved in chemical weapons verification and by the United Nations Inspectorate during the destruction of Iraqi tabun stocks.

REFERENCES

- 1 P. A. D'Agostino and L.R. Provost, *J. Chromatogr.*, 331 (1985) 47-54.
- 2 P. A. D'Agostino and L. R. Provost, *J. Chromatogr.*, 436 (1988) 399-411.
- 3 *Chemical and Instrumental Verification of Organophosphorus Warfare Agents*, The Ministry of Foreign Affairs of Finland, Helsinki, 1977.
- 4 S. Sass and T. L. Fisher, *Org. Mass Spectrom.*, 14 (1979) 257-264.
- 5 P. A. D'Agostino, A. S. Hansen, P. A. Lockwood and L. R. Provost, *J. Chromatogr.*, 347 (1985) 257-266.
- 6 E. R. J. Wils and A. G. Hulst, *Org. Mass Spectrom.*, 21 (1986) 763-765.
- 7 P. A. D'Agostino, L. R. Provost and J. Visentini, *J. Chromatogr.*, 402 (1987) 221-232.
- 8 P. A. D'Agostino, L. R. Provost and K. M. Looye, *J. Chromatogr.*, 465 (1989) 271-283.
- 9 R. G. Gillis and J. L. Occolowitz, in M. Halman (Editor), *The Mass Spectrometry of Phosphorus Compounds*, Interscience, New York, 1972, pp. 295-331.
- 10 M. S. B. Munson and F. H. Field, *J. Am. Chem. Soc.*, 88 (1966) 2621-2630.
- 11 J. R. Chapman, *Organophosphorus Chem.*, 14 (1983) 278-304.
- 12 *Identification of Potential Organophosphorus Warfare Agents*, Ministry of Foreign Affairs of Finland, Helsinki, 1979.
- 13 J. B. Westmore and M. M. Alauddin, *Mass Spectrom. Rev.*, 5 (1986) 381-465.
- 14 P. A. Cload and D. W. Hutchinson, *Org. Mass Spectrom.*, 18 (1983) 57-59.
- 15 R. L. Holmstead and J. E. Casida, *J. Assoc. Off. Anal. Chem.*, 57 (1974) 1050-1055.
- 16 T. Cairns, E. G. Siegmund and R. L. Bong, *Anal. Chem.*, 56 (1984) 2547-2552.
- 17 T. Cairns, E. G. Siegmund, G. M. Doose and A. C. Oken, *Anal. Chem.*, 57 (1985) 572A-576A.
- 18 A. Hesso and R. Kostiaainen, *Proc. 2nd. Int. Symp. Protection Against Chemical Warfare Agents, Stockholm, June 15-19, 1986*, National Defence Research Institute, Umeå, 1986, pp. 257-260.
- 19 P. A. D'Agostino, L. R. Provost and P. W. Brooks, *J. Chromatogr.*, 541 (1991) 121-130.
- 20 *Identification of Degradation Products of Potential Organophosphorus Warfare Agents*, Ministry of Foreign Affairs of Finland, Helsinki, 1980.

Determination of organotin species by capillary gas chromatography with alternating current plasma emission detection

Jackson M. Ombaba and Eugene F. Barry*

Department of Chemistry, University of Massachusetts at Lowell, 1 University Avenue, Lowell, MA 01854 (USA)

(First received October 14th, 1991; revised manuscript received January 21st, 1992)

ABSTRACT

An alternating current plasma (ACP) emission detector is used as a detector for capillary gas chromatography (GC) in the determination of organotin compounds in environmental marine samples. Detection limits for tributyltin chloride (TBT) and tetrabutyltin (TEBT) were found to be 131 and 116 pg/s (as Sn), respectively. Calibration curves exhibited linearity over three orders of magnitude. Precision was found to be less than 8.5% relative standard deviation ($n = 10$) for both TBT and TEBT. Results for the separation and detection of organotin compounds in complex sample matrices are presented to illustrate the selectivity of the ACP emission detector. No prior hydride formation or alkylation reactions were performed on the organotin species prior to gas chromatographic detection. Recovery data ranged from 77 to 100%. The results obtained in this study demonstrate the variability, selectivity and ease of use of the GC-ACP detector for the determination of organotin compounds.

INTRODUCTION

Organotin compounds continue to generate considerable interest among environmental researchers because they exhibit extreme toxicity to a wide variety of aquatic organisms such as fish, mussels and mollusks [1–8]. Tributyltin chloride (TBT), $[\text{CH}_3(\text{CH}_2)_3]_3\text{Sn}$, and tetrabutyltin (TEBT), $[\text{CH}_3(\text{CH}_2)_3]_4\text{Sn}$, are two organotin compounds which are frequently used as fungicides, bactericides as well as anticancer and biochemical agents [2–4], the tri- and tetrabutyl moieties being more toxic than the mono- or dibutyl forms. Consequently, most published data on the toxicity of organotin in aquatic ecosystems focuses on TBT and TEBT [5–8].

Harrison *et al.* [9] have published a compilation of the various analytical techniques developed for the determination of organotin compounds. These include gas chromatography (GC) coupled with various detection modes such as microwave induced plasma [10–12], direct current plasma [13,14],

atomic absorption spectroscopy [2,8,15–17] and flame photometric detection [5,18]. High-performance liquid chromatography (HPLC) has also been used in conjunction with several detection modes including plasma emission spectroscopy [3,10], laser-enhanced ionization detection [6], and furnace atomic absorption spectroscopy [15,19]. Uden [20] has provided an up-to-date review of on-line chromatographic detection by plasma emission spectroscopy in response to the resurgence and potential demonstrated by atomic emission techniques in the past decade.

In the majority of analytical approaches employed in the determination of tin compounds, hydride generation or alkylation [2,5,16] has been used to form volatile derivatives. Although most of these paths have provided low detection limits, they exhibit some minor drawbacks including unpredictable interferences from organic reagents used for hydride generation, contamination of Grignard reagents with TBT and the possibility of molecular rearrangement of organotin compounds accompa-

nying the Grignard reaction [6].

Several recent studies in our laboratory have addressed the interfacing of a capillary gas chromatographic and a HPLC system with an alternating current plasma (ACP) emission detector for selective element detection [21–25]. With an ACP detector, a uniform discharge is generated across two copper electrodes (3 mm diameter) in a controlled helium atmosphere. Therefore, when a primary supply of 115 V at 60 Hz feeds a step-up furnace transformer, an unrectified output voltage of 10 000 V at a current of 23 mA is obtained. The discharge is contained within a quartz tube with emitted radiation incident on the entrance slit of a monochromator, detected and processed. The device produces a remarkably stable signal as it is self-seeding, re-igniting itself every half-cycle (120 times/s) and is easily constructed at modest cost.

The results of the present investigation demonstrate the suitability of GC–ACP emission detection in the analysis of environmentally significant organotin compounds. No hydride formation or alkylation reactions were performed on the species prior to detection. The procedure was applied to mussel, sediment, industrial sludge and wastewater samples.

EXPERIMENTAL

Materials

All solvents employed in this study were pesticide grade. Concentrated hydrochloric acid (Ultrex, J. T. Baker, Philipsburg, NJ, USA), hydrobromic acid (48%) (Fisher Scientific, Fair Lawn, NJ, USA) and organotin standards as tributyltin chloride and tetrabutyltin (Alfa Products, Ward Hill, MA, USA) with stated purities of 96 and 93%, respectively, were used without further purification. Stock solutions of TBT and TEBT were prepared in benzene and refrigerated until use. A regular unleaded Shell gasoline sample was obtained locally.

Instrumentation

The GC–ACP detector system arrangement has been described in detail elsewhere [24,25]. The system includes a Hewlett-Packard 5890A gas chromatograph, a single-beam McPherson grating monochromator (Model EU700 McPherson, Acton, MA), an optical bench equipped with an ad-

justable optical mount and 75-mm biconvex quartz lens (Stratford, CT), a R212 photomultiplier tube (Hamamatsu, Middlesex, NJ, USA) coupled to a McPherson Model 7640 voltage supply and a Hewlett-Packard 3392A integrator. A picoammeter (Model 414S, Keithley instruments, Cleveland, OH, USA) monitored the current generated by the photomultiplier tube. Data acquisition was simultaneously achieved with a Chrom-1AT chromatography data acquisition board controlled by the Lab Calc software (Galactic Industries, Salem, NH, USA) in conjunction with a Zenith AT microcomputer. The Lab Calc software package provided data smoothing algorithms to reduce random noise and permitted selectable sampling rates.

A DB-1 fused-silica capillary GC column (30 m × 0.32 mm I.D., 1.5 μm film thickness) (J&W Scientific, Folsom, CA, USA) was employed. Helium (Linde, ultra-high-purity grade) served as carrier gas at a linear velocity of 30 cm/s and as the plasma supporting gas at a flow-rate of 1800 ml/min. The temperatures of the split injector (split ratio of 100:1) and the interface were maintained at 220°C and 250°C, respectively. The operational parameters for the GC–ACP system appear in Table I.

Preparation of marine samples

Mussels (*Mytilus edulus*) and sediments were collected by hand from Boston Harbor at low tide and were refrigerated to minimize possible changes in-

TABLE I
GENERAL ACP DETECTOR OPERATING CONDITIONS
USED IN THIS STUDY

Parameter	Condition
Helium flow-rate	1800 ml/min
Alternating current power output	11 000 V a.c.
Slit width	200 μm
Slit height	5 mm
Analytical wavelength for Sn(I)	300.91 nm
Picoammeter gain	0.03 · 10 ⁻⁶ to 10 · 10 ⁻⁶ A
Picoammeter time constant	0.2 s
Photomultiplier tube and voltage	R212, -1000 V d.c.
Discharge tube	1 mm I.D. × 6 mm O.D. quartz
RC low-pass filter	Time constant 0.2 s

duced by bacterial action. Mussels were transported to the laboratory in plastic bags while sediments were transported in polycarbonate containers which were prewashed with acid. The industrial sludge and wastewater samples were collected at a local manufacturer of printed circuit boards. Synthetic ocean water was prepared according to the procedure of Parsons *et al.* [26].

The procedure used for the extraction of tin species from mussel tissue and water samples was a modification of the method reported by Martin-Landa *et al.* [27]. After the exterior of the mussel shells was rinsed thoroughly with distilled water, the shells were then opened and the soft tissue removed and washed with distilled water. The analytical sample set consisted of 6 samples, a blank and a spiked blank. The blank consisted of distilled water, glassware and the extracting reagent. The spiked blank was the same except for the addition of known amounts of tributyltin chloride and tetrabutyltin. A 12-g amount of tissue or 100 ml of volume of water (for the case of wastewater and ocean water) were transferred into a 250-ml separatory funnel. A 40-ml volume of concentrated hydrochloric acid was added and the funnel shaken for 2 h followed by a 2-h equilibration period. A 10-ml aliquot of hydrobromic acid (48%) was then added and the solution was allowed to stand for 15 min. A 100-ml aliquot of benzene was then added to the separatory funnel which was subjected to vigorous shaking action for 5 min. After 1 h the organic layer was removed.

The extraction method used for sediments and sludge was a modification of the method reported by Schebek and Andrae [8]. A 50-ml volume of benzene and 1 ml of 30% HCl were added to an appropriate amount of sediment. A PTFE-coated stirring bar was added and the mixture boiled under reflux conditions for 30–40 min in a water bath. After cooling to room temperature, the mixture was distributed among six 10-ml acid-washed glass tubes and centrifuged for 1 h at 1500 g. The supernatants were decanted, combined and transferred into a 50-ml volumetric flask and diluted to the mark with benzene. Each sediment sample was extracted and analyzed in triplicate.

Recovery studies with TBT and TEBT were performed by analyzing a given original sample (*e.g.* mussel tissue, sediment or water) and then spiking

another portion of the original sample at a known level of TBT and TEBT and repeating the same procedure in triplicate; all subsequent GC analyses were also performed in triplicate.

RESULTS AND DISCUSSION

Spectral considerations

A general description of GC-ACP detector interface and the plasma discharge tube appears elsewhere [24,25]; however, in this study a modified quartz plasma discharge tube (2 cm × 1 mm I.D. × 6 mm O.D.) was utilized to enclose the plasma. Approximately 0.5 cm of the capillary column was inserted into the discharge tube after removal of the protective polyimide coating from this segment. A schematic diagram of the GC column-plasma discharge tube interface is shown in Fig. 1. The ACP detector plasma image was focused on the monochromator entrance slit by means of an adjustable optical mount and lens.

An ultrasonic nebulizer (common room humidifier) was subsequently used to generate headspace vapor of TEBT which was transported to the ACP by helium make-up flow. This procedure provided a constant mass introduction of TEBT into the plasma and the emission wavelength-intensity profile of

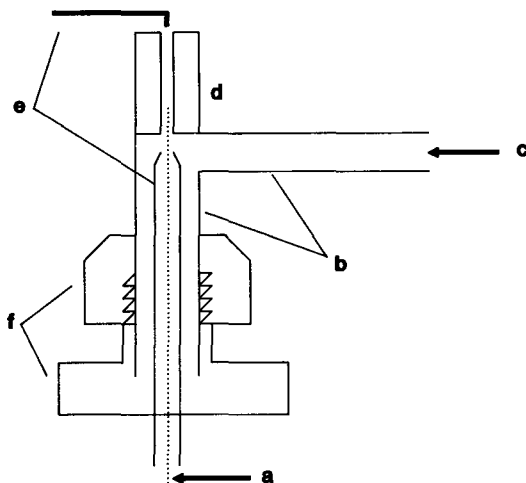


Fig. 1. Gas chromatographic column-plasma discharge tube interface. a = Column from the oven; b = 4 mm I.D. × 6 mm O.D. transfer and electrode holding tubing; c = helium plasma gas inlet; d = 1 mm I.D. × 6 mm O.D. plasma discharge tube; e = copper electrodes; f = 1/4 in O.D. Swagelok tee union.

the tin lines were then determined. Emission intensities at wavelengths of 231.72, 242.95, 254.66, 270.65 and 300.91 nm were observed and corresponded to relative intensities of 0.12, 0.67, 1.00, 0.07 and 0.75, respectively. The 300.91-nm line was selected as the analytical wavelength for this study because of its favorable relative intensity and location in background emission spectrum where no interference from OH, N₂, NH, H, He and O is observed. A tin hollow cathode lamp (Perkin-Elmer, Norwalk, CT, USA) was employed to confirm the analytical emission line (300.91 nm) by positioning the lamp such that its emission lines were incident on the entrance slit of the monochromator. The ACP spectral profile of this region is displayed in Fig. 2. The carbon backbone of TEBT was also eliminated as a source of molecular emission in this spectral region because a scan of benzene vapors in the ACP detector did not produce any major emission bands.

Linearity and detection limits

Calibration plots for TBT and TEBT were prepared by injecting seven repetitive injections of known amounts of each solute into the GC-ACP system. Linearity for each solute extended over three orders of magnitude. Correlation coefficients of the log-log plots were found to be 0.999 for TBT and 0.998 for TEBT, respectively. The detection limits of TBT and TEBT were estimated based on integrated baseline noise [28,29]. Detection limit may be defined as the amount of organotin species needed to produce a signal that is three times the standard deviation of the baseline noise divided by the sensitivity whereas sensitivity is defined as the slope of the calibration plot [30,31] multiplied by the peak-width at half height of the analyte peak to account for k' (capacity factor) [32]. Detection limits were calculated to be 131 and 116 pg/s as Sn for TBT and TEBT, respectively. These detection limits, when converted to mass detection limits, become 0.88 and 0.53 ng as Sn for TBT and TEBT, respectively, and compare favorably with the detection limits of 2.5 ng as Sn for TBT reported by Weber and Han [2]. The precision in response at twice the detection limit was under 8.5% relative standard deviation ($n = 10$) for both TBT and TEBT.

Selectivity

The selectivity ratio may be defined as the ratio of

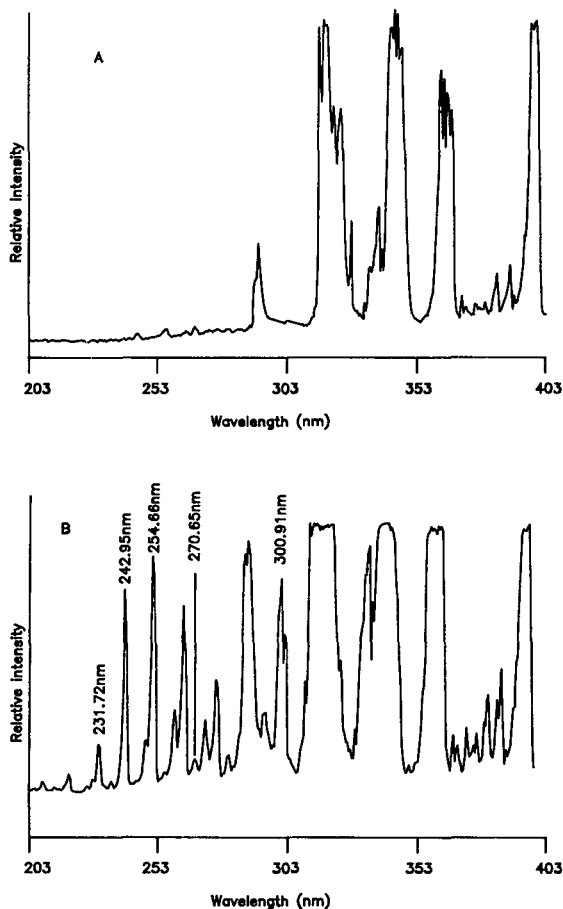


Fig. 2. (A) Background spectrum of the helium alternating current plasma from 203 nm to 403 nm; (B) emission wavelength profile of TEBT in the same spectral region as in (A) (see Table I for experimental conditions of the ACP detector).

peak area response of the ACP detector at 300.91 nm per unit mass of tin to the response per gram weight of carbon in a given compound. The selectivity ratio of the ACP detector towards tin was determined by means of injecting 1- μ l aliquot of standard solutions of selected organics and TEBT with a column temperature of 200°C and a slit width of 200 μ m, after which the responses were then compared. Selectivity ratios of TEBT relative to several organic solvents are listed in Table II and compare favorably with those reported with a GC-microwave-induced plasma [11,12], exhibiting a range of $2.1 \cdot 10^4$ to $5 \cdot 10^5$ for the organic probes under consideration.

TABLE II

ACP SELECTIVITIES OF TETRABUTYL TIN RELATIVE TO SELECTED ORGANICS

The selectivity ratio is defined as the ratio of the peak area response per gram Sn to the peak area response per gram of carbon in the indicated compound.

Compound	Selectivity ratio
Carbon disulfide	21 000
Chloroform	37 200
Ethylene disulfide	53 200
<i>n</i> -Butanol	87 400
Trichloroethylene	90 100
<i>n</i> -Heptane	99 400
Cumene	133 200
<i>n</i> -Hexane	142 300
Pyridine	225 200
Benzene	500 300

Analytical applications

Several applications were conducted in order to demonstrate the practicality and selectivity underlying the ACP response to organotin species present in complex matrices. An appropriate amount of each sample was spiked with a known amount of organotin standard and the appropriate extraction

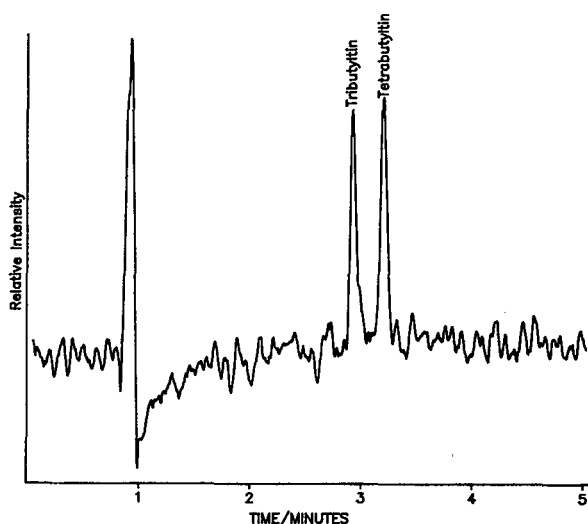


Fig. 3. Chromatogram of spiked distilled water extract; indicated peaks represent 4.8 ng of tributyltin chloride and 4.4 ng of tetrabutyltin. Conditions: column temperature, 170°C; interface temperature 200°C; split ratio, 100:1; amount injected, 1 μ l; $0.03 \cdot 10^{-6}$ A f.s.

TABLE III

RECOVERY OF TRIBUTYL TIN CHLORIDE AND TETRABUTYL TIN COMPOUNDS FROM SPIKED SAMPLES

	Recovery \pm S.D. (%) ($n = 3$)	
	Tributyltin chloride	Tetrabutyltin
Distilled water	98.78 \pm 1.19	101.44 \pm 1.08
Ocean water	89.54 \pm 0.76	91.11 \pm 1.22
Sediment	97.67 \pm 0.78	93.29 \pm 1.74
Wastewater	77.26 \pm 1.94	83.33 \pm 1.10
Sludge	79.97 \pm 1.10	84.81 \pm 1.37

procedure carried out as previously described. The chromatogram presented in Fig. 3 illustrates the separation of TBT (4.8 ng) and TeBT (4.4 ng) in a benzene extract of distilled water initially containing TBT and TeBT at concentrations of 120 and 106 μ g/ml, respectively; likewise a chromatogram of a benzene spiked extract (containing TBT and TeBT) of mussels from Boston Harbor appears in Fig. 4. Percent recovery data for TBT and TeBT spiked in various matrices is listed in Table III and ranges from 77 to 101%. The lower recoveries of organotin from wastewater may be due to associ-

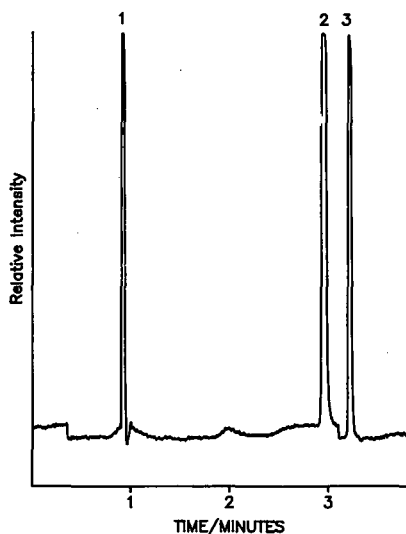


Fig. 4. Chromatogram of extract of mussel tissue from Boston Harbor spiked with tributyltin chloride and tetrabutyltin. Peaks: 1 = solvent; 2 = TBT; 3 = TeBT. Conditions: column temperature, 170°C; interface temperature, 200°C; split ratio, 100:1; $0.1 \cdot 10^{-6}$ A f.s.

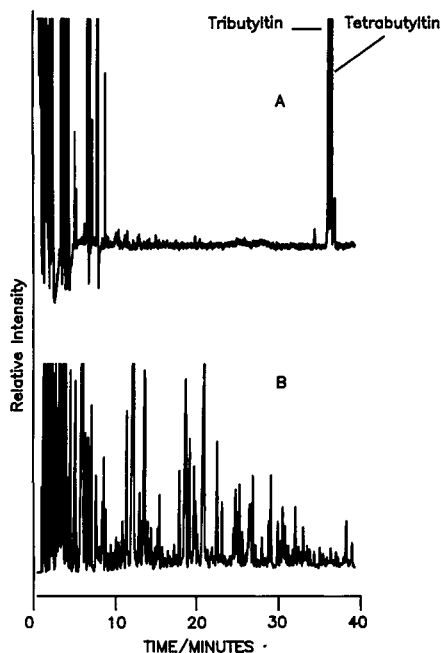


Fig. 5. (A) Chromatogram of regular unleaded gasoline illustrating the detection of 64 ng TBT (26 ng Sn) and 28 ng TEBT (9.6 ng Sn) with ACP detector at 300.91 nm, $0.1 \cdot 10^6$ A f.s. (B) Chromatogram of regular unleaded gasoline detected by flame ionization detection; conditions: 35°C (5 min) to 100°C at 4°C/min then to 230°C at 5°C/min.

ative effects with other organics present whereas secondary partitioning effects may be responsible for the lower recoveries in the sludge samples studied.

An additional application of the detection of organotin in gasoline, a potentially interfering matrix, was then examined to demonstrate the sensitivity and selectivity of the ACP detector. A 5-ml sample of regular gasoline was spiked with 500 μ l of a solution containing 192 ng of TBT and 85 ng of TEBT and a 1- μ l aliquot was then chromatographed. Parallel ACP and flame ionization detection chromatograms are shown in Fig. 5 where the indicated peaks represent 64 ng TBT (26 ng Sn) and 28 ng TEBT (9.6 ng Sn). Although TBT is not an additive to gasoline, the gasoline matrix may be viewed as potentially problematic, as evidenced by the irregular appearance at the beginning of the chromatogram in Fig. 5A due to the rapid coelution of many hydrocarbons associated with gasoline. This coelution results in plasma instability and carbon background

emission and has been observed in previous studies [21,22]. The coelution of these components in Fig. 5 also demonstrates that the ACP detector does not extinguish with the injection of a large solvent plug.

Hydrogen doping of plasma gas

The addition of hydrogen as a doping agent to helium-supported plasmas has been shown to produce signal enhancement in some determinations [12]; signal enhancement factors of two and three have been reported for elements capable of undergoing hydride formation [33]. In the present study, however, the addition of 0.5 to 3 ml/min of hydrogen gas to the helium flow did not produce any enhancement of organotin signals. Also, the hydrogen flow creates intense heating of the plasma and causes added stress on the walls of the discharge tube resulting in reduced life-time of the discharge tube.

CONCLUSIONS

The ACP detector is a viable alternative to other element-selective devices for the detection of organotin species and offers considerable potential. The detector is easily assembled and interfaced with chromatographic equipment at modest cost. The device exhibits a remarkably stable signal because the plasma is self-seeding and reignites itself every half cycle which is 120 times per second for the 60 Hz power supply. A tesla coil is not required to commence operation of the plasma if the ac voltage is greater than the breakdown voltage. As a result, the ACP detector can tolerate high mass flow-rates of solvent without extinguishing and, thus, requires no venting valve which lends itself to a less complex interface design and minimizes band broadening.

The reduction of background spectral interference produced by molecular emission has not been investigated with the ACP detector to date. The use of techniques such as lock-in amplifiers, oscillating quartz plates incorporated within a monochromator and pulsed power sources often lead to an improved signal to noise ratio and better selectivity. These fruitful avenues remain to be studied.

ACKNOWLEDGEMENTS

The authors are grateful to Professor David Ryan and Matthew Staffier for supplying mussel

and sediment samples and to Eric Conte for assistance with the plasma discharge tubes. One of us (J.M.O.) wishes to acknowledge the Graduate School at the University of Massachusetts at Lowell for providing a summer research fellowship. The authors also are appreciative of the data acquisition system donated by Galactic Industries.

REFERENCES

- 1 M. O. Stallard, S. Y. Cola and C. A. Dooley, *Appl. Organomet. Chem.*, 3 (1989) 105.
- 2 J. H. Weber and J. S. Han, *Anal. Chem.*, 60 (1988) 316.
- 3 H. Suyani, D. Heitkemper, J. Creed and J. Caruso, *Appl. Spectrosc.*, 43 (1989) 962.
- 4 Y. Hattori, A. Kobayashi, S. Takemoto, A. Takami, Y. Kuge, A. Sugimae and M. J. Nakamoto, *J. Chromatogr.*, 315 (1984) 341.
- 5 J. J. Sullivan, J. D. Torkelson, M. M. Wekell, T. A. Hollingworth, W. L. Saxton and G. A. Miller, *Anal. Chem.*, 60 (1988) 626.
- 6 K. S. Epler, T. C. O'Haver, G. C. Turk and W. A. MacCrehan, *Anal. Chem.*, 60 (1988) 2062.
- 7 T. L. Wade, B. Garcia-Romero and J. M. Brooks, *Environ. Sci. Technol.*, 22 (1988) 1488.
- 8 L. Schebek and M. O. Andreae, *Environ. Sci. Technol.*, 25 (1991) 871.
- 9 R. M. Harrison, C. N. Hewitt and S. J. deMora, *Trends Anal. Chem.*, 4 (1985) 8.
- 10 H. Suyani, J. Creed, J. Caruso and R. D. Satzger, *J. Anal. At. Spectrom.*, 4 (1989) 777.
- 11 B. D. Quimby, P. C. Uden and R. M. Barnes, *Anal. Chem.*, 50 (1978) 2112.
- 12 S. A. Estes, P. C. Uden and R. M. Barnes, *Anal. Chem.*, 53 (1981) 1829.
- 13 J. O. Beyer, *Ph. D. Dissertation*, University of Massachusetts, Amherst, MA, 1984.
- 14 S. A. Estes, C. A. Poirier, P. C. Uden and R. M. Barnes, *J. Chromatogr.*, 196 (1980) 265.
- 15 E. J. Parks, F. E. Brinckman, K. L. Jewett, W. R. Blair and C. S. Weiss, *Appl. Organomet. Chem.*, 2 (1988) 441.
- 16 V. F. Hodge, S. L. Seidel and E. D. Goldberg, *Anal. Chem.*, 51 (1979) 1256.
- 17 Y. K. Chau, P. T. S. Wong and G. A. Bengert, *Anal. Chem.*, 54 (1982) 246.
- 18 M. D. Muller, *Anal. Chem.*, 59 (1987) 617.
- 19 D. T. Burns, F. Glockling and M. Harriot, *Analyst (London)*, 11 (1983) 921.
- 20 P. C. Uden, in R. M. Harrison and S. Rapsomanikis (Editors), *Environmental Analysis Using Chromatography Interfaced with Atomic Spectroscopy*, Ellis Horwood, Chichester, England, 1989, p. 96.
- 21 R. B. Costanzo and E. F. Barry, *J. High Resolut. Chromatogr.*, 12 (1989) 522.
- 22 R. B. Costanzo and E. F. Barry, *J. Chromatogr.*, 467 (1989) 373.
- 23 L. A. Colon and E. F. Barry, *J. Chromatogr.*, 513 (1990) 159.
- 24 R. B. Costanzo and E. F. Barry, *Anal. Chem.*, 60 (1988) 826.
- 25 R. B. Costanzo and E. F. Barry, *Appl. Spectrosc.*, 42 (1988) 1387.
- 26 T. R. Parsons, Y. Maita and C. M. Lalli, *A. Manual of Chemical and Biological Methods for Seawater Analysis*, Pergamon Press, Oxford, p. 173.
- 27 I. Martin-Landa, F. de Pablos and I. L. Marr, *Anal. Proc.*, 26 (1989) 16.
- 28 H. C. Smith and H. L. Walg, *Chromatographia.*, 8 (1975) 311.
- 29 C. H. Gast, J. C. Kraak, H. Poppe and J. M. Maessen, *J. Chromatogr.*, 185 (1979) 549.
- 30 "Nomenclature, Symbols, Units and Their Usage in Spectrochemical Analysis II: Data Interpretation", *Spectrochim. Acta.*, 33B (1978) 241.
- 31 W. P. Carey and B. R. Kowalski, *Anal. Chem.*, 58 (1986) 3077.
- 32 R. P. W. Scott, *Liquid Chromatography Detectors*, Elsevier, Amsterdam, New York, 2nd ed., 1986, p. 18.
- 33 L. G. Sarto Jr, S. A. Estes, P. C. Uden, S. Siggia and R. M. Barnes, *Anal. Lett.*, 14 (1981) 205.

CHROM. 24 019

Determination of selenium by capillary gas chromatography after high-temperature derivatization with 1,2-diamino-3,5-dibromobenzene

K. Johansson* and Å. Olin

Department of Analytical Chemistry, University of Uppsala, P.O. Box 531, S-751 21 Uppsala (Sweden)

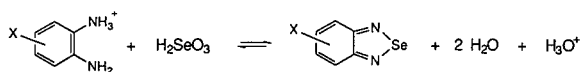
(First received October 2nd, 1991; revised manuscript received January 20th, 1992)

ABSTRACT

The determination of selenium as 4,6-dibromopiazselenol by gas chromatography with electron-capture detection (GC-ECD) was investigated. The rate of formation of the piazselenol from selenium(IV) and 1,2-diamino-3,5-dibromobenzene was studied as a function of temperature. At 100°C the time for quantitative piazselenol formation can be reduced to 5 min without adverse effects on the chromatograms. The use of capillary column results in the separation of the piazselenol from the background without clean-up steps. A capillary column and derivatization at a high temperature facilitate application of the GC-ECD method. The method was applied to the determination of total soluble selenium in water.

INTRODUCTION

The determination of selenium(IV) by gas chromatography with electron-capture detection (GC-ECD) is an established method. It is based on the formation of a volatile compound, generally called a piazselenol (PIAZ), in the reaction between selenious acid and a substituted *o*-phenylenediamine (PDA):



where X is one or several of Cl, Br, NO₂, F or CF₃. The piazselenol is extracted into an organic solvent before injection into the chromatograph.

The unsubstituted piazselenol was first synthesized in 1889 by Hinsberg [1], who showed that only Se(IV) reacts with PDA to form the selenium complex. In 1968, Nakashima and Tôei [2] published a GC method for the determination of selenium using 4-chloro-1,2-diaminobenzene as the ligand. Since then, several papers have been published on the determination of selenium in a range of samples

by GC [3–12]. Various substituted *o*-phenylenediamines [2,3,9,10,12–14] have been employed in order to increase the ECD sensitivity. Shimoishi [3] synthesized a range of differently substituted piazselenols and investigated their chromatographic properties, distribution ratios and relative ECD sensitivities. Amongst the thirteen piazselenols investigated, he found that 1,2-diamino-3,5-dibromobenzene (Br₂-PDA) was the best as regards sensitivity and distribution ratio. Br₂-PDA is perhaps the most commonly used, commercially available ligand today, although it is not the most sensitive.

When fluorine is present in a compound it generally enhances volatility and the ECD sensitivity. Dilli and Sutikno [13] investigated 1,2-diamino-4-fluorobenzene and 1,2-diamino-4-trifluoromethylbenzene. Al-Attar and Nickless [14] prepared and investigated 3-bromo-5-fluoro-1,2-diaminobenzene and 3-bromo-5-trifluoromethyl-1,2-diaminobenzene (Br-CF₃-PDA). Of these ligands, only Br-CF₃-PDA has a higher ECD sensitivity than Br₂-PDA.

In addition, the substituted PDAs 2,3-diaminonaphthalene [12,15] and 1,4-dibromo-2,3-diaminonaphthalene [16] have been used as ligands, but the

sensitivities are inferior to those of the best PDA ligands.

The GC-ECD method is only one of several methods available for the determination of Se(IV). Atomic absorption spectrometry after hydride generation (HG-AAS) [17,18] and cathodic stripping voltammetry (CSV) [19,20] are two commonly used methods. The GC-ECD method is more time consuming than the other two for water samples. In earlier work it has been reported that the piaszelenol reaction takes several hours to reach completion at room temperature [3,4] and generally several clean-up steps are needed before the extract can be injected into the gas chromatograph [4,5,10,13]. Reduction of the time necessary for the formation of the piaszelenol and in the number of clean-up steps required would make the GC-ECD method more attractive. An advantage of the GC-ECD method is that it makes possible the direct determination of Se(IV) in natural water samples. This is not always possible with the CSV and HG-AAS methods, which are subject to interferences from organic material in such samples. Further, low limits of detection can be reached with the GC-ECD method owing to the sensitivity of the electron-capture detector and the preconcentration obtained in the extraction of the piaszelenol.

This paper reports investigations with Br₂-PDA as the ligand. This ligand was selected for several reasons. It is commercially available in high purity, and the lower volatility of the piaszelenol derived from Br₂-PDA is favourable when the derivatization is applied at higher temperatures. It also means a longer retention time, which was needed as natural water samples and the chemicals used generated peaks at short and medium retention times. Further, as will be shown, the values of the protonation constants of Br₂-PDA make the adjustment of the optimum pH for the piaszelenol reaction easy. The rate of piaszelenol formation was determined as a function of temperature and ligand concentration. Further, the chromatographic behaviour of a toluene extract of the reaction products obtained at various temperatures was studied on a capillary column. Derivatization at a high temperature in conjunction with a capillary column separation greatly facilitates the application of GC-ECD to the determination of selenium. The method was applied to the determination of total soluble selenium in water.

EXPERIMENTAL

Instrumentation

Kinetic studies were carried out in a 1-cm quartz cuvette in a Perkin-Elmer Lambda 17 UV-VIS spectrophotometer equipped with a thermostated ($\pm 0.1^\circ\text{C}$) cell holder and a magnetic stirrer.

For the GC measurements a Shimadzu GC-14 gas chromatograph equipped with a constant-current ⁶³Ni electron-capture detector was used. The column was DB-1701 (15 m \times 0.25 mm I.D.) with a 0.25- μm film thickness (J&W Scientific) with the following conditions: carrier gas, helium at 40 cm/s; split vent, 60 ml/min; purge vent, 1 ml/min; make-up gas, nitrogen at 45 ml/min; injector temperature, 225°C; detector temperature, 325°C; and column temperature programme, 100°C held for 2 min, increased at 8°C/min to 175°C, held for 5 min, increased at 15°C/min to 265°C, held for 5 min.

The injections (0.5 μl of sample + 1 μl of toluene) were made in the splitless mode with a Shimadzu AOC-14 automatic injector, with a change to the split mode after 1 min. The peak areas were evaluated with a Shimadzu CR-5A integrator.

The UV destruction of organic material in water samples was performed in a locally built device [21]. The closed quartz tubes (60 ml, 22 mm I.D.) were placed around a 700-W UV lamp (Original Hanau, Hanau, Germany). A temperature-controlled aluminium block [22], made in the laboratory, heated the sample when Se(VI) was reduced to Se(IV) with hydrochloric acid at 100°C.

Reagents

All chemicals except lindane were of analytical-reagent grade. Water purified with a Milli-Q system (Millipore) ("Milli-Q water") was used for preparing standards and dilutions. All glassware was cleaned in 4 M nitric acid and rinsed with Milli-Q water.

1,2-Diamino-3,5-dibromobenzene. A 5.5 mM solution of Br₂-PDA (Merck) in 0.5 M perchloric acid was prepared. The solution was purified by extraction once with toluene and should preferably be kept in the dark. When 100 ml was extracted with 5 ml of toluene the Br₂-PDA concentration decreased to about 5.2 mM.

Selenium(IV). A stock standard solution containing 1 g/l of Se(IV) was prepared from an ampoule of

selenium dioxide in dilute nitric acid (Merck) and its concentration was checked by amperometric titration with thiosulphate after addition of a large excess of iodide [23]. Working standard solutions were obtained by serial dilution of the stock standard solution and contained 1 ml/l of perchloric acid (70–72%).

Lindane. A stock standard solution containing 2 mg/ml of lindane was prepared by dissolving lindane (99%, Applied Science Labs., State College, PA, USA) in toluene. A working standard solution containing 18 ng/ml of lindane was prepared by stepwise dilution of the stock standard solution with toluene.

Lindane is an insecticide and precautions should be taken to avoid inhalation and skin contact, especially when preparing solutions.

4,6-Dibromopiazselenol (PIAZ). This was synthesized according to the literature [3,12–14]. The synthesized piazselenol was analysed for selenium after wet digestion according to a variation of Gould's method [24] using a 10:1 (v/v) mixture of concentrated sulphuric acid and fuming nitric acid and the amperometric titration method mentioned above. The purity was $99.8 \pm 0.4\%$. A stock standard solution containing 0.5 mg/ml of piazselenol was prepared by dissolving piazselenol in toluene. Working standard solutions were prepared by serial dilution with toluene.

Kinetic experiments

To a quartz cuvette 3 ml of 0.10 or 0.30 mM Br₂-PDA were added and the cuvette was placed in a thermostated cuvette holder. When the desired temperature had been reached, 100 μl of 10 mg/l Se(IV) solution were added. The automatic absorbance measurement was started immediately and the absorbance was measured every 15 s at the beginning and every 1 min at the end of the reaction. The reaction was followed at 20, 30, 40, 50 and 60°C. The wavelength used was 343 nm, where the piazselenol has an absorption maximum and the ligand has an absorbance of only 0.002 (Fig. 1).

Lindane as internal standard and the clean-up step

A stock standard solution containing 17 ng/ml of lindane and 1.9 ng/ml of piazselenol in toluene was prepared. A 1-ml volume of this solution was shaken with 1.5 ml of 4, 6, 7, 8 or 9 M perchloric acid. The

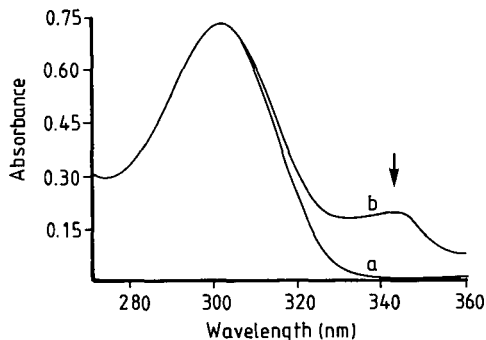


Fig. 1. UV absorption spectrum of 0.23 mM monoprotonated 1,2-diamino-3,5-dibromobenzene. (a) No selenium added; (b) 10 μM selenium added; formation of 10 μM 4,6-dibromopiazselenol. The analytical wavelength (343 nm) is indicated by an arrow.

aqueous phase was discarded and the toluene phase shaken twice with 1.5 ml of Milli-Q water and then injected into the chromatograph. The Milli-Q water and the perchloric acid solutions were extracted with toluene before use.

Extraction efficiency

To five 25-ml volumetric flasks, 15 ml of Milli-Q water, 0.5 ml of 70–72% perchloric acid and 0.5 ml of 5.2 mM Br₂-PDA were added. To five 100-ml volumetric flasks, 75 ml of Milli-Q water, 2 ml of 70–72% perchloric acid and 2 ml of 5.2 mM Br₂-PDA were added. Finally, to five 250-ml volumetric flasks, 200 ml of Milli-Q water, 5 ml of 70–72% perchloric acid and 5 ml of 5.2 mM Br₂-PDA were added. This means that the concentrations of Br₂-PDA and perchloric acid in all flasks were 0.1 mM and 0.25 M, respectively. To each set of five volumetric flasks 0, 1, 2, 3 and 4 ml of a standard solution containing 1 ng/ml of Se(IV) were added, then, the flasks were diluted to the mark. After 3 h the solutions were extracted with 1 ml of toluene containing lindane as internal standard. The aqueous phases were discarded and the toluene phases were transferred into 5-ml test-tubes with PTFE-faced screw-caps. The toluene phases were shaken once with 1.5 ml of 6 M perchloric acid and twice with 1.5 ml of Milli-Q water. Before injection into the chromatograph the organic phase was dried with anhydrous sodium sulphate. Rapid phase separation was obtained by spinning the test-tubes.

Derivatization at elevated temperatures

A 100-ml volume of test solution containing 10 ng/l of Se(IV) and 0.25 M perchloric acid was heated in a conical flask to the appropriate reaction temperature. At temperatures between 20 and 80°C the flask was placed in a low-temperature oven and at 100°C the flask was heated to boiling on an ordinary hot-plate. When the temperature had stabilized, 1.9 ml of 5.5 mM Br₂-PDA were added and after 5*t*_½ (where *t*_½ is the half-life of the piaszelenol reaction) the solution was cooled to room temperature in a water-bath and then transferred quantitatively with 5 ml of Milli-Q water to a separating funnel for extraction. The extract was then treated as described above. Blanks were run with Milli-Q water.

Determination of total soluble selenium in water

The following method was applied to the determination of total soluble selenium in water.

Filter the sample through a 0.45-μm filter, acidify with 1 ml/l of perchloric acid and store the sample in a refrigerator at 4°C. Add 25 ml of pretreated water sample and 25 μl of 30% hydrogen peroxide to a 60-ml quartz tube. Irradiate the sample with a 700-W UV lamp for 3 h. Add 12.5 ml of concentrated hydrochloric acid (extracted with toluene) to the sample [to reduce Se(VI) to Se(IV)] and place the test-tubes in a temperature-controlled aluminium block or equivalent. Boil the sample for 30 min. Remove the tube from the heating source and add 1 ml of 5.5 mM Br₂-PDA extracted with toluene. Wait for 5 min, then cool the sample to room temperature and transfer it quantitatively to a separating funnel with 5 ml of Milli-Q water. Add 1 ml of toluene containing lindane (20 ng/ml) and extract the sample for 2 min by vigorous shaking. Discard the aqueous phase and transfer the toluene phase to a 5-ml test-tube with a PTFE-faced screw-cap. Wash the toluene twice with 1.5 ml of Milli-Q water (rapid phase separation can be obtained by spinning the test-tube). Dry the toluene phase by adding anhydrous sodium sulphate prior to injection into the chromatograph. Evaluate the result from a calibration graph obtained with PIAZ or selenium(IV) standards and lindane as internal standard.

The procedure is adapted to waters containing 10–200 ng/l of selenium. Outside this range, the sample volume should be adjusted.

RESULTS AND DISCUSSION

Rate of the piaszelenol reaction

In the following, the previous abbreviation Br₂-PDA for 1,2-diamino-3,5-dibromobenzene will be retained in general discussions of the ligand; however, if its chemical form is of importance in the context, the ligand will be referred to in italics by *Br*₂-*PDA*, *Br*₂-*PDAH*⁺ or *Br*₂-*PDAH*₂⁺ to indicate a particular species. A symbol in italics within square brackets denotes concentration.

The formation of the piaszelenol has been shown repeatedly [3,25–28] to occur by the reaction between undissociated selenious acid and the diamine in the monoprotonated form. Hence the rate of reaction will be optimum in the pH range where these species predominate. As the dissociation constants of *Br*₂-*PDAH*₂⁺ were unknown, they were determined by spectrophotometric measurements. The p*K*_{a,2} value was found to be 2.6. The value of p*K*_{a,1} could not be properly established but it must be small as it was observed that the spectrum of *Br*₂-*PDAH*⁺ did not change until the medium was 3 M in perchloric acid and it changed continuously in the range 3–7 M acid.

The p*K*_{a,1} value of selenious acid is 2.6. Hence the reaction rate should be virtually independent of the acidity in the range 0.1–3 M. Outside this region the amount of monoprotonated ligand decreases and the reaction rate diminishes. Tôei and Shimoishi [3,8] found that *Br*₂-*PDAH*⁺ reacts quantitatively with selenious acid in 0.01–6 M hydrochloric acid if the ligand is present in more than a 12 000-fold molar excess over selenium(IV).

The kinetic experiments were carried out in 0.25 M perchloric acid. In this medium, Se(IV) will be present almost exclusively as H₂SeO₃ and the ligand as *Br*₂-*PDAH*⁺. The reason for using perchloric acid instead of the commonly employed hydrochloric acid medium is the greater solubility of Br₂-PDA in perchloric acid. This acid also yielded cleaner blank chromatograms than hydrochloric acid.

From the previous discussion, the expected rate law for the formation of the piaszelenol is

$$r = \frac{d[\text{PIAZ}]}{dt} = -\frac{d[\text{Se(IV)}]}{dt} = k'_2[\text{H}_2\text{SeO}_3][\text{Br}_2\text{-PDAH}^+] \quad (1)$$

Under the current experimental conditions, eqn. 1 can be written as, and a new second-order rate constant, k_2 , defined by,

$$r = -\frac{d[Se(IV)]}{dt} = k_2[Se(IV)]_{tot}[Br_2-PDA]_{tot} \quad (2)$$

as the reactants are constant fractions, almost equal to 1, of the total selenium(IV) and ligand concentrations. In the following equations and discussions the subscript tot will be omitted.

Eqn. 2 was experimentally tested by Ostwald's isolation method using an excess of the ligand. Integration of eqn. 2 gives

$$\ln[Se(IV)] = \ln[Se(IV)]_0 - k't \quad (3)$$

where $k' = k_2[Br_2-PDA]$ and $[Se(IV)]_0$ represents the initial selenium concentration. First $[Se(IV)]_0$ was varied at constant $[Br_2-PDA]$. The results are presented in Fig. 2. The slopes of the three lines are equal, which is in agreement with eqn. 3. In a second series of experiments $[Br_2-PDA]$ was varied at constant $[Se(IV)]_0$. The slopes of the lines in Fig. 3, k' , are different but the k_2 values are the same. The proposed rate equation is thus confirmed. These experiments were carried out at 20°C and eqn. 3 was assumed to be valid also at higher temperatures.

The values of k' at higher temperatures were evaluated in the following way in order to account for a possible time lag before the reaction mixture became homogeneous with respect to temperature

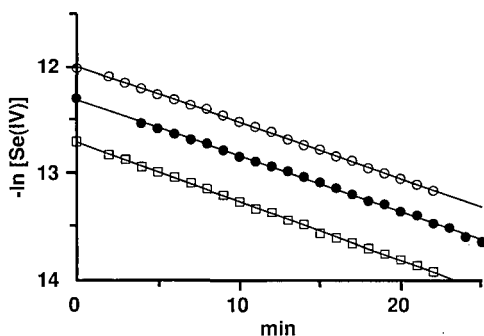


Fig. 2. Determination of the rate constant of piarselenol formation at 20°C by fitting eqn. 3 to the experimental data. The concentration of Br_2 -PDA was kept constant at 0.3 mM and the total selenium(IV) concentration was varied: $\square = 3.02$; $\bullet = 4.52$; $\circ = 6.03 \mu M$.

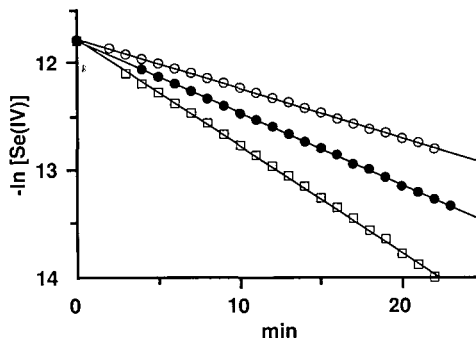


Fig. 3. Determination of the rate constant of piarselenol formation at 20°C by fitting eqn. 3 to the experimental data. The total concentration of selenium was kept constant at 7.5 μM and the concentration of Br_2 -PDA was varied: $\circ = 0.177$; $\bullet = 0.265$; $\square = 0.353 mM$.

and concentration. The total concentration of selenium, C_0 , is

$$C_0 = [PIAZ] + [Se(IV)] \quad (4)$$

With the ligand in excess the combination of eqns. 1, 2 and 4 yields

$$\frac{d[PIAZ]}{dt} = k'(C_0 - [PIAZ]) \quad (5)$$

The selenium(IV) solution is added to the Br_2 -PDA solution in the cuvette at $t = 0$. A certain time will elapse before the solution is homogeneous and the temperature has stabilized at the preset value. At that time, $t = t_0$, the concentrations are $[Se(IV)] = C'_0$ and $[PIAZ] = C_0 - C'_0$. Integration of eqn. 5 between t and t_0 then results in

$$[PIAZ] = C_0 - B e^{-k't} \quad (6)$$

where $B = C'_0 e^{k't_0}$. As the absorbance, A , of the piarselenol formed was measured, eqn. 6 is more conveniently expressed as

$$A_t = A_\infty - b e^{-k't} \quad (7)$$

Eqn. 7 was fitted to the experimental data shown in Fig. 4 by non-linear least-squares calculations.

The results from the kinetic studies of the piarselenol formation are presented in Table I. The temperature dependence of the second-order rate constant between 20 and 60°C can be expressed by

$$\ln k_2 = 22.9 - \frac{42900}{RT} \quad (8)$$

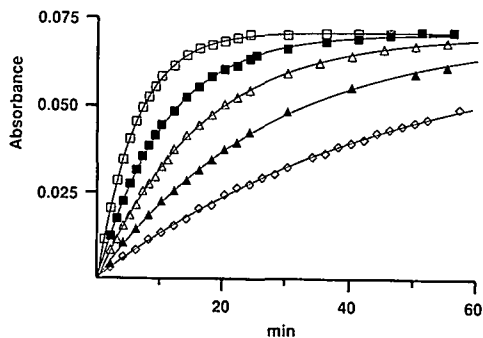


Fig. 4. Determination of the temperature dependence of piazselenol formation. The rate constant at each temperature was found by fitting eqn. 7 to the experimental data. Temperature: \square = 60; \blacksquare = 50; \triangle = 40; \blacktriangle = 30; \diamond = 20°C.

with k_2 in $l \text{ mol}^{-1} \text{ min}^{-1}$ and the activation energy in $J \text{ mol}^{-1}$. Half-lives, $t_{\frac{1}{2}}$, can be calculated from eqns. 8 and 9:

$$t_{\frac{1}{2}} = \frac{\ln 2}{k_2[Br_2-PDA]} \quad (9)$$

Table II contains estimates, expressed as $5t_{\frac{1}{2}}$, of the time for quantitative piazselenol formation with 0.1 mM Br_2 -PDA at temperatures between 20 and 100°C in 0.25 M perchloric acid. The data indicate that the reaction time could be shortened from about 3 h to 4 min if the piazselenol can be formed at 100°C instead of room temperature (20°C). An increased temperature has been used for the piazselenol reaction in the analysis of biological samples

TABLE I
SECOND-ORDER RATE CONSTANTS OF THE PIAZSELENOL FORMATION REACTION

The second-order rate constants (k_2) were determined once with 0.1 and twice with 0.3 mM Br_2 -PDA. The estimated standard deviation is given in parentheses.

Temperature (°C)	k_2 ($l \text{ mol}^{-1} \text{ min}^{-1}$)
20	200 (3)
30	362 (6)
40	616 (12)
50	1035 (39)
60	1658 (73)

TABLE II
TIME REQUIRED FOR QUANTITATIVE PIAZSELENOL FORMATION

The estimated times correspond to five half-lives ($5t_{\frac{1}{2}}$) calculated from Table I or, above 60°C, by extrapolation of eqn. 8. The ligand concentration was 0.1 mM.

Temperature (°C)	$5t_{\frac{1}{2}}$ (min)	Temperature (°C)	$5t_{\frac{1}{2}}$ (min)
20	175	70	13
30	98	80	9
40	57	90	6
50	34	100	4
60	21		

[7,10,13,29], but it has also been reported that a high temperature in the derivatization step leads to a number of spurious peaks in the chromatogram [29].

Chromatographic conditions and clean-up procedure

The piazselenol reaction yields by-products, which together with a co-extracted excess of the diamine result in chromatographic peaks that may overlap the piazselenol peak. Back-extractions of the organic extract with hydrochloric acid [3], perchloric acid [4,6,7,13,14], perchloric acid and sodium hydroxide [5,11] or by passing the organic phase through a Fluorosil column [10] have been used to eliminate the interferences. For Br_2 -PDA it has been reported [29] that a peak partially overlapping the piazselenol peak could not be eliminated completely.

In earlier investigations on the GC determination of selenium, packed columns have been used. With the higher efficiency of a capillary column, interferences are absent in the present system even without a clean-up procedure, as the piazselenol is well separated from the by-products (Fig. 5a). The ligand, which is added in large excess, elutes after the piazselenol as two broad peaks. The effect of one clean-up step on the toluene extract is shown in Fig. 5b. The two broad peaks have almost disappeared and some of the peaks around the piazselenol peak have decreased. A clean-up step could be included in the method to prolong the lifetime of the column and detector and was therefore investigated.

In the clean-up step the toluene phase was extracted once with 1.5 ml of 6 M perchloric acid

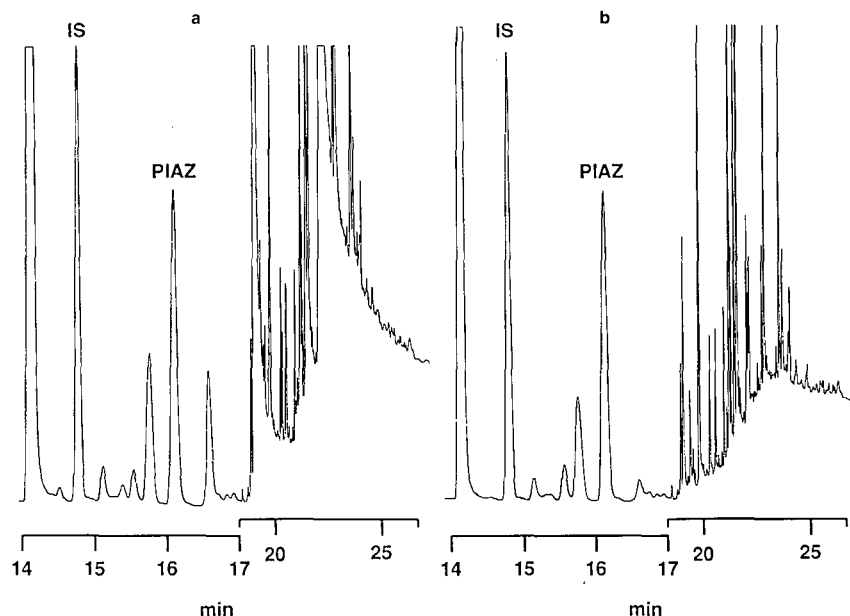


Fig. 5. Chromatograms of toluene extract of the reaction mixture after reduction of Se(VI) to Se(IV) in 4 *M* hydrochloric acid and piazselenol formation at 100°C. Only the analytically relevant part of the chromatogram is shown. A 25-ml volume of 130 ng/l Se solution was made to react with 0.1 *M* Br₂-PDA for 5 min. The reaction mixture was extracted with 1 ml of toluene containing lindane as internal standard. The volume injected was 0.5 μ l. (a) Without clean-up; (b) with clean-up; extraction with 6 *M* perchloric acid.

followed by two washings with 1.5 ml of Milli-Q water. This treatment removed most of the Br₂-PDA (Fig. 5b). The piazselenol was not back-extracted (Table III) unless the perchloric acid concentration exceeded 7 *M*. This finding is in fair agreement with a report [4] that two extractions can be

TABLE III

BACK-EXTRACTION OF PIAZSELENIOL AND LINDANE

A 1-ml volume of toluene containing 1.9 ng of piazselenol and 17 ng of lindane was extracted with perchloric acid solution. *R* is the ratio between the areas of the piazselenol and lindane peaks.

[HClO ₄] (<i>M</i>)	<i>V</i> (ml)	<i>R</i>
—	—	0.353
4	1.5	0.355
6	1.5	0.355
7	1.5	0.350
8	1.5	0.299
9	1.5	0.112
0.25	100	0.346

made with 8 *M* perchloric acid without loss. For 4-bromo-6-fluoropiazselenol losses were observed after washings with 6 *M* perchloric acid [14]. Such differences between piazselenols might be due to differences in their first protonation constants [30].

The temperature programme used gave a good separation of the piazselenol peak from some minor peaks close to it. The resolution between the piazselenol and the two closest peaks were $R_s(1) = 2.2$ and $R_s(2) = 3.3$. It would therefore be possible to use a shorter column. This was not investigated because in the future the column will be used to determine selenium(IV) in water. Decomposition of organic matter (UV destruction) then cannot be made and this will lead to additional peaks in the chromatogram from concomitants in the water.

If the Br₂-PDA reagent was not extracted with toluene before use, then a large peak appeared next to the piazselenol peak.

Lindane as internal standard

Lindane was used as internal standard and about 18 ng/ml of lindane were added to the toluene used

TABLE IV
EFFICIENCY OF THE PIAZSELENOL EXTRACTION

The stated amounts of selenium were derivatized in different volumes of 0.25 *M* perchloric acid and then extracted into 1 ml of toluene. *R* is the ratio between the areas of the piazselenol and lindane peaks corrected for the blank. The blank is the value of *R* when no selenium was added.

Se (ng)	<i>R</i>		
	$V_{\text{aq}} =$ 25 ml	$V_{\text{aq}} =$ 100 ml	$V_{\text{aq}} =$ 250 ml
Blank	0.0263	0.0384	0.0890
1	0.320	0.324	0.317
2	0.630	0.638	0.579
3	0.870	0.885	0.812
4	—	1.14	1.09

for extraction of the piazselenol. It is well separated in the chromatogram (Fig. 5) and gives a good response in the electron-capture detector. No loss of lindane has been observed in the extraction or the clean-up step.

Extraction efficiency

The efficiency of the extraction of the piazselenol was investigated by extracting 0, 1, 2, 3 and 4 ng of

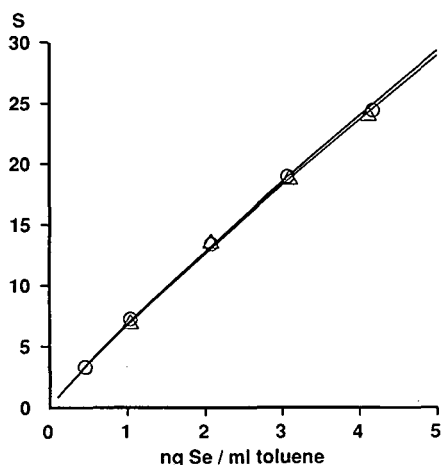


Fig. 6. Calibration graphs. *S* is the area ratio between the piazselenol peak and the internal standard (lindane) peak recalculated to an internal standard concentration of 1 ng/ml in toluene. Results from (□) synthesized piazselenol standards and (○) derivatized selenium(IV) standards.

selenium(IV) derivatized in different volumes of 0.25 *M* perchloric acid into 1 ml of toluene. The results presented in Table IV indicate that the distribution constant is so large that the extraction can be considered to be quantitative. There was, however, a small loss when extraction was made from 250 ml of the aqueous phase. Owing to the sensitivity of the method, the use of sample volumes larger than 100 ml is seldom required. For larger volumes the losses can be compensated for by establishing a calibration graph from standards of the appropriate volume.

Calibration

There was good agreement between calibration graphs obtained from solutions of synthesized piazselenol and derivatized standard solutions of selenium(IV) (Fig. 6). Standard solutions of synthesized piazselenol can therefore be used for calibration purposes. As a check of the calibration, a standard solution of selenium(IV), treated as the sample, should be included in the analysis of real samples. This procedure will correct for extraction losses with large sample volumes.

The calibration graph is non-linear. The function $Y = AX^B$ reproduces the calibration data well after subtraction of the blank. The value of *B* is typically about 0.9.

Derivatization at higher temperatures

The formation of the piazselenol at higher temperatures and hence shorter reaction times, $5t_{\frac{1}{2}}$, was investigated in two series of experiments. In the first series the toluene extracts were subjected to the previously described clean-up step with 6 *M* perchloric acid. This step was excluded in the second series. No special precautions were taken to minimize possible loss of piazselenol, other than covering the mouth of the conical reaction flask with a watch-glass. Losses of the volatile piazselenol would be greatest from boiling solution. In the experiments performed at 100°C the reaction vessel was therefore removed from the hot-plate before adding Br₂-PDA. The calculated reaction time was prolonged by 1 min instead.

At all temperatures the derivatizations resulted in very similar chromatograms. The analytical data are presented in Table V. No decrease in recovery is observed at higher temperatures. The blank value is

TABLE V

RECOVERY OF SELENIUM WHEN THE PIAZSELENOL IS FORMED AT HIGHER TEMPERATURES

The sample consisted of 1 ng of Se(IV) added to 100 ml of 0.25 M perchloric acid. The results are averages of triplicate determinations with relative standard deviations in parentheses.

Temperature (°C)	Reaction time (min)	Selenium found (ng)			
		Without clean-up		With clean-up	
		Sample	Blank	Sample	Blank
20	174	1.00 ^a (4.8%)	0.050	1.01 (2.4%)	0.064
40	56	1.02 (0.2%)	0.051	1.02 (4.2%)	0.049
60	21	1.00 (1.0%)	0.048	1.00 (0.8%)	0.054
80	9	1.03 (7.8%)	0.051	0.99 (1.5%)	0.086
100	5	1.01 (5.0%)	0.060	1.01 (5.4%)	0.062

^a Used as a reference.

not affected by temperature and the clean-up step does not influence the results.

The time for the derivatization step can be reduced by increasing the concentration of Br₂-PDA. Short reaction times can then be achieved at moderate temperatures. For instance, the reaction would be complete after 7 min when the concentration of Br₂-PDA is 0.3 mM and the temperature 60°C. However, a higher Br₂-PDA concentration adversely affects the chromatogram unless one or several clean-up steps are included. Therefore, it is recommended to use a lower Br₂-PDA concentration and a higher temperature.

Determination of total soluble selenium in water

In the determination of total soluble selenium in water it is necessary to decompose organic selenium compounds and reduce selenium(VI) to selenium(IV). The decomposition of the organic material was achieved by UV irradiation of the sample contained in closed quartz tubes after addition of hydrogen peroxide [21]. The lake water analysed contained 24 mg/l of carbon and was completely discoloured after the UV irradiation. The reduction was carried out in 4 M hydrochloric acid at 100°C for 30 min.

It would be convenient to carry out the derivatization directly in the quartz tube after the reduction step. The concentration of monoprotonated ligand is lower in 4 M hydrochloric acid than in 0.25 M

TABLE VI

TOTAL SOLUBLE SELENIUM IN A LAKE WATER SAMPLE

The determination was made according to the procedure described in the text. The results obtained with an HG-AAS method was 131 ± 5 ng/l. This was an average of five different digestion procedures [31].

[HCl] (M)	t _{react.} (min)	Selenium concentration (ng/l)
4	5	128 124
4	10	132 129
3.2	5	127 129
1.5	180 ^a	130

^a The derivatization was made at room temperature.

perchloric acid, so that the previous kinetic data are not directly applicable. Table VI contains data from derivatizations at high hydrochloric acid concentrations. Obviously the high temperature leads to such a high reaction rate that neither the acid concentration need be decreased nor the reaction time increased.

The results from the GC-ECD method agree with those from a study with an HG-AAS method in which also different digestion procedures were evaluated [31].

CONCLUSIONS

Most analytical procedures for selenium determine only selenium(IV). Therefore, selenium(VI) must be reduced to selenium(IV). This is generally accomplished by boiling the sample in about 4 M hydrochloric acid. In the GC-ECD method the derivatization step follows the reduction step. For easy performance, the derivatization conditions should be compatible with the conditions prevailing after the reduction step. This is the case for Br₂-PDA owing to the small value of its second protonation constant. The piazselenol reaction is complete in about 5 min at boiling temperature with little or no increase in the background from decomposed ligand. The use of a capillary column facilitates the isolation of the piazselenol peak and a clean-up step may be

omitted. The sensitivity is good and quantitative determination of a few ng/l of selenium in water can be made.

REFERENCES

- 1 O. Hinsberg, *Ber. Dtsch. Chem. Ges.*, 22 (1889) 862.
- 2 S. Nakashima and K. Tōei, *Talanta*, 15 (1968) 1475.
- 3 Y. Shimoishi, *J. Chromatogr.*, 136 (1977) 85.
- 4 Y. Shimoishi and K. Tōei, *Anal. Chim. Acta*, 100 (1978) 65.
- 5 K. Kurahashi, S. Inoue, S. Yonekura, Y. Shimoishi and K. Tōei, *Analyst (London)*, 105 (1980) 690.
- 6 H. Uchida, Y. Shimoishi and K. Tōei, *Environ. Sci. Technol.*, 14 (1980) 541.
- 7 H. Uchida, Y. Shimoishi and K. Tōei, *Analyst (London)*, 106 (1981) 757.
- 8 K. Tōei and Y. Shimoishi, *Talanta*, 28 (1981) 967.
- 9 Y. Shimoishi and K. Tōei, *Talanta*, 17 (1970) 165.
- 10 T. Stijve and E. Cardinale, *J. Chromatogr.*, 109 (1975) 239.
- 11 Y. Shimoishi, *Analyst (London)*, 101 (1976) 298.
- 12 C. F. Poole, N. J. Evans and D. G. Wibberley, *J. Chromatogr.*, 136 (1977) 73.
- 13 S. Dilli and I. Sutikno, *J. Chromatogr.*, 298 (1984) 21.
- 14 A. F. Al-Attar and G. Nickless, *J. Chromatogr.*, 440 (1988) 333.
- 15 J. W. Young and G. D. Christian, *J. Chromatogr.*, 65 (1973) 127.
- 16 O. Zheng, P.-Y. Xu, G.-L. Xiong and Y. Liu, *Talanta*, 33 (1986) 443.
- 17 J. Piwonka, G. Kaiser and G. Tölg, *Frezenius' Z. Anal. Chem.*, 321 (1985) 225.
- 18 G. A. Cutter, *Anal. Chim. Acta*, 98 (1978) 59.
- 19 C. M. G. van den Berg and S. H. Khan, *Anal. Chim. Acta*, 231 (1990) 221.
- 20 M. Zelić and M. Branica, *Electroanalysis*, 2 (1990) 455.
- 21 I. Gustavsson and L. Hansson, *Int. J. Environ. Anal. Chem.*, 17 (1984) 57.
- 22 J. Pettersson, L. Hansson and Å. Olin, *Talanta*, 33 (1986) 249.
- 23 T. A. Bengtsson, unpublished results.
- 24 E. S. Gould, *Anal. Chem.*, 23 (1951) 1502.
- 25 L. Barcza, *Microchim. Acta*, 1 (1964) 136.
- 26 H. Ariyoshi, M. Kiniwa and K. Tōei, *Talanta*, 5 (1960) 112.
- 27 J. Neve, M. Hanocq and L. Molle, *Microchim. Acta*, 1 (1980) 41.
- 28 J. Neve, M. Hanocq and L. Molle, *Talanta*, 26 (1979) 1173.
- 29 T. Stijve and G. Philopossian, *Trav. Chim. Aliment. Hyg.*, 69 (1978) 74.
- 30 J. Neve, M. Hanocq and L. Molle, *Talanta*, 26 (1979) 15.
- 31 U. Örnemark, J. Pettersson and Å. Olin, *Talanta*, in press.

CHROM. 24 017

Fluorescence detector cell for use in an integrated electrically driven separation system

P. K. de Bokx*, E. E. A. Gillissen, P. van de Weijer, M. H. J. Bekkers
and C. H. M. van Bommel

Philips Research Laboratories, P.O. Box 80 000, 5600 JA Eindhoven (Netherlands)

H.-G. Janssen

Eindhoven University of Technology, P.O. Box 513, 5600 MB Eindhoven (Netherlands)

(First received September 3rd, 1991; revised manuscript received January 27th, 1992)

ABSTRACT

An integrated design for electrically driven separations is presented. The injector, column and detector are all located within the same cartridge, allowing for integral thermostating and short column lengths. Results on the performance of the proposed fluorescence detector are reported. Molar amounts as low as $2 \cdot 10^{-19}$ mol of fluorescein (100- μ l detector cell volume) can be detected. Short column lengths permit very fast separations, as is demonstrated by the separation of four laser dyes within 35 s.

INTRODUCTION

Electrically driven separation methods, including capillary zone electrophoresis (CZE) [1–3], micellar electrokinetic chromatography [4,5] and electrochromatography [6,7], are currently attracting a great deal of attention. Their common characteristic is that the flow through the “separation column” is effected by electroosmosis rather than by a pressure gradient. There are two main analytical reasons for such interest: first, superior separation efficiencies can be attained, with plate counts an order of magnitude higher than are possible in traditional liquid chromatography, and second, extremely small sample volumes can be handled. Depending on the inner diameter of the separation capillary, injection volumes can range from several tens of picolitres to the low nanolitres level, creating possibilities for single-cell sampling in the biological sciences [8] and local dissolution and sampling in materials research.

Owing to their common characteristics, many of the operating parameters (*e.g.*, field strength, buffer

concentration, column diameter, column length) affect the separation performance of all electrically driven separation techniques in a similar fashion. As is outlined in the Theory section, there is a great deal to be gained with respect to efficiency and, more important, time of analysis (seconds rather than minutes) if high field strengths and short column lengths can be employed. In the present generation of instruments, short column lengths cannot be used owing to the physical distance that has to be spanned between the injector and detector. At a given maximum voltage of the power supply, this also limits the attainable field strength. Moreover, high field strengths require active thermostating to dissipate efficiently the Joule heat generated by the current. To benefit from the prospects offered by high field strengths and short column lengths, a new instrument concept is called for that takes into account the stringent requirements placed on injector and detector volumes, and, at the same time, allows for integral thermostating. Such an integrated instrument design is presented under Experimental.

In this paper, we report on the detector cell of the instrument. Owing to the very small detector cell volumes required, the use of several widely employed detection principles, *e.g.*, UV absorbance detection and refractive index detection, is precluded. Detection should be based on phenomena of high inherent sensitivity. Fluorescence and electrochemical detection are the only likely candidates at present. Unfortunately, both methods are highly specific. In order to increase the versatility, one can either turn to derivatization or to indirect detection (adding a detectable compound to the eluent and measuring the decrease in signal due to presence of a solute [9]). Here, we demonstrate the use of a detector cell for fluorescence detection that is compatible with short column lengths and high field strengths and also adheres to the limitations placed on the maximum allowable detector cell volume.

THEORY

In this section, we investigate the separation properties of electrically driven systems. Our main aim is to show how the different operating parameters influence the separation performance with regard to efficiency and speed of analysis and to estimate how large the detector cell volume can be before a significant loss in this performance is observed.

The standard deviation of a chromatographic peak can be expressed in volume units as [10]

$$\sigma_{v,E} = (\pi/4)H\epsilon d_c^2 \sqrt{N} \quad (1)$$

where H is the plate height, ϵ the void fraction (different from unity in the case of packed column electrochromatography), d_c the column diameter and N the plate number. The above standard deviation is a measure of the dispersion due to the column. We now demand that external contributions to the total dispersion do not seriously deteriorate the performance of the instrument. Following Naish *et al.* [11], we use as a criterion that the extra-column contribution to the total standard deviation should be less than half the dispersion caused by the column. Assigning half of the external dispersion to the detector and half to the injector and other sources, the maximum allowable detector cell volume can be obtained from

$$V_{\text{DET}} \leq \sqrt{\kappa} \cdot \frac{\sigma_{v,E}}{2\sqrt{2}} \quad (2)$$

where κ is the detection profile factor [12].

To make eqns. 1 and 2 explicit, we need an expression for the plate height of the peak. It is here, of course, that the specific characteristics of electrically driven separation techniques will become apparent. The great advantage of electrically driven systems is to be found in the plug profile of electroosmotic flow (for a detailed account, see Rice and Whitehead [13]). As there now is no tendency for the solute to be dispersed by radial differences in flow, one expects the only term to remain in the equation for the plate height of a solute that does not participate in any mass-transfer process to be that due to axial diffusion. Hence,

$$H = \frac{2\gamma D_m}{u} \quad (3)$$

where γ is the tortuosity factor, which is different from unity in the case of a packed bed, and D_m is the diffusivity of the solute. In electrically driven systems the linear velocity is given by the von Smoluchowski equation, $u = \epsilon_r \epsilon_0 \zeta E / \eta$, where ϵ_0 and ϵ_r are the permittivity of free space and the relative permittivity, respectively, ζ (the zeta potential) is the potential at the plane of shear, E is the electric field strength and η is the viscosity. Substituting for u in eqn. 3 leads to

$$H = \frac{2\eta\gamma D_m}{\epsilon_r \epsilon_0 \zeta} \cdot \frac{1}{E} \quad (4)$$

As noted by several workers [7,14], eqn. 4 is a simplification. Owing to self-heating of the eluent, a temperature gradient between the centre of the separation capillary and its walls will build up. Knox and Grant [7] calculated the excess temperature at the centre of the capillary, assuming the wall temperature to be constant. The resulting additional dispersion term is derived to be equal to

$$H = \frac{7 \cdot 10^{-9} \cdot \epsilon_r \epsilon_0 \zeta \lambda^2 \epsilon^2 d_c^6 c^2}{D_m \eta K^2} \cdot E^5 \quad (5)$$

where λ is the equivalent conductivity, c is the molar concentration of the eluent and K is its thermal conductivity.

Eqn. 5 indicates that this additional dispersion

term becomes particularly manifest at large column diameters and high field strengths. The total plate height, *i.e.*, the sum of eqns. 4 and 5, is plotted against field strength in Fig. 1 for three different column diameters.

Typical values used in the calculations are collected in Table I. The data clearly illustrate the need for small column diameters. Owing to self-heating, a diameter of 500 μm offers a working range that is extremely limited in voltage. Generally, a diameter of around 100 μm is accepted as a practical upper limit.

Key numerical results are collected in Table II, with values for the elution time of the electroosmotic peak, $t_E = L\eta/\varepsilon_r\varepsilon_0\zeta E$, the analysis time, t_A , assuming the slowest component to have a capacity factor of 10, the standard deviation of the unretained peak, $\sigma_{v,0}$, in volume units (eqn. 1), using eqns. 4 and 5, and the maximum allowable cell volume, V_{DET} (eqn. 2). Values were calculated for two column diameters, 100 and 50 μm . All calculations were performed at the minimum of the $H-E$ curves (values for H_{min} and E_{opt} are indicated in the table title). The corresponding flows for 100- and 50- μm columns are 17.5 and 8.8 nls^{-1} , respectively.

It should be realized that the results in Table II were obtained based on the velocity of the electroosmotic peak (which is necessarily the fastest peak in electrochromatography) and using the values for the physical constants collected in Table I. Notwithstanding these constraints, several very interesting conclusions can be drawn from the results in Fig. 1

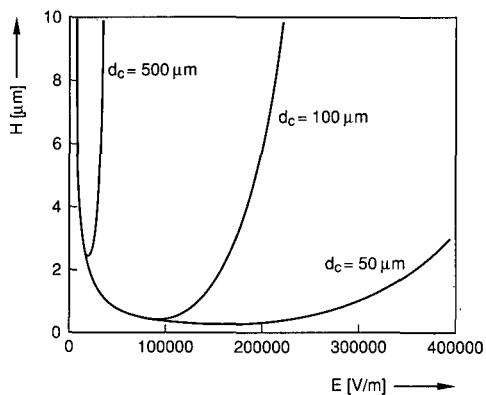


Fig. 1. Plots of total plate height (sum of eqns. 4 and 5) vs. electrical field strength for different capillary diameters. For numerical values used in the calculations, see Table I.

and Table II, as follows. (1) The minima of the $H-E$ curves are located at very high field strengths, far above the currently used values of 30–40 kV m^{-1} . Such high field strengths can only be used in practice if the Joule heat generated can be efficiently removed. (2) For analyses that do not require high plate numbers, very short analysis times can be realized. Owing to the physical dimensions of the currently used instruments, the short column lengths needed (*e.g.*, 0.5 cm for 10 000 plates on a 100- μm column) cannot be used. (3) The maximum allowable detector volume increases with plate number and decreases with column diameter. Detector volumes of the order of 100 pl need to be realized to

TABLE I

TYPICAL VALUES OF PHYSICAL QUANTITIES USED IN THE CALCULATIONS

Symbol	Quantity	Unit	Value
c	Molar concentration	mol m^{-3}	10
D_m	Diffusivity	$\text{m}^2 \text{s}^{-1}$	10^{-9}
K	Thermal conductivity	$\text{W m}^{-1} \text{K}^{-1}$	0.4
γ	Tortuosity factor	—	0.6
ε	Void fraction	—	0.75
ε_0	Permittivity of free space	$\text{C}^2 \text{N}^{-1} \text{m}^{-2}$	$8.85 \cdot 10^{-12}$
ε_r	Relative permittivity	—	80
η	Viscosity	N s m^{-2}	10^{-3}
ζ	Zeta potential	V	$5 \cdot 10^{-2}$
κ	Profile factor	—	6
λ	Equivalent conductivity	$\text{m}^{-2} \text{mol}^{-1} \Omega^{-1}$	0.015

TABLE II

CHARACTERISTIC PARAMETERS FOR TWO COLUMN DIAMETERS: 100 μm ($H_{\text{min}} = 0.49 \mu\text{m}$, $E_{\text{opt}} = 84 \text{ kV m}^{-1}$) AND 50 μm ($H_{\text{min}} = 0.24 \mu\text{m}$, $E_{\text{opt}} = 168 \text{ kV m}^{-1}$)

d_c (μm)	N	t_E (s)	t_A (min)	$\sigma_{v,0}$ (pl)	V_{DET} (pl)
100	10 000	1.6	0.3	290	250
	50 000	8	1.5	640	550
	100 000	16	3.0	900	770
	500 000	80	15	2030	1760
	1 000 000	160	30	2900	2470
50	10 000	0.4	0.07	40	35
	50 000	2.0	0.37	80	70
	100 000	4.1	0.75	110	100
	500 000	20	3.7	250	210
	1 000 000	40	7.5	360	310

exploit fully the advantages of electro-drive separations.

Our integrated design for electrically driven separations aims at meeting the requirements set by the above three conclusions.

EXPERIMENTAL

Instrument design

In Fig. 2 a schematic diagram of the integrated instrument is shown. As can be seen, the injector, column and detector are all located within the same

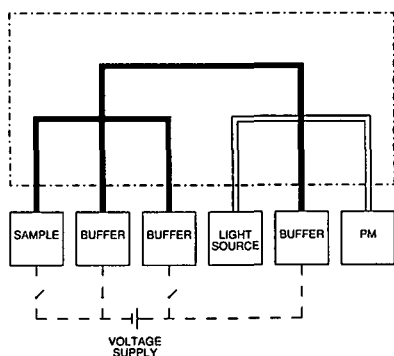


Fig. 2. Schematic diagram of integrated instrument design. The injector is on the left-hand side and the detector on the right-hand side. Heavy solid lines indicate fused-silica capillary, double lines optical fibres. Dashed lines are used for electrical connections. Note that the injector, column and detector are all within the same thermostated enclosure (dot-dashed lines). PM = Photomultiplier.

thermostated enclosure. The enclosure, in fact, is intended to be a small cartridge. The necessity for active thermostating can be appreciated if one bears in mind that electrophoretic and electroosmotic mobilities, and hence retention times, vary by about $2\% \text{ K}^{-1}$. Also, because the optics of the fluorescence detector and also the buffer and sample vials are remote from the actual instrument, the length of the separation capillary can be very short (several millimetres). The design depicted in Fig. 2 is only possible by directly connecting optical fibres and injection capillaries to the separation capillary, *i.e.*, without employing bulky connecting devices. Direct connection is obtained by the use of a carbon dioxide laser to machine bores in the wall of the separation capillary. In the injector design, capillaries are inserted in these bores and an injector similar to that reported by Verheggen *et al.* [15] is the result. Flow through either the injection or the separation capillary can be effected by the appropriate application of the voltage. In the design of the fluorescence detector cell, optical fibres are placed in the two bores, which are now at right-angles. In this paper, we focus on detector performance. A detailed description of the construction of the detector is given in the next section.

Detector cell construction

At the desired position of the cell, 2 cm of the protective, polyimide coating of the fused-silica capillary were removed. A carbon dioxide laser (Edinburgh Instruments, Edinburgh, UK) was used to make the bores in the walls of the capillaries [16]. The design is illustrated in Fig. 3. The diameter of the resulting bores depends on the outer and inner diameters of the capillary (330 and 100 μm , respectively), the power and duration of the laser shot (2.4 W and 400 ms, respectively) and the distance to the object (2.9 mm). Using the above conditions, tapered bores having a top diameter of 35 μm were obtained, centred with an accuracy of 2 μm .

To increase the light intensity in the cell and to decrease the fluorescent background due to fluorescing centres in the adhesive, the detector cell was coated with a silver mirror prior to the application of the adhesive. Silver films were vapour-deposited on the fused silica of the capillary. Vapour deposition was performed in an HV system (Balzers, Liechtenstein) using an Airco-Temesal E-gun at a rate of 0.3

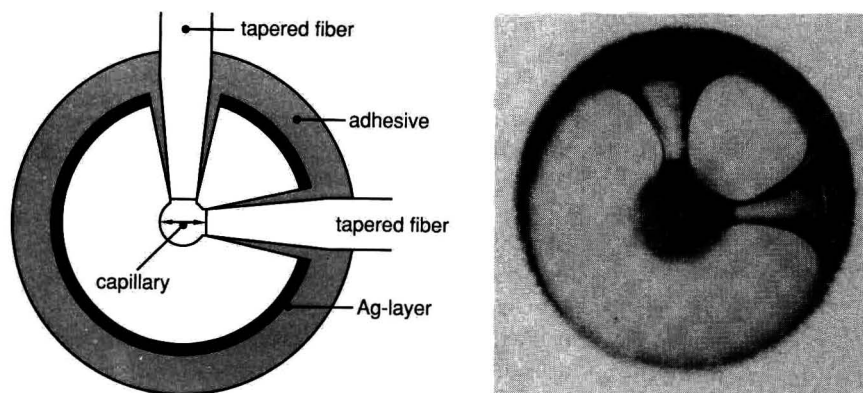


Fig. 3. Fluorescence detector design. A drawing of the cell is shown on the left-hand side and an optical micrograph of the cell (no optical fibres connected) on the right-hand side.

nm s^{-1} . The thickness of the silver layer was 30 nm.

Spectraguide optical fibres with high UV transmission were obtained from Spectrum (Sturbridge, MA, USA). The 100- μm core of the fibres was tapered to 35 μm in order to fit snugly into the bores in the capillary walls. The metal-coated capillary and the optical fibres were joined with a two-component epoxy adhesive (Bison, Middelburg, Netherlands).

Assuming a cylinder with a length of 100 μm and a diameter of 35 μm , the illuminated volume of the detector cell described above is 96 pl.

Experimental set-up

In all experiments, a continuous laser was employed (Model 4210 NB, Liconix, Santa Clara, CA, USA). The 442-nm emission line of the He-Cd laser was used, having an energy of *ca.* 10 mW. The laser was focused on one of the fibres of the detector cell using a lens ($f = 125$ mm). The output from the other fiber was fed to a Model 150UVP photomultiplier (Philips, Eindhoven, Netherlands). The laser-induced fluorescence was measured with a 530-nm short-wavelength cut-off filter in front of the photomultiplier. The signal of the photomultiplier was recorded via a Model 160 boxcar (Princeton Applied Research, Princeton, NJ, USA), using a static gate, with either an $x-t$ recorder or a Model 10B computing integrator (Milton Roy, Riviera Beach, FL, USA).

In all experiments, a Model DA-30 stabilized, high-voltage (0–30 kV) power supply (Spectrovision, Chelmsford, MA, USA) was used.

Procedures

All experiments were performed using phosphate buffers adjusted to the desired pH by titration with phosphoric acid. The test solutes were obtained from various sources and were all of the highest purity available. High-purity deionized water was used to make up the solutions. Samples were introduced into the capillary using electromigration. In determining the calibration graph and the detection limit for fluorescein, concentration fronts were injected and the heights of the resulting blocks were measured. Noise levels were measured by recording the baseline over 1-min intervals and taking the average of six measurements of the peak-to-peak signal as $4\sigma_N$ [17]. Electrophoretic separations were performed by injecting the sample mixture at a voltage of 3 kV for 3 s.

RESULTS AND DISCUSSION

In Fig. 4, a calibration graph for fluorescein is shown. Over the three orders of magnitude investigated, good linearity is observed. From the slope of the plot and the noise (see Experimental), the concentration detection limit is determined to be $2 \cdot 10^{-9}$ M of fluorescein. Using an illuminated volume of 100 pl, this corresponds to $2 \cdot 10^{-19}$ moles (200 zmol) in the detector cell.

Owing to the great variety of experimental systems and test solutes used, a direct comparison with literature data on laser-induced fluorescence detection is not straightforward. The concentration detection limit quoted above compares well with

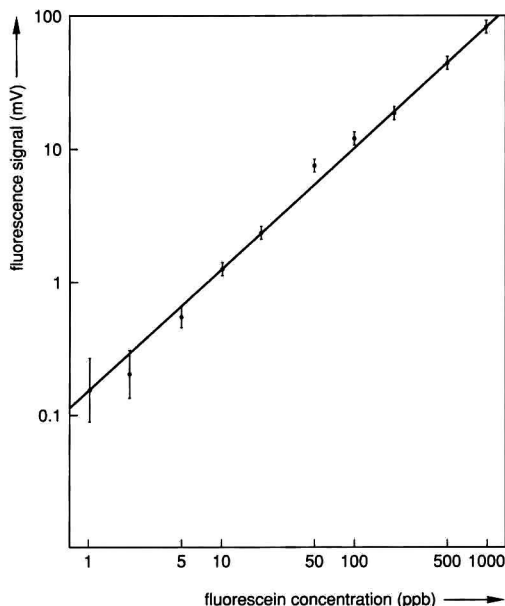


Fig. 4. Calibration graph for fluorescein, obtained using the detector cell in Fig. 3.

earlier values for highly fluorescing compounds using on-column detection [17,18]. Substantially lower detection limits were reported by Folestad *et al.* [19] ($5 \cdot 10^{-14}$ M fluoranthene). However, they used a free-falling jet cell that requires flow-rates far higher than can be attained in electrically driven systems. In CZE very impressive results were obtained by Dovichi and co-workers [20,21] using a sheath flow cuvette [$5 \cdot 10^{-12}$ M of (derivatized) alanine] and by Sweedler *et al.* [22] using axial illumination and a charge coupled device (CCD) readout ($1 \cdot 10^{-12}$ M of fluorescein isothiocyanate). Again, we encounter a compatibility problem. It is not easy to see how either the sheath flow cuvette or axial illumination can be combined with short column lengths and integral thermostating that are necessary to achieve the high efficiencies and separation speeds. In our integrated design, such a compatibility problem does not exist. In addition, we feel that there is ample room for improving the detection limit of our detector cell. As the standard deviation of the background signal is now limiting its performance, increasing the laser power will not be beneficial. Rather, we should either try to decrease the background itself by improving on the optics or to decrease its variance. Several ways to achieve the

latter can be envisaged. One could either contemplate the use of a commercially available laser power stabilizer (Liconix) or build a double-beam instrument in which fluctuations are corrected for by subtracting or ratioing the “blank” and “sample” photocurrents.

The possibility of fast separations is demonstrated in Fig. 5, which shows the separation of four laser dyes within 35 s using a 4-cm capillary. In this work, we used traditional electromigration (3 s, 3 kV) as the injection technique. It is clear that this method of injection has an adverse effect on the separation. Using an electroosmotic mobility of $7.8 \cdot 10^{-8}$ m² V⁻¹s⁻¹ (determined using the technique described by Huang *et al.* [23]), the volume injected is calculated to be 17 nl. Assuming an injection profile factor of 6, the peak width at half-height due to the injection is 0.95 s. Comparing this result with the electropherogram in Fig. 5, it is seen that the width of the peak travelling at the electroosmotic velocity (approximately the first peak) is completely dominated by the contribution of the injection. In practice, the consequence of the large contribution of the injection is that we cannot use the desirable high field strengths without serious resolution losses. Note that the field strength used to obtain the electropherogram in Fig. 6 is much lower than the optimum values quoted in the Theory section. Obviously, injection devices that allow for smaller

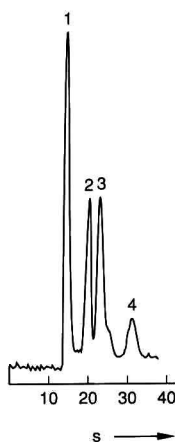


Fig. 5. Electropherogram of the separation of four laser dyes. Conditions: field strength, 33 kV m^{-1} ; buffer, 2 mM phosphate (pH 6); capillary, 4.0 cm \times 100 μm I.D.; temperature, ambient; injection, 3 s at 3 kV. Sample: (1) 7 ppm rhodamine B; (2) 7 ppm sulphorhodamine B; (3) 0.4 ppm fluorescein; (4) 17 ppm 4',5'-diiodofluorescein.

injection volumes than electromigration are necessary to realize the very short analysis times offered by short column lengths. We feel that the injector described in the first paragraph under Experimental, with which injection volumes of the order 100 pl are possible, can serve the purpose.

CONCLUSIONS

An integrated instrument for electrically driven separations has been designed. The design facilitates the use of short columns and high field strengths, so that high resolutions and short analysis times can be attained. The detector cell has the required small volume (100 pl) and allows $2 \cdot 10^{-19}$ mol of fluorescein to be detected. In combination with a short capillary (4 cm), four laser dyes could be separated within 35 s.

The separation speed is currently limited by the injection technique used (electromigration at 3 kV for 3 s). To decrease the contribution of the injection to the total peak width, the injected volume has to be reduced. This may be achieved using the injector of the proposed instrument.

REFERENCES

- 1 F. E. P. Mikkers, F. M. Everaerts and Th. P. E. M. Verheggen, *J. Chromatogr.*, 169 (1979) 11.
- 2 J. W. Jorgenson and K. D. Lukacs, *J. Chromatogr.*, 218 (1981) 209.
- 3 J. W. Jorgenson and K. D. Lukacs, *Anal. Chem.*, 53 (1981) 1298.
- 4 S. Terabe, K. Otsuka, K. Ishikawa, A. Tsuchiya and T. Ando, *Anal. Chem.*, 56 (1984) 111.
- 5 S. Terabe, *Trends Anal. Chem.*, 8 (1989) 129.
- 6 T. Tsuda, K. Nomura and G. Nakagawa, *J. Chromatogr.*, 99 (1982) 248.
- 7 J. H. Knox and I. H. Grant, *Chromatographia*, 24 (1987) 135.
- 8 R. T. Kennedy, M. D. Oates, B. R. Cooper, B. Nickerson and J. W. Jorgenson, *Science*, 246 (1989) 57.
- 9 P. K. de Bokx, P. C. Baarslag and H. P. Urback, *Sep. Sci. Technol.*, in press.
- 10 P. J. Schoenmakers, *The Optimization of Chromatographic Selectivity. A Guide to Method Development*, Elsevier, Amsterdam, 1986.
- 11 P. J. Naish, C. V. Perkins and D. P. Goulder, *Chromatographia*, 20 (1985) 335.
- 12 J. C. Sternberg, *Adv. Chromatogr.*, 2 (1966) 205.
- 13 C. L. Rice and R. Whitehead, *J. Phys. Chem.*, 69 (1965) 4017.
- 14 F. Foret, M. Deml and P. Boček, *J. Chromatogr.*, 452 (1988) 601.
- 15 Th. P. E. M. Verheggen, J. L. Beckers and F. M. Everaerts, *J. Chromatogr.*, 452 (1988) 615.
- 16 X. Huang, T.-K. J. Pang, M. J. Gordon and R. N. Zare, *Anal. Chem.*, 59 (1987) 2747.
- 17 H. P. M. van Vliet and H. Poppe, *J. Chromatogr.*, 346 (1985) 149.
- 18 E. J. Guthrie, J. W. Jorgenson and P. L. Dlugneski, *J. Chromatogr. Sci.*, 22 (1984) 171.
- 19 S. Folestad, L. Johnson, B. Josefsson and B. Galle, *Anal. Chem.*, 54 (1982) 925.
- 20 Y.-F. Cheng and N. J. Dovichi, *Science*, 242 (1988) 562.
- 21 S. Wu and N. J. Dovichi, *J. Chromatogr.*, 480 (1989) 141.
- 22 J. V. Sweedler, J. B. Shear, H. A. Fishman, R. N. Zare and R. H. Scheller, *Anal. Chem.*, 63 (1991) 496.
- 23 X. Huang, M. J. Gordon and R. N. Zare, *Anal. Chem.*, 60 (1988) 1837.

CHROM. 24 000

Assay of protein drug substances present in solution mixtures by fluorescamine derivatization and capillary electrophoresis

Norberto A. Guzman*, John Moschera, Carole A. Bailey, Khurshid Iqbal and A. Waseem Malick

Pharmaceutical Research and Development, Hoffmann-La Roche, Nutley, NJ 07110 (USA)

(First received September 27th, 1991; revised manuscript received January 9th, 1992)

ABSTRACT

A method is described to enhance the resolution and detection sensitivity of proteins, peptides, and amino acids in capillary electrophoretic analysis of solution mixtures. The method consists of derivatizing the analytes with fluorescamine, which is normally used as a fluorogenic reagent for compounds containing a reactive primary amine functional group, and then using the derivative as an ultraviolet chromophore to enhance detection sensitivity (measured at 280 nm) in capillary electrophoresis. The results demonstrated a significant improvement in the separation and detection sensitivity of the derivatized analytes as compared to their underivatized counterparts. The use of chromophores, such as fluorescamine, in capillary electrophoresis facilitates the analysis of components of solution mixtures, such as pharmaceutical formulations, that could not be resolved and/or detected by conventional capillary electrophoresis procedures.

INTRODUCTION

The utility of capillary electrophoresis (CE) for the analysis of protein drug substances present in a solution mixture has been previously demonstrated [1,2]. Because of the complexity of many solution mixtures, however, it is essential to develop CE conditions that will provide a sufficient degree of resolution to separate the components of the analyte mixture. A typical complex solution mixture, for example, is a pharmaceutical formulation. In this case, in addition to optimization of separation conditions, detection sensitivity must be maximized in order to visualize small amounts of drug substances in the presence of relatively large amounts of excipients. With this in mind, we have developed a method for increasing the detection sensitivity in the CE analysis of protein drug substances. The method involves reaction of the analyte mixture with the reagent fluorescamine to form fairly stable derivatives. These derivatives can then be detected

with a conventional UV detector. The fluorescamine-analyte derivatives are separated with a higher degree of resolution than their underivatized counterparts.

Fluorescamine (4-phenylspiro[furan-2(3H),1'-phthalan]-3,3'-dione) has been commonly used as a fluorogenic reagent [3–9]. This reagent reacts readily and rapidly at alkaline pH with primary amines to form intensely fluorescent substances, providing the basis for a rapid and sensitive assay of amino acids, peptides, proteins, and other primary amines [7–12]. Although free fluorescamine is quickly hydrolyzed in aqueous solution, the derivative it forms with primary amines is not. The comparative rates of the hydrolysis and derivatization reactions are crucial parameters. At pH 9 and ambient temperature, the reaction between fluorescamine and primary amines has a half-time of 200–1000 ms, while the hydrolytic reaction has a half-time of several seconds [7]. This assures that, upon mixing fluorescamine with an aqueous solution which con-

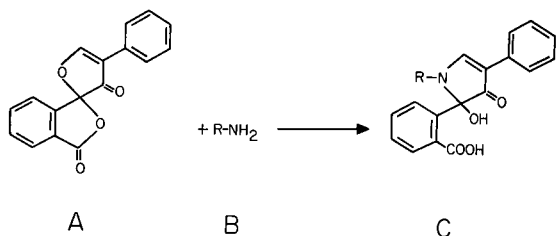


Fig. 1. Schematic representation of the molecular structure of fluorescamine (A), the reacting amino functional group-containing analyte (B) and the derivatized reaction product (C).

tains primary amines, there will be immediate derivatization followed by rapid hydrolysis of unreacted reagent. The proposed reaction scheme of fluorescamine with primary amines [7] is shown in Fig. 1.

The vast amount of data available in the literature has focused on the use of fluorescamine as a fluorogenic reagent (assaying for fluorescent derivatives). Only a few papers [13–16] report the measurement of the fluorescamine-analyte derivative by UV absorption. In this report we have examined the utility of fluorescamine as a UV chromophore, and have evaluated its application to the measurement of protein drug substances in pharmaceutical formulations separated by capillary electrophoresis. As a model system we have used the active drugs recombinant human leukocyte A interferon^a, humanized anti-TAC monoclonal antibody^b and the commonly used excipients glycine, L-arginine and human serum albumin.

EXPERIMENTAL

Reagents and supplies

All chemicals were obtained at the highest purity level available from the manufacturer, and were used without additional purification. Potassium hydroxide, sodium phosphate (Na₂HPO₄), borax (Na₂B₄O₇ · 10H₂O), lithium chloride, crystallized human serum albumin, and fluorescamine were obtained from Sigma (St. Louis, MO, USA). Glycine and L-arginine were purchased from Fluka (Ron-

konkoma, NY, USA). Acetone (HPLC grade), pyridine (Fisher Certified), and hydrochloric acid solution (12 M) were obtained from Fisher Scientific (Fair Lawn, NJ, USA). Recombinant human leukocyte-A interferon and humanized anti-TAC monoclonal antibody were supplied by Hoffmann-La Roche (Nutley, NJ, USA). Albuminar-25 (250 mg/ml solution for injection of human serum albumin) was purchased from Armour Pharmaceutical (Kankakee, IL, USA). Reagent solutions and buffers were prepared using triply distilled and deionized water, and routinely degassed and sonicated under vacuum after filtration.

Millex disposable filter units (0.22 μm) were purchased from Millipore (Bedford, MA, USA), and fused-silica capillary columns were obtained from Scientific Glass Engineering (Austin, TX, USA), and Polymicro Technologies (Phoenix, AZ, USA).

Instrumentation

A commercially available CE instrument (P/ACE System 2000, Beckman, Palo Alto, CA, USA), was used for this work. In this instrument, the capillary is housed in a cartridge constructed so as to allow a flow of recirculating liquid for Peltier-temperature control of the capillary column. Samples were stored in a microapplication vessel assembly, consisting of a 150-μl conical microvial inserted into a standard 4-ml glass reservoir and held in position for injection by an adjustable spring. In order to minimize evaporation of the sample volume (100 μl), about 1–2 ml of cool water was added to the microapplication vessel housing the microvial. The external water serves as a cooling bath for the sample in the microvial, and as source of humidity to prevent sample evaporation and concentration. After insertion of the microvial, the microapplication vessel assembly was covered with a rubber injection septum and placed into the sample compartment of the CE instrument. Samples were injected into the capillary column by pressure. Peak visualization and data acquisition were performed using the UV detection system of the CE instrument and the System Gold chromatography software package (Beckman, San Ramon, CA, USA). Data integration was also carried out with a Model D-2500 Chromato-Integrator (Hitachi, Danbury, CT, USA).

^a Leukocyte A interferon (IFN-αA) is in current nomenclature designated IFN.α2a.

^b Anti-TAC (T-activated cell) is an IgG1 class genetically engineered hybrid antibody, directed against the human receptor for interleukin-2 [26].

Assay procedure

Sample preparation. Equal molarity stock solutions were individually prepared by dissolving L-arginine (1 mg/ml) and glycine (0.43 mg/ml) in 0.1 M sodium tetraborate (borax) buffer, pH 9.0. A stock solution of crystallized human serum albumin (25 mg/ml), used as reference, was prepared in the same buffer. Albuminar-25 (250 mg/ml), recombinant human leukocyte-A interferon (5.8 mg/ml) and humanized anti-TAC monoclonal antibody (8.6 mg/ml) were obtained as concentrated solution and were diluted to their specified working strengths with the same sodium tetraborate buffer.

Sample derivatization. For CE analysis without fluorescamine derivatization, assay samples were diluted to desired concentrations with sample dilution buffer (0.1 M sodium tetraborate buffer, pH 9.0) and directly transferred to the conical vial and then inserted into the microapplication vessel assembly on the CE instrument.

For CE analysis of fluorescamine derivatives, solutions of the respective analyte samples (concentration ranging from 2.1 to 1250 μg , or from 7.4 to 172.2 nmol per 100 μl reaction mixture) were transferred to a 500- μl microcentrifuge tube and their total volume adjusted to 70 μl by addition of sample dilution buffer. Derivatization was performed by the addition of 30 μl of fluorescamine solution (3 mg/ml fluorescamine in acetone, containing 20 μl pyridine) to the sample while continuously and vigorously vortexing. After approximately 2 min, the content of the microcentrifuge tube was transferred to the conical microvial and then inserted into the microapplication vessel assembly for analysis.

For the fluorescamine-derivatized L-arginine the volumes of the sample and reagent were doubled and prepared in a 500- μl microcentrifuge tube. A 100- μl aliquot was transferred to a conical microvial and then inserted into the microapplication vessel assembly as described above. The rest of the sample mixture was maintained in a sealed microcentrifuge tube at 25°C, and used as a replacement sample for the last two experimental points (8.5 and 24.5 hours).

Running conditions. Sample solutions for analysis in microapplication vessels were placed into the sample holder of the analyzer. The analysis program was initiated and the first sample automatically injected into the capillary by a positive nitrogen

pressure of 0.5 p.s.i. (3500 Pa) for 4 s. At the completion of each run, the capillary column was sequentially washed by injection of 2.0 M sodium hydroxide solution, 0.1 M sodium hydroxide solution, distilled-deionized water, and then regenerated with running buffer.

The CE separations reported were performed using three different buffers: (1) 0.05 M sodium tetraborate buffer, pH 8.3, containing 0.05 M lithium chloride; (2) 0.05 M sodium tetraborate buffer, pH 8.3, containing 0.025 M lithium chloride; or (3) 0.05 M sodium phosphate buffer, pH 7.0, containing 0.05 M lithium chloride. The CE instrument was equipped with a 57 cm (50 cm to the detector) \times 75 μm I.D. capillary column. The CE separation was performed at 12 kV when using the 0.05 M lithium chloride-containing sodium phosphate buffer, at 15 kV when using the 0.05 M lithium chloride-containing sodium tetraborate buffer, or at 18 kV when using the 0.025 M lithium chloride-containing sodium tetraborate buffer. Capillary temperature for all experiments was maintained at 25°C during the run. Under these conditions, approximately 24 nl (6 nl/s) was injected into the capillary column [17]. Monitoring of the analytes was performed at wavelengths of 200, 214 or 280 nm.

RESULTS

Fig. 2 depicts the electropherograms of a control fluorescamine solution and of a fluorescamine-derivatized simple mixture of primary amines, *i.e.*, L-arginine and glycine. Both of the fluorescamine-derivatized amino acids, L-arginine (peak 2) and glycine (peak 3), are well separated from each other and from the peaks corresponding to the constituents of the derivatization reagent, fluorescamine (peak 4) and the organic solvents acetone and pyridine (comigrating at peak 1). The observed decreased peak area for the fluorescamine (Fig. 2B, peak 4), in comparison with the control value (Fig. 2A, peak 4), confirms that a significant amount of the reagent is immediately consumed in reaction with the analytes.

In order to optimize the degree of derivatization of the analytes with fluorescamine under the reaction conditions used, *i.e.*, pH 9.0 in a sodium tetraborate buffer at 25°C, a fixed amount of L-arginine (115 nmol) was reacted with increasing concentra-

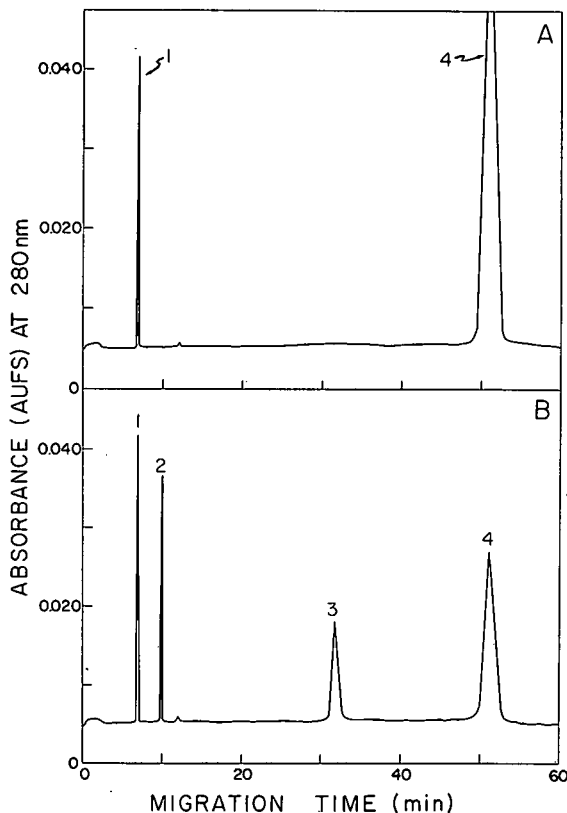


Fig. 2. Capillary electrophoresis profile of fluorescamine-derivatized amino acids. (A) Electropherogram of the fluorescamine solution control; peaks: 1 = acetone; 4 = fluorescamine reagent. (B) Electropherogram of glycine and L-arginine; peaks: 1 = acetone; 2 = fluorescamine-derivatized L-arginine; 3 = fluorescamine-derivatized glycine; 4 = fluorescamine reagent. The procedure was carried out as described in the Experimental section. The separation buffer consisted of 0.05 M sodium tetraborate buffer, pH 8.3, containing 0.05 M lithium chloride.

tions of the fluorescamine reagent. As shown in Fig. 3, peak area of the derivative appeared to be maximal at a fluorescamine concentration of 250–300 nmol (per 100 μ l reaction mixture volume). Therefore, for this amino acid, a two- to three-fold molar excess of fluorescamine reagent should be sufficient to saturate the reaction mixture and form an optimal fluorescamine-amino acid derivative.

Using these conditions, the linearity of the derivative peak area as a function of L-arginine concentration was investigated. As shown in Table I and Fig. 4, a linear response (at 280 nm) was observed at L-arginine concentrations ranging from 14.3

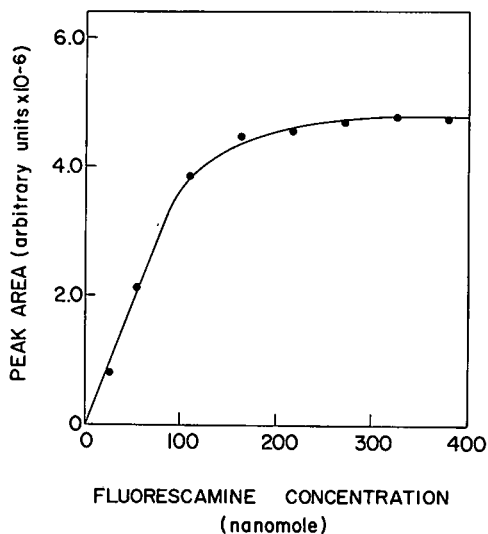


Fig. 3. Relationship between peak area of derivatized analyte formed and concentration of fluorescamine consumed. The amount of excess fluorescamine reagent was calculated by reacting a fixed concentration of L-arginine (115 nmol/100 μ l reaction mixture volume) with an increasing concentration of fluorescamine. The procedure was carried out as described in the Experimental section. The separation buffer consisted of 0.05 M sodium tetraborate buffer, pH 8.3, containing 0.05 M lithium chloride.

nmol/100 μ l to 172.2 nmol/100 μ l of reaction mixture. A similar molar excess fluorescamine ratio and saturation response curve were observed for glycine (data not shown).

The stability of the fluorescamine-L-arginine derivative over a 24-h period, which might constitute a normal day's assay requirements, was also investigated. For this study, caution was taken to avoid evaporation during the 24-h storage period. This is particularly important in view of the volatile nature of the fluorescamine solvent (acetone). As shown in Table II, no loss in derivative was observed over the test period. On the contrary, peak area was observed to increase slightly over the first 2.5 h of storage and then remain constant. The progressive increase in peak area during the initial phase of storage is most likely the result of evaporative concentration, which appears to occur to some extent despite the precautions taken. This is probably due in part to: (a) storage of the sample in the ambient temperature environment of the CE instrumentation sample handling compartment, and (b) poor or

TABLE I

TYPICAL AMOUNTS OF FLUORESCAMINE-DERIVATIZED L-ARGININE ANALYZED BY CAPILLARY ELECTROPHORESIS AT 280 nm

For this experiment, increasing amounts of L-arginine were reacted with a fixed concentration of fluorescamine reagent (324 nmol/100 μ l reaction mixture). The separation buffer consisted of 0.05 M sodium tetraborate buffer, pH 8.3, containing 0.05 M lithium chloride.

Amount of L-arginine present in 100 μ l reaction mixture			Amount of L-arginine injected into the capillary column			peak area (arbitrary units $\times 10^{-6}$)
μ l	μ g	nmol	nl	ng	pmol	
2.5	2.5	14.3	24	0.6	3.4	0.57
5	5	28.7	24	1.2	6.7	1.09
10	10	57.4	24	2.4	13.8	2.20
15	15	86.1	24	3.6	20.7	3.18
20	20	114.8	24	4.8	27.6	4.48
25	25	143.5	24	6.0	34.4	5.59
30	30	172.2	24	7.2	41.3	6.92

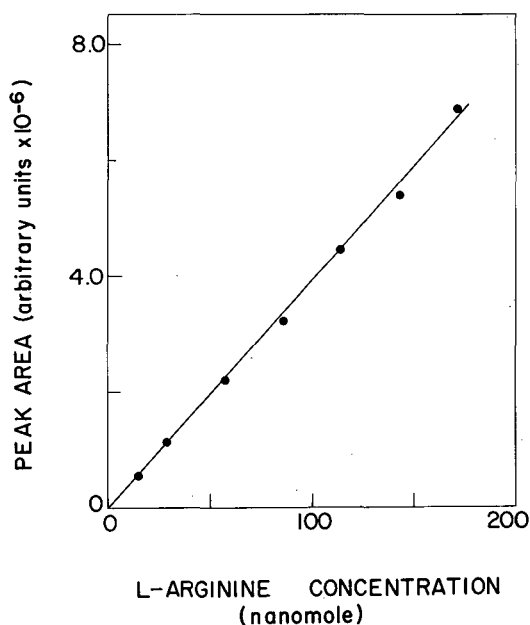


Fig. 4. Relationship between peak area of the derivatized analyte formed and the concentration of reacting L-arginine. The linearity of the formation of fluorescamine-derivatized amino acid was calculated by reacting increasing concentrations of L-arginine (ranging from 14.3 to 172.2 nmol/100 μ l reaction mixture) with an excess amount of fluorescamine reagent (324 nmol/100 μ l reaction mixture). The procedure was carried out as described in the Experimental section. The separation buffer consisted of 0.05 M sodium tetraborate buffer, pH 8.3, containing 0.05 M lithium chloride.

incomplete sealing of the microapplication vessel assembly. Without the precautions taken, *i.e.* humidification of the chamber and water cooling of the sample, evaporation occurred much more rapidly and resulted in a dramatic loss of acetone and a corresponding concentration of the fluorescamine-L-arginine derivative (results not shown). Similarly, evaporative concentration effects have been previously demonstrated for benzoic acid derivatives [18].

TABLE II

STABILITY OF FLUORESCAMINE-L-ARGININE DERIVATIVE

For this experiment, the microapplication sample vessel containing the microvial was filled with an appropriate amount of deionized water in order to avoid evaporation. For details see the Experimental Section. The separation buffer consisted of 0.05 M sodium tetraborate buffer, pH 8.3, containing 0.05 M lithium chloride.

Time of incubation (h)	Peak area (arbitrary units $\times 10^{-6}$)
0.5	4.58
1.5	4.61
2.5	4.72
4.5	4.78
8.5	4.79
24.5	4.76

The fluorescamine derivatization procedure developed with the simple amino acid model compounds was applied to CE analysis of recombinant human leukocyte A interferon and human serum albumin, which represent a typical protein drug substance and a common protein excipient. For derivatization, fluorescamine concentration was maintained at 324 nmol/100 μ l of reaction mixture and analyte samples containing 13.3 nmol of interferon and 4.2 nmol of albumin, respectively, were analyzed. CE analysis was performed using the 0.05 M sodium phosphate buffer, pH 7.0, containing 0.05 M lithium chloride. As shown in Fig. 5, the derivatization with fluorescamine resulted in a 20- to 30-fold increase in detection response for the

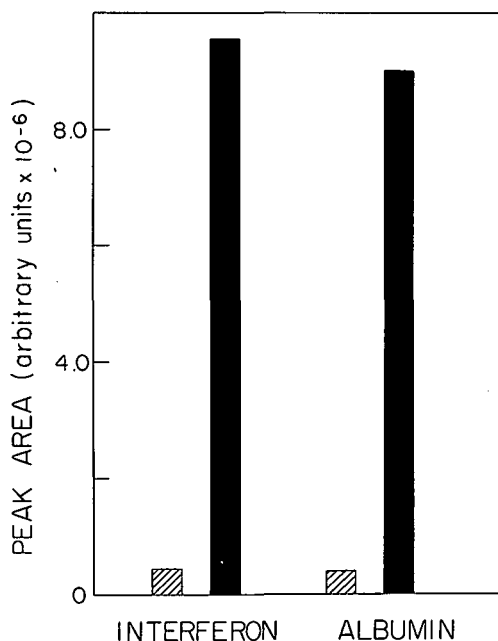


Fig. 5. Comparison of the peak areas of the non-derivatized proteins versus fluorescamine-derivatized human serum albumin and recombinant human leukocyte A interferon. Dashed bars represent the peak areas of non-derivatized proteins. Solid bars represent the peak areas of fluorescamine-derivatized proteins. The concentration of non-derivatized samples used in this experiment was 580 μ g (29.6 nmol)/100 μ l reaction mixture of recombinant leukocyte A interferon, and 1250 μ g (18.4 nmol)/100 μ l reaction mixture of human serum albumin. The concentration of fluorescamine-derivatized samples was 290 μ g (14.8 nmol)/100 μ l reaction mixture of recombinant leukocyte A interferon, and 250 μ g (3.7 nmol)/100 μ l reaction mixture of human serum albumin. The separation buffer consisted of 0.05 M sodium phosphate buffer, pH 8.3, containing 0.05 M lithium chloride.

protein analytes. Under these conditions (280 nm), interferon at a concentration down to 400 μ g/ml (20.4 nmol/ml), and albumin at a concentration down to 800 μ g/ml (11.7 nmol/ml) were easily detected when derivatized with fluorescamine.

Derivatization with fluorescamine was also observed to have a marked effect on analyte mobility in CE analysis. As indicated in Table III, derivatization increased the migration times for both the amino acid and protein analytes. The magnitude of the shift appears to be mostly determined by the net charge of the analyte after derivative formation, which is a function of both the *pI* of the underivatized analyte and the number of reacting amino groups present. The molar ratio of fluorescamine to analyte in the derivative also influences migration rate, and would play a major role in determining the mobility of analytes migrating in buffers at or near their *pI* values.

This mobility shift is graphically illustrated in Fig. 6, which shows the electropherograms obtained for leukocyte A interferon samples (2.9 nmol/100 μ l, 24 nl injection) assayed with and without fluorescamine derivatization. Analysis of the non-derivatized sample (Fig. 6A) indicated a single peak migrating at 10.2 min and detected near the lower limits of detector sensitivity (at 280 nm). Derivatization with fluorescamine (Fig. 6B) shifted the interferon to 22.2 min (peak 4), increased its peak area dramatically, and enabled detection of an un-

TABLE III

EFFECT OF FLUORESCAMINE ON THE MIGRATION TIME OF COMPONENTS PRESENT IN A FORMULATION MIXTURE

For this experiment, CE detection of separated native amino acids (non-fluorescamine derivatized) was performed at 200 nm. All other measurements were carried out at 280 nm. For the separation of the formulation mixture sample components by CE, 0.05 M sodium tetraborate buffer, pH 8.3, containing 0.025 M lithium chloride was used.

Substance	Migration time (min)	
	Native	Derivatized
L-Arginine	3.9	7.3
Glycine	5.2	20.0
Humanized anti-TAC	5.9	10.1
Interferon	7.2	14.0
Human serum albumin	9.7	17.8

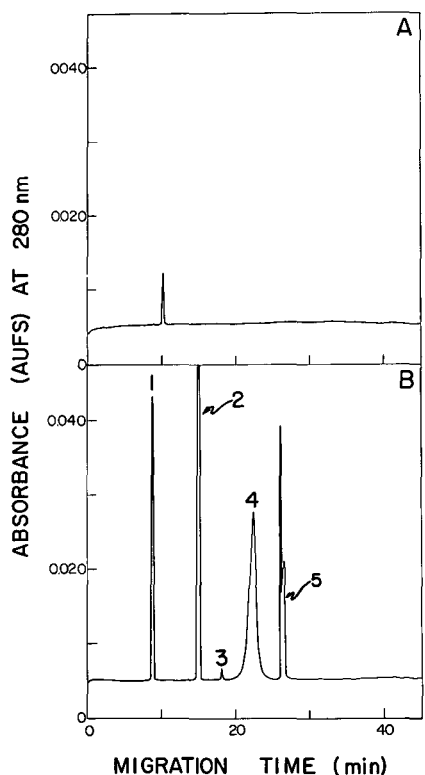


Fig. 6. Capillary electrophoresis profile of recombinant leukocyte A interferon. (A) Electropherogram of non-derivatized interferon. (B) Electropherogram of fluorescamine-derivatized interferon. Peaks: 1 = acetone; 2 = ammonia; 3 = unknown; 4 = interferon; 5 = fluorescamine reagent. The separation buffer consisted of 0.05 *M* sodium phosphate buffer, pH 7.0, containing 0.05 *M* lithium chloride. The concentration of interferon used in this experiment was 580 μg (29.6 nmol)/100 μl reaction mixture (A), and 232 μg (11.8 nmol)/100 μl reaction mixture (B).

known component (peak 3) and ammonia (peak 2), an interferon buffer constituent. The enhanced sensitivity afforded by fluorescamine derivatization is even greater when detection is performed at lower wavelengths (Fig. 7).

The procedures developed using the model compounds were applied to CE analysis of recombinant leukocyte A interferon (Fig. 8A) and recombinant humanized anti-TAC antibody (Figure 8B) in formulation mixtures. To demonstrate the versatility of CE, the formulation mixtures were supplemented with the excipients human serum albumin, glycine and L-arginine, which may also serve as reference compounds for mobility comparison. As shown in

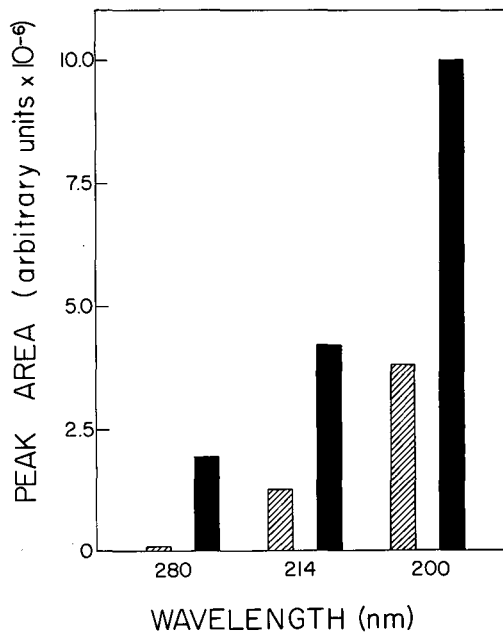


Fig. 7. Comparison of the peak areas of non-derivatized and fluorescamine-derivatized interferon at various wavelengths. Dashed bars represent the peak areas of the non-derivatized interferon and solid bars represent fluorescamine-derivatized interferon. The separation buffer consisted of 0.05 *M* sodium tetraborate buffer, pH 8.3, containing 0.025 *M* lithium chloride. The concentration of interferon used in this experiment was 58 μg (2.9 nmol)/100 μl reaction mixture.

the figure, all of the compounds were well separated.

DISCUSSION

Proteins and peptides are playing an ever increasing role in today's pharmaceutical industry. Although capillary zone electrophoresis and other variants of CE methods have developed over the last decade into analytical tools of remarkable performance [19–25], the use of this technology for the separation and analysis of proteins is not yet generally accepted. Difficulties in separating the proteins of interest from components of the formulation matrix and the high levels of sensitivity required for their detection, have contributed to the problem. Furthermore, detection of proteins is difficult owing to a lack of good chromophore groups in easily accessible spectral regions.

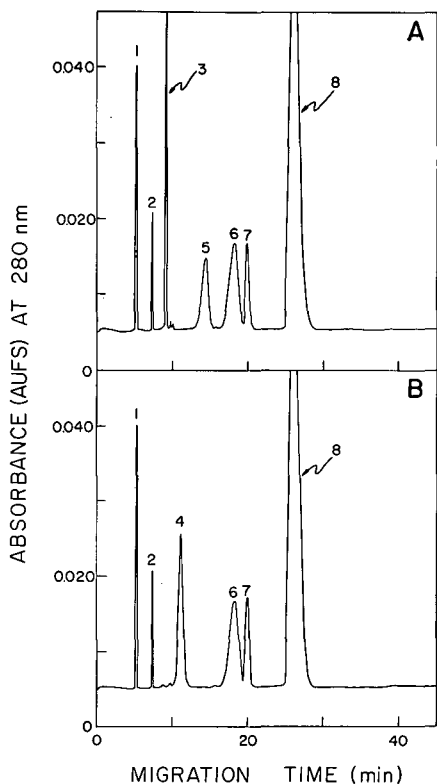


Fig. 8. Capillary electrophoresis profile of fluorescamine-derivatized formulation mixture components. (A) Electropherogram of a formulation mixture containing human leukocyte A interferon; peaks: 1 = acetone; 2 = L-arginine; 3 = ammonia; 5 = interferon; 6 = human serum albumin; 7 = glycine; 8 = fluorescamine reagent. (B) Electropherogram of a formulation mixture containing humanized anti-TAC monoclonal antibody; peaks: 4 = anti-TAC monoclonal antibody; all other peaks as in (A). The separation buffer consisted of 0.05 M sodium tetraborate buffer, pH 8.3, containing 0.025 M lithium chloride. The concentration of analytes, per 100 μ l reaction mixture, used in this experiment were as follows: L-arginine, 5 μ g (28.7 nmol); anti-TAC monoclonal antibody, 215 μ g (1.4 nmol); interferon, 145 μ g (7.4 nmol); glycine, 2.1 μ g (28.7 nmol); and human serum albumin, 125 μ g (1.8 nmol).

The experiments described in this report demonstrate that the addition of a chromophore, such as fluorescamine, to an amino functional group of a protein, peptide, or amino acid, or any other amine-containing substance, dramatically improves its detection sensitivity in the UV region. Furthermore, derivatization with fluorescamine shifts analyte migration time, as a function of analyte structure and buffer conditions, and may result in an enhanced degree of resolution as compared to underivatized

counterparts. For maximum utility, conditions for derivatization with fluorescamine should be optimized for the analyte of interest. For simple compounds, containing only a single reactive amino group, a 2- to 3-fold molar excess of reagent and a reaction pH of 9.0 were sufficient to show a dramatic increase in detection sensitivity when monitored at 280 nm. For more complex analytes, having many reactive groups, an increased molar ratio of fluorescamine and slightly altered reaction pH, may be called for. Also, it may be possible that the extent of derivatization could be dependent on the sample matrix. Thus, if this problem occurs, post-column derivatization may be used as an alternative method.

Optimization of CE running conditions, to consider the effects of buffer salt, pH and the inclusion of inorganic ions [24,25], is also essential in order to assure the required degree of analyte resolution. For example, the experiments described in this report demonstrated that for the analysis of the fluorescamine-derivatized protein analytes by CE, 50 mM lithium chloride-containing sodium tetraborate buffer, pH 8.3, produces adequate separation with reproducible migration times and peak areas. Similar results are obtained with 50 mM lithium chloride-containing sodium phosphate buffer, pH 7.0. However, when the analysis of all formulation mixture components is carried out simultaneously, the separation seems to be better when the concentration of lithium chloride is reduced to 25 mM in the sodium tetraborate buffer, pH 8.3.

In conclusion, the incorporation of fluorescamine derivatization in the CE analysis of amino acids, peptides or proteins, or of molecules in general containing a reactive primary amine functional group, significantly improves detection sensitivity and separation. The method is simple, quite fast, and very reproducible. The derivatives formed also appear to be stable and show no loss in UV response over the period tested.

REFERENCES

- 1 N. A. Guzman, H. Ali, J. Moschera, K. Iqbal and A. W. Malick, *J. Chromatogr.*, 559 (1991) 307-315.
- 2 E. Monnot-Chase, C. W. Demarest, M. Y. Baratta and J. Jiu, presented at the 3rd International Symposium on High Performance Capillary Electrophoresis, San Diego, CA, February 3-6, 1991, abstract PT-42.

- 3 K. Samejima, W. Dairman, J. Stone and S. Udenfriend, *Anal. Biochem.*, 42 (1971) 237–247.
- 4 M. Weigele, S. L. DeBernardo, J. P. Tengli and W. Leimgruber, *J. Am. Chem. Soc.*, 94 (1972) 4052–4053.
- 5 M. Weigele, J. F. Blount, J. P. Tengli, R. Czaikowski and W. Leimgruber, *J. Am. Chem. Soc.*, 94 (1972) 5927–5928.
- 6 S. Udenfriend, *J. Res. Nat. Bureau Stds.*, 76A (1972) 637–640.
- 7 S. Udenfriend, S. Stein, P. Böhlen, W. Dairman, W. Leimgruber and M. Weigele, *Science (Washington, D.C.)*, 178 (1972) 871–872.
- 8 S. Stein, P. Böhlen, J. Stone, W. Dairman and S. Udenfriend, *Arch. Biochem. Biophys.*, 155 (1973) 202–212.
- 9 P. Böhlen, S. Stein, W. Dairman and S. Udenfriend, *Arch. Biochem. Biophys.*, 155 (1973) 213–220.
- 10 C. H. Evans and J. D. Ridella, *Anal. Biochem.*, 142 (1984) 411–420.
- 11 P. M. Horowitz, *J. Chromatogr.*, 319 (1985) 446–449.
- 12 M. C. Miedel, J. D. Hulmes and Y.-C. E. Pan, *J. Biochem. Biophys. Meth.*, 18 (1989) 37–52.
- 13 A. M. Felix, V. Toome, S. De Bernardo and M. Weigele, *Arch. Biochem. Biophys.*, 168 (1975) 601–608.
- 14 L. D. Libera, *J. Chromatogr.*, 536 (1991) 283–288.
- 15 N. A. Guzman, M. A. Trebilcock and J. P. Advis, *Anal. Chim. Acta*, 249 (1991) 247–255.
- 16 N. A. Guzman, J. Moschera, K. Iqbal and A. W. Malick, *J. Liq. Chromatogr.*, 15 (1992) 1163–1177.
- 17 J. Harbaugh, M. Collette and H. E. Schwartz, *Technical Information Bulletin No. TIBC-103 (4SP-890-10B)*, Beckman Instruments, Palo Alto, CA, 1990.
- 18 R. J. Nelson, *Technical Information Bulletin No. TIBC-101 (4SP-590-10B)*, Beckman Instruments, Palo Alto, CA, 1990.
- 19 B. L. Karger, A. S. Cohen and A. Guttman, *J. Chromatogr.*, 492 (1989) 585–614.
- 20 N. A. Guzman, L. Hernandez and S. Terabe, in C. Horváth and J. G. Nikelly (Editors), *Analytical Biotechnology — Capillary Electrophoresis and Chromatography (ACS Symposium Series, No. 434)*, American Chemical Society, Washington, DC, 1990, Ch. 1, pp. 1–35.
- 21 R. A. Wallingford and A. G. Ewing, *Adv. Chromatogr.*, 29 (1990) 1–76.
- 22 M. Novotny, K. A. Cobb and J. Liu, *Electrophoresis*, 11 (1990) 735–749.
- 23 Z. Deyl and R. Struzinsky, *J. Chromatogr.*, 569 (1991) 63–122.
- 24 J. S. Green and J. W. Jorgenson, *J. Chromatogr.*, 478 (1989) 63–71.
- 25 M. M. Bushey and J. W. Jorgenson, *J. Chromatogr.*, 480 (1989) 301–310.
- 26 M. A. Costello, C. Woititz, J. de Feo, D. Stremlo, L.-F. L. Wen, D. J. Palling, K. Iqbal and N. A. Guzman, *J. Liq. Chromatogr.*, 15 (1992) 1181–1197.

Systematic optimization of capillary electrophoretic separation of sulphonamides

C. L. Ng, H. K. Lee and S. F. Y. Li*

Department of Chemistry, National University of Singapore, Kent Ridge, Singapore 0511 (Singapore)

(First received October 24th, 1991; revised manuscript received January 13th, 1992)

ABSTRACT

The use of an optimization scheme for the separation of a group of sulphonamides is described. This scheme utilizes an interpretive optimization approach to predict the optimum conditions for the separation of a group of eight sulphonamides. By conducting nine preplanned experiments that span the maximum working range of the system, overall optimum conditions for separation can be obtained. To confirm the validity of the optimization procedure, additional experiments using the optimum conditions predicted by the scheme were performed. The results demonstrated that satisfactory separation could be achieved by using the optimum separation conditions predicted by the scheme.

INTRODUCTION

Sulphonamides are drugs which are extensively used in the treatment of bacterial infections in both animals and man, and there is currently great interest in their separation and assay [1–3]. High-performance liquid chromatography (HPLC) is commonly used for this purpose but, as most of these compounds are ionic, it is expected that capillary electrophoresis (CE) may be a valuable alternative method.

CE is a highly efficient and rapid technique that is being increasingly used in the biological and pharmaceutical fields [4–6]. Extremely high separation efficiencies have been demonstrated using this technique. However, optimum separation conditions using CE are normally obtained by trial-and-error methods and these approaches result only in local optimum conditions rather than overall optima. A systematic approach for CE separation was recently reported by Vindevogel and Sandra [7], in which a Plackett–Burman statistical design was used. The method required only eight experiments for the optimization of five factors, all related to buffer

composition. However, no fixed rules existed for the selection of low and high levels of the parameters used in the optimization procedure and further optimization may need to be attempted based on the conclusion of the optimization experiments [7].

In this investigation, CE with β -cyclodextrin as modifier was used for the assay of eight sulphonamides. A systematic optimization scheme was utilized. This scheme, known as the overlapping resolution mapping (ORM) scheme, had been previously applied for the optimization of HPLC separations [8,9]. In this paper, the use of a modified ORM scheme for the optimization of the CE separation of sulphonamides is described.

EXPERIMENTAL

Experiments were conducted on a laboratory-built CE system. A Spellman (Plainview, NY, USA) Model RM15P10KD power supply capable of delivering up to 15 kV was used. Fused-silica capillary tubing of 50 cm \times 50 μ m I.D. with an optically transparent coating was obtained from Polymicro Technologies (Phoenix, AZ, USA). A Shimadzu

(Kyoto, Japan) Model SPD-6A UV spectrophotometric detector and a microUVIS20 UV detector (Carlo Erba, Milan, Italy) were used for the detection of peaks. Chromatographic data were collected and analysed using a Shimadzu Chromatopac C-R6A data processor.

The pH of the buffer solutions used in the CE system was obtained by mixing appropriate portions of sodium dihydrogenphosphate and sodium tetraborate solutions. β -Cyclodextrin, which was used as a modifier in the electrophoretic medium, was purchased from Fluka (Buchs, Switzerland). The eight sulphonamide standards used (Table I) were purchased from Sigma (St. Louis, MO, USA). The sulphonamide standards were each dissolved in HPLC-grade methanol (BDH, Poole, UK) at a concentration of 1000 ppm.

Sample solutions were introduced manually. One end of the capillary was placed in a sample vial containing the sample solution and the sample was introduced by siphoning from the sample solution at a level 9 cm higher than the electrophoretic solution in which the other end of the tube was immersed. The injection time was about 4 s. Each injection was estimated to be 1 nl.

RESULTS AND DISCUSSION

Initial attempts to separate the sulphonamides using CZE conditions in which the pH of the electrophoretic media was adjusted to 6, 7 and 8 proved unsuccessful. Owing to the ionic nature of the sulphonamides, slight changes in pH was found to affect the separation adversely. In fact, it was found that the resolution of the peaks could be

affected by as small as 0.05 unit change in the pH of the electrophoretic medium. In view of the susceptibility of resolution to pH changes for this group of compounds, optimization through pH variation by the trial-and-error method was considered to be unsatisfactory. The addition of a suitable modifier to the buffer, which would serve to stabilize the system in response to slight changes in pH and to enhance the separation efficiency, was therefore considered. As the sulphonamides are relatively polar, we would not expect that the use of sodium dodecyl sulphate (SDS) in the electrophoretic medium, as is normally employed in micellar electrokinetic chromatography (MEKC) [10–12], would be effective in solvating the compounds. This is because the sulphonamides would prefer to remain in the aqueous buffer medium rather than partition with the micelles. A better choice would be β -cyclodextrin, as it is neutral and yet possesses polar hydroxy groups. β -Cyclodextrin was therefore chosen as a modifier in the electrophoretic medium.

An ORM scheme was used to determine the optimum conditions for the separation of sulphonamides. The ORM scheme is a statistical experimental model used to define the region of interest in which the optimum conditions reside. The term ORM used in this investigation implies that the optimum conditions were achieved by overlapping all resolution plots. The scheme predicts the optimum operating pH and β -cyclodextrin composition of the electrophoretic medium from nine preliminary experiments.

A schematic flow chart for the optimization scheme is shown in Fig. 1. The initial step for this scheme involved setting the criteria for the separation. Two criteria were considered: first, the peaks should be baseline separated, and second, the overall migration time should be less than 15 min. For this scheme, there is great flexibility in choosing the migration range for the system. This depends on the type of compounds under investigation and the nature of the investigation. As the sulphonamides would be expected to be ionized in the electrophoretic medium, the migration times for this group of compounds under CZE conditions would be relatively short. In addition, it is desirable not to choose too long a migration range for the separation. In this instance, an overall migration time of 15 min was chosen.

TABLE I
SULFONAMIDES INVESTIGATED

Compound	Abbreviation
Sulphamethoxypyridazine	SMP
Sulphachloropyridazine	SCP
Sulphasalazine	SS
Sulphamerazine	SM
Sulphaguanidine	SG
Sulphadiazine	SD
Sulphaquinoxaline	SQX
Sulphamethazine	SMZ

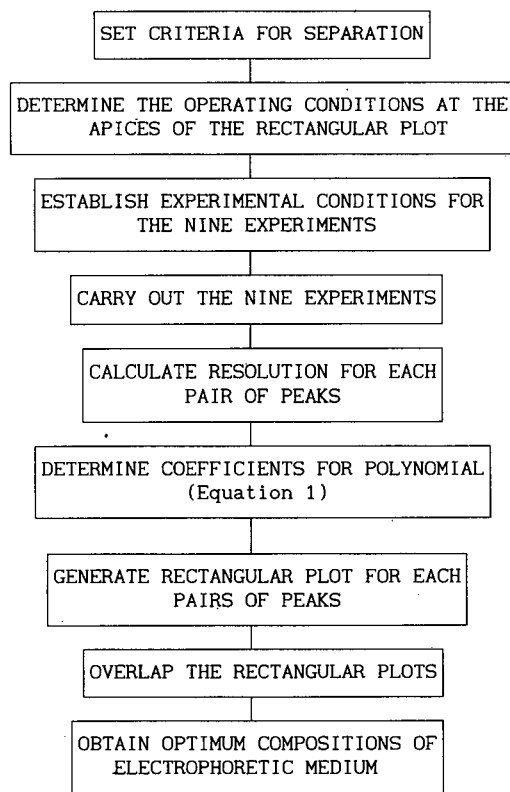


Fig. 1. Schematic representation of the optimization scheme.

After the criteria had been set, the operating conditions at the four apices of the rectangular plot were determined. The nine experiments were strategically chosen at appropriate positions in the rectangular plot as shown in Fig. 2. The ORM scheme is flexible in that it allows the four experiments at the vertices of the rectangular plot to cover as much as possible the whole working range of the system. These four experiments are only subjected to the preset criteria mentioned earlier and the type of compounds under investigation. In determining the working range for the pH of the buffer, it was considered undesirable to use extreme pH conditions because they were known to be detrimental to the untreated column. Therefore, a moderate pH of 8 was chosen. Otsuka and Terabe [13], in investigations on the effect of pH on electroosmotic flow, showed that the electroosmotic flow, v_{eo} , decreased as pH decreased. The use of a low-pH buffer would obviously lead to an increase in analysis time. In view of the preset criteria which stipulated that the

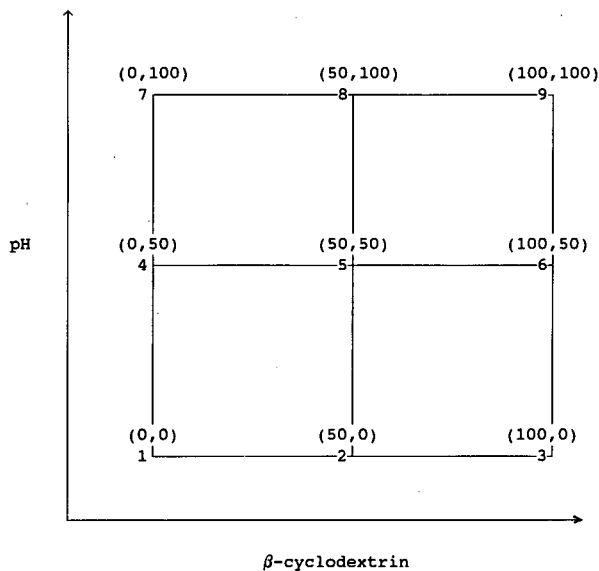


Fig. 2. Locations of the nine experiments chosen from the rectangular plot. The composition at each point is represented as a percentage at the respective apices.

total analysis time should not be greater than 15 min, the lower limit of pH was set at 6.

β -Cyclodextrin as modifier in the electrophoretic medium has been shown to effect separation through a host-guest relationship [14] with the analytes. Small amounts of β -cyclodextrin in the separation media have been found to be sufficient for optimizing the separation of water- and fat-soluble vitamins [15]. Therefore, concentrations higher than 10 mM were considered unnecessary. In addition, higher concentrations of β -cyclodextrin in the buffer solution would pose a solubility problem. Consequently, minimum and maximum β -cyclodextrin concentrations of 0 and 10 mM were chosen.

After setting the operational conditions at the four apices of the rectangular plot, the other five experiments as shown in Fig. 2 would then be easily defined. For example, the pH of the buffer and the amount of β -cyclodextrin in the electrophoretic media for point 5 (5 mM β -cyclodextrin and pH 7.0) shown in Fig. 2 are calculated as follows: the amount of β -cyclodextrin is the sum of the amount of β -cyclodextrin at point 4 (0 mM β -cyclodextrin) and the mean of the difference between point 4 (0 mM β -cyclodextrin) and point 6 (10 mM β -cyclodextrin). Similarly, the pH of the buffer can be obtained from point 2 (pH 6) and point 8 (pH 8). The detailed

TABLE II
EXPERIMENTAL CONDITIONS USED FOR THE NINE
EXPERIMENTS

Experiment No.	pH	β -CD concentration (mM)
1	6.0	0
2	6.0	5
3	6.0	10
4	7.0	0
5	7.0	5
6	7.0	10
7	8.0	0
8	8.0	5
9	8.0	10

conditions at the various points of the rectangular plot are listed in Table II.

Once all the conditions for the nine experiments had been determined, the experiments were conducted. The resolutions, R , between adjacent peak pairs in each of the electropherograms were then calculated from the migration times obtained from the nine experiments using the equation

$$R = \frac{2(t_2 - t_1)}{W_1 + W_2} \quad (1)$$

where t_1 and t_2 are the migration times of two adjacent peak pairs and W_1 and W_2 are the widths of the peak pairs. These values were fitted into a polynomial equation:

$$R = a_0 + a_1x_1 + a_2x_2 + a_{12}x_1x_2 + a_{11}x_1^2 + a_{22}x_2^2 + a_{112}x_1^2x_2 + a_{122}x_1x_2^2 + a_{1122}x_1^2x_2^2 \quad (2)$$

where a_i are the polynomial coefficients and x_i are the proportions of each variable in percentage as defined in Fig. 2. A BASIC program was used to determine the coefficients of the polynomial. Once the coefficients had been determined, the resolution between peak pairs for conditions other than those in the nine experiments could be calculated using eqn. 2. As there are eight compounds, there would be seven pairs of adjacent peaks. The rectangular plots for the seven pairs of peaks were then generated. Fig. 3 shows a typical rectangular plot for one of the peak pairs, where the different symbols correspond to different ranges of resolution between peak pairs. By overlapping the seven rectangular plots, the final

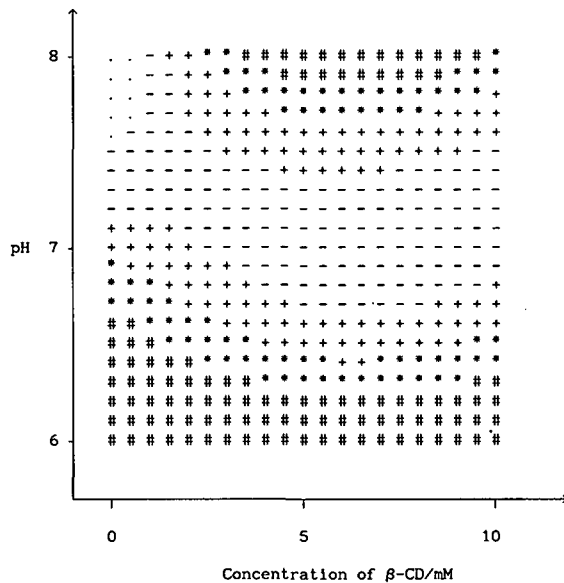


Fig. 3. Typical rectangular resolution plot of a pair of peaks. Notation: ·, $R < 0.5$; -, $0.5 \leq R < 1.0$; +, $1.0 \leq R < 1.5$; *, $1.5 \leq R < 2.0$; #, $R \geq 2.0$.

overlapped rectangular plot was obtained and is shown in Fig. 4. Fig. 5 is a three-dimensional representation of such a plot. The final overlapped resolution plot represents the minimum values of the

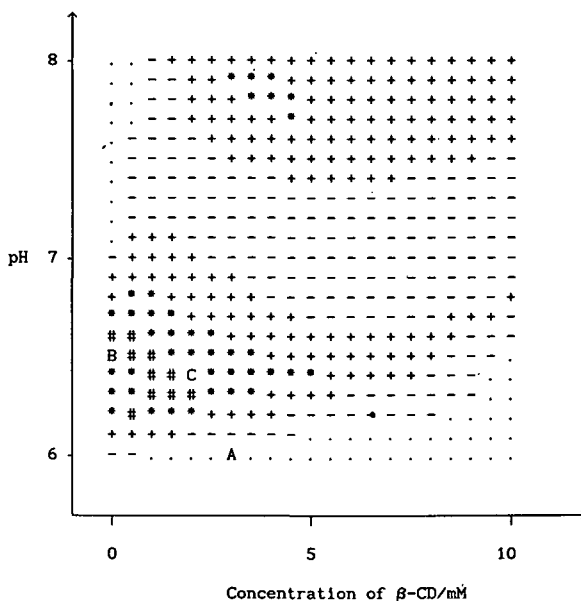


Fig. 4. Final overlapped resolution plot for all seven pairs of peaks. Notation as in Fig. 3.

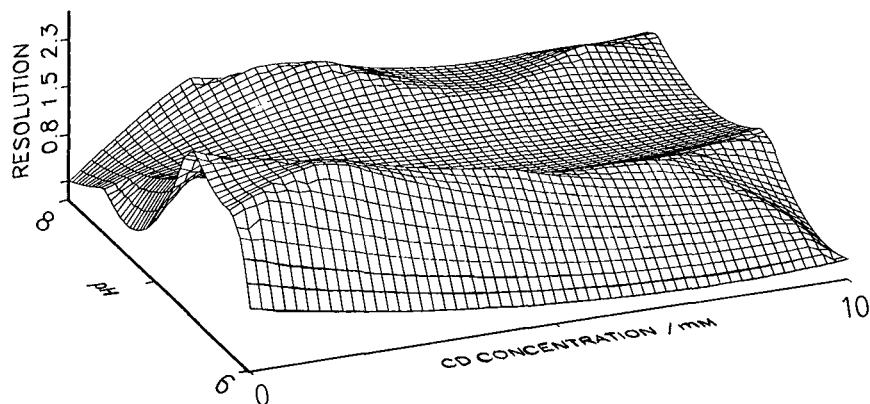


Fig. 5. Three-dimensional representation of the final overlapped resolution plot.

resolution between all peak pairs under the conditions bounded by the rectangular plot. The region marked with # indicates the highest resolution between all peak pairs and this is where the optimum conditions are expected to be found. It is noted in Figs. 4 and 5 that the overall optimum corresponds to pH 6.4 and 2 mM β -cyclodextrin ($R = 2.24$). Although satisfactory separation can also be obtained at pH 6.5 or 6.6 without β -cyclodextrin ($R = 2.03$ and 2.10, respectively), the use of β -cyclodextrin as a modifier served to stabilize the system and resulted in enhanced separation.

In order to evaluate the validity of the ORM scheme, experimental conditions corresponding to points A, B and C in Fig. 4 (the final overlapped resolution plot) were chosen from the regions re-

presented by the symbols \cdot and #, respectively. Poor resolution ($R < 0.5$) would be expected for the condition represented by point A whereas high resolution ($R \geq 2.0$) would be expected for conditions represented by points B and C. Point B represented the optimum conditions when no modifier is added. Point C represented the overall optimum conditions, *i.e.*, the conditions with the highest resolution within the range of experimental conditions. Typical electropherograms using these conditions (represented by points A, B and C) are shown in Figs. 6, 7 and 8, respectively. As can be seen from Fig. 6, the first two peaks (SG and SMZ) co-elute for experimental conditions corresponding to point A, which lies outside the optimum region. From Figs. 7 and 8, it can be observed that for experimental

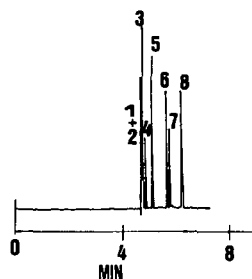


Fig. 6. Electropherogram for the eight sulphonamides with electrophoretic conditions corresponding to point A in Fig. 4: 0.05 M phosphate-0.05 M borate (pH 6.0) and 3 mM β -cyclodextrin; Separation tube, 50 cm \times 50 μ m I.D.; detection wavelength, 210 nm; voltage, 15 kV. Peaks: 1 and 2 = methanol, SG and SMZ; 3 = SMP; 4 = SM; 5 = SD; 6 = SQX; 7 = SS; 8 = SCP.

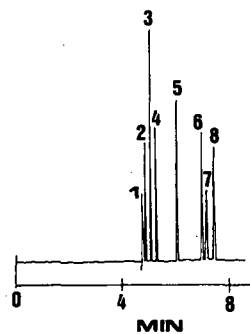


Fig. 7. Electropherogram for the eight sulphonamides with electrophoretic conditions corresponding to point B in Fig. 4: 0.05 M phosphate-0.05 M borate (pH 6.5); separation tube, 50 cm \times 50 μ m I.D.; detection wavelength, 210 nm; voltage, 15 kV. Peaks: 1 = methanol and SG; 2 = SMZ; 3 = SMP; 4 = SM; 5 = SD; 6 = SQX; 7 = SS; 8 = SCP.

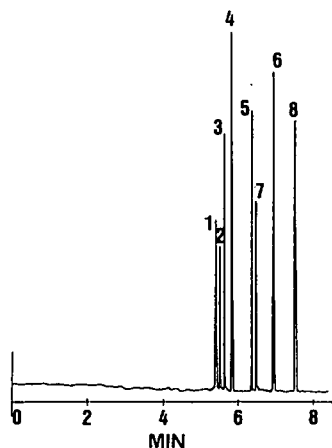


Fig. 8. Electropherogram for the eight sulphonamides with electrophoretic conditions corresponding to point C in Fig. 4: 0.05 M phosphate–0.05 M borate (pH 6.4) and 2 mM β -cyclodextrin; separation tube, 50 cm \times 50 μ m I.D.; detection wavelength, 210 nm; voltage, 15 kV. Peaks: 1 = methanol and SG; 2 = SMZ; 3 = SMP; 4 = SM; 5 = SD; 6 = SQX; 7 = SS; 8 = SCP.

conditions corresponding to points B and C selected from the optimum region, all the peaks are baseline separated and the values of the resolution between all the pairs of peaks are more than the preset value of 2. The total analysis time was less than 8 min, which is considerably less than the preset criterion of a maximum analysis time of 15 min.

The results clearly demonstrated the versatility of the ORM scheme for CE separations. The most important feature of the scheme is that it could be used to determine the overall optimum conditions for the separation, which involved optimization of both pH and β -cyclodextrin concentration. Further, it could be used to determine the optimum conditions for separation by varying pH alone (corresponding to pH 6.5 or 6.6 and 0 mM β -CD). From the results obtained, it is concluded that overall optimum conditions for CE separation can be obtained much more readily using the systematic optimization scheme than by trial-and-error approaches.

CONCLUSIONS

An ORM scheme was employed for the optimization of CE separation of eight sulphonamides. The scheme provided a systematic procedure which could be used to obtain the overall optima within the range of experimental conditions investigated. To confirm the validity of the optimization procedure, additional experiments were performed which demonstrated that satisfactory separation could be obtained using experimental conditions selected from the optimum region of the resolution plot. In view of the promising results obtained, it is believed that the scheme can be readily extended to obtain optimum experimental conditions for other CE separations.

ACKNOWLEDGEMENT

The authors thank the National University of Singapore for financial assistance.

REFERENCES

- 1 M. M. L. Aerts, W. M. J. Beek and U. A. Th. Brinkman, *J. Chromatogr.*, 435 (1988) 97.
- 2 R. F. Cross, *J. Chromatogr.*, 478 (1989) 422.
- 3 A. R. Long, C. R. Short and S. A. Barker, *J. Chromatogr.*, 502 (1990) 87.
- 4 H. Nishi, T. Fukuyama, M. Matsuo and S. Terabe, *J. Microcol. Sep.*, 1 (1989) 234.
- 5 A. Guttman, A. S. Cohen, D. N. Heiger and B. L. Karger, *Anal. Chem.*, 62 (1990) 137.
- 6 P. D. Grossman, K. J. Wilson, G. Petrie and H. H. Lauer, *Anal. Biochem.*, 173 (1988) 265.
- 7 J. Vindevogel and P. Sandra, *Anal. Chem.*, 63 (1991) 1530.
- 8 J. L. Glajch, J. J. Kirkland, K. M. Squire and J. M. Minor, *J. Chromatogr.*, 199 (1980) 57.
- 9 C. P. Ong, H. K. Lee and S. F. Y. Li, *J. Chromatogr.*, 464 (1989) 405.
- 10 S. Terabe, K. Otsuka and T. Ando, *Anal. Chem.*, 57 (1985) 834.
- 11 H. Nishi, T. Fukuyama and M. M. Matsuo, *J. Chromatogr.*, 515 (1990) 245.
- 12 M. M. Bushy and J. W. Jorgenson, *Anal. Chem.*, 61 (1989) 491.
- 13 K. Otsuka and S. Terabe, *J. Microcol. Sep.*, 1 (1989) 150.
- 14 S. Terabe, Y. Miyashita and O. Shibata, *J. Chromatogr.*, 516 (1990) 23.
- 15 C. P. Ong, C. L. Ng, H. K. Lee and S. F. Y. Li, *J. Chromatogr.*, 547 (1991) 419.

Short Communication

High-performance liquid chromatographic separation of *cis-trans* isomers of proline-containing peptides

I. Separation on cyclodextrin-bonded silica

S. Friebe and G. J. Krauss*

Martin-Luther University Halle, Department of Biochemistry/Biotechnology, Bioanalytical Division, Weinbergweg 16a, O-4050 Halle/S. (Germany)

H. Nitsche

Serva Feinbiochemica, Carl-Benz-Strasse, Heidelberg (Germany)

(Received November 28th, 1991)

ABSTRACT

β -Cyclodextrin-bonded silica is shown to be a suitable stationary phase for high-performance liquid chromatography of conformational isomers of proline-containing peptides. A variety of selective interactions may be used to separate *cis-trans* conformers by steric discrimination. The formation of an inclusion complex seems to be particularly effective if an aromatic amino acid N-terminal-bonded to proline is enclosed in the analyte. Unusually high resolution values for such separations under low-temperature conditions suggest a steric hindrance of isomer conversion owing to the formation of inclusion complexes.

INTRODUCTION

cis-trans Isomerism of the prolyl peptide bond seems to be of central importance for the folding and biological activity of various oligopeptides and small proteins [1]. Enzymes exhibiting peptidyl prolyl *cis-trans* isomerase (PPIase) activity efficiently catalyse the *cis-trans* isomerization of proline imidic peptide bonds [2,3]. In order to investigate the enzymatic catalysis of conformational changes applying pure conformers instead of mixtures of *cis-trans* short peptides with C-terminal proline or N-alkylamino acid can be utilized to study the

separation of conformers. Such oligopeptides show particularly high barriers of rotation of the peptide bond [4,5]. In the equilibrium the *trans* conformation is favoured in most peptides, but the *cis* conformers occur in detectable amounts. Quantitative data about this type of conformational interconversion could be obtained by different spectroscopic and kinetic methods [3,6–10].

Reversed-phase high-performance liquid chromatographic (HPLC) studies of di- and oligopeptides with C-terminal proline were published by Melander *et al.* [11] and others [12,13]. Chromatographic resolution of conformers by solvophobic interaction

with the reversed-phase was described as a possible method for separating pure peptide bond isomers, but the relaxation times of conformational changes have to be comparable to the time scale of the HPLC run used.

It was assumed that the elution behaviour of *cis* and *trans* isomers is determined by the larger solvophobic surface area of the *cis* isomer, interacting with hydrocarbons bonded to silica gel. In relation to aqueous solution, the isomer distribution and the relaxation times of the isomerization may be seriously affected by the chromatographic conditions. Therefore, experimental selection of the optimum eluent composition, pH, ionic strength, system temperature and flow-rate is necessary for the successful separation of conformational isomers.

In this paper, we present an HPLC method which allows the separation of *cis* and *trans* isomers of proline-containing di- and oligopeptides by steric discrimination on cyclodextrin-bonded silica.

EXPERIMENTAL

Materials

Optically pure dipeptides were purchased from Bachem Biochemica (Heidelberg, Germany). Biologically active oligopeptides were synthesized by K. Neubert and co-workers at the Department of Biochemistry/Biotechnology, Martin-Luther University Halle, Germany. Chiral β -cyclodextrin Si 100 (10 μ m) columns were obtained from Serva (Heidelberg, Germany). All other solvents and chemicals were of analytical-reagent grade.

Apparatus

HPLC measurements were performed with a Merck-Hitachi LiChroGraph system using an L-6200 low-gradient pump, an L-3000 photodiode-array detector and an HM computing integrator. The columns and the eluents were immersed in a Lauda RM 6 constant-temperature bath.

HPLC conditions

The columns, both 125 mm \times 4.6 mm I.D., were connected. Chromatographic experiments were performed isocratically using various 0.02 M ammonium dihydrogenphosphate-acetonitrile mixtures. The analyte absorptions were monitored at 210 nm. The flow-rate was 2 ml/min. Before elution, the

columns were equilibrated with the mobile phase at 5°C for 60 min. Peak splitting as a result of isomerization kinetics was demonstrated by peak collection and rechromatography of the fractions.

RESULTS AND DISCUSSION

Cyclodextrin (CD)-bonded silicas as stationary phases in HPLC were developed for separating enantiomers by forming diastereomers with chiral centres of cyclodextrins. In addition to chiral applications, CD-bonded phases have been used as packings for the separation of polynuclear aromatics, substituted aromatics, stilbenes and structural isomers [14], and also as stationary phases for the separation of selected groups of di- and tripeptides [15,16].

The introduction of CD-bonded silicas for separating conformational isomers offers the opportunity to exploit a variety of selective interactions between peptides and cyclodextrins, such as host-guest and hydrophobic interactions, hydrogen bonding and dipole-dipole interactions. Using phosphate buffer of low ionic strength and pH values that force peptides into their zwitterionic form, a number of conformers of di-, tri- and tetrapeptides were resolved. To separate both conformers of Ala-Pro, Ile-Pro, Leu-Pro, Phe-Pro, Phe-D-Pro, Ile-Pro-Ile, Val-Pro-Leu, Tyr-Pro-Phe and Pro-D-Phe-Pro-Gly by inclusion complexation and hydrophobic interaction for each individual peptide, the organic solvent content has to be adjusted.

Lowering the temperature below ambient decreases the interconversion rates and can improve the resolution of isomer peaks. As demonstrated in Fig. 1, peptides bearing aromatic amino acids N-terminal to proline (phenylalanine or tyrosine) show baseline separations between the two conformers with relative resolution (R_s) values up to 5. The unusually high R_s values and the absence of the typical plateau between the two isomer peaks, in contrast to reversed-phase chromatographic runs, suggest a steric hindrance of isomer conversion owing to the formation of inclusion complexes. In contrast to these results, peptides consisting of aliphatic amino acids N-terminal-bonded to proline show well resolved peaks without baseline resolution.

It seems that aromatic amino acids are essential

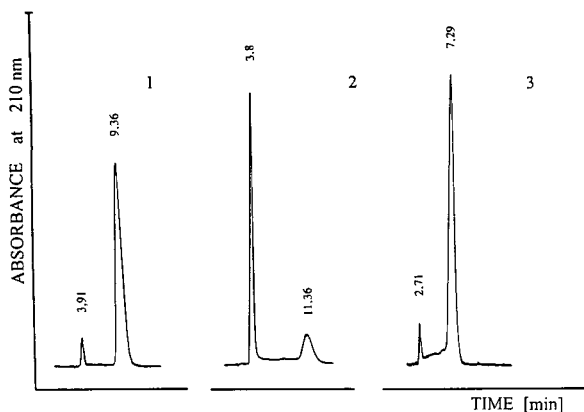


Fig. 1. Elution profiles of (1) Phe-Pro, (2) Tyr-Pro-Phe and (3) Pro-D-Phe-Pro-Gly on chiral β -cyclodextrin Si-100 at 5°C. For chromatographic conditions, see Experimental. Mobile phase: (1) 0.02 M ammonium dihydrogenphosphate (pH 6.2)-acetonitrile (90:10); (2) 0.02 M ammonium dihydrogenphosphate (pH 6.2)-acetonitrile (80:20); (3) 0.02 M ammonium dihydrogenphosphate (pH 6.2)-acetonitrile (70:30). Detector: 0.0128 a.u.f.s.

parts in the sequence to distinguish conformers by inclusion complexation. These results are in accordance with those of other workers [15,17,18], which suggested that the formation of an inclusion complex for exploiting the chiral recognition principle and a separation system for geometric isomers is particularly effective if an aromatic ring system is enclosed in the analyte.

In contrast to reversed-phase techniques, the elution pattern of conformer separations on CD-bonded silica may be affected by additional different interactions. Starting from the hypothesis that *cis* or *trans* isomers are selectively included in the CD cavity by steric discrimination, some of the observed phenomena, e.g., elution order of *cis* and *trans* isomers and the *cis-trans* ratio of conformers, could be explained. Enzymatic and NMR spectroscopic studies of fractionated single isomers are in progress to establish the elution order.

In order to demonstrate that peak splitting was a result of dynamic equilibrium during the chromatographic run, fractions of effluents were collected. Using rechromatography in each instance the original chromatogram was obtained after relaxation of the conformer distribution, as demonstrated for Phe-Pro in Fig. 2. Refrigeration of the fractionated

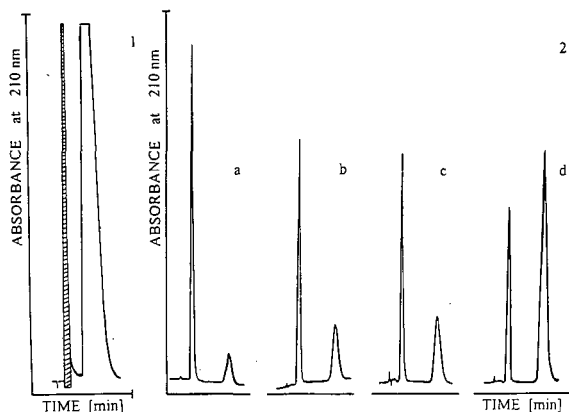


Fig. 2. Semi-preparative low-temperature fractionation of Phe-Pro on chiral β -cyclodextrin Si-100 (see Experimental). (1) Isolation of the minor isomer (shaded peak); injection 0.5 mg per 100 μ l. (2) Rechromatography of the first-eluting peak from (1), corresponding to the minor isomer; rechromatography of this fraction as a function of incubation time and temperature. (a) 15 min, -10°C; (b) 45 min, -10°C; (c) 60 min, -10°C; (d) 90 min, 25°C. Detector: (1) 1.0 a.u.f.s.; (2) 0.01 a.u.f.s.

conformers offers the opportunity to delay conformer relaxation for a substantial period and allows the acquisition of nearly pure *cis* and *trans* isomers for further studies, e.g., structural and enzymatic investigations.

In conclusion, low-temperature HPLC on CD-based silicas has been found to be applicable to the determination of conformational changes in proline-containing peptides and for the fractionation of *cis* and *trans* conformers as valuable substrates for advanced studies. Cyclodextrin additives should provide versatile chromatographic systems for the investigation of conformational changes in prolyl peptides. These applications are under investigation.

ACKNOWLEDGEMENTS

The authors thank Dr. K. Neubert and his co-workers for synthesizing some of the peptides and Dr. G. Fischer for helpful discussions.

REFERENCES

- 1 J. F. Brandts, H. R. Halvorson and M. Brennan, *Biochemistry*, 14 (1975) 4953-4963.
- 2 K. Lang, F. X. Schmid and G. Fischer, *Nature (London)*, 329 (1987) 268-270.

- 3 G. Fischer, H. Bang and C. Mech, *Biomed. Biochem. Acta*, 43 (1984) 1104–1111.
- 4 C. Grathwohl and K. Wütherich, *Biopolymers*, 20 (1981) 2632–2633.
- 5 W. E. Stuart and T. H. Siddall, *Chem. Rev.*, 70 (1970) 517.
- 6 D. Hübner, G. Fischer, D. Ströhl, E. Kleinpeter, B. Hartrodt and W. Brandt, *Fresenius' J. Anal. Chem.*, 337 (1990) 131–132.
- 7 D. Hübner, T. Drakenberg, St. Forsen and G. Fischer, *FEBS Lett.*, 284 (1991) 79–81.
- 8 D. Hübner, B. Hartrodt, E. Kleinpeter, D. Ströhl, W. Brandt, H. Schinke, M. Wahab and G. Fischer, *Biochem. Biophys. Res. Commun.*, 177 (1991) 271–278.
- 9 V. L. Hsu, R. E. Handschumacher and I. M. Armitage, *J. Am. Chem. Soc.*, 112 (1990) 7456–6747.
- 10 J. T. Gerig, *Biopolymers*, 10 (1971) 2435–2443.
- 11 W. R. Melander, J. Jacobsen and Cs. Horváth, *J. Chromatogr.*, 234 (1982) 269–276.
- 12 L. Rusconi, G. Perseo, L. Franzoi and P. C. Montecucci, *J. Chromatogr.*, 349 (1985) 117–130.
- 13 J. C. Gesquiere, E. Diesis, M. T. Cung and A. Tartar, *J. Chromatogr.*, 478 (1989) 121–129.
- 14 T. M. Ward and D. W. Armstrong, in M. Zief and L. Y. Crane (Editors), *Chromatographic Chiral Separation (Chromatographic Science Series, Vol. 40)*, Marcel Dekker, New York, 1988, pp. 131–163.
- 15 H. J. Issaq, *J. Liq. Chromatogr.*, 9 (1986) 229–233.
- 16 C. A. Chang, H. Ji and G. Lin, *J. Chromatogr.*, 522 (1990) 143–152.
- 17 D. W. Armstrong, T. J. Ward, R. D. Armstrong and T. E. Beesley, *Science (Washington, D.C.)*, 232 (1982) 1132.
- 18 R. R. West and H. Cardelline, *J. Chromatogr.*, 539 (1991) 15–23.

Short Communication

Identification and determination of honokiol and magnolol from *Magnolia officinalis* by high-performance liquid chromatography with photodiode-array UV detection

Tung-Hu Tsai

National Research Institute of Chinese Medicine, Taipei Hsien (Taiwan)

Chieh-Fu Chen*

National Research Institute of Chinese Medicine, Taipei Hsien, and *Department and Institute of Pharmacology, National Yang-Ming Medical College, Taipei (Taiwan)

(First received October 31st, 1991; revised manuscript received January 17th, 1992)

ABSTRACT

An improved high-performance liquid chromatographic technique with photodiode-array detection was developed for the identification and determination of the active principles of *Magnolia officinalis* extracts such as honokiol and magnolol. A reversed-phase column (Nucleosil 7C₁₈) was eluted with a isocratic system of acetonitrile-0.1% phosphoric acid (65:35). It was found that 19.13 ± 0.62 mg of honokiol and 75.24 ± 3.48 mg of magnolol were contained in the methanol extracts of 1 g of *Magnolia officinalis*.

INTRODUCTION

The root and stem bark of *Magnolia officinalis* (Chinese name: houpo) has been used as a folk medicine in China for the treatment of thrombotic stroke, typhoid fever and headache [1]. Two isomers of neolignans, honokiol and magnolol, have been isolated from the bark of this plant and other *Magnoliaceae* [1]. These two compounds possess antimicrobial activities against Gram-positive and acid-fast bacteria and fungi [2] and central depressant effects [3]. Recent studies indicated that magnolol inhibits intracellular calcium mobilization in platelets caused by collagen, even in the presence of

indomethacin [4], and relaxes vascular smooth muscle by releasing endothelium-derived relaxing factor and by inhibiting calcium influx through voltage-gated calcium channels [5].

The determination of honokiol and magnolol by

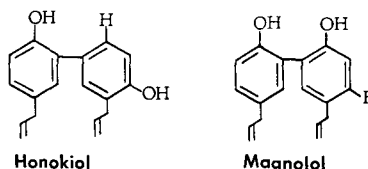


Fig. 1. Structures of honokiol and magnolol.

high-performance liquid chromatography (HPLC) [6] and of magnolol and its metabolites by liquid chromatography–mass spectrometry [7–9] have been described. However, none of the methods permits the ultraviolet spectral identification of honokiol and magnolol from *Magnolia officinalis*. In this work, we developed a simple method displaying three-dimensional patterns for the identification and to check the purity of honokiol and magnolol.

EXPERIMENTAL

Materials and reagents

Magnolia officinalis was purchased from a traditional Chinese herbal drug store in Taipei. Authentic compounds, honokiol and magnolol (Fig. 1), were obtained from Nacalai Tesque (Kyoto, Japan) and acetonitrile, methanol, *n*-hexane, ethanol (99.5%) and phosphoric acid (70%) from E. Merck (Darmstadt, Germany).

Apparatus

The HPLC system consisted of a Rheodyne (Cotati, CA, USA) Model 7125 injector, a Waters (Mil-

ford, MA, USA) Model 990 photodiode-array detector, which permits the scanning of chromatographic and spectral data, and two Waters Model 510 chromatographic pumps. Separation was achieved on a reversed-phase Nucleosil 7C₁₈ (particle size 7 μm) column (250 \times 4 mm I.D.) (Macherey–Nagel, Düren, Germany) fitted with a column inlet filter (3 mm \times 0.5 μm) (Rheodyne) at room temperature. The mobile phase was acetonitrile–water–phosphoric acid (65:35:0.1, v/v/v) of pH 2.4–2.7 at a flow-rate of 1.0 ml/min. The detection wavelengths were 209 nm for honokiol and 218 nm for magnolol.

Extraction

Magnolia officinalis powder (0.5 g) was boiled with 50 ml of extraction solvent [water, methanol, ethanol (99.5%), ethanol (50%), *n*-hexane, 0.1 M HCl or 0.1 M NaOH] for 15 min. This procedure was repeated twice. The two filtrates were combined and diluted to 100 ml in a volumetric flask.

Authentic samples

The compounds separated by the proposed

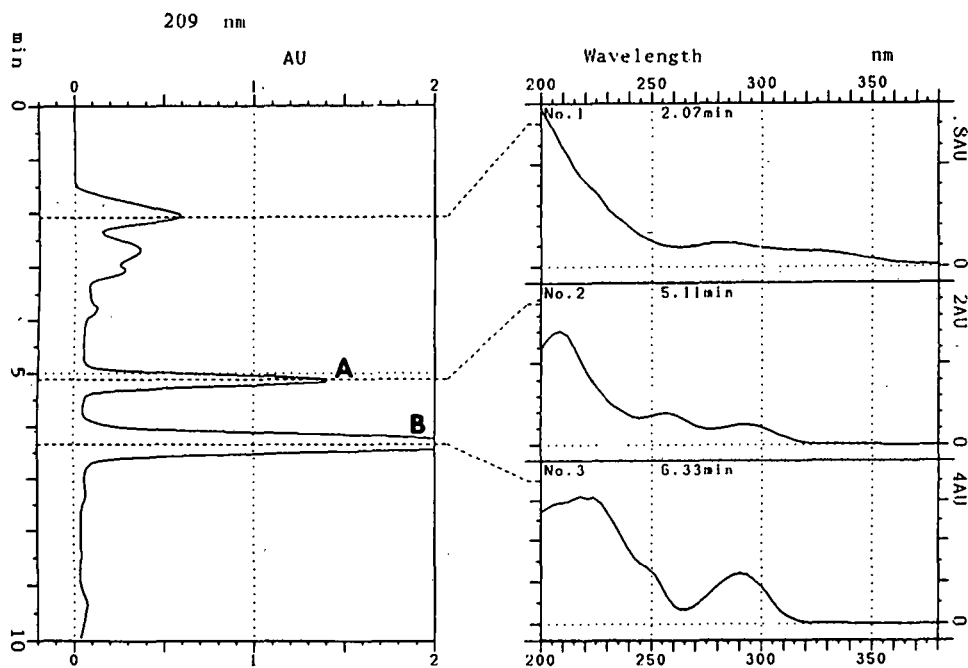


Fig. 2. Chromatogram and UV spectra of ethanol (99.5%) extract of *Magnolia officinalis*. A = honokiol (3.89 μg); B = magnolol (16.18 μg).

HPLC method were identified by comparison of their retention times and spectra with those of authentic samples of honokiol and magnolol.

Determination of honokiol and magnolol

Calibration graphs for honokiol and magnolol dissolved in methanol were constructed by HPLC of various known amounts of these compounds (0.25, 0.5, 1 and 2 μg). The contents of honokiol and magnolol in the crude extract of *Magnolia officinalis* were determined from the regression equations for the lines constructed for the two compounds.

RESULTS AND DISCUSSION

Under the above conditions, the retention times for honokiol and magnolol were 5.11 and 6.33 min, respectively. Fig. 2 shows the chromatogram and UV spectra of an ethanol (99.5%) extract of *Magnolia officinalis*. The peaks corresponding to honokiol and magnolol were confirmed by the retention

times and the UV spectra obtained with photodiode-array detection. Fig. 3 illustrates a three-dimensional chromatogram where both honokiol and magnolol are present. This plot was very useful in the identification of each compound because it allowed the observation of the full UV absorption spectrum of each peak as it eluted from the chromatographic column [10]. Hence the detection of other compounds was easily noted, and co-eluting components could be observed.

The content of each compound in the crude herbal extract was determined from the linear regression equation of the calibration graph for each compound. The equations for honokiol and magnolol were $y = 0.0862x + 0.0028$ ($r = 0.999$) and $y = 0.0655x + 0.0057$ ($r = 0.999$), respectively, where x is amount of compound and y is peak-area response. The linearity range was between 5 ng and 2 μg . The detection limits for honokiol and magnolol, at a signal-to-noise ratio of 4, were 2 and 1 ng, respectively.

Table I gives the contents of honokiol and mag-

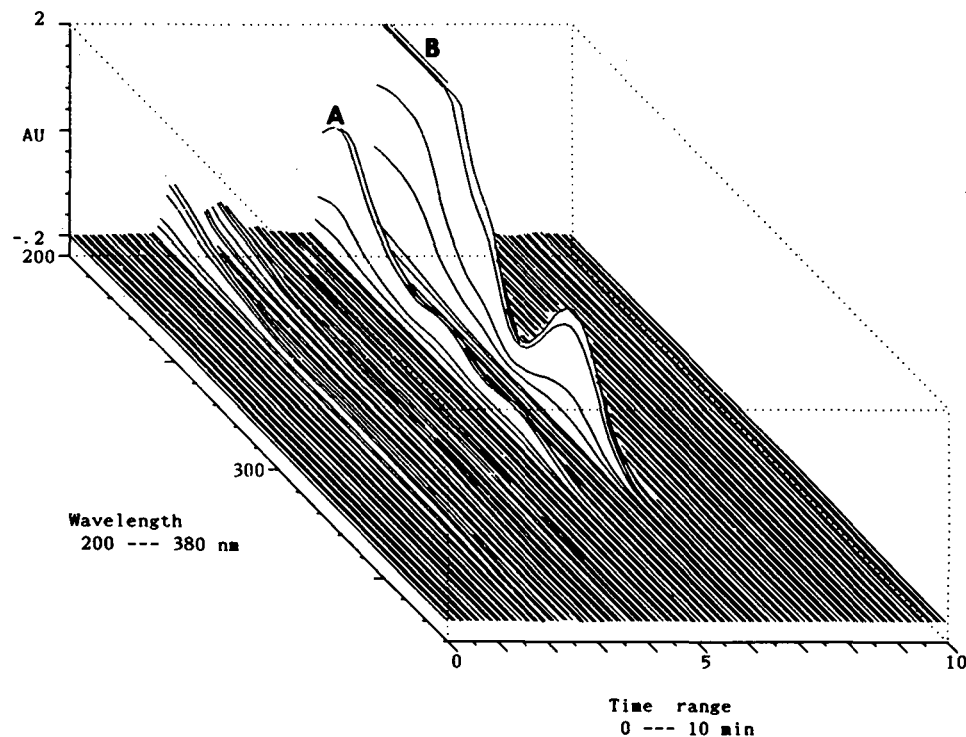


Fig. 3. Three-dimensional chromatogram of ethanol (99.5%) extract of *Magnolia officinalis*. x-Axis is retention time, y-axis absorbance and z-axis UV wavelength. A = honokiol; B = magnolol.

TABLE I

CONTENTS OF HONOKIOL AND MAGNOLOL IN DIFFERENT EXTRACTS OF 1 g OF *MAGNOLIA OFFICINALIS*

Results are means \pm S.D. ($n=4$).

Extraction solvent	Honokiol (mg/g)	Magnolol (mg/g)
Water	0.59 \pm 0.09	2.29 \pm 0.89
Methanol	19.13 \pm 0.62	75.24 \pm 3.48
Ethanol (99.5%)	18.88 \pm 0.98	83.62 \pm 5.23
Ethanol (50%)	17.27 \pm 0.21	77.67 \pm 0.69
<i>n</i> -Hexane	22.11 \pm 1.84	89.87 \pm 3.27
0.1 M HCl	0.57 \pm 0.12	1.70 \pm 0.73
0.1 M NaOH	18.29 \pm 0.27	84.01 \pm 1.73

nolol in extracts of *Magnolia officinalis* obtained with different solvents. It appears that *n*-hexane is the best and 0.1 M HCl the worst solvent for the extraction of honokiol and magnolol.

In conclusion, the proposed technique should be useful for the quality control of *Magnolia officinalis*,

for stability testing and for pharmacokinetic studies of honokiol and magnolol.

REFERENCES

- 1 Juangsu New Medical College, *Zhong Yao Da Ci Dian (Dictionary of Chinese Materia Medica)*, Shanghai Scientific and Technological Publishers, Shanghai, 1985.
- 2 A. M. Clark, F. S. El-Feraly and W. S. Li, *J. Pharm. Sci.*, 70 (1981) 951.
- 3 K. Watanabe, H. Watanabe, Y. Goto, N. Yamamoto and M. Yoshizaki, *Jpn. J. Pharmacol.*, 25 (1975) 605.
- 4 C. M. Teng, C. C. Chen, F. N. Ko, L. G. Lee, T. F. Huang, Y. P. Chen and H. Y. Hsu, *Thromb. Res.*, 50 (1988) 751.
- 5 C. M. Teng, S. M. Yu, C. C. Chen, Y. L. Huang and T. F. Huang, *Life Sci.*, 47 (1990) 1153.
- 6 W. Z. Song, J. F. Cui and G. D. Zhang, *Yao Hsueh Hsueh Pao*, 24 (1989) 295.
- 7 M. Hattori, T. Sakamoto, Y. Endo, K. Kobasho, T. Mizuno and T. Namba, *Chem. Pharm. Bull.*, 32 (1984) 5010.
- 8 M. Hattori, Y. Endo, S. Takebe, K. Kobashi, N. Fudasaku, *Chem. Pharm. Bull.*, 34 (1986) 158.
- 9 Y. H. Ma, J. N. Ye, N. Fukasaku, M. Hattori and T. Namba, *Shoyakugaku Zasshi*, 42 (1988) 130.
- 10 T. Takeuchi and D. Ishii, *J. Chromatogr.*, 288 (1984) 451.

Short Communication

Studies on stress metabolites

XVI[☆]. High-performance liquid chromatographic analysis of cruciferous phytoalexins using complex ternary mobile phase gradients

Kenji Monde* and Mitsuo Takasugi

Department of Chemistry, Faculty of Science, Hokkaido University, Sapporo 060 (Japan)

(First received September 4th, 1991; revised manuscript received January 29th, 1992)

ABSTRACT

A reversed-phase high-performance liquid chromatographic analysis of cruciferous phytoalexins, antimicrobial compounds synthesized *de novo* by plants after exposure to microorganisms, was performed using an acetonitrile–methanol–water complex solvent gradient system. A well resolved chromatogram of thirteen phytoalexins and three related indole metabolites isolated from cruciferous plants was obtained by this method. Accumulation of phytoalexins in *Pseudomonas cichorii*-inoculated turnip tissue was followed by this high-performance liquid chromatographic analysis.

INTRODUCTION

Phytoalexins are low-molecular-weight antimicrobial compounds that are synthesized *de novo* by plants in response to infection by microorganisms [for recent reviews see refs. 1–3]. Accumulation of phytoalexins is considered to be one of the important disease resistance mechanisms. We have recently isolated and characterized several phytoalexins (1–12) (Fig. 1) from cruciferous plants, Japanese radish (*Raphanus sativus*) [4], Chinese cabbage (*Brassica campestris* ssp. *pekinensis*) [5–7], cabbage

(*B. oleracea*) [8–10] and turnip (*B. campestris* L. ssp. *rapa*) [11].

These phytoalexins are structurally unique indole or indole-related compounds possessing one or two sulphur atoms. Devys and co-workers [12,13] have described the accumulation of additional phytoalexins, brassilexin (13) and cyclobrassinin sulphoxide, in Indian mustard (*B. juncea*) treated with abiotic elicitors. Also, Dahiya and Rimmer [14] have reported the isolation of methoxybrassinin (2) and cyclobrassinin (4) from oilseed rape (*B. napus*) inoculated with *Leptosphaeria maculans*. Phytoalexin accumulation was related to resistance to *L. maculans*, a fungus which causes the blackleg disease of crucifers [15,16].

Cruciferous plants contain a group of structur-

* For part XV, see ref. 10.

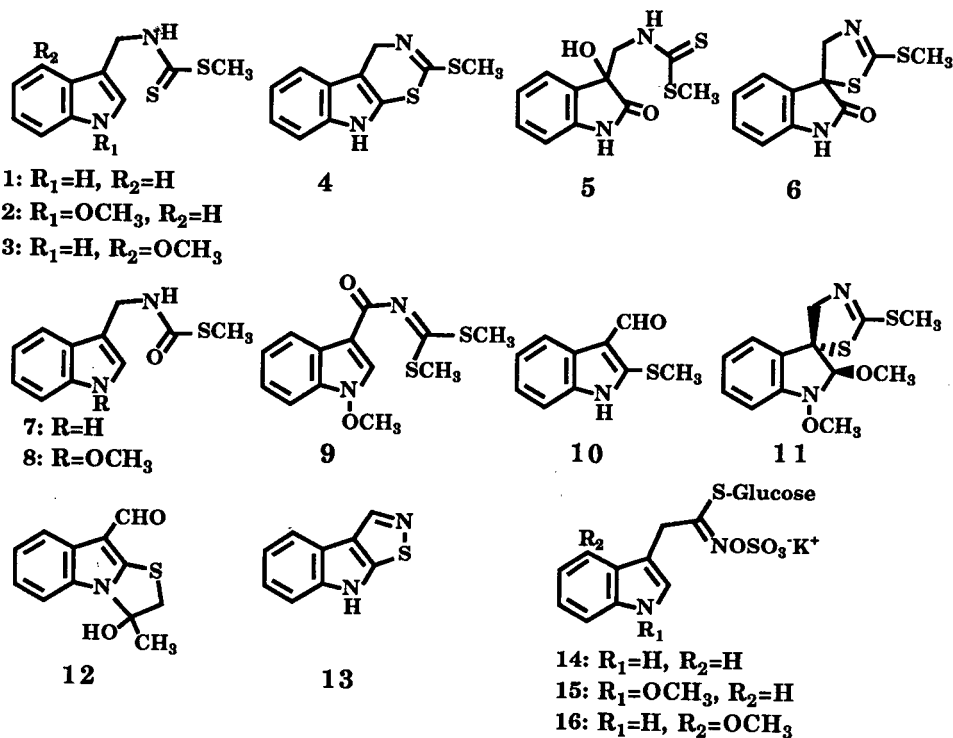


Fig. 1. Chemical structures of cruciferous phytoalexins and indole glucosinolates. **1** = Brassinin; **2** = methoxybrassinin; **3** = 4-methoxybrassinin; **4** = cyclobrassinin; **5** = dioxibrassinin; **6** = spirobrassinin; **7** = brassitin; **8** = methoxybrassinin; **9** = methoxybrassinin B; **10** = brassicanal A; **12** = brassicanal B; **13** = brassilexin; **14** = glucobrassicin; **15** = neoglucobrassicin; **16** = 4-methoxyglucobrassicin. Compound **11** was isolated from both Chinese cabbage and cabbage, but its structure has not been published. The absolute configurations of **6** and **11** have not been determined as yet. The spectroscopic data will be published elsewhere.

ally related secondary metabolites, the glucosinolates (**14–16**) [17]. The breakdown of such compounds, brought about by the action of another enzyme, thioglucoside glucohydrolase, yields a variety of products possessing a variety of biological effects, especially indole glucosinolates [18,19]. Recently, interest in the biosynthetic relationship between these indole or indole-related phytoalexins and indole glucosinolates has increased.

In order to study the biosynthesis of the cruciferous phytoalexins, it is important to develop an efficient method of analysing all phytoalexins and related metabolites. In this paper, we describe a practical high-performance liquid chromatographic (HPLC) analysis of these thirteen cruciferous phytoalexins and three related indole metabolites in a single run. We believe that this method is very useful and powerful for research on the biosynthesis of cruciferous phytoalexins and the analysis of phytoalexins of other crucifers.

EXPERIMENTAL

Apparatus

The HPLC analyses were performed on a Japan Spectroscopic (Tokyo, Japan) liquid chromatographic system equipped with a Model 801-SC system controller, a Model 851-AS automatic sampler, a Model 880-50 line degasser, a Model 880-02 low-pressure gradient unit, a Model 865-CO column oven, a Model 880-PU pump and a Model UVI-DEC-100-V UV detector. A Chromatopac C-R6A integrator was used for measuring peak areas (Shimadzu, Tokyo, Japan).

HPLC analytical conditions

The analytical column was μ Bondapak C_{18} (10 μ m, irregular) (300 mm \times 3.9 mm I.D.) (Waters Assoc., Milford, MA, USA). Water, methanol and acetonitrile used as the mobile phase were HPLC grade (Wako Chemicals, Tokyo, Japan, and Kanto

Chemicals, Tokyo, Japan). These solvents were kept at 35°C in a water bath. The HPLC column was eluted with water (A)–methanol (B)–acetonitrile (C) under a ternary gradient mode [20–22] at a flow-rate of 2 ml/min at 35°C in a column oven. The column was eluted for 4 min with 75% A + 10% B + 15% C, followed by successive linear gradients: to 60% A + 10% B + 30% C over 10 min; to 50% A + 50% B + 0% C over 3 min; to 100% B over 15 min. The eluent was held at 100% B for 5 min and then brought back to 75% A + 10% B + 15% C over 5 min, and allowed to equilibrate for 5 min (Fig. 2). The UV detector was operated at 254 nm.

Phytoalexin standards

An authentic standard mixture was prepared from thirteen phytoalexins (Fig. 1, 1–13) and three related indole compounds [3-indolecarboxaldehyde (17), 3-indolylacetonitrile (18) and 1-methoxy-3-indolecarboxaldehyde (19)]. These were isolated from *Pseudomonas cichorii*-inoculated Japanese radish [4], Chinese cabbage [5–7] and cabbage [8–10] as previously described, except for brassilexin (13) [12]. Authentic brassilexin (13) was supplied by Dr. Barbier (Institut de Chimie des Substances Naturelles, CNRS, Gif-sur-Yvette, France). The authentic standard mixture contained 0.1 µg of each component in 5 µl of methanol. Cyclobrassinin sulphoxide was not determined in this analysis. The internal standard wighteone (20) was isolated from *Ficus carica* inoculated with *Fusarium solani* [23].

Quantitative analysis of phytoalexins

Under the analysis conditions, the retention times (in minutes) of the phytoalexins were as follows: 3-indolecarboxaldehyde (17), 6.6 ± 0.2; dioxybrassinin (5), 9.6 ± 0.2; 3-indolylacetonitrile (18), 11.4 ± 0.3; brassicanal B (12), 12.0 ± 0.2; brassitin (7) and brassicanal A (10), 12.6 ± 0.2; 1-methoxy-3-indolecarboxaldehyde (19) and brassilexin (13), 13.3 ± 0.2; spirobrassinin (6), 15.5 ± 0.2; me-

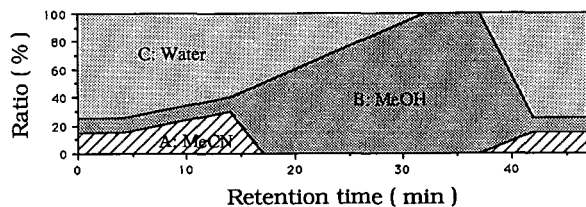


Fig. 2. Solvent composition in the gradient system.

thoxybrassinin (8), 18.7 ± 0.3; brassinin (1), 19.9 ± 0.3; 4-methoxybrassinin (3), 21.3 ± 0.3; methoxybrassinin (2), 24.4 ± 0.2; cyclobrassinin (4), 24.9 ± 0.2; methoxybrassinin B (9), 25.3 ± 0.1; and compound 11, 26.7 ± 0.2 min. Each value is the mean ± S.D.

A known quantity (0.50 µg) of wighteone (20) was chromatographed as an internal standard. The area of each peak in comparison with that of the standard was used for quantitative purposes. In the case of brassinin (1), the calculated equation for the regression curve at 254 nm was $y = -0.002 + 0.229x$ where y = weight in µg and x = ratio of peak area between brassinin (1) and wighteone (20) with $r = 0.997$. The regression line was linear from 0.05 to 2.5 µg. The other areas were calculated from their absorption coefficients recorded with a Japan Spectroscopic Ubest-30 spectrophotometer. The UV detector permitted detection of 10 ng of the substances. Statistical analyses were obtained through Delta Graph 1.5 software, loaded onto an Apple Macintosh SE computer (Apple Computer, Cupertino, CA, USA).

Material

Turnip plants (*B. campestris* L. ssp. *rapa* cv. Tokyo Cross) were cut into 3-mm-thick discs (ca. 5 cm in diameter). After an ageing period of 24 h, the discs were divided into two series: control tissues and tissues inoculated with *P. cichorii*. The control discs were incubated at 25 °C for the indicated periods. Two discs were taken out each time and freeze dried. The other series of discs were inoculated with *P. cichorii* (ca. 10⁸ cells/ml). The inoculated discs and controls were kept under similar conditions and processed similarly. Freeze-dried disc tissue was suspended in acetone and homogenized using a Polytron homogenizer (5 min); after being set aside for 5 min the mixture was filtered under vacuum. The filtrate was evaporated to dryness under reduced pressure and taken up in methanol (2 × 2 ml). The methanol solution was passed through Adsorbex SI (100 mg) and Adsorbex RP-18 (100 mg) cartridges connected in a series, to remove highly polar/non-polar substances, and the cartridges were washed with 5 ml of methanol. The combined methanol eluate and washings were evaporated under vacuum and the residue redissolved in a proportional amount of methanol [11].

RESULTS AND DISCUSSION

An authentic standard mixture was prepared from the thirteen phytoalexins and three related indole metabolites and their resolution was investigated using HPLC under several analytical conditions. At first, two simple gradient systems, acetonitrile–water and methanol–water, were tried. However, a well resolved chromatogram could not be obtained. In the case of the acetonitrile–water gradient system, peaks of polar compounds were well resolved, but those of non-polar compounds were not. On the other hand, in the case of the methanol–water gradient system, the opposite result was obtained. So an acetonitrile–methanol–water combination [20–22] was adopted, and gradient conditions were examined. Several kinds of columns were also tried, e.g. RCM8 × 10 with cartridge columns of 10- μ m Radial-PAK 5PAH (C₁₈), 10- μ m 8MBPH (alkylphenyl type), 10- μ m 8CN and μ Bondapak C₁₈ (Waters). When the 10- μ m 5PAH cartridge column was used, eight compounds were eluted within 10 min without separation, and all peaks were broadened considerably. In the case of 10- μ m 8BPH, most peaks were symmetrical, but only eleven peaks were observed. Sharp peaks could be obtained with 10- μ m 8CN columns, but all phytoalexins were eluted within 17 min without complete separation because of weak affinity between the CN group and the indole phytoalexins. Finally, the best resolution was found with the μ Bondapak C₁₈ column using the complex solvent system as illustrated in Fig. 2. In this ternary mobile phase gradients, all the peaks of the phytoalexins and the related indole metabolites were well resolved except those of brassitin (7), brassicanal A (10), brassilexin (13) and 1-methoxy-3-indolecarboxaldehyde (19) (Fig. 3E, standard sample). When the UV detector was operated at wavelengths \geq 300 nm, only brassicanal A (10) and 1-methoxy-3-indolecarboxaldehyde (19) could be detected since brassilexin (13) and brassitin (7) show weak UV absorption in this range. On the other hand, brassicanal A (10) and 1-methoxy-3-indolecarboxaldehyde (19) exhibit strong UV absorption in this range. For instance, brassicanal A (10) exhibits its absorption maximum at 311 nm (ϵ = 9740) [7], and 1-methoxy-3-indolecarboxaldehyde (19) at 300 nm (ϵ = 10 400) [24].

Using this method all cruciferous phytoalexins

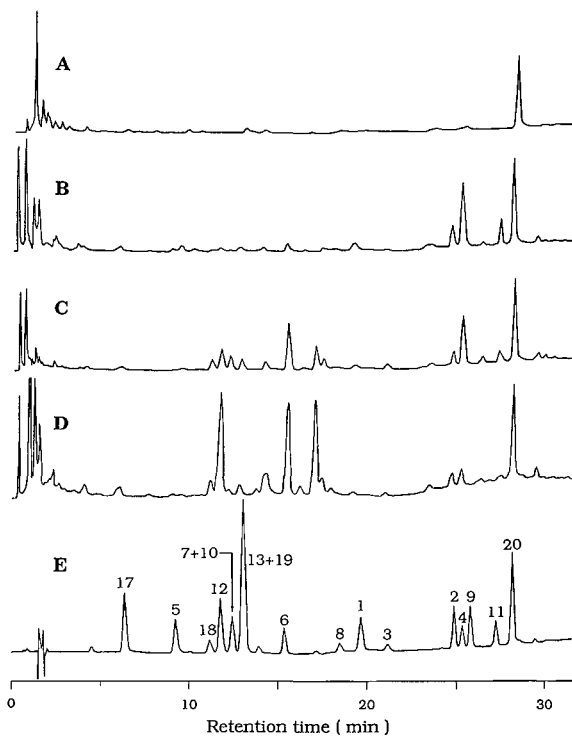


Fig. 3. HPLC of the crude extracts of turnip tissues and standard sample. Column, μ Bondapak C₁₈, 10 μ m 300 × 3.9 mm I.D.; solvent system, acetonitrile–methanol–water; flow-rate, 2 ml/min; UV detection at 254 nm. (A) Control tissue after 3 days. (B) *P. cichorii*-inoculated tissue after 12 h. (C) Inoculated tissue after 2 days. (D) Inoculated tissue after 4 days. (E) Standard sample. Peaks: 1–13, see Fig. 1; 17 = 3-indolecarboxaldehyde; 18 = 3-indolylacetone; 19 = 1-methoxy-3-indolecarboxaldehyde.

and related indole metabolites can be analysed in a single run within a reasonable time (50 min per run). Many samples can be analysed automatically, even at night, in combination with an automatic sampler. Reproducible chromatograms were obtained by maintaining the temperature of both the column oven and the solvent reservoirs at 35°C. Fig. 3 illustrates the HPLC chromatograms of the crude extracts obtained from control and *P. cichorii*-inoculated turnip tissues and Table I shows their phytoalexin contents. Accumulation of brassinin (1), methoxybrassinin (2) and cyclobrassinin (4) was clearly observed after 12 h of inoculation. Spirobrassinin (6) became the major phytoalexin at day 4, with a decline in brassinin (1) and cyclobrassinin (4). This result agrees with our biosynthetic studies: spirobrassinin (6) is biosynthesized from

TABLE I

PHYTOALEXIN CONTENTS OF *P. CICHORII*-INOCULATED TURNIP ROOT TISSUE

N.D. = Not detected. Each value represents the mean \pm S.D. Experiments were repeated three times with three samples per experiment.

Time	Phytoalexin production (μg per g dried weight)			
	Spirobrassinin	Brassinin	Methoxybrassinin	Cyclobrassinin
Control (3 days)	N.D.	N.D.	N.D.	N.D.
12 h	10.1 \pm 1.7	8.8 \pm 1.0	20.0 \pm 0.9	112.6 \pm 8.9
2 days	61.9 \pm 5.0	3.7 \pm 0.4	10.9 \pm 0.2	82.2 \pm 3.5
8 days	130.2 \pm 3.9	3.9 \pm 0.4	14.0 \pm 0.8	30.4 \pm 2.0

brassinin (**1**) [25]. A detailed discussion of the time course studies of the phytoalexins is provided elsewhere [11].

Prior to this report, two groups have described procedures for the determination of cruciferous phytoalexins. Dahiya and Rimmer [26] have reported the HPLC analysis of methoxybrassinin (**2**) and cyclobrassinin (**4**) from elicited *B. napus* and *B. juncea* tissues and Kollmann *et al.* [27] have also demonstrated efficient clean-up of coloured plant extract with reversed-phase cartridges and reported the HPLC analysis of three phytoalexins. Recently, Rouxel *et al.* [28] reported the HPLC analysis of five indole phytoalexins [brassinin (**1**), methoxybrassinin (**2**), brassilexin (**13**), cyclobrassinin (**4**) and cyclobrassinin sulphoxide] using Kollmann's binary gradient system, and discussed the relationship between these indole phytoalexins and resistance to *L. maculans* within Brassicaceae. However, as they indicated in their paper, it seems difficult to be to determine polar phytoalexins such as brassilexin (**13**) using a simple gradient, since the slope of the methanol gradient is too steep. Furthermore, they did not analyse spirobrassinin (**6**), which is a major phytoalexin in Japanese radish (*R. sativus*) and turnip root (*B. campestris*), as illustrated in Fig. 3.

Recently, we have confirmed that spirobrassinin (**6**) and cyclobrassinin (**4**) are biosynthesized from brassinin (**1**) by incorporation studies of labelled compounds [25]. Devys and Barbier [29] suggested that brassilexin (**13**) is also biosynthesized from brassinin (**1**) via cyclobrassinin (**4**) and cyclobrassinin sulphoxide. In order to determine these biosynthetic pathways, spirobrassinin (**6**) and other polar and less polar phytoalexins must be analysed together with non-polar ones. Using our gradient sys-

tem, thirteen phytoalexins from polar to non-polar and three related metabolites can be analysed in a single run.

Because Japanese radish and turnip roots were used as material, the analyses were not complicated by pigments, waxes, sterols and other interfering compounds, as illustrated in Fig. 3A (control tissue after 3 days). However, other coloured cruciferous plant materials could be also analysed by our method in combination with Kollmann's protocol. The combined method may be a standard analytical procedure of cruciferous phytoalexins.

ACKNOWLEDGEMENTS

This work was supported in part by a Grant-in-Aid (to M.T., No. 63470019) from the Ministry of Education, Science and Culture, Japan. The authors thank Dr. Barbier (Institut de Chimie des Substances Naturelles, CNRS, Gif-sur-Yvette, France) for supplying a sample of brassilexin.

REFERENCES

- 1 J. A. Bailey and J. W. Mansfield, *Phytoalexins*, Blackie, Glasgow, 1982.
- 2 C. J. W. Brooks and D. G. Watson, *Natl. Prod. Rep.*, 2 (1985) 427.
- 3 H. D. Van Etten, D. E. Mathews and P. S. Mathews, *Annu. Rev. Phytopathol.*, 27 (1989) 143.
- 4 M. Takasugi, K. Monde, N. Katsui and A. Shirata, *Chem. Lett.*, (1987) 1631.
- 5 M. Takasugi, N. Katsui and A. Shirata, *J. Chem. Soc., Chem. Commun.*, (1986) 1077.
- 6 M. Takasugi, K. Monde, N. Katsui and A. Shirata, *Bull. Chem. Soc. Jpn.*, 61 (1988) 285.
- 7 K. Monde, N. Katsui, A. Shirata and M. Takasugi, *Chem. Lett.*, (1990) 209.

- 8 K. Monde, K. Sasaki, A. Shirata and M. Takasugi, *Phytochemistry*, 29 (1990) 1499.
- 9 K. Monde, K. Sasaki, A. Shirata and M. Takasugi, *Phytochemistry*, 30 (1991) 2915.
- 10 K. Monde, K. Sasaki, A. Shirata and M. Takasugi, *Phytochemistry*, 30 (1991) 3921.
- 11 K. Monde, M. Takasugi, J. A. Lewis and G. R. Fenwick, *Z. Naturforsch., C* 46 (1991) 189.
- 12 M. Devys, M. Barbier, I. Loiselet, T. Rouxel, A. Sarniguet, A. Kollmann and J. F. Bousquet, *Tetrahedron Lett.*, 29 (1988) 6447.
- 13 M. Devys, M. Barbier, A. Kollmann, T. Rouxel and J. F. Bousquet, *Phytochemistry*, 29 (1990) 1087.
- 14 J. S. Dahiya and S. R. Rimmer, *Phytochemistry*, 27 (1988) 3105.
- 15 T. Rouxel, A. Sarniguet, A. Kollmann and J. R. Bousquet, *Physiol. Mol. Plant. Pathol.*, 34 (1989) 507.
- 16 M. S. C. Pedras and J. L. Taylor, *J. Org. Chem.*, 56 (1991) 2619.
- 17 G. R. Fenwick, R. K. Heaney and W. J. Mullin, *CRC Crit. Rev. Food Sci. Nutr.*, 18 (1983) 123.
- 18 G. R. Fenwick, R. K. Heaney and R. Mawson, in P. R. Cheeke (Editor), *Toxicants of Plant Origin, Vol. II, Glycosides*, CRC Publishing, Boca Raton, FL, 1989, pp. 3-41.
- 19 R. McDannell, A. E. M. MacLean, A. B. Hanley, R. K. Heaney and G. R. Fenwick, *Food Chem. Toxicol.*, 26 (1988) 59.
- 20 P. Jandera and B. Prokes, *J. Liq. Chromatogr.*, 14 (1991) 3125.
- 21 T. Kowalska, *Chromatographia*, 29 (1990) 389.
- 22 A. Bartha, H. A. H. Billiet and L. de Galan, *J. Chromatogr.*, 458 (1988) 371.
- 23 N. Tanimoto and M. Takasugi, unpublished results.
- 24 R. M. Acheson, P. G. Hunt, D. M. Littlewood, B. A. Murrer and H. E. Rosenberg, *J. Chem. Soc., Perkin Trans. 1*, (1978) 1117.
- 25 K. Monde and M. Takasugi, *J. Chem. Soc., Chem. Commun.*, (1991) 1582.
- 26 J. S. Dahiya and S. R. Rimmer, *J. Chromatogr.*, 448 (1988) 448.
- 27 A. Kollmann, T. Rouxel and J. F. Bousquet, *J. Chromatogr.*, 473 (1989) 293.
- 28 T. Rouxel, A. Kollmann, L. Boulidard and R. Mithen, *Planta*, 184 (1991) 271.
- 29 M. Devys and M. Barbier, *J. Chem. Soc., Perkin Trans. 1*, (1990) 2856.

PUBLICATION SCHEDULE FOR 1992

Journal of Chromatography and Journal of Chromatography, Biomedical Applications

MONTH	O 1991–F 1992	M	A	M	J	
Journal of Chromatography	Vols. 585–593	594/1 + 2 595/1 + 2	596/1 596/2 597/1 + 2	598/1 598/2 599/1 + 2 600/1 600/2	602/1 + 2	The publication schedule for further issues will be published later.
Cumulative Indexes, Vols. 551–600					*	
Bibliography Section		610/1			610/2	
Biomedical Applications	Vols. 573 and 574	575/1 575/2	576/1	576/2 577/1	577/2	

* Cumulative Indexes will be Vol. 601, to appear early 1993.

INFORMATION FOR AUTHORS

(Detailed *Instructions to Authors* were published in Vol. 558, pp. 469–472. A free reprint can be obtained by application to the publisher, Elsevier Science Publishers B.V., P.O. Box 330, 1000 AH Amsterdam, The Netherlands.)

Types of Contributions. The following types of papers are published in the *Journal of Chromatography* and the section on *Biomedical Applications*: Regular research papers (Full-length papers), Review articles and Short Communications. Short Communications are usually descriptions of short investigations, or they can report minor technical improvements of previously published procedures; they reflect the same quality of research as Full-length papers, but should preferably not exceed five printed pages. For Review articles, see inside front cover under Submission of Papers.

Submission. Every paper must be accompanied by a letter from the senior author, stating that he/she is submitting the paper for publication in the *Journal of Chromatography*.

Manuscripts. Manuscripts should be typed in double spacing on consecutively numbered pages of uniform size. The manuscript should be preceded by a sheet of manuscript paper carrying the title of the paper and the name and full postal address of the person to whom the proofs are to be sent. As a rule, papers should be divided into sections, headed by a caption (*e.g.*, Abstract, Introduction, Experimental, Results, Discussion, etc.). All illustrations, photographs, tables, etc., should be on separate sheets.

Introduction. Every paper must have a concise introduction mentioning what has been done before on the topic described, and stating clearly what is new in the paper now submitted.

Abstract. All articles should have an abstract of 50–100 words which clearly and briefly indicates what is new, different and significant.

Illustrations. The figures should be submitted in a form suitable for reproduction, drawn in Indian ink on drawing or tracing paper. Each illustration should have a legend, all the *legends* being typed (with double spacing) together on a *separate sheet*. If structures are given in the text, the original drawings should be supplied. Coloured illustrations are reproduced at the author's expense, the cost being determined by the number of pages and by the number of colours needed. The written permission of the author and publisher must be obtained for the use of any figure already published. Its source must be indicated in the legend.

References. References should be numbered in the order in which they are cited in the text, and listed in numerical sequence on a separate sheet at the end of the article. Please check a recent issue for the layout of the reference list. Abbreviations for the titles of journals should follow the system used by *Chemical Abstracts*. Articles not yet published should be given as "in press" (journal should be specified), "submitted for publication" (journal should be specified), "in preparation" or "personal communication".

Dispatch. Before sending the manuscript to the Editor please check that the envelope contains four copies of the paper complete with references, legends and figures. One of the sets of figures must be the originals suitable for direct reproduction. Please also ensure that permission to publish has been obtained from your institute.

Proofs. One set of proofs will be sent to the author to be carefully checked for printer's errors. Corrections must be restricted to instances in which the proof is at variance with the manuscript. "Extra corrections" will be inserted at the author's expense.

Reprints. Fifty reprints of Full-length papers and Short Communications will be supplied free of charge. Additional reprints can be ordered by the authors. An order form containing price quotations will be sent to the authors together with the proofs of their article.

Advertisements. The Editors of the journal accept no responsibility for the contents of the advertisements. Advertisement rates are available on request. Advertising orders and enquiries can be sent to the Advertising Manager, Elsevier Science Publishers B.V., Advertising Department, P.O. Box 211, 1000 AE Amsterdam, Netherlands; courier shipments to: Van de Sande Bakhuysenstraat 4, 1061 AG Amsterdam, Netherlands; Tel. (+31-20) 515 3220/515 3222, Telefax (+31-20) 6833 041, Telex 16479 els vi nl. UK: T. G. Scott & Son Ltd., Tim Blake, Portland House, 21 Narborough Road, Cosby, Leics. LE9 5TA, UK; Tel. (+44-533) 753 333, Telefax (+44-533) 750 522. USA and Canada: Weston Media Associates, Daniel S. Lipner, P.O. Box 1110, Greens Farms, CT 06436-1110, USA; Tel. (+1-203) 261 2500, Telefax (+1-203) 261 0101.

For Superior Chiral Separation

From Analytical to Semi-preparative column

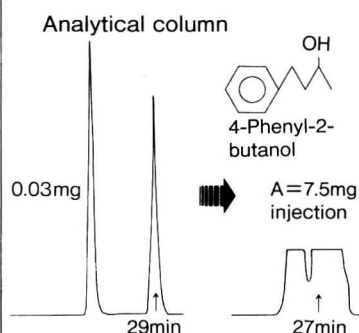
HPLC column output is directly proportional to cross section

- Analytical column
0.46cm ϕ \times 25cm

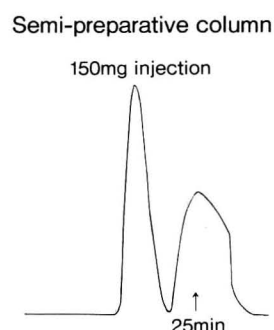
- Semi-preparative column
2cm ϕ \times 25cm

$$A \text{ mg} \times \left(\frac{1^2 \times 3.14}{(0.29)^2 \times 3.14} \right) \div A \text{ mg} \times 20$$

A = maximum sample amount of Analytical column



CHIRALCEL OD	column	CHIRALCEL OD
0.46cm ϕ \times 25cm	column size	2cm ϕ \times 25cm
10 μ m	Particle size	10 μ m
Hexane/IPA (9:1)	eluent	Hexane/IPA (9:1)
0.3ml/min.	flow rate	6ml/min.
UV 254nm	detection	UV 254nm
max 0.03mg	injection amount	7.5mg \times 20 = 150mg



Standard Available Column

- CHIRALPAK[®]/CHIRALCEL[®] (Particle size 10 μ m)

	I. D.	Length
Analytical column	0.46cm ϕ \times 25cm	
Pre-column	0.46cm ϕ \times 5cm	
Semi-preparative column	1cm ϕ \times 25cm	
	2cm ϕ \times 25cm	

- CROWNPAK[™] (Particle size 5 μ m)

	I. D.	Length
Analytical column	0.4cm ϕ \times 15cm	
Pre-column	0.4cm ϕ \times 1cm	

CHIRAL TECHNOLOGIES, INC.

730 SPRINGDALE DRIVE
DRAWER I
EXTON, PA 19341
Phone: 215-594-2100
Fax: 215-594-2325

DAICEL (EUROPA) GmbH

Oststr. 22
4000 Düsseldorf 1, Germany
Phone: 49/211/369848
Telex: (41) 8588042 DCEL D
Fax: 49/211/364429

DAICEL CHEMICAL INDUSTRIES, LTD.

8-1, Kasumigaseki 3-chome, Chiyoda-ku, Tokyo 100, Japan
Phone: 81-3-3507-3151 Fax: 81-3-3507-3193

CHIRALCEL, CHIRALPAK and CROWNPAK are trademarks of DAICEL CHEMICAL IND., LTD.